TECHNISCHE UNIVERSITÄT MÜNCHEN

Lehrstuhl für Ernährung und Immunologie

Complex bacterial consortia reprogram the colitogenic activity of *Enterococcus faecalis* in a gnotobiotic mouse model of chronic immune-mediated colitis

Isabella Brigitta Lengfelder

Vollständiger Abdruck der von der Fakultät Wissenschaftszentrum Weihenstephan für Ernährung, Landnutzung und Umwelt der Technischen Universität München zur Erlangung des akademischen Grades eines

Doktors der Naturwissenschaften (Dr. rer. nat.)

genehmigten Dissertation.

Vorsitzender: Prof. Dr. Siegfried Scherer

Prüfer der Dissertation: **1.** Prof. Dr. Dirk Haller

                           2. Prof. Dr. Wolfgang Liebl

Die Dissertation wurde am 01.07.2019 bei der Technischen Universität München eingereicht und durch die Fakultät Wissenschaftszentrum Weihenstephan für Ernährung, Landnutzung und Umwelt der Technischen Universität München am 11.10.2019 angenommen.

ABSTRACT

Inflammatory bowel diseases (IBD) are associated with compositional and functional changes of the intestinal microbiota, but specific contributions of individual bacteria to chronic intestinal inflammation remain unclear. *Enterococcus faecalis* is a resident member of the human intestinal core microbiota that has been linked to the pathogenesis of IBD and induces chronic colitis in susceptible monoassociated IL10-deficient (IL-10$^{-/-}$) mice. In this study, we characterized the colitogenic activity of *E. faecalis* as part of a simplified microbial consortium based on human strains (SIHUMI).

RNA sequencing analysis of *E. faecalis* isolated from monoassociated wild type and IL-10$^{-/-}$ mice identified 408 genes including 14 genes of the ethanolamine utilization (*eut*) locus to be significantly upregulated in response to inflammation. Despite considerable upregulation of *eut* genes, deletion of ethanolamine utilization (Δ*eutVW*) had no impact on *E. faecalis* colitogenic activity in monoassociated IL-10$^{-/-}$ mice. However, replacement of the *E. faecalis* wild type bacteria by a Δ*eutVW* mutant in SIHUMI-colonized IL-10$^{-/-}$ mice resulted in exacerbated colitis, suggesting protective functions of *E. faecalis* ethanolamine utilization in complex bacterial communities.

To better understand *E. faecalis* gene response in the presence of other microbes, we purified wild-type *E. faecalis* cells from the colon content of SIHUMI-colonized wild type and IL10$^{-/-}$ mice using immuno-magnetic separation and performed RNA sequencing. Transcriptional profiling revealed that the bacterial environment reprograms *E. faecalis* gene expression in response to inflammation, with the majority of regulated genes not being shared between monocolonized and SIHUMI conditions. While in *E. faecalis* monoassociation a general bacterial stress response could be observed, expression of *E. faecalis* genes in SIHUMI-colonized mice was characterized by up-regulation of genes involved in growth and replication. Interestingly, in mice colonized with SIHUMI lacking *E. faecalis* enhanced inflammation was observed in comparison to SIHUMI-colonized mice, supporting the hypothesis that *E. faecalis* ethanolamine metabolism protects against colitis in complex consortia.

In conclusion, this study demonstrates that complex bacterial consortia interactions reprogram the gene expression profile and colitogenic activity of the opportunistic pathogen *E. faecalis* towards a protective function.

ZUSAMMENFASSUNG

Chronisch entzündliche Darmerkrankungen gehen mit kompositionellen und funktionellen Veränderungen der Darmmikrobiota einher, allerdings ist der spezifische Beitrag einzelner Bakterien zum entzündlichen Geschehen weitgehend unklar. *Enterococcus faecalis* ist ein residentes Mitglied der menschlichen Darmkernmikrobiota, das mit der Pathogenese chronisch entzündlicher Darmerkrankungen in Verbindung gebracht wird und chronische Kolitis in suszeptiblen monoassoziierten IL10-defizienten (IL-10$^{-/-}$) Mäusen induziert. In dieser Studie haben wir die kolitogene Aktivität von *E. faecalis* als Teil eines vereinfachten mikrobiellen Konsortiums basierend auf menschlichen Stämmen (SIHUMI) charakterisiert.

Eine RNA-Sequenzierungsanalyse von *E. faecalis* Zellen, die aus monoassoziierten Wildtyp- und IL-10$^{-/-}$-Mäusen isoliert wurden, identifizierte 408 Gene, darunter 14 Gene des Ethanolaminverwertungs-Locus (*eut)*, die als Reaktion auf Entzündungen signifikant hochreguliert werden. Trotz erheblicher Hochregulierung der *eut*-Gene hatte die Deletion der Ethanolaminverwertung (ΔeutVW) keinen Einfluss auf die kolitogene Aktivität von *E. faecalis* in monoassoziierten Mäusen. Der Austausch des *E. faecalis* Wildtyp-Stammes durch eine Δ*eutVW*-Mutante in SIHUMI-kolonisierten IL-10$^{-/-}$-Mäusen führte jedoch zu einer Verschlimmerung der Entzündung. Dies deutet auf eine protektive Funktion der Ethanolaminverwertung durch *E. faecalis* in einer komplexen Gemeinschaft hin.

Um die Genexpression von *E. faecalis* in Gegenwart anderer Mikroben besser zu verstehen, haben wir Wildtyp-*E. faecalis*-Zellen aus dem Darminhalt von SIHUMI-kolonisierten Wildtyp- und IL-10$^{-/-}$-Mäusen mittels immunomagnetischer Trennung isoliert und mittels RNA-Sequenzierung analysiert. Die transkriptionelle Analyse ergab, dass das bakterielle Umfeld die Genexpression von *E. faecalis* in Reaktion auf Entzündungen neu programmiert. Nur ein kleiner Teil der regulierten Gene waren sowohl in *E. faecalis* in Monoassoziation, als auch in Co-Kolonisation mit dem SIHUMI Konsortium parallel reguliert. Während bei monoassoziiertem *E. faecalis* eine allgemeine Stressreaktion beobachtet werden konnte, war das Expressionsprofil von *E. faecalis* in SIHUMI kolonisierten Mäusen durch Gene gekennzeichnet, die an Wachstum und Replikation beteiligt sind. Interessanterweise führte die Kolonisation von IL-10$^{-/-}$ Mäusen mit SIHUMI unter Ausschluss von *E. faecalis* zu einer Verschlimmerung des inflammatorischen Phänotyps. Dies unterstützt die Hypothese, dass *E. faecalis* als Mitglied eines komplexen Konsortiums durch die Verwertung von Ethanolamin eine protektive Funktion in suszeptiblen IL-10$^{-/-}$ Mäusen vermittelt.

Abschließend zeigt diese Studie, dass Interaktionen mit einem komplexen bakteriellen Konsortium das Genexpressionsprofil und die kolitogene Aktivität des opportunistischen Pathogens *E. faecalis* in Richtung einer protektiven Aktivität umprogrammieren.

TABLE OF CONTENTS

1. INTRODUCTION

1.1 IBD – a multifactorial chronic disease associated with a westernized lifestyle

Inflammatory bowel diseases (IBD) with the two dominant types Crohn's disease (CD) and Ulcerative colitis (UC) are chronic relapsing inflammatory disorders affecting the gastrointestinal (GI) tract. CD is characterized by discontinuous, transmural inflammation occurring most commonly in the terminal ileum and colon (Baumgart and Sandborn, 2012). In UC, inflammation is restricted to the colon and only affects the mucosal surface. Tissue inflammation always begins at the rectum and extends continuously in the proximal direction (Ordas et al., 2012).

Both diseases are on the rise worldwide, with the highest incidence rates in westernized countries. While developing countries had a low incidence of IBD, incident rates increased with increasing industrialization of those countries, indicating a strong influence of environmental factors on the onset of disease (Loftus, 2004; Molodecky et al., 2012). Several factors appear to be involved in the pathogenesis of IBD, including genetic susceptibility (Jostins et al., 2012) and diverse environmental triggers resulting in an inappropriate T-cell mediated activation of immunity towards components of the intestinal microbiota (Xavier and Podolsky, 2007; Sartor, 2008). The environmental triggers of disease identified so far include smoking, diet, antibiotics, nonsteroidal anti-inflammatory drug use, stress and infection. However, the mechanisms underlying disease initiation by these factors are not well understood. It has been suggested that environmental triggers influence intestinal barrier integrity, immune responses or the luminal microenvironment, eventually leading to an inflammatory response in a genetically susceptible host (Sartor, 2006).

It is well established that genetic factors influence the susceptibility to IBD with an increased risk of disease in relatives of IBD patients. The degree of heritability is different for disease subtypes with a lower genetic component in UC compared to CD (Moller et al., 2015). This is consistent with monozygotic twin studies, which show a concordance rate of only 10–15% in UC compared to 30–35% in CD (Spehlmann et al., 2008; Brant, 2011). To date, more than 230 single nucleotide polymorphisms (SNPs) associated with an increased risk for IBD have been identified by genome-wide association studies (Turpin et al., 2018). The majority of these SNPs appear for both UC and CD, indicating a common genetic basis for the IBD subtypes, with multiple genes contributing to disease risk (Jostins et al., 2012).

Many genetic risk loci associated with IBD development are involved in the modulation of host immune responses towards intestinal microbes including bacterial recognition and clearance, intestinal barrier function and cellular stress responses. These defects can lead to a loss of tolerance to commensal microbiota, together with the inability to down-regulate immune responses after

exposure to luminal antigens, resulting in relapsing inflammation with chronic tissue damage (Sartor, 2008; Jostins et al., 2012).

1.2 Physiologic Microbe-Host Interactions

The control of the intestinal microbiota with a dynamic balance between immune recognition and defense seems to play a central role in IBD pathogenesis. Usually, the commensal microbiota and the host coexist in a mutualistic relationship that has been established through co-evolution. The GI tract hosts a diverse community of bacterial species with bacterial counts ranging from very low levels in the stomach up to 10^{12}/g in the colon. The human gut microbiota is a dynamic ecosystem consisting of an estimated 400-1000 bacterial species with large variations between individuals, especially for less abundant species (Qin et al., 2010; Donaldson et al., 2016). However, most people share a core set of microbially encoded genes and thus metabolic core functions provided by the microbiome (Turnbaugh et al., 2009; Human Microbiome Project, 2012).

The commensal microbiota confers metabolic functions beyond those of the host alone and enables the host to obtain energy from dietary compounds that would otherwise be indigestible. Some bacterial metabolites, such as short-chain fatty acids (SCFA), are not only an important source of energy but also influence intestinal barrier function and immune responses (Turnbaugh et al., 2006; Kau et al., 2011; Marchix et al., 2018). In addition, the endogenous commensal microbiota competes with invading microorganisms for nutrients and space, thus providing a colonization resistance against incoming pathogens (Sorbara and Pamer, 2018).

The mucosal surfaces of the GI tract are constantly exposed to microbial antigens derived from the diverse community of endogenous bacteria, underlining the importance of maintaining immune tolerance to commensal microbiota while combating pathogens. This balance between tolerance and defense is mediated through extensive microbe-host interactions. The commensal microbiota is essential for the development and function of the host immune system. Vice versa, a functioning host immune system is essential for maintaining a symbiotic relationship with the microbiota by maintaining mucosal homeostasis. The immune system of germfree animals is underdeveloped with hypoplastic Peyer's patches, a greatly reduced number of IgA-producing plasma cells and CD4+ T-cells in the lamina propria, poorly matured spleen and lymph nodes and reduced serum IgG levels. All these defects can be reversed by colonization of GF animals with a complex commensal microbiota (Bauer et al., 1963; Benveniste et al., 1971; Macpherson et al., 2001; Macpherson et al., 2002).

A key strategy of the host to maintain mucosal homeostasis is to maintain a spatial separation between the microorganisms and the host. A single cell layer of intestinal epithelial cells (IECs) separates the large number of intestinal microorganisms from underlying tissues. This barrier is

further enhanced by a mucus layer, the production of IgA by plasma cells and the secretion of antimicrobial peptides (AMPs) by Paneth cells (Macpherson and Uhr, 2004; Johansson et al., 2008; Bevins and Salzman, 2011; Johansen and Kaetzel, 2011). These reinforcement strategies minimize the contact between microorganisms and the epithelial cell surface, thereby limiting immune overactivation and microbial translocation.

Goblet cells secrete mucin glycoproteins, the constituents of the intestinal mucus layer which restricts the access of microorganisms to the epithelial surface. While the mucus in the small intestine consists of a single layer that allows the microbes to get into contact with the epithelium, a structurally different bi-layer forms in the large intestine. Herein, the inner mucus layer is impenetrable for most microorganisms, while the outer mucus layer provides a habitat for a large number of bacteria (Johansson et al., 2011).

A second line of defense against microorganisms is provided by the production of AMPs. AMPs have antimicrobial functions including the disruption of bacterial cell wall or inner membrane. (Hooper and Macpherson, 2010). A small number of bacteria that overcome the host's first line defense mechanisms and breach the epithelial barrier are killed by macrophages or processed by dendritic cells (DCs) that promote the induction of secretory IgA. Secretory IgA can be produced by both T-cell independent (innate IgA) and T-cell dependent mechanisms (adaptive IgA). The local secretion of innate IgA limits penetration and overgrowth of microbiota, but is not as potent as adaptive IgA in shaping microbiota composition and with this a mutualistic relationship between host and microbiota (Kawamoto et al., 2014; Sutherland et al., 2016).

It is hypothesized that enteric pathogens induce the production of specific high-affinity IgA, whereas commensal species induce low-affinity IgA with low specificity (Pabst, 2012; Slack et al., 2012). Interestingly, it was demonstrated that high IgA-coating identifies indigenous bacterial species, which trigger intestinal inflammation (Palm et al., 2014). Furthermore, certain commensal bacteria induce systemic IgA, which confers protection against polymicrobial sepsis. This supports the hypothesis that IgA has an important function in maintaining immune homeostasis (Wilmore et al., 2018).

In healthy hosts, commensal bacteria stimulate a program of immune responses that is dominated by homeostatic mechanisms such as down-regulation of microbe-sensing receptors and secretion of anti-inflammatory molecules that terminate immune responses and mediate mucosal barrier function (Sartor, 2008). Some of these mechanisms are controlled by the sensing of microbes or microbe-derived products by the host. Bacterial recognition depends on a repertoire of pattern recognition receptors (PRR) expressed by IECs and innate immune cells residing in the lamina propria. The activation of these PRR by bacterial ligands stimulates central signaling cascades such as

nuclear factor-κB (NF-κB) and mitogen-activated protein kinase (MAPK) pathways resulting in the expression of pro- or anti-inflammatory proteins (Sartor, 2008).

The integration of these multiple signals by IECs and immune cells ensures the homeostasis of the tissue and the integrity of the barrier at the interface between the microbiota and host tissue. Disorders of this tightly balanced system can lead to the development of a chronic overactivation of the host's immune system characteristic for IBD.

1.2 Importance of microbe-host interactions in IBD pathogenesis

Several lines of evidence, including clinical and experimental studies, suggest that microbial agents play a central role in the pathogenesis of IBD (Figure 1). The most convincing evidence is the absence of inflammation in several rodent models that are genetically susceptible to chronic immune-mediated intestinal inflammation when kept under germfree (sterile) conditions (Hormannsperger et al., 2015). In addition, genes related to innate immune recognition and response are enriched among IBD risk loci, which suggests that defects in intestinal microbiota containment increase IBD susceptibility (chapter 1.2.1). CD and UC occur mainly in the colon and distal ileum, the intestinal areas with the highest bacterial concentrations and the diversion of the fecal stream prevents and treats CD (Sartor and Mazmanian, 2012).

Furthermore, it has been shown that the composition and function of the microbiota in IBD patients is altered compared to healthy controls. These alterations are referred to as dysbiosis. Among the dysbiotic changes characteristic for IBD are a reduced bacterial diversity associated with the expansion of supposedly harmful microbes combined with a loss of supposedly protective microbes (chapter 1.2.2) (Sartor and Wu, 2017). The functional relationship between IBD pathogenesis and the intestinal microbiota is further illustrated by substantial T-cell and serologic responses to a variety of microbial antigens in IBD patients indicating defective immune regulation after microbial stimulation (Mow et al., 2004; Sartor, 2008; Harmsen et al., 2012).
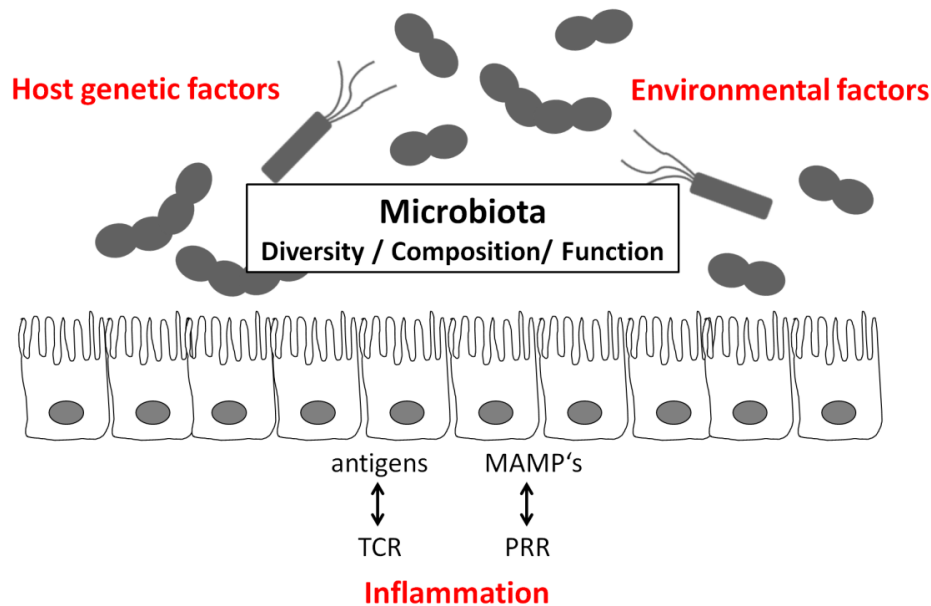
Figure 1: Microbe-Host interactions in IBD pathogenesis.
IBD etiology involves genetic susceptibility, environmental triggers, and the gut microbiome. Bacterial antigens and microbe-associated molecular patterns (MAMP's, e.g. lipoproteins, lipopolysaccharide) are processed by host receptors (TCR, T-cell receptor; PRR, pattern recognition receptor) and induce inappropriate T-cell mediated activation of immunity towards components of the intestinal microbiota leading to inflammation and tissue damage The intestinal microbiota is influenced in diversity, composition and function by internal (inflammation, genetic factors, microbe-microbe interactions) and environmental factors (e.g. diet, antibiotics). Alterations of the microbial ecosystem that are associated with pathology are defined as dysbiosis.

1.2.1 Host genetic defects in the containment of intestinal microbes

The strongest genetic risk factor associated with CD is the nucleotide-binding oligomerization domain 2 (NOD2) gene. The NOD2 gene encodes a cytoplasmic PRR that senses muramyl dipeptide, a component of the peptidoglycan present in bacterial cell walls (Hugot et al., 2001; Ogura et al., 2001; Girardin et al., 2003). IBD-associated mutations of the NOD2 locus are thought to cause defective bacterial recognition accompanied by impaired NF-kB activation, Paneth cell function (reduced defensin production) and finally clearance of intracellular pathogens (Bonen et al., 2003; Hisamatsu et al., 2003; Wehkamp et al., 2004; Kobayashi et al., 2005).

It has also been reported that NOD2 controls the commensal microbiota composition. In NOD-deficient mice, increased bacterial load and reduced capability to prevent colonization with pathogenic bacteria were observed (Petnicki-Ocwieja et al., 2009). This is consistent with a study from Frank and colleagues showing that NOD2 polymorphisms were associated with shifts in microbiota composition in CD patients (Frank et al., 2011).

Other IBD susceptibility loci affecting microbial recognition and killing include ATG16L1, IRGM, NCF4 and TLR receptors. ATG16L1 is an integral protein of the autophagy pathway involved in the clearance of intracellular pathogens (Rioux et al., 2007; Cadwell et al., 2008). In line with this, IRGM plays a role in killing of phagocytosed bacteria and is associated with abnormal Paneth cell morphology (Singh et al., 2006; Roberts et al., 2008; Liu et al., 2013). NCF4 is a component of NADPH oxidase and crucial for the production of reactive oxygen species by phagocytic cells (Rioux et al., 2007; Roberts et al., 2008). TLR receptors identified as IBD risk loci include TLR2, 4 and 5. These PRRS sense bacterial lipoproteins, lipopolysaccharide and flagellin, respectively (Beutler, 2000; Pierik et al., 2006; Meena et al., 2013; Chassaing et al., 2014).

1.2.2 Dysbiosis of the intestinal microbiota

Alterations of the microbial ecosystem that are associated with pathology are defined as dysbiosis. Characteristic dysbiotic changes reported for IBD are a reduced microbial diversity, an expansion of supposedly pathogenic bacteria and a loss of supposedly protective species. There is evidence that dysbiosis can be both cause and consequence of intestinal inflammation. This will be discussed in detail in the following section.

A causative role is supported by a therapeutic efficacy of antibiotics, probiotics and fecal microbiota transplantation (FMT) in some IBD patients. All these treatment strategies target the dysbiotic microbiota. Antibiotics remove large communities of bacteria, while probiotic treatment and FMT attempt to correct a dysbiotic ecosystem by introducing new and potentially beneficial bacterial species (Hansen and Sartor, 2015). Narrow-spectrum antibiotics like metronidazole and ciprofloxacin provide some benefit to CD patients, while UC patients seem to benefit only from broad antibiotic combinations (Hansen and Sartor, 2015).

The use of probiotics like *E. coli* Nissle and the probiotic combination VSL#3 appears to maintain and possibly induce remission in a number of UC patients (Rembacken et al., 1999; Kruis et al., 2004; Sood et al., 2009; Tursi et al., 2010). So far, however, no beneficial effect of probiotic treatment has been observed for CD (Kruis, 2013). FMT treatment appears to induce remission in a subset of UC patients. However, additional studies are needed to support these findings and the optimal composition of donor microbiota and FMT conditions (mode and intensity of administration) need to be defined (Hansen and Sartor, 2015; Moayyedi et al., 2015; Rossen et al., 2015; Costello et al., 2017; Paramsothy et al., 2017). Another strong evidence of dysbiosis as a cause of IBD is the induction of colitis in wild type (WT) mice through the transfer of fecal microbiota from mice suffering from colitis (Elinav et al., 2011).

In contrast, there is also convincing evidence that the dysbiosis observed in IBD is the consequence of inflammation, antibiotic treatment or diet (Lewis et al., 2015). Active IBD and experimental chronic intestinal inflammation are associated with changes in bacterial community composition (Gevers et al., 2014; Berry et al., 2015; Schaffler et al., 2016; Osaka et al., 2017) and gene expression (Patwa et al., 2011; Tchaptchet et al., 2013; Ocvirk et al., 2015).

Schaffler and colleagues were able to show that the mucosa-attached bacterial community of CD patients is related to disease state, with dysbiotic changes being associated with high disease activity scores (Schaffler et al., 2016). Gevers and colleagues also observed a strong correlation between the dysbiotic status of the intestinal microbiota and the disease activity in new-onset CD patients (Gevers et al., 2014). In accordance with this, a recent study by Schirmer and colleagues demonstrated that the severity of the baseline disease in new-onset UC patients is associated with the depletion of core gut microbes and the expansion of oral bacteria (Schirmer et al., 2018).

Dysbiotic changes occurring in a chronic inflammatory environment are characterized by a reduced bacterial diversity, a reduction of obligate anaerobic bacteria such as SCFA-producing Ruminococcaceae and Lachnospiraceaea and an expansion of facultative anaerobic bacteria from the phylum Proteobacteria, mainly belonging to the family Enterobacteriaceae (Baumler and Sperandio, 2016; Duvallet et al., 2017; Pascal et al., 2017). These changes are likely to reflect alterations in the nutritional environment and epithelial defense mechanisms by the inflammatory host response.

A prominent hypothesis that attempts to explain the shift from obligate to facultative anaerobic bacteria, is referred to as the "Oxygen hypothesis" (Rigottier-Gois, 2013). It has been suggested that intestinal inflammation is associated with an increase in intraluminal oxygen concentrations due to hyperemia and increased vascular and mucosal permeability. O_2 would inhibit the growth of oxygen-sensitive obligate anaerobes and at the same time serve as an electron acceptor for facultative anaerobes and thereby promote their growth. In the mouse intestine, a radial gradient of microbes linked to oxygen levels was observed, wherein aerotolerant bacteria were enriched at the mucosa, while anaerobic microbes dominate the intestinal lumen. (Rigottier-Gois, 2013; Albenberg et al., 2014; Sartor and Wu, 2017). In accordance with the "Oxygen hypothesis", new-onset CD patients exhibit an altered mucosal bacterial community with a higher number of aerotolerant species than healthy controls (Gevers et al., 2014; Haberman et al., 2014).

A central mechanism that shapes the bacterial community is nutrient availability. It has been shown that mucosal inflammation is associated with dysregulated epithelial electrolyte transport. In mice, the disruption of a Na^+/H^+ exchanger caused dysbiosis of the gut microbiota and microbiota-dependent inflammatory symptoms (Laubitz et al., 2016). In addition, the production and

composition of mucus is altered in inflammatory processes (McGuckin et al., 2011). A change associated with inflammation is an increase in carbohydrate fucosylation. Fucose from mucus carbohydrates can be liberated and utilized by members of the gut microbiota, providing a growth advantage for these species (Baumler and Sperandio, 2016). In line with this, mucosa-associated bacteria are increased in IBD, with a disproportionate enrichment of some mucus-degrading bacteria (Png et al., 2010). For instance, *Ruminococcus gnavus*, a known utilizer of mucin glycans, appears to be particularly enriched in CD patients (Prindiville et al., 2004; Willing et al., 2010; Joossens et al., 2011; Crost et al., 2013).

Another mechanism that supports the bloom of certain members of the microbiota during inflammation-associated dysbiosis is the production of alternative respiratory electron acceptors as by-product of inflammatory host responses. Alternative electron acceptors such as nitrate or tetrathionate promote the anaerobic respiration of some facultative anaerobes. Anaerobic respiration enables the utilization of non-fermentable substrates or fermentation end products as carbon sources. This confers facultative anaerobes a fitness advantage over obligate anaerobes that lack the necessary genes and can lead to their uncontrolled expansion in the intestinal lumen (Winter et al., 2010; Thiennimitr et al., 2011; Winter et al., 2013; Winter and Baumler, 2014).

An example is the bloom of *Salmonella enterica* serovar Thypimurium (*S.* Thypimurium) in the inflamed intestine through the utilization of Ethanolamine (EA) upon tetrathionate respiration (Thiennimitr et al., 2011). EA is derived from the membrane phospholipid phosphatidylethanolamine by microbial activity and can be used by some bacteria as valuable source of carbon and/or nitrogen. Most species that are able to utilize intestinal EA are pathogens, the only commensals that contain the necessary genes are *Enterococcus faecalis* (*E. faecalis*) (chapter 1.5) and some strains of *Escherichia coli* (*E. coli*) (Tsoy et al., 2009; Kaval and Garsin, 2018; Rowley et al., 2018).

Inflammation alters not only the nutritional environment, but also epithelial defense mechanisms such as the generation of reactive oxygen (Harper et al., 2005; Haberman et al., 2014) and nitrogen species (Lundberg et al., 1994; Salzman et al., 1996) as well as the production of antimicrobial molecules and IgA (Ramanan and Cadwell, 2016). All this influences the composition of the bacterial community by providing a fitness advantage for bacterial species that can quickly adapt to and take advantage of this particular environment.

Interestingly, several bacterial species showing an altered frequency during active IBD affect immune responses in experimental colitis models either by mediating homeostasis or inflammation. A prominent indicator species lost in IBD is *Faecalibacterium prausnitzii* (*F. prausnitzii*), a member of the Clostridiaceae family. *F. prausnitzii* was found specifically decreased in microbiota samples of IBD

patients compared to healthy specimens (Ramanan and Cadwell, 2016) and the low-mucosal abundance of this species was associated with post-resection relapse of CD (Sokol et al., 2008). It has been shown that *F. prausnitzii* and other Clostridium species exert positive immune suppressive effects on the host, including the suppression of experimental colitis and the induction of T-regulatory cells (Treg cells) (Sokol et al., 2008; Atarashi et al., 2013). Together with the decline of protective species, the expansion of potentially pathogenic species is characteristic for an IBD-associated dysbiotic microbiota.

However, the significance of correlation analyses is limited. Bloom et al. isolated Bacteroides and Enterobacteriaceae species from spontaneously colitic dnKO mice. In these mice, the abundance of Bacteroides was not altered compared to noncolitic control animals, whereas Enterobacteriaceae were strikingly enriched in spontaneous disease. Surprisingly, colonization of antibiotic-treated dnKO mice with Bacteroides isolates induced colitis, whereas colonization with Enterobacteriaceae isolates did not (Bloom et al., 2011). Similar results were also obtained by Perez-Munoz et al. in TM-IEC C1galt1(-/-) mice. Monoassociation with a *Lactobacillus johnsonii* isolate, that was found to be enriched in colitic TM-IEC C1galt1(-/-) mice, did not induce disease (Perez-Munoz et al., 2014).

Bacterial species that are usually blooming under inflammatory conditions are not classical pathogens, but mostly commensal species with functional alterations. Intestinal inflammation creates a special environment that boosts the growth of those species that are well adapted and resistant to immune defense mechanisms. Under homeostatic conditions, these "opportunistic pathogens" are commensal members of the microbiota, but can have detrimental inflammation-promoting effects in immune-compromised hosts.

Adherent and invasive *E. coli* (AIEC) were found in high prevalence in the mucosa of patients with ileal CD (Darfeuille-Michaud et al., 2004). Baumgart et al. showed that invasive *E. coli* are restricted to inflamed mucosa in ileal CD patients and that their number correlates with disease severity (Baumgart et al., 2007). AIEC use different strategies to interact with the host to promote bacterial growth and survival. AIEC strongly adhere to and invade IECs, leading to pro-inflammatory cytokine secretion. Furthermore, they can survive and replicate within macrophages, thereby inducing a strong TNF-α response (Agus et al., 2014). Bacterial adhesion to IECs is mediated via the interaction of bacterial type1 pili with the host receptor carcinoembryonic antigen-related cell adhesion molecule 6 (CEACAM6) (Barnich et al., 2007) or via binding of the bacterial ChiA protein to the host chitinase 3-like-1 receptor (Low et al., 2013). CEACAM6 has been shown to be highly expressed in ileal IECs of CD patients and in a transgenic mouse expressing human CEACAMs to mimic the situation in CD patients, the AIEC reference strain LF82 induced the development of colitis (Carvalho et al., 2009). AIECs can actively resist against AMPs and translocation across the epithelial barrier is

mediated by different mechanisms, including the modulation of tight junctions. Furthermore, AIEC outer membrane vesicles interact with the endoplasmatic reticulum (ER) stress response glycoprotein Gp69 that is over-expressed in the apical IEC membrane in CD patients (Agus et al., 2014).

A second species often mentioned in the context of IBD pathogenesis is Gram-positive *E. faecalis*. Enterococci have been found to be increased in fecal samples from CD patients compared to healthy controls (Kang et al., 2010; Shiga et al., 2012; Zhou et al., 2016). This is consistent with an increased frequency of *E. faecalis* housekeeping as well as virulence genes in CD cohorts (Roche-Lima et al., 2018) and a high likelihood of *E. faecalis* isolates from inflamed IBD mucosa to carry virulence genes (Golinska et al., 2013).

UC patients show an increased number of mucosa-associated *E. faecalis* correlating with disease activity (Fite et al., 2013) and high *E. faecalis* specific IgG reactivity (Furrie et al., 2004). *E. faecalis* induces chronic colitis in monoassociated IL-10-deficient mice (IL-10$^{-/-}$ mice), a well characterized model to mimic human colitis (Balish and Warner, 2002; Barnett et al., 2010). In previous studies we could assign the colitiogenic activity of *E. faecalis* to certain bacterial structures, suggesting that the contribution of bacteria to IBD pathogenesis depends on microbe-host interactions via specific structures (Steck et al., 2011; Ocvirk et al., 2015). This makes the situation even more complex, as these structures are often strain-specific and their degree of expression can be regulated in response to environmental cues (chapter 1.4).

1.3 Animal models of experimental colitis: Microbe-Host interactions

Animal models are a useful tool to study microbe-host interactions and their role in the pathogenesis of IBD without confounding factors such as diet, genetic background and the microbial environment. The development of intestinal inflammation in animal models can be triggered either by a chemical inductor (e.g. DSS or TNBS) or preferably by genetic background. Many genetically driven IBD mouse models are disease-free when kept under GF conditions and clearly demonstrate the importance of microbial triggers for IBD pathogenesis.

The IL-10$^{-/-}$ mouse, incapable of producing the anti-inflammatory cytokine IL-10, is an extensively studied model of spontaneous colitis. GF housed IL-10$^{-/-}$ mice are free of disease, while mice colonized with a complex microbiota develop chronic intestinal inflammation (Sellon et al., 1998). Colitis development in IL-10$^{-/-}$ mice is mediated by an abnormal response of Th1/Th17 cells to microbial triggers leading to massive production of pro-inflammatory cytokines such as IFNγ, IL-12 and IL-17 (Berg et al., 1996; Davidson et al., 1996; Yen et al., 2006). It is noteworthy that disease

onset and severity depend on the microbial environment, the time of colonization and the genetic background (Sellon et al., 1998; Mähler M, 2002; Kim et al., 2005).

Monoassociation studies (colonization of GF mice with a single bacterial strain) revealed that not all microorganisms, even including some opportunistic pathogens like *Helicobacter hepaticus*, trigger inflammation in IL-10$^{-/-}$ mice. This demonstrates that some species have higher colitogenic activity than others (Whary et al., 2011) (Figure 2). Of note, species that trigger colitis in one experimental colitis model may not necessarily induce disease in other experimental models (Hormannsperger et al., 2015). For example, *Bacteroides vulgatus* induces inflammation in monoassociated HLA/B27-ß2m rats, but not in IL-10$^{-/-}$ or IL-2$^{-/-}$ mice (Rath et al., 1999; Sydora et al., 2005; Frick et al., 2006). Monoassociation of IL-10$^{-/-}$ mice with different strains of *E. coli* or *E. faecalis* was sufficient to induce disease supporting the colitogenic character of these species (Balish and Warner, 2002; Kim et al., 2005; Kim et al., 2007; Patwa et al., 2011). However, the absence of disease in monoassociated WT animals indicates that these species are not pathogens.
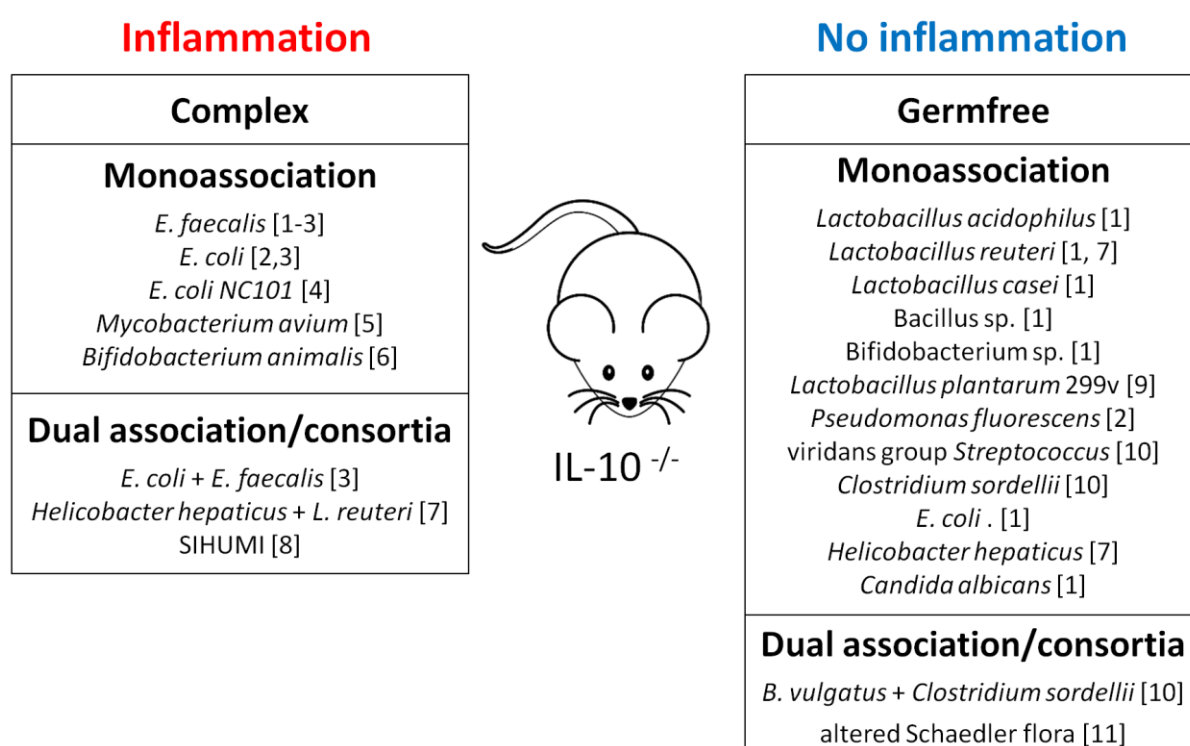
Figure 2: Impact of microbial colonization on disease development in gnotobiotic IL-10$^{-/-}$ mice

Interestingly, the location of inflammation and onset of disease varies from species to species. *E. faecalis*-driven inflammation develops primarily in the distal colon with only a weak phenotype in the cecum, while *E. coli*-driven inflammation is most pronounced in the cecum (Kim et al., 2005). This demonstrates that different bacterial species can induce variable inflammatory phenotypes in a

single susceptible host. Geva-Zatorsky et al. screened in an elaborate study 53 human-derived microbes for their immunomodulatory activities in gnotobiotic WT mice. They were able to show that the majority of microbes analyzed induced immunophenotypic and/or transcriptomic changes in the host, with only a few bacteria having no influence on the host organism according to the parameters measured. Most microbes elicited a distinct immunophenotype, but the effects could be redundant and even complementary. Surprisingly, the immunophenotypic and transcriptomic effects were independent of microbial phylogeny (Geva-Zatorsky et al., 2017).

Since the microbiota of conventional animals is too complex to dissect the mechanisms of disease development, gnotobiotic animals colonized by a defined simplified microbial consortium are used as a model system to mimic the conditions in conventional hosts. This allows the manipulation of the bacterial community and its individual members, which is crucial for studying the complex interactions between microbes themselves and between microbes and their host.

Brugiroux et al. have established a defined mouse consortium comprising 12 bacterial isolates that provides partial colonization resistance against *S. Typhimurium* infection. Reinforced with 3 facultative anaerobes selected according to functional characteristics, the consortium provided complete colonization resistance to *S. Typhimurium* (Brugiroux et al., 2016). This shows that a simplified microbial consortium can mimic a complex microbiota in terms of colonization resistance. However, the composition of the consortium is important. Furthermore, it should be noted that gnotobiotic mice colonized with a simplified microbial consortium may be morphologically and functionally similar to conventional mice, but so far there is no minimal consortium available that fully restores all functions conducted by a conventional microbiota (Becker et al., 2011; Eun et al., 2014; Hormannsperger et al., 2015; Brugiroux et al., 2016).

A simplified human microbiota consortium (SIHUMI) has been shown to induce antigen-specific colitis in gnotobiotc IL-10$^{-/-}$ mice (Eun et al., 2014). The SIHUMI consortium is composed of 7 well-characterized species of human origin known to show shifts in the microbiota of IBD patients. In gnotobiotic animals, SIHUMI forms a stable community with the abundance of individual SIHUMI species being influenced by host genetic background and the presence of intestinal inflammation. In IL-10$^{-/-}$ mice, the individual bacterial strains induce differential effector immune responses with no direct correlation to bacterial abundance (Eun et al., 2014).

1.4 *E. faecalis* as model organism for microbe-host interactions in IBD

E. faecalis is a Gram-positive resident member of the human intestinal core microbiota, but also carries a number of pathogenic traits that explain the association of this bacterium with IBD and fatal nosocomial infections (Qin et al., 2010; Sava et al., 2010; Lebreton et al., 2014). This dualistic

character as an opportunistic pathogen makes *E. faecalis* an exemplary model for the investigation of microbe-host interactions that are relevant for the pathogenesis of chronic colitis.

In the IL-10$^{-/-}$ mouse model, monoassociation with *E. faecalis* causes severe colitis that is characterized by a defective resolution of TLR-2 mediated pro-inflammatory gene expression in the intestinal epithelium (Ruiz et al., 2005). We were able to show that the colitogenic activity of *E. faecalis* in monoassociated IL-10$^{-/-}$ mice can be assigned to certain bacterial structures (Steck et al., 2011; Ocvirk et al., 2015). The secreted protease Gelatinase E (GelE) impairs intestinal barrier integrity by cleavage of the epithelial tight junction protein E-cadherin, which promotes the development of chronic inflammation in susceptible IL-10 $^{-/-}$ mice (Steck et al., 2011). Furthermore, we found that enterococcal polysaccharide antigen (epa) influences biofilm formation and *in vivo* mucus penetration, which partially contributes to disease development, while functional *E. faecalis* lipoproteins involved in TLR2-mediated activation and recruitment of innate immune cells are required as primary bacterial structures responsible for *E. faecalis* colitogenic activity (Ocvirk et al., 2015).

1.5 Ethanolamine utilization in *E. faecalis*

The ability to catabolize EA is encoded by the *eut* genes, a locus consisting of 19 genes in *E. faecalis* (Del Papa and Perego, 2008; Fox et al., 2009; Kaval and Garsin, 2018). The central enzyme in EA catabolism is the ethanolamine ammonia lyase consisting of the two subunits EutB and EutC. In the presence of the cofactor adenosylcobalamin (AdoCbl), EutB/C breaks down EA into acetaldehyde and ammonia, which serve as cellular supply for carbon and nitrogen, respectively (Kaval and Garsin, 2018). *E. faecalis* can grow on EA as sole carbon source, but only under anaerobic conditions. It is presumed that *E. faecalis* ferments EA, as no alternative electron acceptor was provided in the minimal medium (Garsin, 2010).

The *eut* gene expression is controlled by the EutV/W two-component system, which comprises the sensor histidine kinase EutW and the response regulator EutV. In the presence of EA, the histidine kinase EutW undergoes autophosphorylation and the phosphoryl group is transferred to a recipient domain on EutV (Del Papa and Perego, 2008; Fox et al., 2009). Phosphorylated EutV interacts with transcriptional terminators that precede certain *eut* open reading frames (ORFs). The binding of EutV prevents the formation of terminators and enables the RNA polymerase to generate full-length transcripts (Ramesh et al., 2012; DebRoy et al., 2014a). In addition to EA, *eut* gene expression also depends on the presence of Adenosylcobalamin (AdoCbl). AdoCbl binds to a riboswitch which is part of the small, trans-acting RNA EutX. This small RNA contains also a binding site that normally sequesters active EutV. Only in the presence of AdoCbl, a shorter form of EutX devoid of the EutV

binding site is generated, which leads to the transcriptional read through of multiple *eut* genes (DebRoy et al., 2014b).

It is important to note that the gastrointestinal tract is a rich source of EA, a component of the phospholipid phosphatidylethanolamine present in bacterial and eukaryotic cell membranes and in the host diet. The utilization of this compound could represent a colonization and fitness advantage for *E. faecalis* over other members of the microbiota, as it has already been demonstrated for enteric pathogens such as *S.* Typhimurium and enterohemorrhagic *E. coli* (EHEC) (Thiennimitr et al., 2011; Winter et al., 2013).

1.6 Major facilitator superfamily transporter of *E. faecalis*

Drug extrusion through multidrug efflux pumps serves as an important mechanism of clinically relevant bacterial resistance to antibiotics. In addition to antibiotic resistance, accumulating evidence suggests that efflux pumps also have physiological functions that enable bacterial survival in their ecological niche. They can confer resistance to host-derived molecules including bile, fatty acids and host-defence molecules and some bacterial efflux pumps have been shown to be important for the survival and persistence of bacteria in the host (Piddock, 2006; Sun et al., 2014).

Bacterial efflux pumps are classified into five families, with the major facilitator superfamily (MFS) being the clinically relevant one in Gram-positive bacteria. MFS is one of the largest and most diverse families of transport proteins. Individual MFS members show a high substrate specificity, yet the diversity of transported substrates is enormously (e.g. ions, simple sugars, oligosaccharides, inositols, drugs, amino acids, nucleosides, organophosphate esters, Krebs cycle metabolites) (Pao et al., 1998; Law et al., 2008).

The substrate of *E. faecalis* MFS transporter (OG1RF_10079) has not been identified yet. The transporter shows sequence homology to NorA, a protein involved in the resistance of *Staphylococcus aureus* to norfloxacine, and is the most homologous gene to *hpt* from *L. monocytogenes*, a gene involved in virulence and fosfomycin resistance (Yamada et al., 1997; Scortti et al., 2006). However, Riboulet-Bisson et al. could show that *E. faecalis* MFS transporter is neither implicated in the resistance to these antibiotics nor in *E. faecalis* virulence in a mouse peritonitis model (Riboulet-Bisson et al., 2008).

Furthermore, they identified *E. faecalis* MFS as a member of the Ers regulon. The transcriptional regulator Ers is involved in bacterial survival against oxidative stress, virulence and the regulation of several metabolic pathways (Giard et al., 2006; Riboulet-Bisson et al., 2008). They suggested glycerol transport as a possible function of *E. faecalis* MFS transporter, because growth of a MFS mutant on

glycerol was slightly impaired. However, the weak phenotype indicates that glycerol is not the main substrate of this transporter (Riboulet-Bisson et al., 2009).

1.7 Aim of the study

Dysbiotic changes associated with IBD are characterized by an over-representation of opportunistic pathogens and a loss of beneficial organisms, indicating that the pathogenic potential of a dysbiotic community can be linked to certain organisms. Consequently, the specific contribution of individual bacteria to disease pathogenesis needs to be investigated in detail. We are using *E. faecalis*, a resident member of the intestinal microbiota at the interphase between commensal and pathogen, as model organism to study microbe-host interactions relevant for the development of chronic colitis in a genetically susceptible host.

Bacterial interactions have been implicated in the pathogenesis of IBD, but the influence of co-colonizing microbes on gene expression and colitogenic activity of an opportunistic pathogen is hardly investigated. For this purpose, we are investigating the transcriptional and functional activity of *E. faecalis* in two gnotobiotic experimental settings. First in a monoassociated system and second as part of a simplified microbial consortium (SIHUMI). *E. faecalis* disease-associated gene expression was addressed by RNA sequencing of bacteria isolated from healthy WT and inflamed IL-10$^{-/-}$ mice. We show that *E. faecalis* adapts transcriptionally to inflammatory conditions and, more remarkably, to co-colonizing bacteria. We targeted genes highly upregulated in response to inflammatory conditions to study their influence on *E. faecalis* survival and colitogenic activity, namely a major facilitator superfamily transporter (MFS) and genes of the ethanolamine utilization (eut) locus. Using *E. faecalis* deletion mutants, we were able to establish a novel correlation between *E. faecalis* ethanolamine utilization and a protective function in the context of experimental colitis.

To unravel the etiology of SIHUMI-induced colitis, we colonize WT and IL-10$^{-/-}$ mice with SIHUMI consortium in the presence and absence of the opportunistic pathogens *E. faecalis* or *E. coli.* We demonstrate that bacterial consortia interactions reprogram the colitogenic activity of opportunistic pathogens which indicates that the colitogenic function of a bacterial strain is not only defined its gene repertoire, but also by interaction with co-colonizing microbes.

3. MATERIAL & METHODS

3.1 Supplier of experimental material

Table 1. Companies purchasing experimental material used for the thesis

Company	City of residence	State/Country of residence
4titude	Wotton	UK
Agilent	Böblingen	Germany
Ambion	Foster City	CA, USA
AppliChem	Darmstadt	Germany
Applied Biosystems	Foster City	CA, USA
BD Difco	Franklin Lakes	NJ, USA
Bender	Baden-Baden	Germany
Biochrom	Berlin	Germany
Bioline	London	UK
Biorad	Munich	Germany
MP Biomedicals	Santa Ana	CA, USA
Carl Roth	Karlsruhe	Germay
Covaris	Woburn	MA, USA
Dunnlab	Hanau	Germany
eBioscience	San Diego	CA, USA
GE Healthcare Amersham	Uppsala	Sweden
GraphPad Software	San Diego	CA, USA
Illumina	San Diego	CA, USA
Immunology Consultants Laboratory	Portland	OR, USA
Leica	Soest	Germany
Macherey-Nagel	Düren	Germany
Medite	Burgdorf	Germany
Meintrup DWS Laborgeräte	Herzlake	Germany
Merck	Kenilworth	NJ, USA
Millipore	Billerica	MA, USA
Miltenyi Biotec	Bergisch Gladbach	Germany
New England Biolabs	Ipswich	MA, USA
Olympus	Shinjuku	Japan
PerkinElmer	Waltham	MA, USA
Phenomenex	Aschaffenburg	Germany
Promega	Mannheim	Germany
Qiagen	Hilden	Germany
Roche Diagnostics	Mannheim	Germany
Sciex	Framingham	MA, USA
Shimadzu	Duisburg	Germany
Sigma Aldrich	St. Louis	MO, USA
Stratec	Washington DC	USA
Thermo Fisher Scientific	Waltham	MA, USA
Vector Laboratories	Burlingame	CA, USA
VWR	Leuven	Germany

ZEFA Laborservice	Harthausen	Germany

3.2. Bacterial strains and cultivation

For this study, we used the characterized *E. faecalis* strain OG1RF. The *eut VW* double deletion mutant (Debroy et al., 2012) was kindly provided by Danielle Garsin (The University of Texas, Department of Microbiology and Molecular Genetics). The isogenic *mfs* deletion mutant was generated in this study (for details see 3.5). *E. faecalis* strains (Table 2) were cultivated in Brain Heart Infusion (BHI) broth or on BHI agar (BD Difco) at 37°C under aerobic conditions, unless otherwise indicated.

For *E. faecalis* growth experiments on EA, minimal medium M9HY was prepared as described previously (Del Papa and Perego, 2008). The M9HY medium was supplemented with glucose at 100mM or EA at 40 mM final concentration. Cyanocobalamin (Carl Roth) was used as exogenous vitamin B12 source. The M9HY medium was inoculated with the different *E. faecalis* strains from overnight (ON) cultures. Cells were washed twice in nitrogen-gased M9HY medium without carbon sources and grown at 37°C under anaerobic conditions in an anaerobic chamber (Whitley Hypoxystation H85, Meintrup DWS Laborgeräte GmbH) containing a H_2/ N_2 gas mixture (10:90).

The SIHUMI (Eun et al., 2014) consortium (Table 2, members of the consortium are highlighted in red color) was kindly provided by Prof. Balfour R. Sartor (Division of Gastroenterology and Hepatology, University of North Carolina,Chapel Hill, USA). SIHUMI species were cultivated under anaerobic conditions on Wilkins-Chalgren-Agar (WCA, Thermo Fisher Scientific) in an anaerobic chamber or in hungate tubes (VWR International) containing WCA medium gassed with N_2 and supplemented with 0.05% (w/v) L-cystein (Carl Roth), 0.002% (w/v) dithiothretiol (DTT, Sigma Aldrich) and 0.0025% phenosafranin (Sigma Aldrich).

Bacterial cryo-stocks were prepared from ON cultures by mixing the bacterial suspension 1:1 with filter-sterilized glycerol in culture medium (40% v/v) in cryo-tubes before freezing and storage at -80°C. The purity of bacterial stocks was controlled by aerobic and anaerobic culture on agar plates and by sequencing of the 16S rRNA gene using primer 27F (5'-AGAGTTTGATCCTGGCTCAG-3') and 1492R (5'-GGTTACCTTGTTACGACTT-3'), as described previously (Lane, 1991; Klaring et al., 2013).

Table 2. Bacterial strains used in this study

Strain	Characteristics	Reference
Enterococcus faecalis OG1RF	WT strain	(Murray et al., 1993)

Enterococcus faecalis **OG1RF Δ*eut VW***	OG1RF *eutV* and *eutW* double deletion mutant	(Debroy et al., 2012)
Enterococcus faecalis **OG1RF Δ*mfs***	OG1RF *mfs* deletion mutant	This study
Escherichia coli **LF82**	WT strain	(Eun et al., 2014)
Ruminococcus gnavus **ATCC 29149**	WT strain	(Eun et al., 2014)
Bacteroides vulgatus **ATCC 8482**	WT strain	(Eun et al., 2014)
Faecalibacterium prausnitzii **A2-165**	WT strain	(Eun et al., 2014)
Lactobacillus plantarum **WCFS1**	WT strain	(Eun et al., 2014)
Bifidobacterium longum subsp. longum **ATCC 15707**	WT strain	(Eun et al., 2014)

3.3 Animal experiments – Ethical statement and housing

129S6/SvEv WT and IL-10$^{-/-}$ mice were used for monoassociation experiments and housed in isolators in the National Gnotobiotic Rodent Center, University of North Carolina, USA. All animal procedures were approved by the Institutional Animal Care and Use Committee, Harvard Medical School, and the University of North Carolina.

129S6/SvEv WT and IL-10$^{-/-}$ mice were used for SIHUMI colonization experiments and housed in isolators at the Core Facility Mikrobiom/Gnotobiologie of the Technical University Munich, ZIEL – Institute for Food & Health. All animal procedures were approved by the Committee on Animal Health and Care of the local government (Regierung von Oberbayern, AZ 55.2-1-54-2532-109-2015).

3.4 Animal experiments – Experimental design

Mice were fed a standard Chow diet (ssniff) ad libitum and were killed by CO_2. Littermates were used when possible, or siblings from multiple breeders were combined and randomly assigned before assignment to experimental groups.

For monoassociation, germfree 129S6/SvEv WT and IL-10$^{-/-}$ mice were colonized at the age of 10–12 weeks with either *E. faecalis* WT OG1RF or Δ*eut VW* mutant strain by oral and rectal swab. The mice were sacrificed after different periods of colonization (1, 4, 8, 16, 20, 24 weeks).

For colonization with the SIHUMI consortium, a bacterial mixture was prepared as follows. The bacteria were grown individually in hungate tubes for 24 h. A mixture of all strains with an equal cell density of 1×10^9 cells/ml was prepared in sterile glass tubes, mixed 1:1 with sterile glycerol in culture medium (40% v/v, gassed with N_2) and sealed with a rubber septum. The bacterial mixture was stored at -80°C until use. Germfree 129S6/SvEv WT and IL-10$^{-/-}$ mice were colonized at the age of 10 weeks with 1×10^8 cells/species by repetitive oral gavage (1x week 0, 1x week 1). The composition of the bacterial consortium differed between the experimental groups as shown in Table 3. All mice were sacrificed 4 or 16 weeks after colonization.

Table 3. Composition of the bacterial consortium in the respective experimental groups

Experimental group	Strains included in consortium
SIHUMI (Eun et al., 2014)	*E. coli* LF82, *E. faecalis* OG1RF, *R. gnavus* ATCC 29149, *B. vulgatus* ATCC 8482, *F. prausnitzii* A2-165, *L. plantarum* WCFS1, *B. longum* ATCC 15707
SIHUMI -E. faecalis	*E. coli* LF82, *R. gnavus* ATCC 29149, *B. vulgatus* ATCC 8482, *F. prausnitzii* A2-165, *L. plantarum* WCFS1, *B. longum* ATCC 15707
SIHUMI -E. coli	*E. faecalis* OG1RF, *R. gnavus* ATCC 29149, *B. vulgatus* ATCC 8482, *F. prausnitzii* A2-165, *L. plantarum* WCFS1, *B. longum* ATCC 15707
SIHUMI Δeut VW	*E. coli* LF82, *E. faecalis* Δ*eut vw*, *R. gnavus* ATCC 29149, *B. vulgatus* ATCC 8482, *F. prausnitzii* A2-165, *L. plantarum* WCFS1, *B. longum* ATCC 15707
SIHUMI Δmfs	*E. coli* LF82, *E. faecalis* Δ*mfs*, *R. gnavus* ATCC 29149, *B. vulgatus* ATCC 8482, *F. prausnitzii* A2-165, *L. plantarum* WCFS1, *B. longum* ATCC 15707

3.5 Generation of the *mfs* deletion mutant

An in-frame deletion of 81% of the *E. faecalis* OG1RF gene *mfs* (Locus Tag: OG1RF_10079, GeneID: 12289265) was generated using a method described before (Thurlow et al., 2009) with the following modifications: The mutagenesis strategy (Figure 3) and relevant primers (Table 4) were designed by Luis Felipe Romero Saavedra (Dr. von Hauner Children's Hospital, Ludwig Maximilians University). Fragments up- and downstream (935 bp and 1060 bp) of the *mfs* open reading frame were amplified by PCR using primers 10079_5, 10079_22, 10079_33 and 10079_66. The PCR products were digested with HindIII (Thermo Fisher Scientific) and ligated using T4 DNA ligase (Thermo Fisher Scientific). The ligation product was reamplified using the primer 10079_1 and 10079_44 resulting in a 1942 bp PCR product, lacking 81 % of the *mfs* gene (Δ*mfs*).

For all PCR reactions, a high-fidelity DNA polymerase (Phusion HS II, Thermo Fisher Scientific) was used following manufacturer's instructions. The PCR product was purified using the MSB® Spin PCRapace kit (Stratec), digested with the restriction enzymes BamHI and NcoI (Thermo Fisher

Scientific) and ligated with the replication-thermosensitive vector pLT06 (Thurlow et al., 2009) previously digested with the same restriction enzymes.

Subsequently, the ligated products were electroporated into electro-competent *E. coli* XL-1 Blue (Agilent) for propagation and grown on LB agar plates containing 10 μg/ml chloramphenicol (Cm, Carl Roth), 20 μg/ml X-Gal (VWR) and 0.1 mM IPTG (Applichem) at 30°C under aerobic conditions. Blue colonies were isolated and screened for the presence of the Δ*mfs* insert using pLT06_fwd and pLT06_rev primers.

Positive colonies were grown overnight (ON) in LB broth containing Cm at 30°C. The plasmid was purified using NucleoSpin Plasmid EasyPure kit (Macherey-Nagel) and sequenced using the primers 10079_seq_Fw and 10079_seq_Rv to verify the desired construct. Subsequently, the Δ*mfs* deletion construct was transformed into electrocompetent *E. faecalis* OG1RF cells (chapter 3.6). After transformation, bacteria were grown for 1.5 h at 37°C and then transferred onto BHI plates containing 20 μg/ml Cm, 20 μg/ml X-Gal and 0.1 mM IPTG. After ON incubation at 30°C, blue colonies were screened for the presence of the pLT06/Δ*mfs* construct by PCR using primers pLT06_for and pLT06_rev. Positive colonies were grown in BHI broth supplemented with 20 μg/ml Cm at 30 °C ON.

The liquid cultures were diluted 1:1000 in fresh BHI broth supplemented with Cm (pre-warmed to 44°C) and incubated ON at 44 °C, driving the integration of the construct into the bacterial chromosome by homologous recombination. Bacterial culture was then diluted and plated on BHI plates containing Cm, X-Gal and IPTG incubated ON at 44 °C. The integration was confirmed by PCR using primer 10079_seq_Fw in combination with 10079_22 and 10079_seq_Rv with 10079_33.

Positive isolates were grown in BHI media without antibiotic selection at 30 °C for 3 h followed by an immediate temperature switch to 44°C and ON incubation, thereby forcing the excision of the plasmid from the chromosome. The positive isolates were serially passaged in the same way for 3 times, followed by plating on BHI agar containing X-Gal and IPTG at 30 °C. The resulting white colonies indicate the absence of the plasmid and were screened for the loss of Cm resistance. The presence of the deletion was tested by PCR using primers 10079_5 and 10079_6. Positive clones were selected and isolated genomic DNA (chapter 3.8) was sent for sequencing with 10079_seq_Fw primer (GATC) to confirm the deletion of the *mfs* gene. The generated deletion mutant OG1RF Δ*mfs* containing a 1005 bp deletion is listed in Table 2.

Table 4. Primers used for the generation of the Δ*mfs* deletion mutant from *E. faecalis* OG1RF

Primer	Sequence	Restriction site

10079_1	AGGCGGATCCCATGACGACAGCCGATGAGC	BamHI (GGATCC)
10079_5	GCGAACCAACTGAAAGGAGC	
10079_6	GTGTTCATGCGTTGAATTTCC G	
10079_22	TCAAAAGCTTTGTTGGTGTTTG	HindIII (AAGCTT)
10079_33	TCAAAAGCTTGGTTTAGACCTTGGATTAGGGGT	HindIII (AAGCTT)
10079_44	AGGCCCATGGCGTGTCTTAGTAAGGACCAATCAAAG	NcoI (CCATGG)
10079_66	CGAAATCTTTACCACCGATTCG	
pLT06_fwd	CAATAATCGCATCCGATTGCAG	
pLT06_rev	CCTATTATACCATATTTTGGAC	
10079_seq_Fw	GCCAAACGCTCAATAGAAAATGC	
10079_seq_Rv	CCACGCTCTTCTTGCTTATTTTCT	
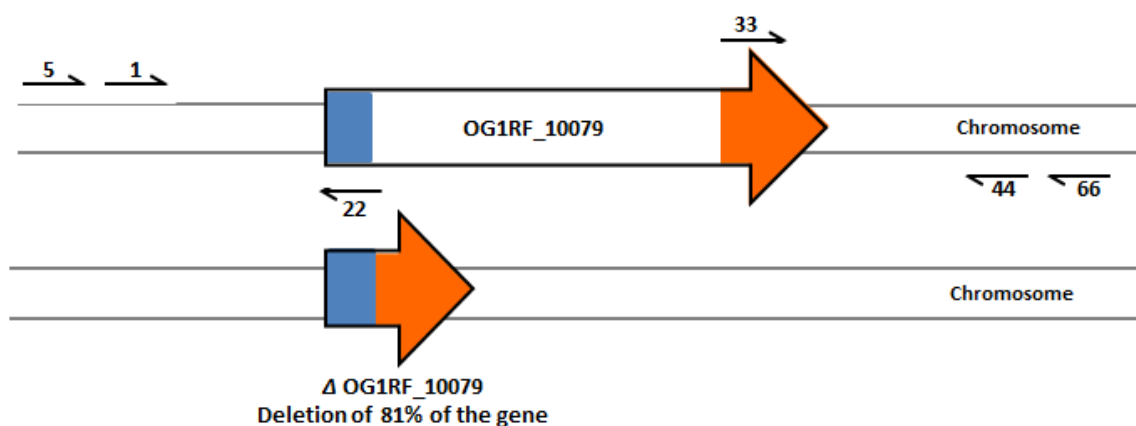
Figure 3: Mutagenesis strategy
Mutagenesis strategy for the construction of the Δ*mfs* deletion mutant from *E. faecalis* OG1RF. Different PCRs were performed to generate an 81% deletion of *E. faecalis mfs* gene. The binding sites of the relevant primers on the *E. faecalis* genome are shown in the upper part, the resulting deletion of the *mfs* gene is shown in the lower part of the figure.

3.6 Preparation of electrocompetent *E. faecalis* cells

E. faecalis OG1RF was inoculated in 10 ml BHI broth and grown at 37°C. The ON culture was diluted 1:20 with 100 ml fresh BHI broth and incubated at 37°C until an Optical Density (OD) at 600 nm between 0.5 and 1 was reached. The bacterial cells were chilled on ice for 20 min and harvested by

centrifugation at 3000 rpm for 10 min at 4°C. The cell pellet was resuspended in 2 ml sterile ddH$_2$O and centrifuged at 13000 rpm for 1 min at 4°C.

Subsequently, the cell pellet was resuspended in 500 µl lysozyme solution (10 mM Tris pH 8.0, 20 % sucrose, 10 mM EDTA, 50 mM NaCl) containing freshly added mutanolysin (Sigma Aldrich) and lysozyme (Sigma Aldrich), at a final concentration of 2 µg/ml and 25 µg/ml, respectively. The bacterial suspension was incubated for 20 min at 37 °C with gentle shaking. Subsequently, bacteria were washed 3 times with 1 ml of electroporation buffer (10 mM Tris pH 8.0, 0.5 M sucrose, 10 % glycerol). Finally, cells were resuspended in 500 µl of electroporation buffer and divided into 50 µl aliquots. The generated electrocompetent *E. faecalis* cells were stored at -80 °C until use.

3.7 Preparation of bacterial lysates

Bacterial lysates were prepared as described previously (Eun et al., 2014). Briefly, individual bacterial colonies were inoculated under anaerobic conditions in 20 ml broth for 24 hours. The bacterial cultures were washed twice with and resuspended in sterile PBS. Per 1 ml bacterial suspension, 250 µl freshly prepared MD solution (0.1 M MgCl$_2$, 100 µg/ml DNaseI) was added. Bacteria were disrupted using a FastPrep®-24 (MP Biomedicals) and the suspension was sterilized using a 0.2 µm syringe filter. The protein concentration was determined by using the Roti®-Nanoquant Bradford assay (Carl Roth). The lysates were stored at -80°C until use.

3.8 Bacterial DNA extraction

Bacterial cells or intestinal contents were resuspended in 600 µl stool stabilizer (Stratech), mixed with 400 µl phenol/chloroform/iso-amyl alcohol (Carl Roth) and lysed by mechanical lysis using a FastPrep®-24 (MP Biomedicals). The homogenized mixture was incubated for 8 min at 95°C and DNA was isolated by phase separation via centrifugation at 16000 g for 5 min at 4°C. Contaminating RNA was digested with 0.1 µg/µl RNase A (VWR) for 30 min at 37°C. Subsequently, DNA was purified using the gDNA clean-up kit (Macherey-Nagel) according to the manufacturer's instructions. DNA concentration and purity were analyzed with a NanoDrop® 1000 spectrophotometer (Thermo Fisher Scientific).

3.9 Bacterial community analysis via quantitative real-time PCR (qPCR) assay

For bacterial community analysis, oligonucleotide primers were used to target species-specific regions of the 16S ribosomal RNA gene. Quantification was performed using the LightCycler 480 Universal Probe Library System (UPL, Roche) with the following 2-step program: 95°C for 3 min, 40 cycles of 95°C for 5 sec and 60°C for 10 sec. Reactions were carried out in 10 µl volumes containing

1x PCR master mix (Brilliant III, Agilent), 200 nM of each primer, 100 nM of probe and 1 ng of DNA template. Primers (Sigma Aldrich) and corresponding probes (Roche) are listed in Table 5. Positive and negative controls were included in every run. The specificity of primer pairs was validated by using an equal mixture of DNA from all SIHUMI species spiked with increasing concentrations of target species DNA. The Ct-value was only affected by changes in DNA concentration of the target species while not being affected by non-target DNA. Standard curves were generated for each species and used to enumerate the 16S gene copy numbers per species in intestinal content. 16S gene copy number per ng DNA was calculated via the molecular weight of the genome and 16S copy numbers/genome. The relative abundance of each species in intestinal content was calculated as previously described (Eun et al., 2014) using the following formula: [(copies of 16S rRNA gene for a specific SIHUMI bacterium/cumulative copies of 16S rRNA gene of all bacteria) × 100].

Table 5. Species specific 16S-targeted primers and UPL probes used for bacterial community analysis

Target bacterial species	Oligonucleotide sequence (5'–3')	UPL probe	Reference
Escherichia coli **LF82**	L: GGGACCTTAGGGCCTCTTG R: GCCTAGGTGAGCCTTTACCC	104	This study
Enterococcus faecalis **OG1RF**	L: GGTCATTGGAAACTGGGAGA R: TTCACCGCTACACATGGAAT	91	This study
Ruminococcus gnavus **ATCC 29149**	L: GGGACTGATTTGGAACTGT R: CGCATTTCACCGCTACACTA	55	This study
Bacteroides vulgatus **ATCC 8482**	L: CGCAACCCTTGTTGTCAGT R: CATCTTACGATGGCAGTCTTGT	73	This study
Faecalibacterium prausnitzii **A2-165**	L: TATTGCACAATGGGGGAAAC R: CAACAGGAGTTTACAATCCGAAG	69	This study
Lactobacillus plantarum **WCFS1**	L: CGAAGAAGTGCATCGGAAAC R: TCACCGCTACACATGGAGTT	35	This study
Bifidobacterium longum subsp. longum **ATCC 15707**	L: TGGTAGTCCACGCCGTAAA R: TAGCTCCGACACGGAACC	42	This study
Total bacteria	L: YAACGAGCGCAACCC R: AAGGGSCATGATGAYTTGACG	69	(Zhu et al., 2014)

3.10 Droplet Digital PCR

Droplet digital PCR (ddPCR^{TM}, Bio-rad) was performed at the Technical University Munich Campus in Straubing with the generous help of Dr. Josef Sperl (Chair: Chemie Biogener Rohstoffe). Therefore, DNA isolated from pure bacterial culture or colonic content of germfree or SIHUMI colonized mice was digested with BamHI-HF restriction enzyme (New England Biolabs) for 1 h to improve amplicon accessibility. The following DNA amouts were used for ddPCR reactions:

- DNA isolated from colon content: 50 ng

- DNA isolated from pure culture for standard curve generation: 50 ng, 5 ng, 0.5 ng, 0.05 ng,
    5 pg, 0.5 pg, 0.05 pg

The ddPCR mixture contained 10 µl of 2x ddPCR^{TM} Supermix for Probes (Bio-Rad), 900 nM of both forward and reverse primers and 125 nM of the respective UPL probe (Roche) in a total reaction volume of 20 µl. Primers and probes are listed in Table 5. The 20 µl reaction and 70 µl/reaction Droplet Generation Oil for Probes (Bio-Rad) were loaded into a droplet cartridge (Bio-Rad). After droplet generation, the emulsion was transferred into a 96 well plate and PCR was performed in a C-1000 thermal cycler (Bio-Rad) with following conditions: 95°C for 10 min, 40 cycles of 94°C for 30 sec and 60°C for 1 min. PCR-positive and PCR-negative droplets were detected using a Bio-Rad droplet reader. The Quantasoft software was used for downstream analysis.

3.11 Bacterial RNA isolation

Bacterial total RNA was isolated as described previously (Ridaura et al., 2013). Briefly, bacterial cells were mechanically disrupted using a FastPrep®-24 bead beater (MP Biomedicals). RNA was isolated by phenol:chloroform:iso-amyl alcohol (25:24:1, pH 4.5, Carl Roth) extraction, precipitated with isopropanol and purified using the NucleoSpin® RNA extraction kit (Macherey-Nagel). RNA concentration and purity was analyzed using a NanoDrop® 1000 spectrophotometer (Thermo Fisher Scientific). The RNA integrity was assessed by Gel Electrophoresis. Contaminating genomic DNA was digested using TURBO DNase (Thermo Fisher Scientific) according to the manufacturer's instructions.

3.12 Reverse transcription and gene expression analysis via qPCR (bacteria)

Complementary DNA (cDNA) was synthesized from 500 ng RNA using the Moloney murine leukemia virus (MMLV) Point Mutant Synthesis System (Promega) and random hexamers. The absence of contaminating gDNA was ensured for each sample by negative controls, whereby no reverse transcriptase was added to the reaction. Quantification was performed by using the LightCycler 480 Universal Probe Library System (UPL, Roche) with the following 2-step program: 95°C for 3 min, 40

cycles of 95°C for 5 s and 60°C for 10 sec. The reactions were carried out in 10 µl volumes containing 1x PCR master mix (Agilent), 400 nM of each primer, 200 nM of probe and 1 µl of cDNA template. Primers (Sigma Aldrich) and corresponding UPL probes (Roche) are listed in Table 6. Relative quantification of gene expression was calculated by means of $2^{-\Delta\Delta Ct}$ values: $2^{-[(Ct_{target\ gene} - Ct_{housekeeping\ gene})treated - (Ct_{target\ gene} - Ct_{housekeeping\ gene})untreated]}$. The values were normalized to the *E. coli* LF82 housekeeping genes cysG, pyrA and rpoA.

Table 6. Primers and corresponding UPL probes used for bacterial gene expression analysis

Targeted gene and Locus Tag	Oligonucleotide sequence (5'-3')	UPL probe
fimH (LF82_0665)	L: TCCAGCGAATAACACGGTATC R: TTGCCGTTAATCCCAGACTT	68
yfgI (LF82_3097)	L: ACGTCGAAGATGGTCGTTTC R: TCAGTCTGGAAACCGGAACT	107
ompA (LF82_1559)	L: CGCTCCGAAAGATAACACCT R: CCATTGTTGTTGATGAAACCAG	26
ompC (LF82_1560)	L: CACTGGTGGTCTGAAATACGAC R: GCGAGTTGCGTTGTAGGTCT	71
fliC (LF82_0291)	L: GGCTACGCTTGATGGTTTATTC R: GCAGTCTTATTAAACCCGATTGA	9
fliD (LF82_0698)	L: TGGGTGAATGCCTATAACTCG R: TCTACGGCGGTGTATTTGGT	66
csgA (LF82_0360)	L: GGCAGGTGTTGTTCCTCAGT R: AATTCGGGCCGCTATTATTAC	70
flhA (LF82_0692)	L: TTATCGACTGATCCCGATGG R: CGTATACGGCCCAACAACTC	18
flgH (LF82_0685)	L: GCGATACGCTGACTATCGTG R: GCATTCGCAGAGGAGCTTT	2
cysG (LF82_0414)	L: ATGAAAGCCTTCTCGACACC R: TAAGCGCGTCATCATCTGTC	70
gyrA (LF82_0962)	L: TCGGTCAGGTAGTACAGACCATC R: CCTGCAGAAGCGAAAACC	18
rpoA (LF82_1958)	L: GAAGCAGCGCGTGTAGAAC R: GGTTTCCATTTCGATGACCA	2
pyrC (OG1RF_11429)	L: AACGCACCTTTTGGTATTGTC R: GCCTGTTTCGACAAAGTTCG	97
OG1RF_10076	L: GCAATCGAGCAAACCATTCT R: TGCTAAGAGAAAACTTTACCGTC	84
OG1RF_10077	L: TGCTAAGAGAAAACTTTACCGTC R: ACTTTCCCGCTGTGCATTTA	103
OG1RF_10082	L: TTCAAATTCACTCAGATTAACAA R: GATTTTAGCGCGTTGGAAAG	69

3.13 Immunomagnetic separation of *E. faecalis* cells from the intestinal content

The isolation method was modified after Nolle (2017) (Nolle, 2017). Frozen colonic content from SIHUMI colonized mice was disrupted by bead beating in 1 ml RNAlater (Sigma Aldrich) using glass beads (1 mm, Carl Roth). Subsequently, samples were diluted with wash buffer (PBS, 0.5% biotin-free BSA, 10% RNAlater) and filtered through 3 cell strainers with decreasing pore size (VWR, 100 μm/70 μm/30 μm).

The samples were kept on ice throughout the protocol and only pre-chilled buffer solutions were used. The bacterial cells were pelleted by centrifugation at 5000 g for 5 min at 4°C and resuspended in 1 ml wash buffer. The samples were mixed with 10 μl *Enterococcus* specific antibody (biotinylated, Thermo Fisher Scientific PA1-73123) and incubated for 10 min at 4°C with gentle agitation. The specificity of the anti-*Enterococcus* antibody was tested by western blot analysis (chapter 3.19.2).

The ideal antibody concentration was determined by spiking of intestinal content from germfree mice with *E. faecalis*, *E. coli* and *L. plantarum* in different mixing ratios followed by immunomagnetic separation (IMS) with distinct antibody concentrations. *E. faecalis* cell number in relation to other bacterial species was determined by plating and CFU determination before and after IMS. The samples were centrifuged for 2 min at 9600 g. After a washing step, the cells were resuspended in 100 μl wash buffer and 10 μl Streptavidin MicroBeads (Miltenyi Biotec) were added per sample. After incubation for 15 min at 4°C with gentle agitation, the cells were washed with wash buffer and resuspended in 500 μl separation buffer (PBS, 0.5% biotin-free BSA, 2 mM EDTA, 10% RNAlater). Magnetically labeled *E. faecalis* cells were isolated using MACS filter columns (LS, Miltenyi Biotec) in a MidiMACS™ Separator (Miltenyi Biotec) according to the manufacturer's instructions and total bacterial RNA was isolated.

3.14 Microbial RNA sequencing (RNA seq)

3.14.1 RNA seq of *E. faecalis* isolated from monoassociated mice

Bacterial RNA prepared from the colonic content of *E. faecalis* OG1RF monoassociated WT and IL-10$^{-/-}$ mice (n=8 mice/group; colonization period: 16 weeks) was sequenced as described previously (Ocvirk et al., 2015). RNA isolation and rRNA depletion was done by Jonathan Hansen and Sandrine Tchaptchet from the Division of Gastroenterology and Hepatology of the University of North Carolina in Chapel Hill. Library preparation and sequencing was performed at the Washington University St. Louis Genome Technology Access Center generating in total 190 million unidirectional 50 bp reads using an Illumina HiSeq2000 instrument (Illumina).

3.14.2 RNA seq of *E. faecalis* isolated from SIHUMI colonized mice

E. faecalis cells in the colonic content of SIHUMI colonized Wt (n=6 mice/group; colonization period: 16 weeks) and IL-10$^{-/-}$ mice (n=13 mice/group; colonization period: 16 weeks) were isolated by IMS. Total bacterial RNA was isolated as described above (chapter 3.11) and purified using the RNeasy® MinElute^{TM} Cleanup kit (Qiagen). Contaminating gDNA was eliminated using TURBO DNase (Thermo Fisher Scientific) and RNA integrity was validated by agarose gel electrophoresis.

Ribosomal RNA was depleted by using the RiboMinus™ Transcriptome Isolation Kit (Bacteria, Thermo Fisher Scientific) according to the manufacturer's instructions. Subsequently, the RNA was fragmented for 180 sec using a Covaris E220 sonicator set at 10% duty cycle, intensity of 5 and 200 cycles/burst in 120 µl 1 mM Tris-EDTA pH 8. The fragmented RNA was precipitated with 1 µl glycogen (Thermo Fisher Scientific), 1:10 sample volume 3 M sodium acetate (Ambion) and 2.5 sample volume of 100% EtOH.

Next, RNA was dephosphorylated using 10 U per 300 ng RNA Antarctic phosphatase at 37 °C for 30 min (New England Biolabs). The RNA fragments were recovered using the miRNeasy® Mini kit (Qiagen) followed by 5' phosphorylation using 20 U T4 polynucleotide kinase at 37°C for 60 min (Thermo Fisher Scientific). Again, the miRNeasy® Mini kit was used for recovery. RNA fragment size was examined using the BioAnalyzer on an RNA Pico Chip (Agilent Technologies).

The cDNA library was prepared as described in the TruSeq® Small RNA Library Prep Reference Guide (Illumina) with the following exception. After adapter ligation and reverse transcription, fragments were size selected between 145 bp and 300 bp corresponding to an insert length between 18 bp and 173 bp. The sequencing was conducted at the Core Facility Microbiome/NGS (ZIEL – Institute for Food & Health, Technical University of Munich), generating in total 300 million unidirectional 50 bp reads using an Illumina HiSeq2000 instrument.

3.14.3 Bioinformatics

Data analysis was performed using tools implemented in the Galaxy web platform (Afgan et al., 2018) (server: usegalaxy.eu). Quality of the raw sequence data was assessed with the FastQC tool (version 0.71). After adapter clipping with the Clip adapter sequences tool (version 1.0.3), Illumina FASTQ files were mapped to the reference genome of *E. faecalis* OG1RF (GenBank: NC_017316.1) using Bowtie2 (version 2.3.4.2). Using htseq-count, the aligned reads overlapping with genomic features were counted. Differentially expressed genes between bacteria isolated from inflamed IL-10$^{-/-}$ versus healthy WT mice were determined using DEseq2 (version 2.11.40.2). KEGG gene set enrichment

analysis was executed using the Bioconductor clusterProfiler package (version 3.8.1) implemented in R (Yu et al., 2012).

3.15 Cytokine quantification

IFNγ, TNF, IL-12p40, IL-6 and IL-17A concentration in cell culture supernatant was quantified using commercially available ELISA kits (eBioscience). Serum amyloid A (SAA) concentration in murine plasma was determined using a commercially available ELISA kit from Immunology Consultants Laboratory (ICL).

3.16 Histological analysis

3.16.1 Tissue processing

The intestinal tract of gnotobiotic WT and IL-10$^{-/-}$ mice was removed immediately after killing and cleaned from stool. Cross-sections or "swiss-roles" (Moolenbeek and Ruitenberg, 1981) of parts of the intestinal tract were fixed in 10% phosphate buffered formaldehyde (VWR) or Carnoy's solution (60% dry Methanol, 30% Chloroform, 10% glacial acetic acid), dehydrated (Leica TP1020, Table 7) and embedded in paraffin (Paramat extra, VWR) by using a Leica EG1150 embedding station .

Table 7. Dehydration and paraffin embedding of fixed tissue sections

Step	Reagent	Time
1	70% EtOH	60 min
2	70% EtOH	60 min
3	80% EtOH	60 min
4	96% EtOH	60 min
5	96% EtOH	60 min
6	100% EtOH	60 min
7	100% EtOH	60 min
8	100% EtOH	60 min
9	Xylene	60 min
10	Xylene	60 min
11	Paraffin	60 min
12	Paraffin	60 min

3.16.2 H&E staining and histological analysis

For histological analysis, fixed paraffin embedded tissue samples were cut into 5 μm sections using a Leica rotary microtome RM2255, mounted on SuperFrost® microscope slides (VWR) and dried over night. The tissue sections were deparaffinized, rehydrated and stained with hematoxylin and eosin (MEDITE) in an automated manner using the multistainer station LeicaST5020 (Table 8). The slides were mounted with Roti®-Histokitt (Carl Roth) and covered with a glass slide (VWR). The histopathology was evaluated by an independent examiner in a blinded manner as described previously (Katakura et al., 2005), resulting in a score from 0 (not inflamed) to 12 (highly inflamed).

Table 8. Deparaffinization, rehydration and H&E staining of tissue sections (LeicaST5020)

Deparaffinization and Rehydration			H&E staining		
Step	**Reagent**	**Time**	**Step**	**Reagent**	**Time**
1	Xylene	3 min	**6**	dH$_2$O	1 min
2	Xylene	3 min	**7**	Hematoxylin	2 min
3	100% EtOH	2 min	**8**	dH$_2$O	2 min
4	96% EtOH	2 min	**9**	Eosin	2 min
5	70% EtOH	1 min	**10**	70% EtOH	1 min
			11	96% EtOH	1 min
			12	100% EtOH	1 min
			13	100% EtOH	1.5 min
			14	Xylene/EtOH	1.5 min
			15	Xylene	2 min
			16	Xylene	2 min

3.17 RNA isolation, reverse transcription and gene expression analysis (mouse)

3.17.1 RNA isolation

Tissue sections of distal colon were stored in RNAlater (Sigma Aldrich) at -80°C. Tissue samples were transferred into 500 μl RA1 buffer (Macherey Nagel) supplemented with 10 mM DTT (Sigma Aldrich) and the tissue was homogenized using a Miccra D-1 homogenizer. RNA was isolated using the NucleoSpin® RNA Kit (Macherey Nagel) according to the manufacturer's instructions. The quantity and purity of the isolated RNA was measured with a NanoDrop® ND-1000 spectrophotometer (Thermo Fisher Scientific).

3.17.2 Reverse transcription and gene expression analysis via qPCR

Reverse transcription and gene expression analysis was performed as described for bacterial RNA (chapter 3.12) with following exceptions. cDNA was synthesized from 1000 ng RNA. Relative gene expression values were normalized to GAPDH and HPRT expression. Primers (Sigma Aldrich) and corresponding probes (Roche) are listed in Table 9.

Table 9. Primers and corresponding UPL probes used for mouse gene expression analysis

Targeted gene	Gene ID (NCBI gene)	Oligonucleotide sequence (5'-3')	UPL probe
GAPDH	14433	L: GGGTTCCTATAAATACGGACTGC R: CCATTTTGTCTACGGGACGA	52
HPRT	110286595	L: TCCTCCTCAGACCGCTTTT R: CCTGGTTCATCATCGCTAATC	95
TNFα	21926	L: TGCCTATGTCTCAGCCTCTTC R: GAGGCCATTTGGGAACTTCT	49
IFNγ	15978	L: GGAGGAACTGGCAAAAGGAT R: TTCAAGACTTCAAAGAGTCTGAGG	21
IL-12p40	16160	L: ATCGTTTTGCTGGTGTCTCC R: GGAGTCCAGTCCACCTCTACA	78
IL-17A	16171	L: TGTGAAGGTCAACCTCAAAGTC R: AGGGATATCTATCAGGGTCTTCATT	50

3.18 Mesenteric lymph node cell cultures

Mesenteric lymph nodes (MLN) were aseptically harvested from gnotobiotic WT and IL-10$^{-/-}$ mice. The tissue was homogenized and filtrated through 70 μm cell strainers (VWR) resulting in unfractionated single cell suspensions. MLN cells (5×10^5 cells per well), isolated from individual mice (for IL-10$^{-/-}$ mice) or a pool of mice (for WT mice), were cultured in RPMI-1640 medium (Sigma Aldrich) containing 10% fetal calf serum (Biochrom) and 1% antibiotics/antimycotics (Sigma Aldrich). Cells were stimulated for 72 hours with corresponding bacterial lysates (15 μg/ml) from the strain/species that was used for colonization. The supernatants were collected for cytokine analysis, as indicated in 3.15.

3.19 SDS-PAGE and immunoblotting

3.19.1 Mouse serum IgG or IgA against bacterial lysates

Bacterial lysates were prepared as described in 3.7, mixed with TruPAGE 4x LDS buffer (Sigma Aldrich) and denatured for 10 min at 70°C. The lysates were subjected in a concentration of 3 µg/lane to discontinuous denaturing polyacrylamid gel electrophoresis (SDS-PAGE), transferred onto a polyvinylidene difluoride membrane (PVDF, GE Healthcare Amersham) and blocked at RT for 1 h in 5% skim milk-TBST (0.05% Tween in TBS). After over-night incubation with a 1:500 dilution of mouse serum (pool of serum from 6 WT or 10 IL-10^{-/-} mice) in 5% skim milk-TBST, the membrane was washed 3 times in TBST and incubated with either a 1:2500 dilution of goat anti mouse immunoglobulin G (IgG) alkaline phosphatase conjugate (Sigma Aldrich) or a 1:1000 dilution of goat anti mouse immunoglobulin A (IgA) FITC conjugate (Invitrogen) for 2 h. Subsequently, the membrane was washed 3 times with TBST and antibody binding was detected using nitro-blue tetrazolium (NBT) /5-bromo-4-chloro-3'-indolyphosphate (BCIP) tablets (Roche) for IgG or by using a Typhoon Trio+ imager (GE Healthcare Amersham) for IgA.

3.19.2 Specificity testing of *Enterococcus* antibody

The specificity of *Enterococcus* polyclonal antibody (Biotin coupled, Thermo Fisher Scientific) was confirmed via western blot analysis as described in 3.19.1 with following changes. After SDS-PAGE and transfer, the membranes were incubated with the polyclonal rabbit antibody raised against *Enterococcus* whole cells (*Enterococcus faecium*) in a dilution of 1:2000 in 5% skim milk-TBST ON at 4°C. After washing in TBST and incubation for 1 h at RT with a streptavidin-peroxidase polymer (Sigma Aldrich) diluted 1:2000 in 5% dry skim milk-TBST, the membrane was washed again 3 times with TBST, incubated with ECL-Prime (GE Healthcare Amersham) for 5 min and exposed to X-ray film (Bender).

3.20 Ethanolamine quantitation in colonic content by LC-MS/MS analysis

Quantitation of ethanolamine in colonic content from WT and IL10^{-/-} mice monoassociated with *E faecalis* OG1RF or Δeut VW was performed at the Bavarian Center for Biomolecular Mass Spectrometry (BayBioMS). Sample preparation and mass spectrometry quantitation was modified after Bertin et al (Bertin et al., 2011). Briefly, colonic content was diluted 1:20 with purified ddH$_2$O (Millipore) and debris was removed by two centrifugation steps at 4°C (2000 g for 20 min, 6000 g for 5 min).

1 ml of colonic content was spiked with 65 µL of a 1 mg/ml solution of ethanol-1,1,2,2-d$_4$-amine (Sigma Aldrich) as internal standard. For protein removal, 1 ml supernatant was incubated with 100

μl 40% sulfosalicylic acid (Sigma Aldrich) followed by centrifugation at 11000 g for 15 min. Precipitated proteins were removed and ethanolamine (EA) was derivatized with dansyl chloride (Sigma Aldrich) for mass spectrometry quantitation. For derivatization, supernatants were mixed with 300 μl of 0.5 M NaHCO$_3$ (Merck), 2 ml of 10 mg/ml dansyl chloride in acetone (Sigma Aldrich) and 200 μl of 1 M NaOH (Sigma Aldrich).

The samples were incubated for 20 min at RT in the dark and residual dansyl chloride was removed by addition of 200 μl 25% NH$_4$OH (Sigma Aldrich). Subsequently, the sample volume was adjusted to 5 ml with acetonitrile (Sigma Aldrich) and 10 μl of the solution was injected for LC-MS/MS analysis. The LC-MS/MS system consisted of a Shimadzu-Prominence LC system, including a LC-20AD pump, a DGU-20A3 degasser, a SIL-20A autosampler and a CTO-20A column oven, with a QTRAP® 4000 mass spectrometer equipped with an Turbo V ion source (Applied Biosystems).

Analyst® software (Applied Biosystems, version 1.6.2) was used for instrument control, data acquisition and data processing. Chromatographic separation was performed on a Kinetex 5u XB-C18 100 A column (100 x 2.1 mm, 5 μm, Phenomenex) using water/formic acid (100/0.1 *v/v*) as solvent A and acetonitrile/formic acid (100/0.1, *v/v*) as solvent B at a flow rate of 400 μl/min and a column temperature of 40°C. Starting with 5% solvent B, the amount of B in the mobile phase was increased to 100% in 3 min and hold for 2 min, followed by re-equilibration at starting conditions for 3 min. The mass spectrometer was operated at 450°C in the positive electrospray ionization mode with the ion spray voltage set at 5500 V. Dansyl-ethanolamine was detected with MRM mode using the following settings: *m/z* 295.1/157 (entrance potential (EP) 10, declustering potential (DP) 70, collision energy (CE) 37, cell exit potential (CXP) 7, quantifier), 295.1/170 (EP 10, DP 72, CE 31, CXP 8, qualifier) and dansylethanol-1,1,2,2-*d$_4$*-amine was used as internal standard:*m/z* 299.1/158 (EP10, DP 70, CE 37, CXP 7).

3.21 Statistical analysis

Statistical analyses were performed using Prism version 6.05 (GraphPad). Unless otherwise stated, data are presented as mean ± standard deviation. Statistical significant differences were determined using one- or two-way ANOVA followed by pair wise comparison testing (Tukey). Differences were considered significant for *$p<0.05$, **$p<0.01$, ***$p<0.001$, ****$p<0.0001$.

Analysis of RNAseq data was performed using Galaxy platform web platform (Afgan et al., 2018) or R as described in detail above.

4. RESULTS

4.1 Kinetic of *E. faecalis*-induced colitis in monoassociated IL-10^{-/-} mice

To analyse the kinetics of *E. faecalis*-driven inflammation, we monoassociated germ-free WT and IL-10^{-/-} mice at the age of 10 weeks with *E. faecalis* WT OG1RF for different periods of time. After 4, 8 and 12 weeks of colonization, IL-10^{-/-} mice showed mild signs of inflammation in the distal colon as indicated by the histological score. Between the 12th and the 20th week of colonization, IL-10^{-/-} mice started to develop severe distal colonic inflammation reaching a plateau after week 20 (Figure 4).

A similar disease pattern was also observed in mid colon with an overall lower level of inflammation (Figure 4B). In proximal colon, the inflammation persisted at a very low level throughout the analysed colonization periods (Figure 4C). All WT mice remained disease-free (Figure 4A-C). The colonization density as detected by countable colony forming units (CFU) in luminal colon contents was not affected by the level of inflammation (Figure 4D).
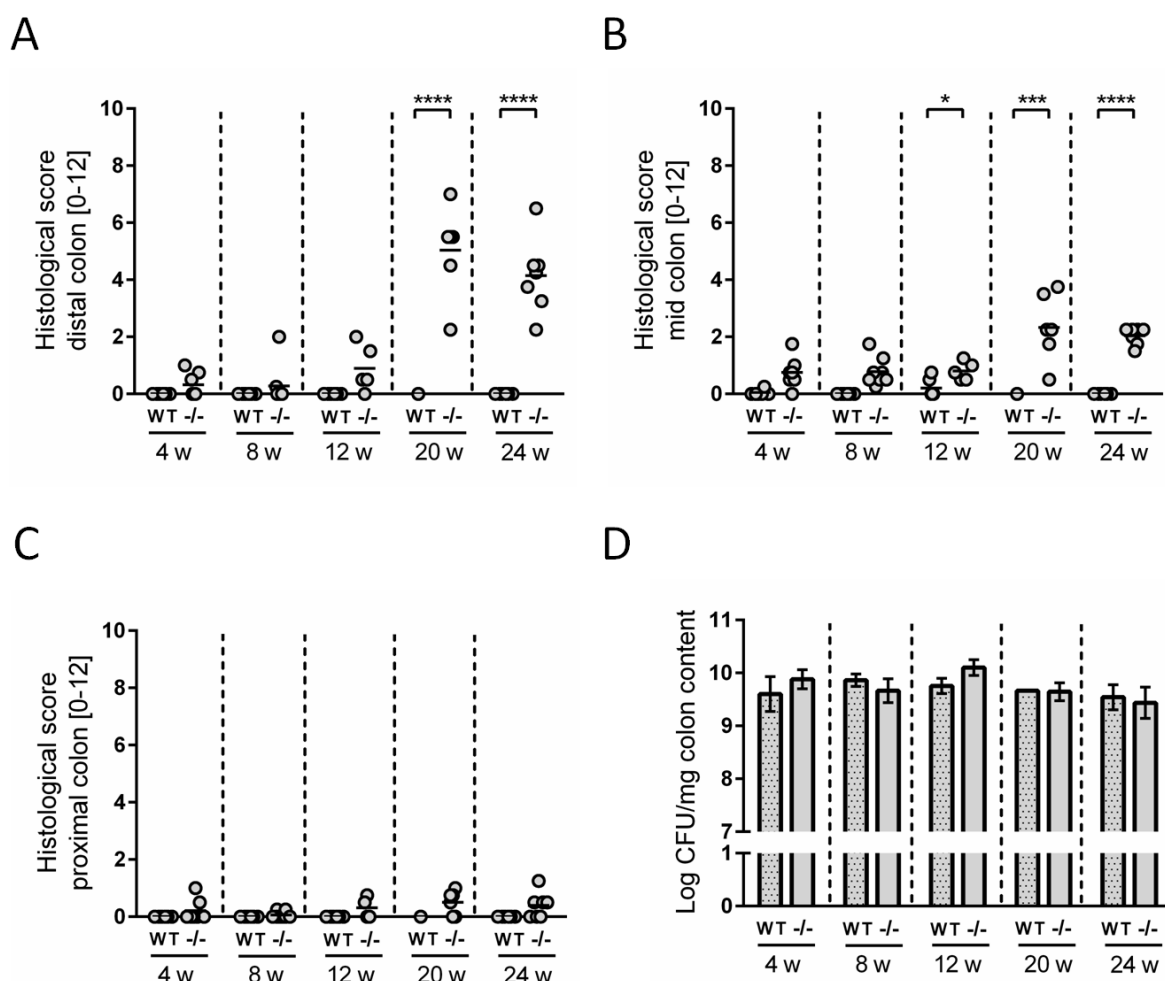
Figure 4: *E. faecalis* induces colitis in IL-10^{-/-} mice between 12 and 20 weeks of colonization.

WT and IL-10$^{-/-}$ mice were monoassociated with *E. faecalis* for 4, 8, 12 and 24 weeks (w). (**A**) Histological inflammation score in the distal, (**B**) mid and (**C**) proximal colon. (**D**) *E. faecalis* counts/mg in luminal contents from colon.

The body weight increased with the age of the mice, but was not influenced by the degree of colonic inflammation (Figure 5). Cecum weight was generally slightly reduced in IL-10$^{-/-}$ compared to WT mice, but significance was only reached at a colonization time of 8 weeks (Figure 5B). Compared to WT mice, the weights of spleen and mesenteric lymph nodes (MLN) of IL-10$^{-/-}$ mice were significantly increased after a colonization period of 20 weeks and 8 weeks, respectively (Figure 5C and D).

Based on the kinetic of distal colonic inflammation and previous publications, 16 weeks of colonization were used in subsequent experiments. At this time, inflammation was still in the ascending phase and is therefore advantageous for the analysis of factors modulating disease severity.
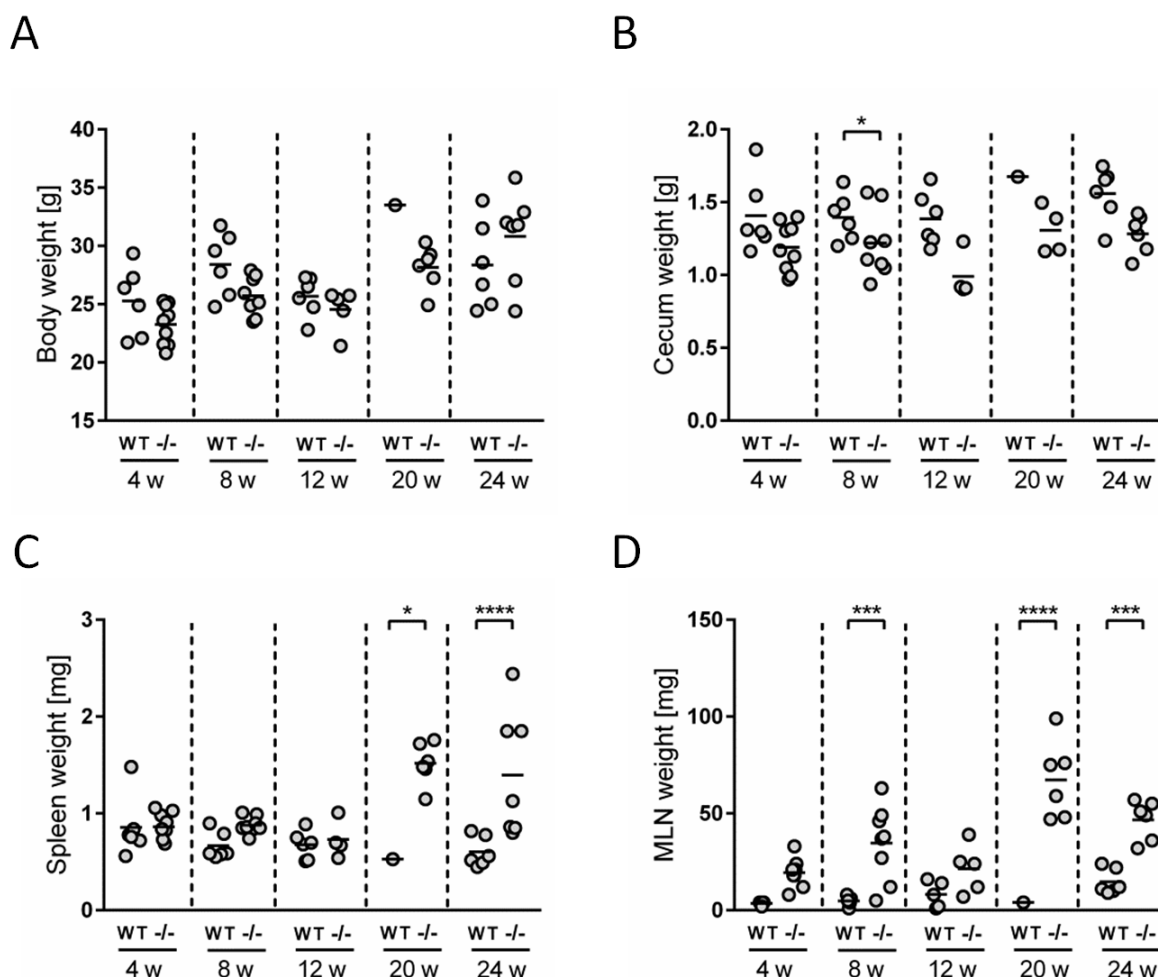
Figure 5: Spleen and MLN weights increase with the degree of intestinal inflammation.
WT and IL-10$^{-/-}$ mice were monoassociated with *E. faecalis* for 4, 8, 12 and 24 weeks (w). (**A**) Body weight, (**B**) Cecum weight, (**C**) Spleen weight and (**D**) MLN weight.

4.2 *E. faecalis* adapts transcriptionally to a chronic inflammatory environment

We hypothesized that *E. faecalis* quickly adapts to a chronic inflammatory environment by altering its gene expression profile. These adaptation mechanisms are likely to be responsible for the persistence and virulence of these bacteria in a susceptible host. To assess *E. faecalis* disease-associated transcriptome, we monoassociated mice with *E. faecalis* OG1RF for 16 weeks and performed RNA sequencing of bacteria isolated from luminal colon content of healthy WT and inflamed IL-10$^{-/-}$ mice.

Transcriptional profiling identified 408 significantly up-regulated and 486 significantly down-regulated genes under conditions of chronic inflammation (Figure 6A and Figure S1A, Table S1). The samples clearly clustered according to mouse genotype as detected by principal component analysis (PCA), indicating that inflammation modulates *E. faecalis* gene expression (Figure S1B).

E. faecalis response to inflammation was characterized by an up-regulation of genes associated with bacterial stress response to unfavourable growth conditions. KEGG pathway enrichment analysis showed an enrichment of the biosynthesis of amino acids, quorum sensing, mismatch repair and oxidative phosphorylation among up-regulated genes (Figure 6B). Induction of these processes has also been observed in previous studies analyzing *E. faecalis* and *E. coli* adaptation during periods of stress (van de Guchte et al., 2002; Durfee et al., 2008; Ran et al., 2015).

Nucleotide synthesis genes in general down regulated, as indicated by an enrichment of purine and pyrimidine metabolism transcripts in wild type mice. Furthermore, a large number of genes involved in metabolism and nutrient acquisition were differentially expressed. Sugar metabolism and transport were repressed with an enrichment of starch and sucrose metabolism, ABC transport, PTS transport and glycolysis among down-regulated genes. On the other hand, genes necessary for the utilization of alternative carbon sources were up regulated with an enrichment of inositol phosphate metabolism, glycerolipid metabolism and ethanolamine utilization genes (Figure 6B and C).
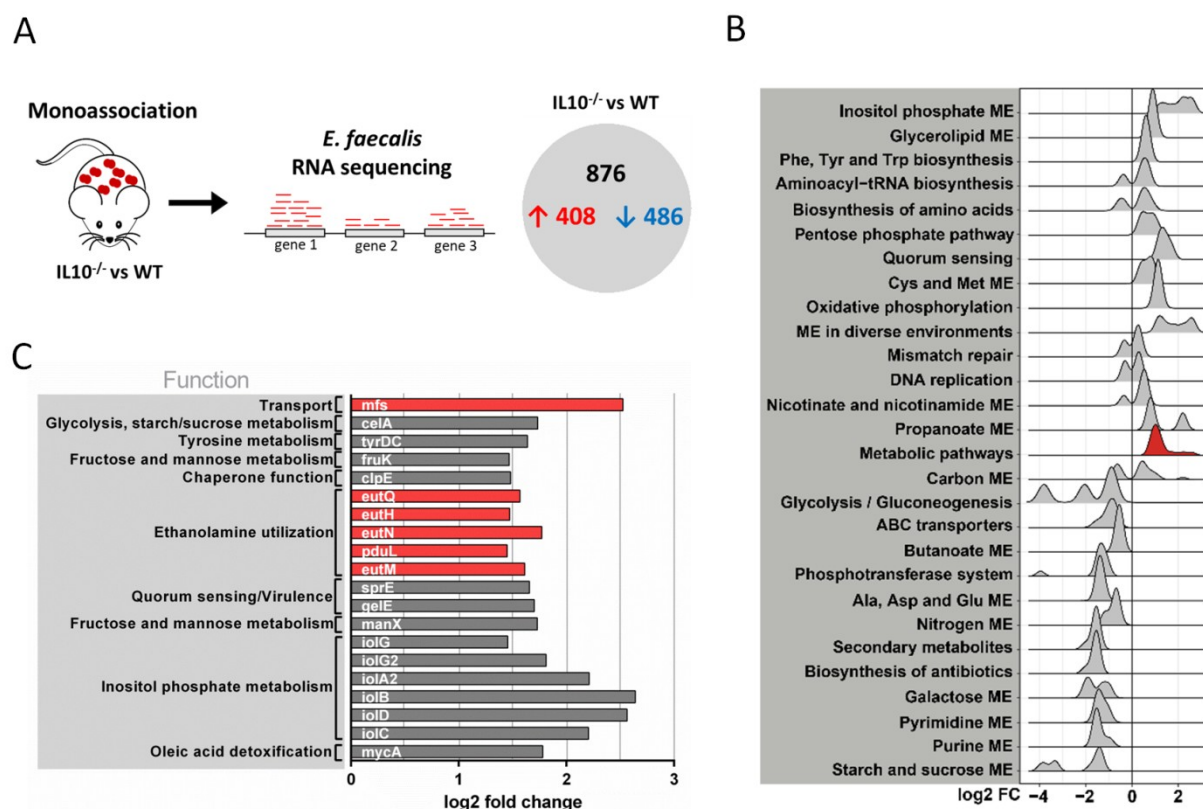
Figure 6: *E. faecalis* adapts transcriptionally to chronic colitis in monoassociated IL-10^{-/-} mice.

(A) Experimental setup: Transcriptional profiling of luminal bacteria isolated from the colon of monoassociated IL-10$^{-/-}$ (inflamed) and healthy WT mice (n=8/group) revealed 408 significantly up-regulated genes and 486 down-regulated genes in *E. faecalis* under inflammatory conditions. **(B+C)** Expression profiles of *E. faecalis* in an inflamed (IL-10-/-) vs. a non-inflamed (WT) environment in monoassociated mice **(B)** Expression distribution (log2 lower or higher) of genes for GSEA enriched categories (KEGG). The gene group containing *eut*-genes is highlighted red **(C)** Top 20 up-regulated genes. Only annotated genes with known function are shown. Genes of the *eut* locus and major facilitator transporter (OG1RF_10079) are highlighted red. Gene functions were assigned according to KEGG database.

4.3 Bacterial genes highly up-regulated in inflamed mice do not affect the colonization and colitogenic activity of *E. faecalis* in a monoassociated system

Among the top up-regulated genes in inflamed IL-10$^{-/-}$ mice, 14 genes of the ethanolamine utilization (*eut*) locus and a major facilitator superfamily transporter (*mfs*) were identified (Figure 6C and Figure 7A). Up regulation in response to inflammation suggests important functions of these genes in the inflamed intestine. We hypothesized that the deletion of *eut* genes or *mfs* gene from *E. faecalis* may reduce bacterial survival and virulence under inflammatory conditions, leading to attenuated intestinal inflammation in monoassociated IL-10$^{-/-}$ mice (Figure 7B and C).
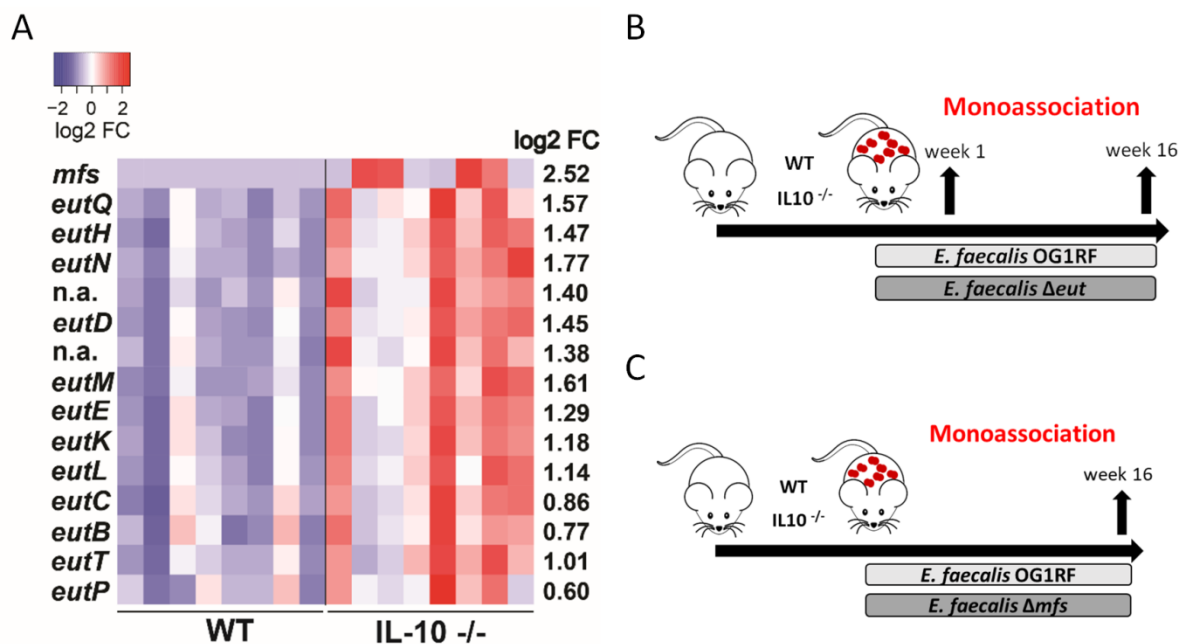
Figure 7: *E. faecalis eut* operon and *mfs* gene are highly up-regulated in inflamed IL-10$^{-/-}$ mice.
(A) Differential expression of genes in relation to a chronically inflamed environment is shown for significantly regulated *eut* genes and *mfs* gene. The log2 ratio of mean abundance (IL-10$^{-/-}$ vs. WT) of normalized expression levels is shown (up regulation is indicated red, down regulation is indicated blue). **(B)** Experimental setup. Germfree WT and IL-10$^{-/-}$ mice were monoassociated with *E. faecalis* WT or Δ*eut* mutant strain for 1 and 16 weeks. **(C)** Experimental setup. Germfree WT and IL-10$^{-/-}$ mice were monoassociated with *E. faecalis* WT or Δ*mfs* mutant strain for 16 weeks

4.3.1 Ethanolamine utilization

To determine whether the utilization of ethanolamine (EA) is relevant for *E. faecalis* colonization and colitogenic activity, we monoassociated germ-free WT and IL-10$^{-/-}$ mice with *E. faecalis* WT OG1RF or an Δ*eutVW* mutant strain (Δ*eut*) for 1 week to analyze early colonization effects or 16 weeks to analyze disease progression (Figure 7B). The Δ*eut* strain does not express the *eut* genes and is not able to utilize EA (Fox et al., 2009; Debroy et al., 2012; Ramesh et al., 2012). *E. faecalis* OG1RF can utilize EA as sole carbon source under anaerobic growth conditions, while Δ*eut* mutant strain is not able to grow on minimal medium supplemented with EA (Figure 8) (Del Papa and Perego, 2008).
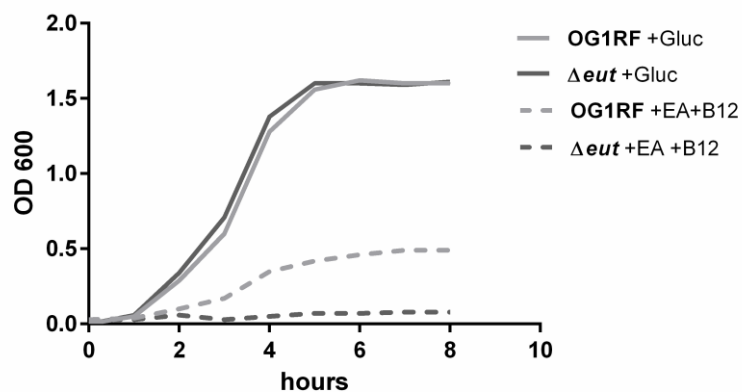
Figure 8: *E. faecalis* Δ*eut* mutant is not able to utilize EA as carbon source.

E. faecalis OG1RF and Δ*eut* mutant were grown in M9HY minimal medium supplemented with glucose (+Gluc) or EA and vitamin B12 (+EA +B12) under anaerobic conditions and bacterial density was measured using OD_{600}.

After 1 week of colonization, WT and IL-10$^{-/-}$ mice showed no signs of inflammation. After 16 weeks of colonization, IL-10$^{-/-}$ mice developed severe inflammation in the distal colon, independent of the *E. faecalis* strain used for monoassociation (OG1RF histopathological score: 5.0 ± 0.9, Δ*eut* histopathological score: 4.6 ± 0.5). All WT mice remained disease-free (Figure 9A and B).

E. faecalis OG1RF and Δ*eut* mutant strains showed a similar colonization density as detected by CFU in luminal contents from colon (Figure 9C). The colon inflammation in IL-10$^{-/-}$ mice was accompanied by elevated spleen weights (Figure 9D) and increased expression of pro-inflammatory markers in the distal colon tissue. The expression levels of TNFα, IL-12p40 and IL-17 were similar for both colonization groups, only IFNγ expression levels were increased in *E. faecalis* WT OG1RF compared to Δ*eut* mutant monoassociated IL-10$^{-/-}$ mice (Figure 9E).
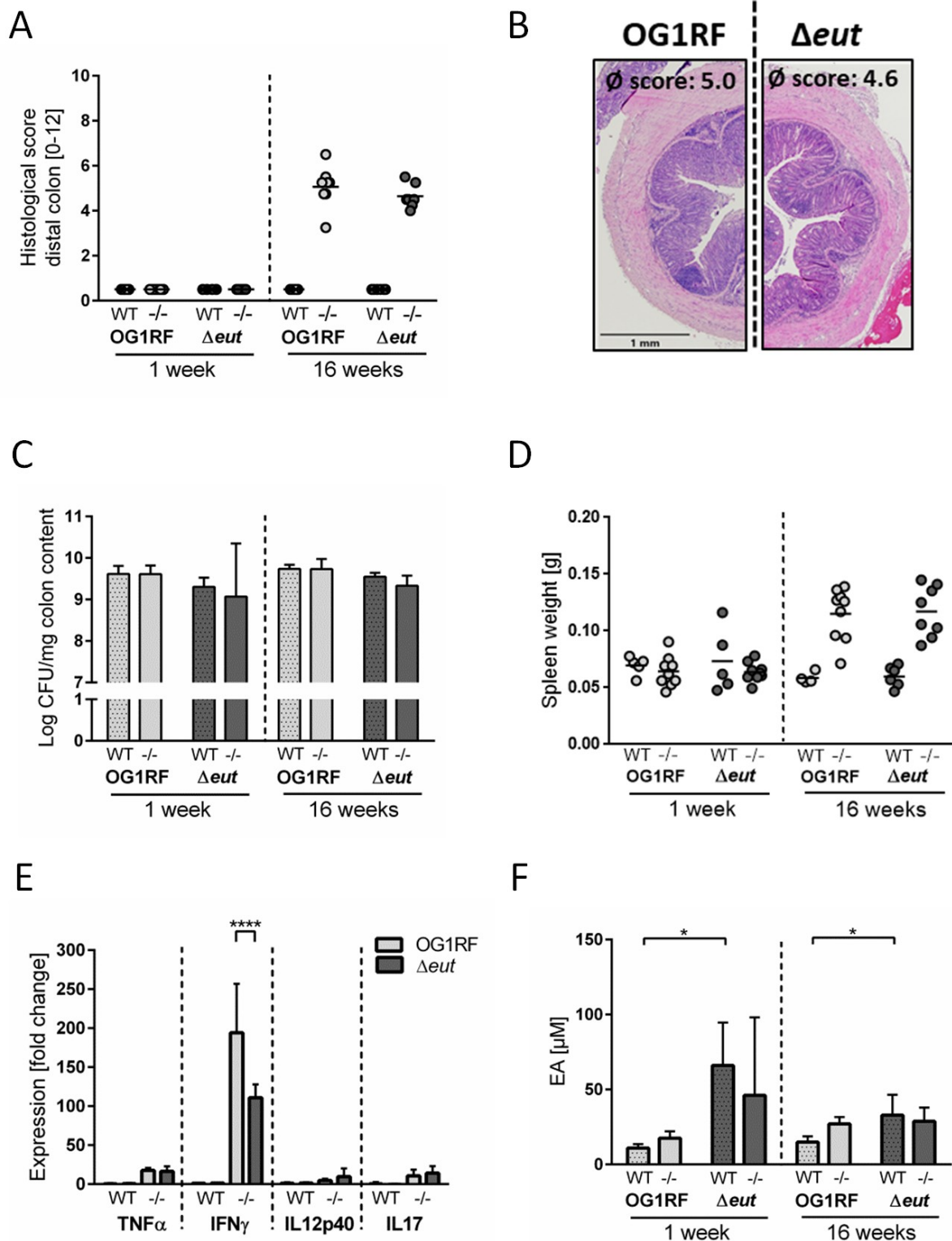
Figure 9: Ethanolamine utilization has no influence on the colitogenic activity and colonization density of *E. faecalis* in monoassociated IL-10$^{-/-}$ mice.

Germ-free WT and IL-10$^{-/-}$ mice were monoassociated with *E. faecalis* WT or Δ*eut* mutant strain for 1 and 16 weeks, respectively. **(A)** Histological inflammation in the distal colon. **(B)** Representative hematoxylin/eosin-stained sections of distal colon after 16 weeks of colonization. **(C)** *E. faecalis* presence in luminal contents from colon as log CFU counts/mg. **(D)** Spleen weights. **(E)** Cytokine expression in colon tissue sections. Values are shown as fold-change normalized to cytokine

expression levels in WT mice colonized with *E. faecalis* WT strain. **(F)** Quantitation of ethanolamine in luminal contents from colon.

To determine whether *E. faecalis* catabolizes EA *in vivo*, we measured EA concentrations in the intestinal fluid. Luminal EA concentrations were significantly higher in WT mice monoassociated with Δ*eut* mutant, indicating catabolism of EA by *E. faecalis* OG1RF. This trend was also observed in IL-10$^{-/-}$ mice after 4 weeks of colonization, but after 16 weeks of colonization intestinal EA concentrations were similar in both *E. faecalis* OG1RF and Δ*eut*-mutant monoassociated mice (Figure 9F).

Antigen-specific T cell responses were addressed *ex vivo*. MLN cells were isolated from IL-10$^{-/-}$ and WT mice monoassociated with *E. faecalis* OG1RF or Δ*eut* mutant strain and re-activated with lysates of the corresponding *E. faecalis* strain. Already after 1 week of colonization, re-activated MLN cells from IL-10$^{-/-}$ mice secreted high amounts of IL-12p40 in response to *E. faecalis* lysate stimulation (Figure 10A). MLN cells isolated from WT mice also responded to stimulation with *E. faecalis* lysate by secretion of IL-12p40, but to a lesser extent than MLN cells from IL-10$^{-/-}$ mice (Figure 10A and B). Interestingly, IL-12p40 secretion from re-activated MLN cells was decreased in IL-10$^{-/-}$ mice colonized with Δ*eut* mutant strain, suggesting an attenuated MLN immune response to Δ*eut* mutant strain (Figure 10B). However, this difference in immune activation was independent of colonic pathology (Figure 9A).

Taken together, deletion of ethanolamine utilization revealed no impact on *E. faecalis* colitogenic activity and survival in monoassociated mice.
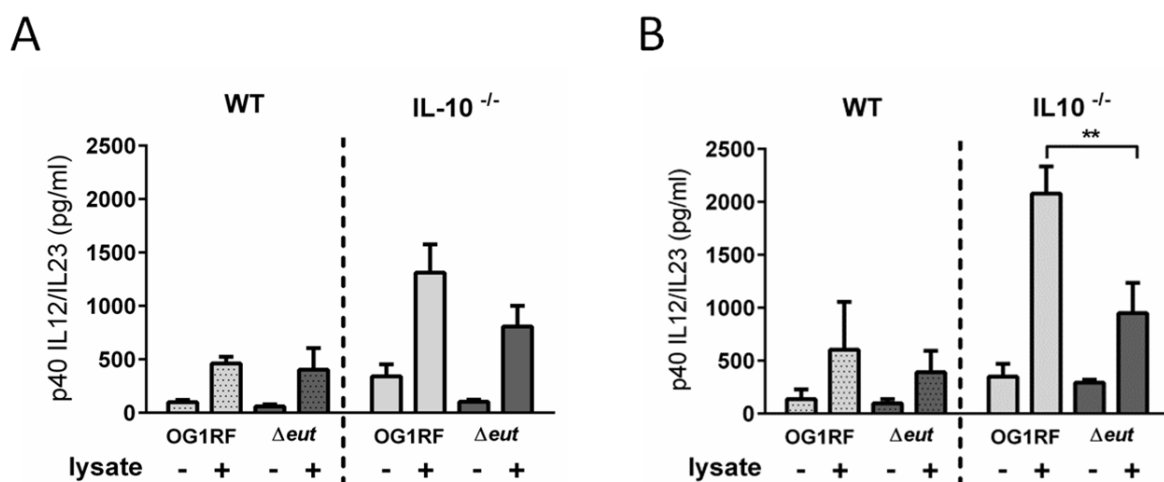
Figure 10: IL-12p40 secretion of re-activated MLN cells is decreased for *E. faecalis* Δ*eut* mutant.

(A) IL-12p40 secretion of MLN cells isolated from *E. faecalis* OG1RF or Δ*eut* mutant colonized IL10$^{-/-}$ and WT mice after 1 week and **(B)** 16 weeks of colonization that were re-activated with the corresponding bacterial lysate for 72 hours.

4.3.2 Major facilitator superfamily transporter

In order to test the hypothesis that the MFS transporter is important for the colonization and colitogenic activity of *E. faecalis* under inflammatory conditions, we constructed a mutant strain of *E. faecalis* OG1RF lacking *mfs* (Δ*mfs*) and confirmed the absence of *mfs* expression in *E. faecalis* Δ*mfs* using real-time PCR (Figure 11A).

To ensure that the absence of *mfs* causes no alterations in the expression of adjacent genes, mRNA levels of genes adjacent to *mfs* (OG1RF_10079) in *E. faecalis* Δ*mfs compared to E. faecalis* WT OG1RF were measured. The expression of OG1RF_10076, OG1RF_10077 and OG1RF_10082 was not influenced by the deletion of *mfs* (data not shown). The *in vitro* growth of *E. faecalis* OG1RF and Δ*mfs* mutant was similar as measured by OD$_{600}$ and CFU counts/ml culture (Figure 11B).
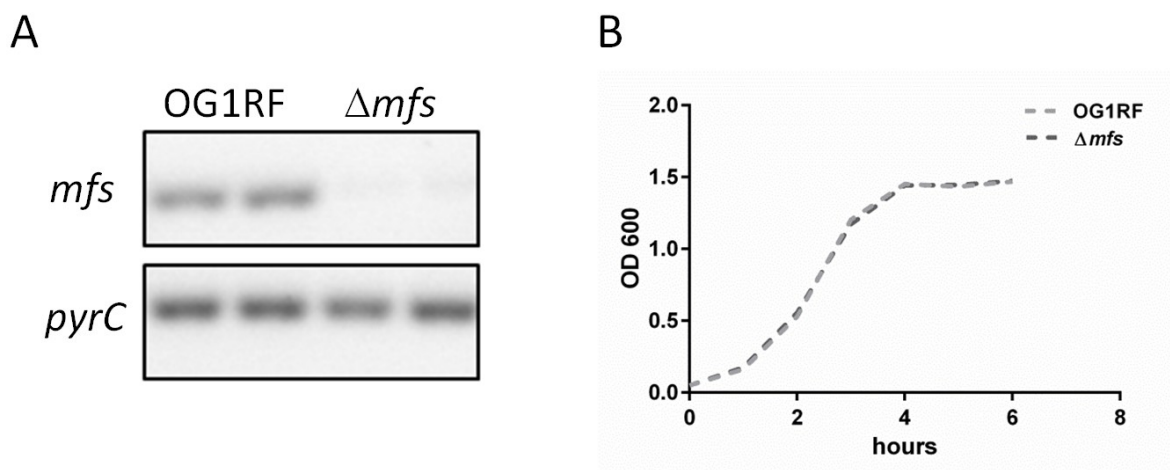
Figure 11: Characterization of Δ*mfs* deletion mutant from *E. faecalis* OG1RF.
(A) Expression of *mfs* (OG1RF_10079) and pyrC (housekeeping gene) in *E. faecalis* WT OG1RF and Δ*mfs* mutant. Quantitative real-time PCR product was applied to an agarose gel. **(B)** *E. faecalis* OG1RF and Δ*mfs* mutant were grown in BHI under anaerobic conditions and bacterial density was measured using OD$_{600}$ and CFU counts/ml culture.

Since the function of *E. faecalis* MFS efflux pump is not known, we measured the resistance of the Δ*mfs* mutant towards different antibiotics, but the deletion did not influence the minimal inhibitory concentration of ampicillin, quinolones (norfloxacin and naldixic acid), kanamycin, erythromycin, tetracycline, chloramphenicol, nisin, polymyxin B, vancomycin, puromycin and streptomycin (data not shown).

Furthermore, we could not detect any involvement of this transporter in the resistance to bile, antimicrobial peptides (cryptidin-4 and lysozyme) and alkaline or acidic conditions (data not shown). Riboulet-Bisson and colleagues suggested glycerol transport as function of *E. faecalis* MFS transporter, but we could not confirm that the growth of *E. faecalis* Δ*mfs* mutant on glycerol is impaired (data not shown) (Riboulet-Bisson et al., 2009).

Germfree WT and IL-10$^{-/-}$ mice were monoassociated with *E. faecalis* WT OG1RF or Δ*mfs* and bacterial colonization density and indicators of chronic, immune-mediated colitis were measured (Figure 7C). After 16 weeks of colonization, IL-10$^{-/-}$ mice developed severe inflammation in the distal colon, independent of the *E. faecalis* strain used for monoassociation (OG1RF histopathological score: 9.6 ± 1.8, Δ*mfs* histopathological score: 9.4 ± 2.0). All WT mice remained disease-free (Figure 12A). It was noticeable that the inflammation in the colon of IL-10$^{-/-}$ mice after 16 weeks of colonization was much more pronounced than in the previous monoassociation experiments with *E. faecalis* (chapter 4.1 and 4.3.1). A later colonization time (at the age of 12 weeks compared to the age of 10 weeks) may explain this phenotype.

The colonization density of *E. faecalis* OG1RF and Δ*mfs* mutant was similar as detected by CFU counts in luminal contents from colon (Figure 12C). Histological inflammation in IL-10$^{-/-}$ mice was accompanied by elevated spleen weights (Figure 12B) and increased expression of pro-inflammatory cytokines in distal colon tissue (Figure 12D). The expression levels of IFNγ, IL-12p40 and IL-17 were similar in both colonization groups, only the expression level of TNFα was increased in *E. faecalis* Δ*mfs* compared to OG1RF monoassociated IL-10$^{-/-}$ mice (Figure 12D).
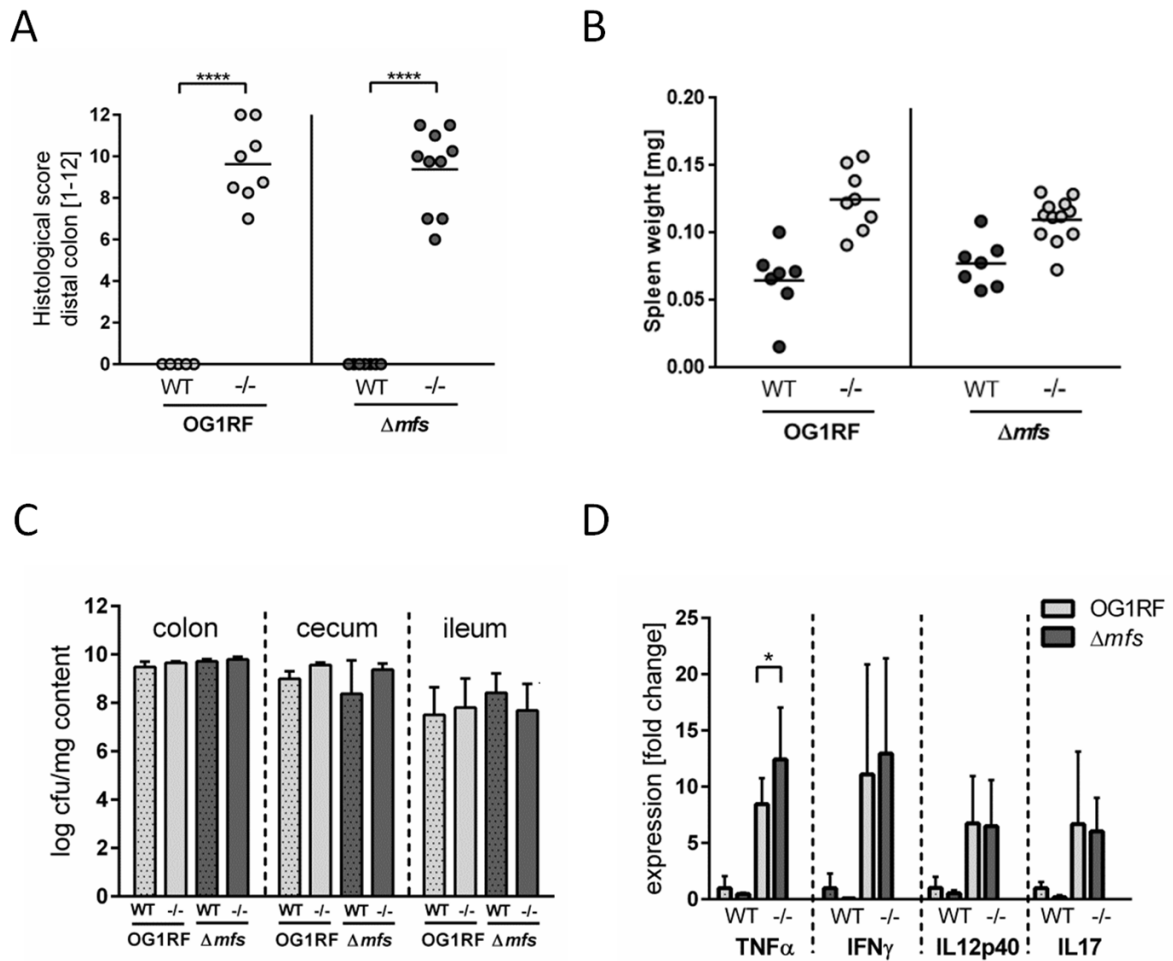
Figure 12: *E. faecalis* **MFS transporter has no impact on the colitogenic activity and colonization density in monoassociated IL-10$^{-/-}$ mice.**

Germfree WT and IL-10$^{-/-}$ mice were monoassociated with *E. faecalis* WT or Δ*mfs* mutant strain for 16 weeks. **(A)** Histological inflammation in the distal colon. **(B)** Spleen weights. **(C)** *E. faecalis* presence in luminal contents from colon, cecum and ileum according to the CFU counts/ml. **(D)** Cytokine expression in colon tissue sections shown as fold change normalized to cytokine expression levels in WT mice colonized with *E. faecalis* WT.

IFNγ and IL-12p40-secretion of re-activated MLN cells was similar for all IL-10$^{-/-}$ mice suggesting that MLN cells are fully capable of responding to bacterial antigens independently of the monoassociated *E. faecalis* strain (Figure 13A and B).

A

B
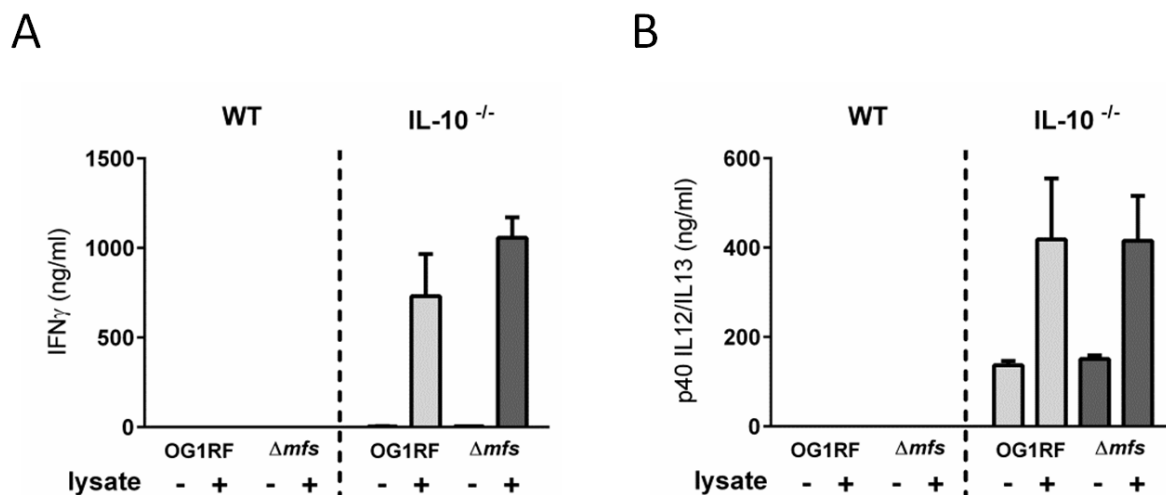
Figure 13: The antigen-specific immune response of re-activated MLN cells was not influenced by the deletion of *mfs*.

(A) IFNγ and **(B)** IL-12p40 secretion of MLN cells isolated from *E. faecalis* OG1RF or Δ*mfs* mutant monoassociated IL-10^{-/-} and WT mice that were re-activated with the corresponding bacterial lysate for 72 hours.

In summary, we tested the functional relevance of *E. faecalis* genes that were up-regulated in response to inflammation, namely genes of the *eut* operon and *mfs* transporter. Despite their massive up-regulation in inflamed monoassociated IL-10^{-/-} mice, their deletion had no impact on the colitogenic activity and survival of *E. faecalis* in monoassociated WT and IL-10^{-/-} mice. Since the function of *E. faecalis* MFS transporter is not known, we decided to further characterize only *E. faecalis* ethanolamine utilization.

4.4 *E. faecalis* EA utilization has protective functions in a microbial consortium

Despite considerable up-regulation of *eut* genes, the deletion of ethanolamine utilization had no impact on the colitogenic activity of *E. faecalis* in monoassociated mice. To test the hypothesis that *E. faecalis* EA utilization is only important for bacterial fitness in competition with other microbes, we characterized the colitogenic activity of *E. faecalis* Δ*eut* mutant strain in the context of a simplified microbial consortium based on seven enteric bacterial strains (SIHUMI).

We colonized germ-free WT and IL-10^{-/-} mice with SIHUMI consortium either containing *E. faecalis* WT OG1RF (SIHUMI) or *E. faecalis* Δ*eut* (SIHUMI Δ*eut*) mutant strain for a period of 16 weeks (Figure 14A). When we introduced the bacterial consortium to germ-free mice, 6 out of 7 species successfully colonized the mouse intestine, as determined by 16S rRNA gene-based quantitative qPCR (Fig. 14B).

Faecalibacterium prausnitzii could not be detected by qPCR and droplet digital PCR at any time (Figure 14B, Figure S2A and B) in intestinal content (taken at week 4 and 16 of colonization) and feces (taken at week 2, 4, 8 and 16 of colonization). *Bacteroides (B.) vulgatus* and *Ruminococcus (R.) gnavus* were the most predominant species in the consortium, while the proportion of *E. faecalis* was relatively low (Figure 14B). However, the total bacterial numbers determined by plating on selective agar are comparable to those found for monoassociated *E. faecalis* (Figure 16A). The replacement of *E. faecalis* WT OG1RF strain by the Δ*eut* mutant strain resulted in a shift in the bacterial community with a significant increase of *B. vulgatus* relative abundance accompanied by a decrease in *R. gnavus* abundance (Figure 14B).
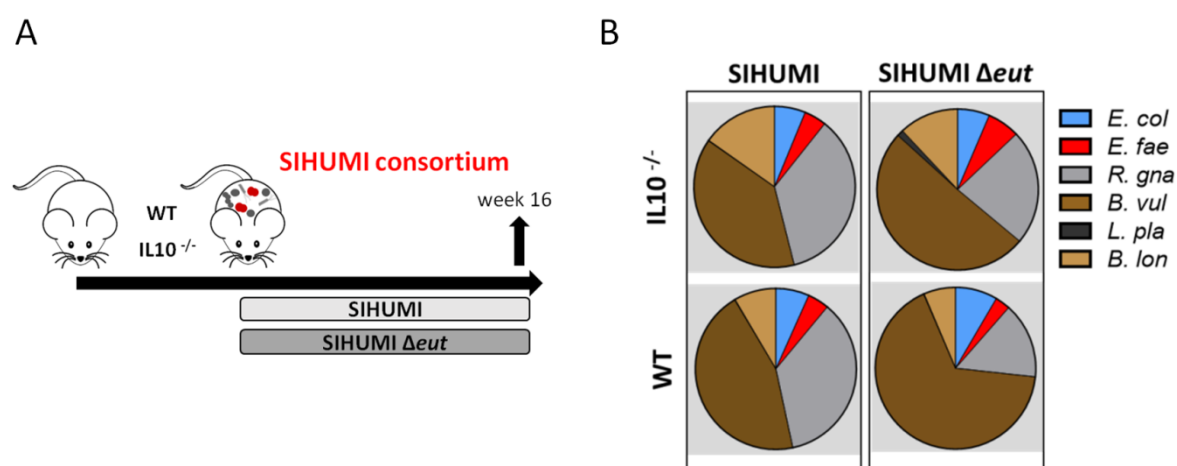
Figure 14: Replacement of *E. faecalis* WT OG1RF strain by Δ*eut* mutant strain results in a shift in the community of a complex bacterial consortium.
Germfree WT and IL-10$^{-/-}$ mice were colonized with SIHUMI consortium including *E. faecalis* WT (SIHUMI) or Δ*eut* strain (SIHUMI Δ*eut*) for 16 weeks. **(A)** Experimental setup. **(B)** Relative abundances of SIHUMI bacterial species in luminal colon content by 16S targeted qPCR. *E. col*, *Escherichia coli*; *E. fae*, *Enterococcus faecalis*; *R. gna*, *Ruminococcus gnavus*; *B. vul*, *Bacteroides vulgatus*; *L. pla*, *Lactobacillus plantarum*; *B. lon*, *Bifidobacterium longum*

While IL-10$^{-/-}$ mice colonized with the SIHUMI consortium gradually developed inflammation in the distal colon (SIHUMI histopathological score: 3.1 ± 2.3), colitis severity was significantly increased when *E. faecalis* OG1RF was replaced by Δ*eut* mutant strain (SIHUMI Δ*eut* histopathological score: 6.1 ± 1.8) (Figure 15A and B). These results surprisingly suggest protective functions of *E. faecalis* EA utilization in the context of chronic intestinal inflammation. Tissue pathology was accompanied by increased spleen weights in IL-10$^{-/-}$ mice colonized with the SIHUMI Δ*eut* consortium (Figure 15C). It is noteworthy that the severity of inflammation appeared to be affected by sex, with higher inflammatory scores and spleen weights in female animals (Figure 15A and C). As expected, all colonized WT remained disease-free.

Tissue sections from the distal colon of IL-10$^{-/-}$ mice showed high expression of pro-inflammatory cytokines in comparison to WT mice. Tissue expression of TNF and IL-12p40 reflected the degree of histopathology with higher expression levels in SIHUMI Δ*eut* colonized compared to SIHUMI colonized IL-10$^{-/-}$ mice. Expression levels of IFNγ were similar between SIHUMI and SIHUMI Δ*eut* colonized IL-10$^{-/-}$ mice, while IL-17 expression was decreased in SIHUMI Δ*eut* colonized IL-10$^{-/-}$ mice (Figure 15D).
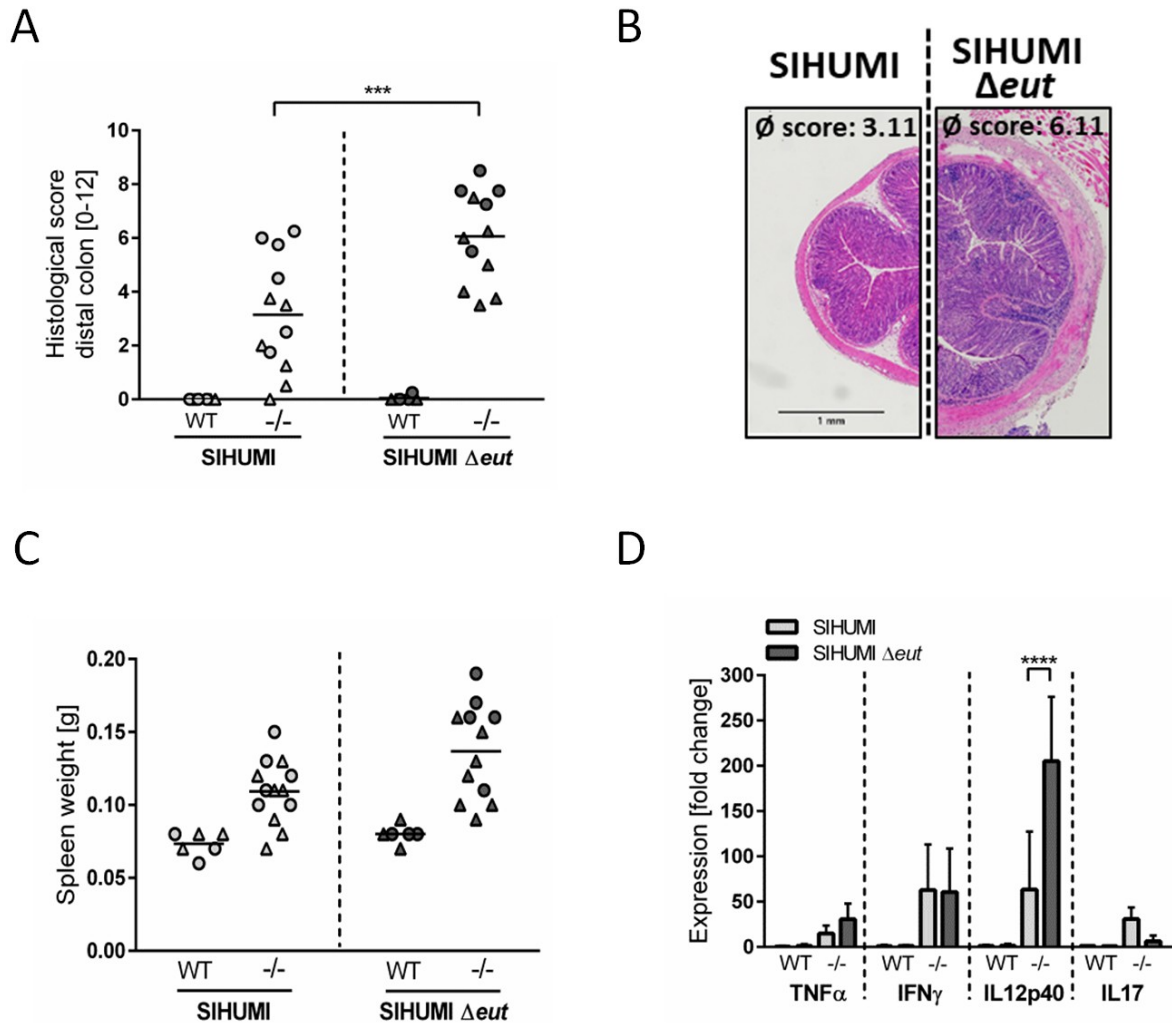
Figure 15: *E. faecalis* **ethanolamine utilization has protective functions in IL-10**$^{-/-}$ **mice colonized by a complex bacterial consortium.**

Germfree WT and IL-10$^{-/-}$ mice were colonized with SIHUMI consortium including *E. faecalis* WT (SIHUMI) or Δ*eut* strain (SIHUMI Δ*eut*) for 16 weeks. **(A)** Histological inflammation in the distal colon. Male mice are displayed as triangle, female mice as circles. **(B)** Representative hematoxylin/eosin-stained sections of distal colon after 16 weeks of colonization. **(C)** Spleen weight. Male mice are displayed as triangle, female mice as circles. **(D)** Cytokine expression in colon tissue sections shown as fold-change normalized to cytokine expression levels in WT mice colonized with the SIHUMI consortium.

Interestingly, the *E. faecalis* Δ*eut* mutant strain showed an increased colonization density compared to the WT OG1RF strain, as detected by CFU in luminal contents from colon (Figure 16A). However, *E. faecalis* abundance did not correlate with the histopathology score of the distal colon (Figure 16B). The only significant correlation between bacterial abundance and the level of colonic inflammation was detected for *R. gnavus* with a decreased abundance being associated with higher inflammatory scores (Figure 16C).

To address the bacterial antigen-specific immune responses in colonized mice, we isolated MLN cells from IL-10^{-/-} mice colonized with SIHUMI or SIHUMI Δ*eut* consortium and re-stimulated them with respective lysates of each of the colonizing species. Unfractionated MLN cells produced high levels of IL-12p40 when stimulated with *E. coli* lysate, while IL-12p40 secretion in response to all other lysates was similar to the negative control. The level of MLN activation was similar for all *E. faecalis* strains (Figure 16D).
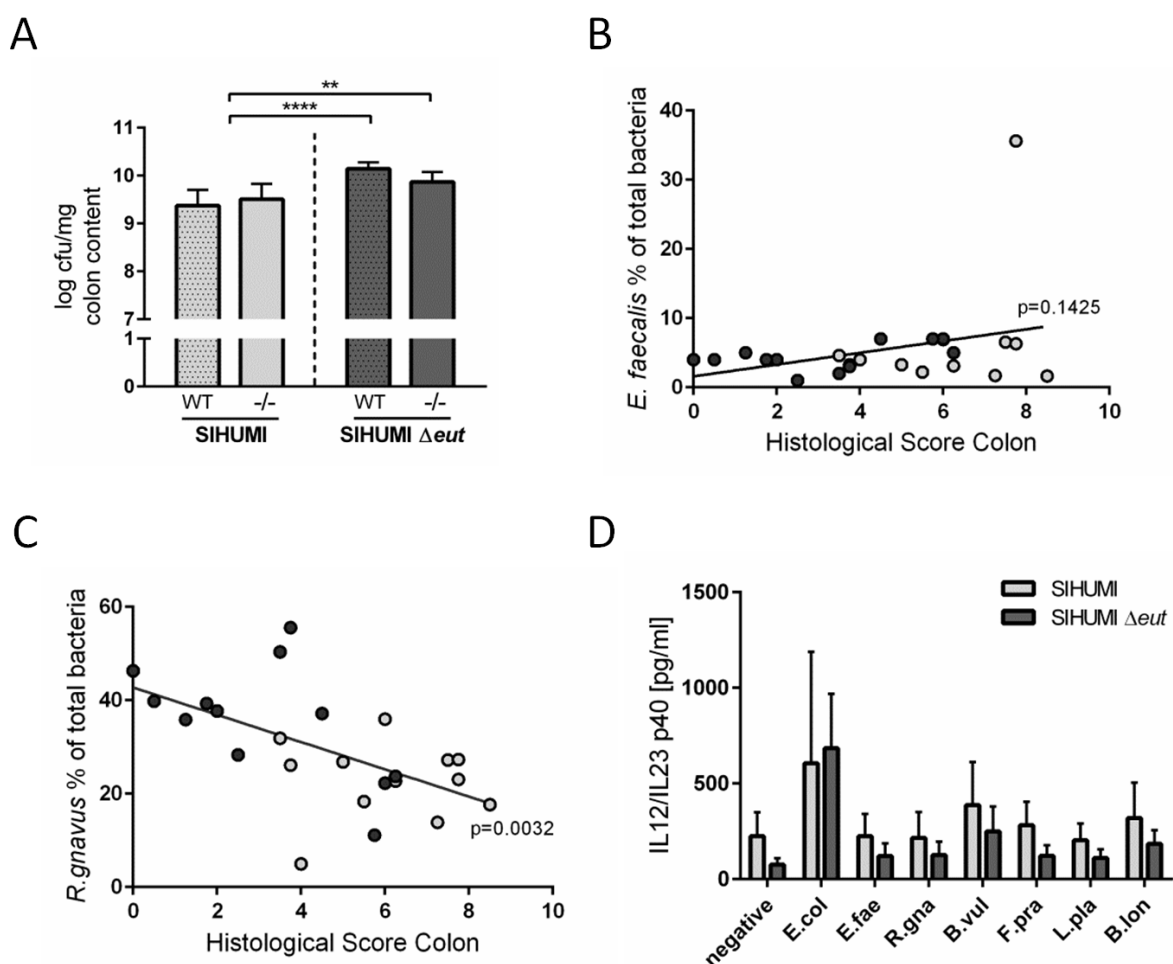
Figure 16: The deletion of ethanolamine utilization increases the colonization rate of *E. faecalis*, but an increased number of *E. faecalis* does not explain the aggravated inflammatory phenotype.

Germfree WT and IL-10$^{-/-}$ mice were colonized with SIHUMI consortium including *E. faecalis* Wt (SIHUMI) or Δ*eut* strain (SIHUMI Δ*eut*) for 16 weeks. **(A)** *E. faecalis* presence in luminal contents from colon as log CFU counts/ml. **(B)** Correlation between *E. faecalis* and **(C)** *R. gnavus* abundance (luminal colon content) and histological scores of distal colon. Light grey indicates SIHUMI experimental group, dark grey indicates SIHUMI Δ*eut* experimental group. **(D)** IL-12p40 secretion of MLN cells isolated from SIHUMI or SIHUMI Δ*eut* colonized mice that were re-activated with the respective bacterial lysate for 72 hours. *E. col*, *Escherichia coli*; *E. fae*, *Enterococcus faecalis*; *R. gna*, *Ruminococcus gnavus*; *B. vul*, *Bacteroides vulgatus*; *L. pla*, *Lactobacillus plantarum*; *B. lon*, *Bifidobacterium longum*

Since replacement of the WT *E. faecalis* by the mutant Δ*eut* resulted in a more severe inflammatory phenotype, we investigated whether increased inflammation was associated with an enhanced humoral immune response against specific SIHUMI species. It has been demonstrated by others that certain commensal bacteria induce serum IgA responses that confer immunity against polymicrobial sepsis (Wilmore et al., 2018). When we probed lysates of SIHUMI species with sera from SIHUMI or SIHUMI Δ*eut* colonized IL-10$^{-/-}$ mice, we observed the highest number of IgA immunoreactive bands for lysates of *B. vulgatus* and *R. gnavus*, the two most prevalent species in colonized mice (Figure 17 and Figure 14B). Similar results have been obtained for serum IgG antibodies (data not shown). *E. faecalis* lysate produced only a weak immunoreactive band. Interestingly, the serum IgA response was not influenced by the level of inflammation, as the number and intensity of immunoreactive bands was similar for lysates probed with SIHUMI or SIHUMI Δ*eut* sera (Figure 17).
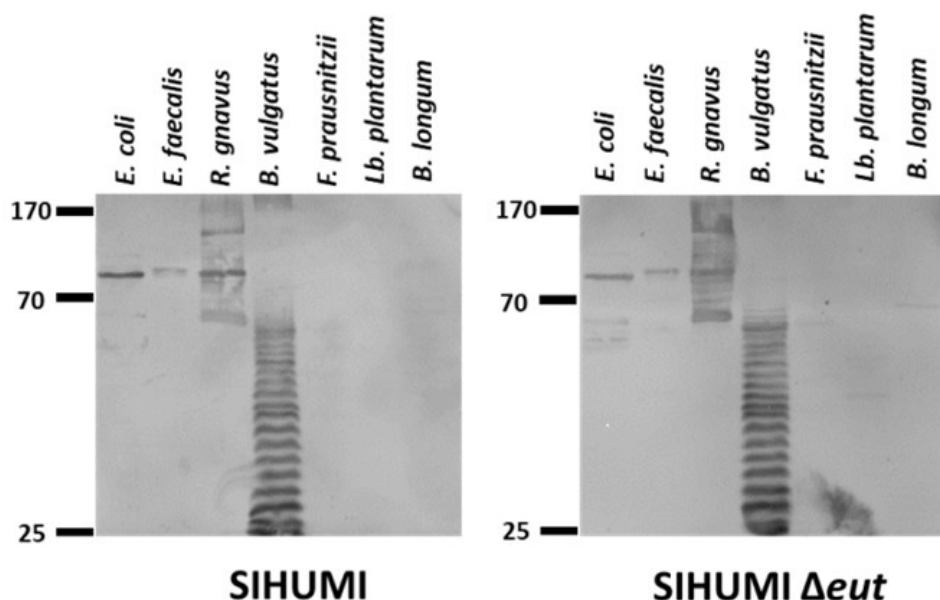
Figure 17: The serum IgA level against *E. faecalis* was not affected by the deletion of ethanolamine utilization.

Serum IgA against SIHUMI species: Western blots of the indicated bacterial lysates using sera from SIHUMI or SIHUMI Δ*eut* colonized IL10$^{-/-}$ mice.

4.5 Complex bacterial consortia interactions reprogram *E. faecalis* gene expression

Since we observed a protective effect of *E. faecalis* EA utilization only in a complex bacterial community and not under conditions of *E. faecalis* monoassociation, we aimed to gain a better understanding of *E. faecalis* gene expression in the presence of other microbes.

We purified *E. faecalis* cells from the colon content of SIHUMI colonized WT and IL-10$^{-/-}$ mice using immuno-magnetic separation and performed RNA sequencing (Figure 18A). Transcriptional profiling identified 180 significantly up- and 148 significantly down-regulated genes under inflammatory conditions (Figure S3A, Table S2). The samples clustered according to mouse genotype, as shown by PCA analysis (Figure S3B).

Among the top 20 up-regulated genes, several genes associated with arginine biosynthesis and glycerol metabolism were identified (Figure 18C). Arginine biosynthesis genes have been shown to be up-regulated in lactic acid bacteria in response to acid stress (van de Guchte et al., 2002) and glycerol is an important substrate for *E. faecalis* adaptive fitness during mouse colonization (Lindenstrauss et al., 2014; Muller et al., 2015). Surprisingly, we observed no overlap with the top up-regulated genes of *E. faecalis* isolated from monoassociated mice (Figure 18C and Figure 6C). Additionally, the functional categories enriched among all differentially regulated genes were mainly different between *E. faecalis* monoassociation or in the context of the SIHUMI community (Figure 18B and Figure 6B).
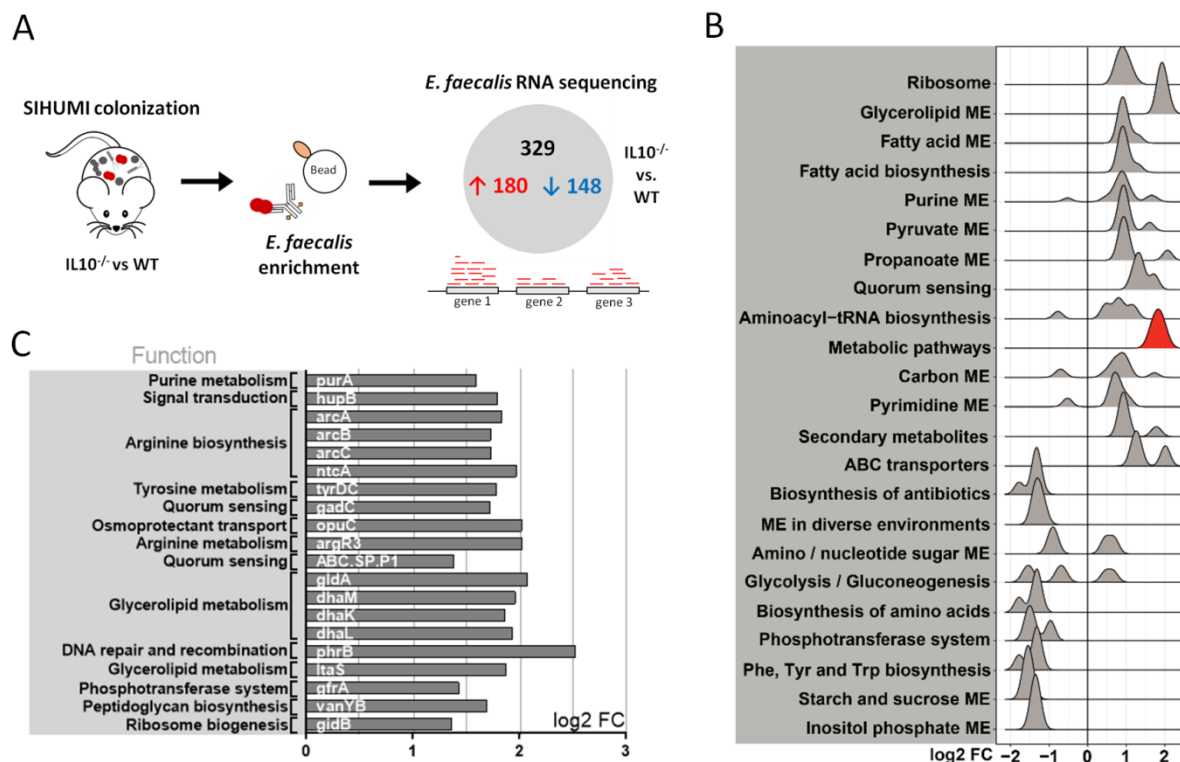
Figure 18: Complex bacterial consortia interactions reprogram *E. faecalis* gene expression in response to inflammation.

Luminal *E. faecalis* cells were isolated from the colon of inflamed IL-10$^{-/-}$ (n=13) and healthy WT mice (n=6) colonized with SIHUMI consortium (16 weeks of colonization), using immuno-magnetic separation and subjected to RNA sequencing analysis. **(A)** Experimental setup: Transcriptional profiling revealed 180 significantly up-regulated and 148 significantly down-regulated genes in *E. faecalis* isolated from IL-10$^{-/-}$ mice compared to *E. faecalis* isolated from WT mice colonized with the SIHUMI consortium. **(B)** Expression distribution of enriched genes for GSEA enriched categories (KEGG) (IL-10$^{-/-}$ vs. WT). The gene group highlighted red contains the *eut*-genes. **(C)** Top 20 up-regulated genes in *E. faecalis* isolated from SIHUMI colonized mice (IL-10$^{-/-}$ vs. WT). Only annotated genes with known function are shown. Gene functions were assigned according to KEGG database.

In the SIHUMI consortium, *E. faecalis* response to inflammation was characterized by an induction of cellular pathways required for growth and replication including ribosome, aminoacyl tRNA biosynthesis, nucleotide synthesis, pyruvate and propanoate metabolism, ABC transport and fatty acid biosynthesis and metabolism. In contrast to *E. faecalis* monoassociation, inositol phosphate metabolism and the biosynthesis of amino acids were repressed (Figure 18B).

Quorum sensing and glycerolipid metabolism were induced, whereas phosphotransferase systems and starch and sucrose metabolism were repressed in both mono- and complex-association of IL-10$^{-/-}$ mice (Figure 18B and Figure 6B). Interestingly, *E. faecalis* isolated from SIHUMI colonized mice showed higher expression of *eut* genes in healthy (Figure 19A) and mildly inflamed (Figure 19B) compared to inflamed animals. This is in line with our finding that *E. faecalis* ethanolamine utilization has a protective function in SIHUMI colonized mice (Figure 15).
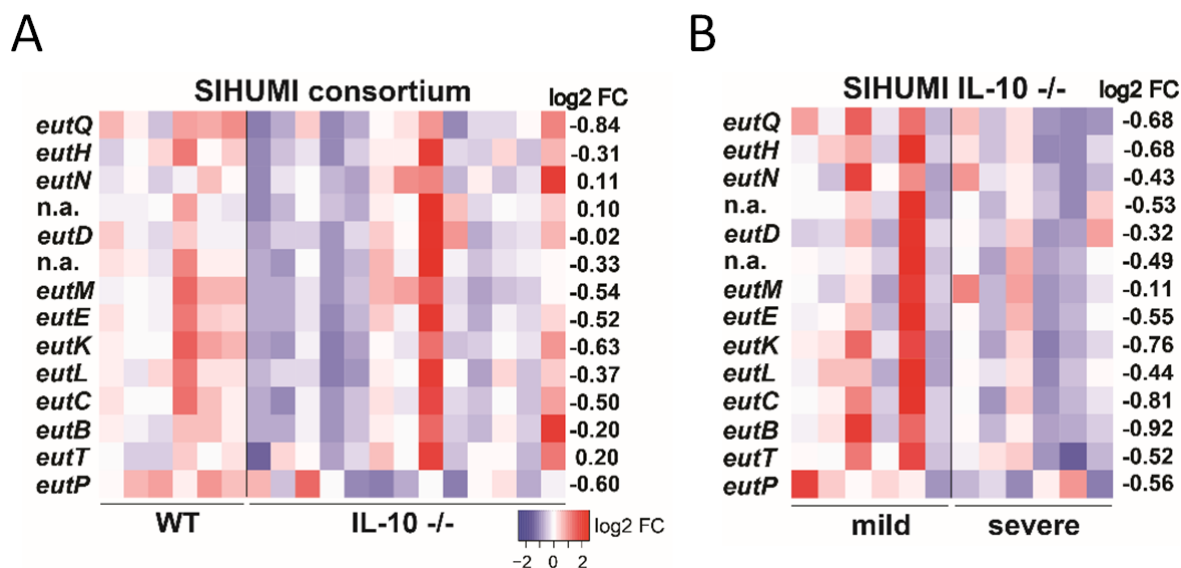
Figure 19: *E. faecalis eut* **genes are down-regulated in inflamed IL-10**^{-/-} **mice colonized with the SIHUMI consortium.**

(A) Differential expression of genes in relation to an inflamed environment is shown for selected *E. faecalis eut* genes. **(B)** Differential expression of *eut* genes in *E. faecalis* of a severely inflamed vs. a mildly inflamed environment. The log2 ratios of mean abundance of normalized expression levels are shown; Up regulation is indicated red, down regulation is indicated blue.

In IL-10^{-/-} mice colonized with the SIHUMI consortium, we observed a gradient of colitis severity. 6 out of 12 mice had a colitis score < 3 and were defined as mildly inflamed animals, the remaining 6 mice with a colitis score > 3 were defined as severely inflamed animals (Figure 20A). When comparing *E. faecalis* gene expression between severely and mildly inflamed IL-10^{-/-} mice, only 11 genes showed statistical significant regulation (Figure S4A and B). In particular, the lipoprotein SpoIIIJ (OG1RF_12576), which has been shown to be important for bile resistance of *E. faecalis* (Dale et al., 2018) and a cell wall surface anchor family protein (OG1RF_10871), which is associated with *E. faecalis* biofilm formation (Nallapareddy et al., 2006), appeared to be interesting candidates for *E. faecalis* survival and virulence (Figure 20B).
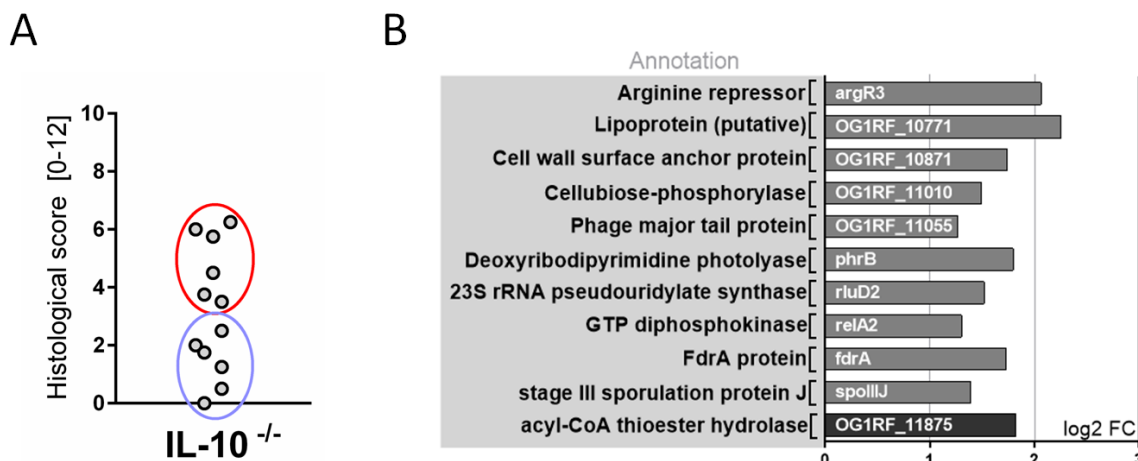
Figure 20: The severity of intestinal inflammation influences the gene expression of *E. faecalis*.
(A) Histological inflammation scores in the distal colon of SIHUMI colonized IL-10$^{-/-}$ mice comparing severely inflamed mice (red) and mildly inflamed mice (blue). **(B)** Significantly differentially regulated genes of *E. faecalis* isolated either from severely inflamed or mildly inflamed SIHUMI colonized IL-10$^{-/-}$ mice (up regulation is indicated by grey bar color, down regulation is indicated by black bar color).

When comparing *E. faecalis* transcriptional response to inflammation between bacteria isolated from mono- and complex-associated mice on the gene level, the majority of differentially regulated genes were not shared. This suggests that the bacterial environment reprograms *E. faecalis* gene expression. Only 125 genes were shared between both colonization environments, while 751 genes were exclusively regulated in monoassociation and 203 genes were exclusively regulated in the SIHUMI community (Figure 21A).

In addition, the majority of overlapping genes showed opposite patterns of regulation. Several genes associated with fundamental cellular pathways were down regulated in *E. faecalis* of monoassociated mice, whereas these genes were strongly up regulated in *E. faecalis* of the SIHUMI community. This includes genes associated with the translation apparatus (*lysS*, *trpS2*, *rpmB2*, *rpmH*, *rpsT*, *engA*), RNA synthesis (*rpoZ*), DNA replication (*parE*), citrate cycle (*fdrA*), peptidoglycan biosynthesis (*amiD*, *cwlO*), nucleotide metabolism (*gmk2*, *guaD*, *upp2*) and transport (*ecfA1*, *tagH*, *ctpE*, *secA*) (Figure 21B).
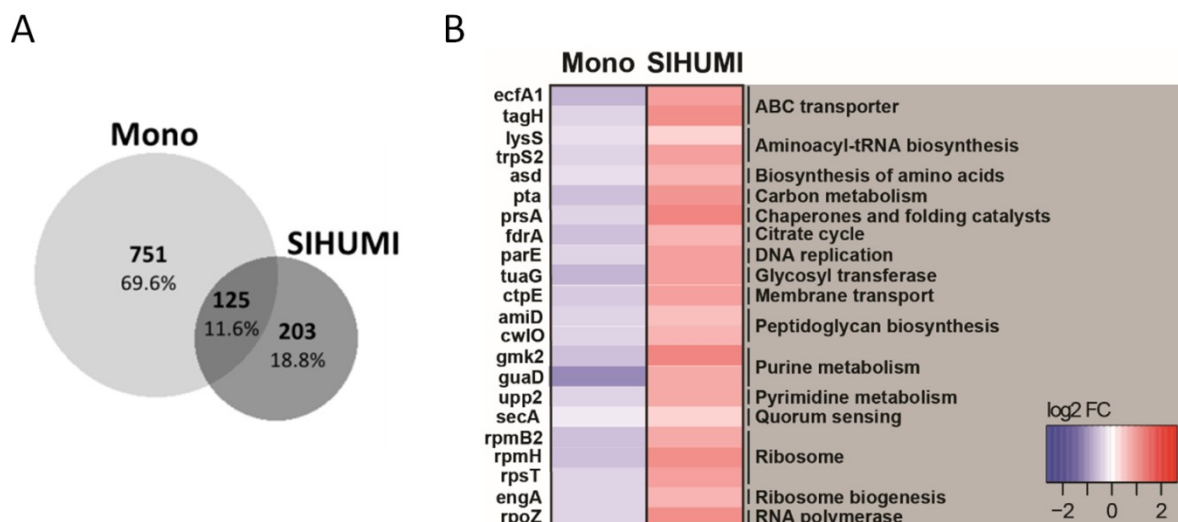
Figure 21: The majority of regulated genes were not shared between *E. faecalis* isolated from monoassociated and SIHUMI colonized mice.

(A) Venn diagram showing the differentially regulated genes shared (IL-10$^{-/-}$ vs. WT) between *E. faecalis* isolated from monoassociated and SIHUMI colonized mice. **(B)** Genes down regulated in monoassociated and up regulated in SIHUMI-associated mice, respectively. The log2 ratios of mean abundances of normalized expression levels are shown (up regulation is indicated red, down regulation is indicated blue). Gene functions were assigned according to KEGG database. Only annotated genes with known function are shown.

Vice versa, we observed an up regulation of several stress-response genes in *E. faecalis* of monoassociated mice, including genes that encode for proteases and chaperones (*clpE*, *clpP*, *dnaK*, *dnaJ*, *groEL*, *groES*), a ribosomal stress protein (*rplY*), a detoxifying enzyme (*gloA2*) and proteins associated with DNA repair (*ung*, *dinB2*) and oxidative stress resistance (*gor*) (van de Guchte et al., 2002; Gaca et al., 2012). In addition, genes associated with the biosynthesis of amino acids (*luxS*, *aroA*, *aroB*, *tyrA*, *pheA*), transport (*yidK*, *nhaC*), transcriptional regulation (*glcR*, *lacI*) and a protein homologous to RNA polymerase subunit RpoE were up-regulated in monoassociated *E. faecalis*, but down-regulated in *E. faecalis* colonizing in the SIHUMI consortium (Figure 22).
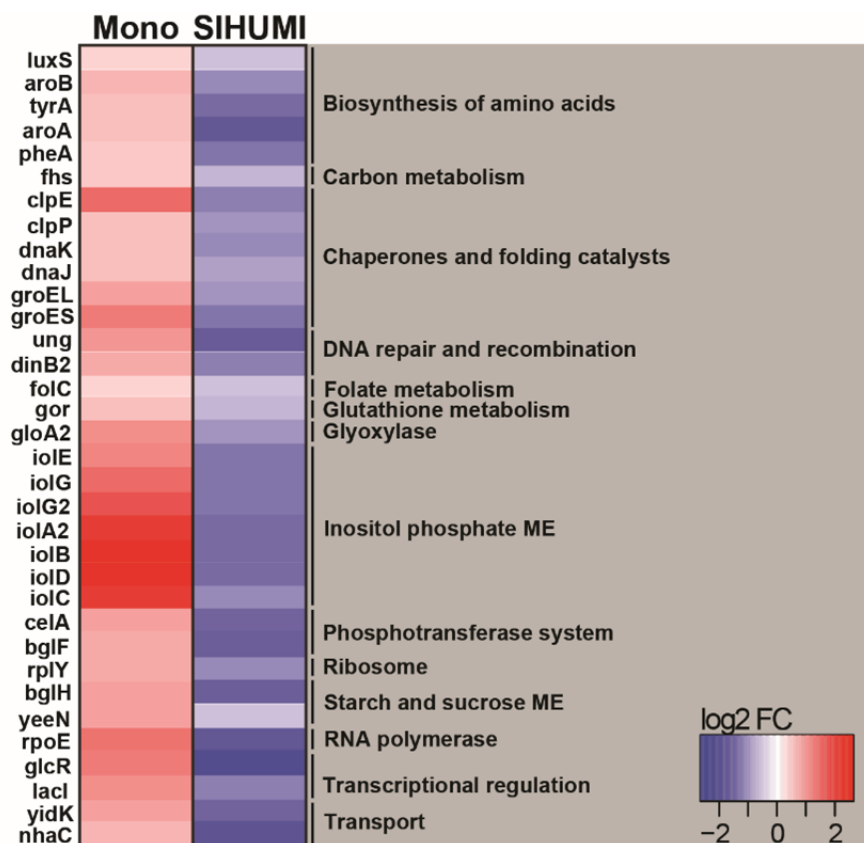
Figure 22: General stress-response genes were up-regulated in *E. faecalis* colonizing in monoassociation, but down-regulated in *E. faecalis* colonizing in a bacterial community.
Differentially regulated genes (IL-10$^{-/-}$ vs. WT) overlapping between *E. faecalis* isolated from monoassociated and SIHUMI colonized mice (only genes with opposing regulation pattern are shown). The log2 ratios of mean abundances of normalized expression levels are shown (up regulation is indicated red, down regulation is indicated blue). Gene functions were assigned according to KEGG database, only annotated genes with known function are shown.

4.6 Bacterial consortia interactions reprogram *E. faecalis* colitogenic activity

We next addressed the question of whether the transcriptional differences of *E. faecalis* colonizing in mono- or complex-associated mice have functional consequences by applying the SIHUMI consortium with (SIHUMI) or without *E. faecalis* (SIHUMI -*E. fae*).

WT and IL-10$^{-/-}$ mice were colonized at the age of 10 weeks for a period of 4 weeks to analyze early effects at the onset of disease, or 16 weeks to analyze disease progression (Figure 23A). Quantification of bacterial concentrations in colon content showed that the 6 (SIHUMI group) or 5 (-*E. fae* group) colonizing species formed a stable community under gnotobiotic conditions (Figure 23B and C). The relative bacterial abundances were slightly different between the early (4 weeks) and late (16 weeks) colonization period. The proportion of *B. longum* was relatively high after 4 weeks of colonization, but after 16 weeks of colonization *R. gnavus* and *B. vulgatus* were the only dominant species (Figure 23B and C). The absence of *E. faecalis* resulted in changes of the relative abundances of specific SIHUMI species in luminal contents of colon. After 16 weeks of colonization,

the relative concentrations of *E. coli* and *B. longum* were slightly higher, while *B. vulgatus* concentrations were lower in SIHUMI -*E. fae* colonized mice as compared to SIHUMI colonized mice (Fig. 23C).
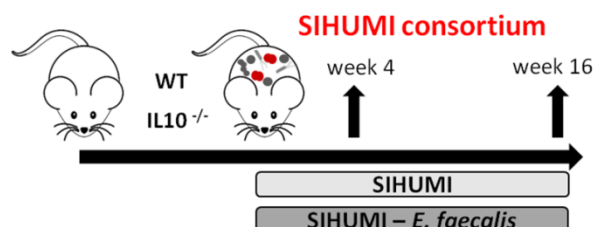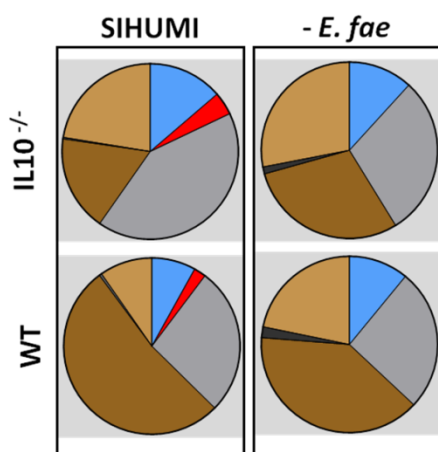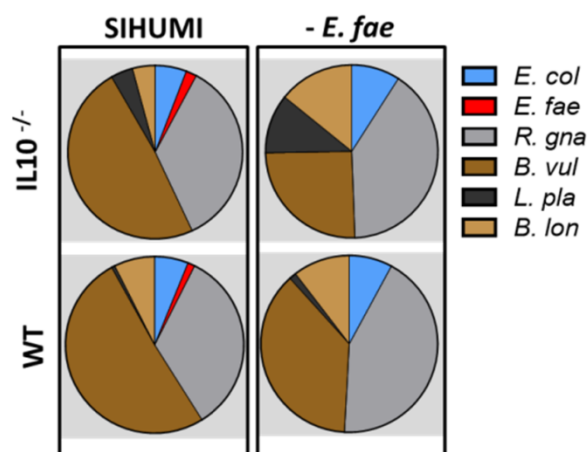
Figure 23: *E. coli* **and** *B. longum* **relative abundances were slightly shifted in SIHUMI colonized mice under omission of** *E. faecalis.*
Germfree IL-10$^{-/-}$ and WT mice were colonized with SIHUMI consortium or SIHUMI consortium without *E. faecalis* (-*E. fae*) for a period of 4 and 16 weeks. **(A)** Experimental setup. **(B)** Relative abundances of SIHUMI bacterial species in luminal colon content by 16S targeted qPCR after 4 weeks and **(C)** 16 weeks of colonization. *E. col*, *Escherichia coli*; *E. fae*, *Enterococcus faecalis*; *R. gna*, *Ruminococcus gnavus*; *B. vul*, *Bacteroides vulgatus*; *L. pla*, *Lactobacillus plantarum*; *B. lon*, *Bifidobacterium longum*

Surprisingly, the colonization of IL-10$^{-/-}$ mice with SIHUMI in the absence of *E. faecalis* not only induced inflammation, but resulted in an aggravated inflammatory host response compared to the control. After 16 weeks of colonization, IL-10$^{-/-}$ mice colonized with SIHUMI -*E. fae* consortium developed severe inflammation in the distal colon (histopathological score: 4.8 ± 2.4), while the degree of colitis was significantly reduced in IL-10$^{-/-}$ mice colonized with SIHUMI in the presence of *E. faecalis* (histopathological score: 2.8 ± 2.5) (Figure 24A and B). After 4 weeks of colonization, IL-10$^{-/-}$

mice showed mild pancolitis independent of the colonizing bacteria. All colonized WT mice remained disease-free (Figure 24A and B).

Again, we observed on average higher histological inflammation in females, suggesting an influence of sex on disease progression in IL-10$^{-/-}$ mice colonized with a complex bacterial consortium (Figure 24A). Increased spleen weights and a high level of pro-inflammatory cytokine expression accompanied the histopathological inflammation in IL-10$^{-/-}$ mice after a colonization period of 16 weeks (Figure 24C). Of note, the expression of IFNγ was significantly higher in IL-10$^{-/-}$ mice that were colonized with SIHUMI -E. fae consortium compared to SIHUMI colonized mice. TNF and IL-17 expression levels followed the same pattern, whereas IL-12p40 expression was not influenced by the composition of the colonizing consortium (Figure 24D).
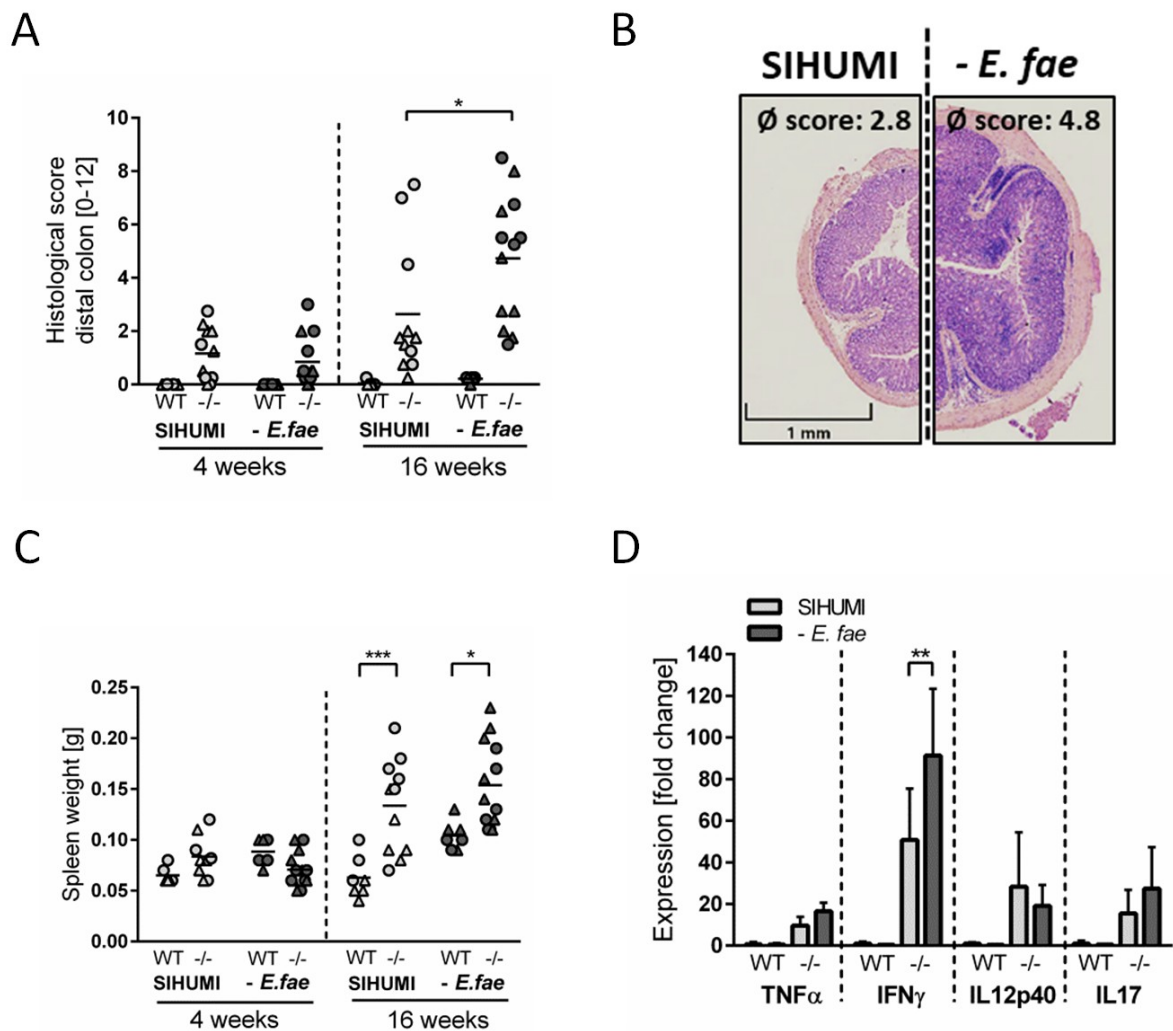
Figure 24: _E. faecalis_ has protective functions in IL-10 $^{-/-}$ mice colonized with a complex bacterial consortium.

Germfree IL-10$^{-/-}$ and WT mice were colonized with SIHUMI consortium or SIHUMI consortium without _E. faecalis_ (-_E. fae_) for a period of 4 and 16 weeks. **(A)** Histological inflammation in the distal colon. Male mice are displayed as triangle, female mice as circles. **(B)** Representative hematoxylin/eosin-stained sections of distal colon after 16 weeks of colonization colon. **(C)** Spleen weight. Male mice are displayed as triangle, female mice as circles. **(D)** Cytokine expression in colon

tissue sections shown as fold change normalized to cytokine expression levels in WT mice colonized with SIHUMI consortium.

Since the colonization of IL-10$^{-/-}$ mice under omission of *E. faecalis* exacerbated the severity of colitis, another species appears to trigger disease in the SIHUMI setting. The relative abundance of *E. coli* and *B. longum* in large intestinal content were positively correlated with the develpment of histopathology, while no correlation was observed for *E. faecalis* abundance and colitis activity (Figure 25A and B, Figure S5).

To address the bacterial antigen-specific immune responses of colonized mice, we isolated MLN cells from IL-10$^{-/-}$ mice colonized with SIHUMI in the presence and absence of *E. faecalis* and re-stimulated them with respective lysates of each of the colonizing SIHUMI species. After 4 weeks of colonization, the secretion of IFNγ and IL-12p40 in response to *E. coli* lysate stimulation was slightly increased in MLN cells isolated from mice colonized with SIHUMI. All other lysates failed to activate the MLN cell cultures (Figure 25C and E). After 16 weeks of colonization, MLN cells produced maximal levels of IFNγ and IL-12p40 upon stimulation with *E. coli* lysate, although the relative luminal concentrations of this bacterium were quite low (Figure 23C). The MLN response towards *E. coli* lysate was even more pronounced in MLNs isolated from mice colonized with SIHUMI -*E. fae* consortium (Figure 25D and F), suggesting compensatory mechanisms in the absence of *E. faecalis*.
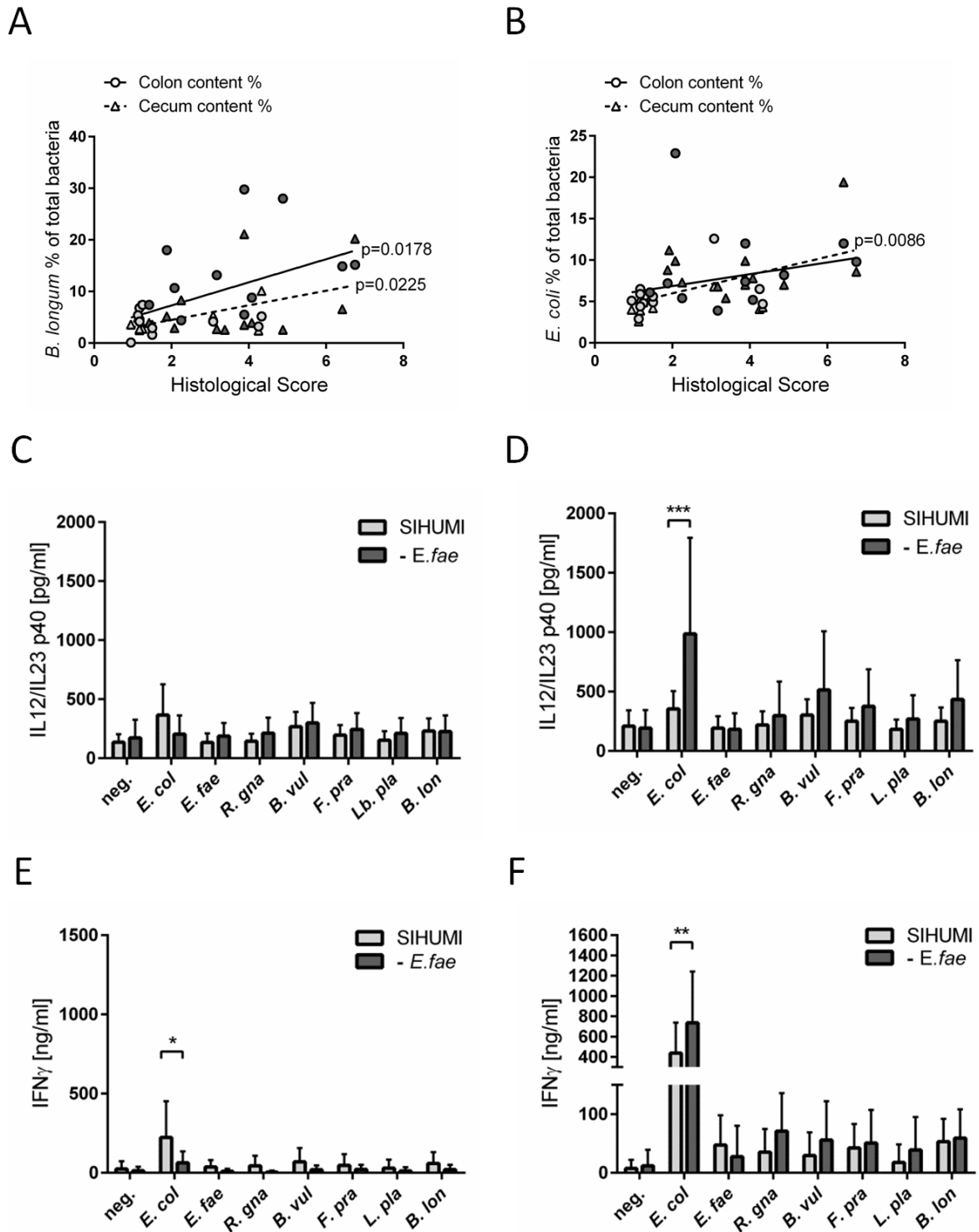
Figure 25: MLN response and bacterial abundance indicate *E. coli* as driver of SIHUMI-mediated colitis in IL-10$^{-/-}$ mice.

Germfree IL-10$^{-/-}$ and WT mice were colonized with SIHUMI consortium or SIHUMI consortium without *E. faecalis* (SIHUMI *-E. fae*) for a period of 4 and 16 weeks. **(A)** Correlation between *B. longum* and **(B)** *E. coli* abundance (colon and cecum luminal content) and mean histological scores of cecum tip and distal colon. Light grey indicates SIHUMI experimental group, dark grey indicates SIHUMI *-E. fae* experimental group. **(C)** IL-12p40 secretion of MLN cells isolated from SIHUMI or SIHUMI *-E. fae* colonized mice that were re-activated with the respective bacterial lysate after 4 weeks or **(D)** 16 weeks of colonization. **(E)** IFNγ secretion of MLN cells isolated from SIHUMI or

SIHUMI *-E. fae* colonized mice that were re-activated with the respective bacterial lysate after 4 weeks or **(F)** 16 weeks of colonization. *E. col, Escherichia coli*; *E. fae, Enterococcus faecalis*; *R. gna, Ruminococcus gnavus*; *B. vul, Bacteroides vulgatus*; *L. pla, Lactobacillus plantarum*; *B. lon, Bifidobacterium longum*

The level of serum IgA antibodies against SIHUMI species was only slightly influenced by the composition of the bacterial consortium. When we probed lysates of SIHUMI species with sera from SIHUMI or SIHUMI *-E. fae* colonized IL-10$^{-/-}$ mice, we observed the highest number of immunoreactive bands for lysates of *B. vulgatus*, *R. gnavus* and *E. coli*. The number and intensity of immunoreactive bands against *E. coli* and *B. vulgatus* lysates were slightly increased when probed with SIHUMI *-E. fae* sera, indicating increased levels of IgA antibodies against these species in mice colonized with SIHUMI in the absence of *E. faecalis* (Figure 26).
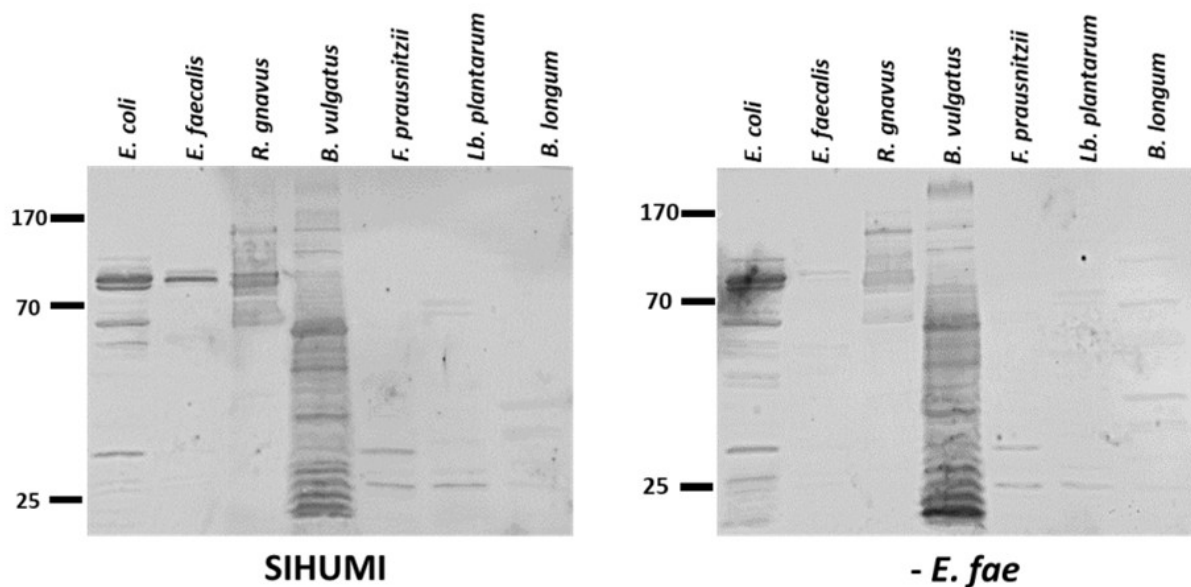
Figure 26: Higher number and intensity of immunoreactive bands (IgA) against *E. coli* and *B. vulgatus* in the absence of *E. faecalis*.
Serum IgA against SIHUMI species: Western blots of the indicated bacterial lysates using sera from SIHUMI or SIHUMI *-E. fae* colonized IL10 $^{-/-}$ mice.

A massive pro-inflammatory response of re-activated MLN cells to *E. coli* lysate stimulation (Figure 25D and F) and a positive correlation between histological inflammation and *E. coli* abundance (Figure 25B) points to this bacterium as main driver of SIHUMI-mediated colitis. In addition, the number of IgA (Figure 26) and IgG (data not shown) immunoreactive bands against *E. coli* lysate was increased in gnotobiotic mice colonized with SIHUMI in the absence of *E. faecalis* compared to mice colonized with the whole SIHUMI consortium.

Since it has been shown that *E. faecalis*, which provides protective mechanisms in our experimental environment, can influence the expression of *E. coli* virulence genes (Neuhaus et al., 2017), we analyzed the expression of selected *E. coli* virulence genes via qPCR. Of 9 genes analyzed, only the expression of *E. coli ompC* in IL-10$^{-/-}$ mice was significantly reduced when *E. faecalis* was present (Figure S6). *OmpC* encodes for an outer membrane porin that is involved in bacterial multidrug resistance and has been shown to be a major immunogen in human serum (Liu et al., 2012).

4.7 In the absence of *E. coli* other SIHUMI species increase their colitogenic activity

Since our data suggest that *E. coli* is the main colitogenic organism in the SIHUMI consortium, while *E. faecalis* provides protective activity, we wanted to confirm our hypothesis by colonizing germfree WT and IL-10$^{-/-}$ mice with the SIHUMI consortium under omission of *E. coli* (SIHUMI -*E. col*). The corresponding control mice colonized with SIHUMI consortium have already been shown in chapter 4.4.

Mice were colonized at the age of 10 weeks for a period of 16 weeks and bacterial concentrations as well as indicators of chronic, immune-mediated colitis were measured (Figure 27A and B). Quantification of bacterial concentrations in colon content showed that the 5 (SIHUMI -*E. col*) colonizing species formed a stable community under gnotobiotic conditions (Figure 27B). Interestingly, the omission of *E. coli* caused a large shift in the SIHUMI community with an increase in the proportion of *B. vulgatus* and a decrease in the concentrations of *R. gnavus* and *B. longum* (Figure 27B).
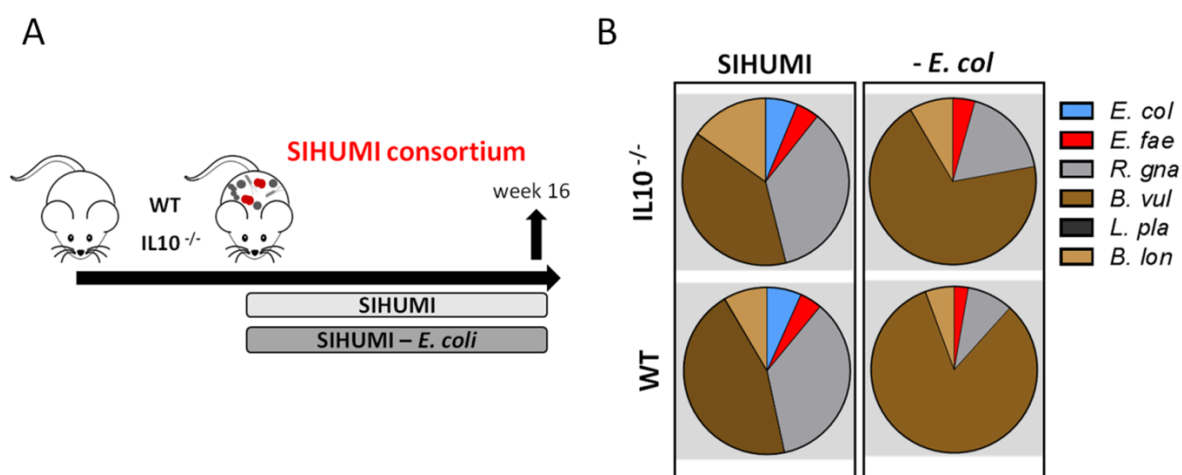
Figure 27: Omission of *E. coli* results in a major shift of the SIHUMI community.
Germfree IL-10$^{-/-}$ and WT mice were colonized with SIHUMI consortium (see 4.4) or SIHUMI consortium without *E. coli* (-*E. col*) for a period of 16 weeks. **(A)** Experimental setup. **(B)** Relative abundances of SIHUMI bacterial species in luminal colon content by 16S targeted qPCR. *E. col*,

Escherichia coli; *E. fae*, *Enterococcus faecalis*; *R. gna*, *Ruminococcus gnavus*; *B. vul*, *Bacteroides vulgatus*; *L. pla*, *Lactobacillus plantarum*; *B. lon*, *Bifidobacterium longum*

Contrary to our hypothesis, the SIHUMI *-E. col* consortium induced a more severe inflammatory phenotype in IL-10$^{-/-}$ mice compared to the complete SIHUMI consortium (Figure 28A). After 16 weeks of colonization, IL-10$^{-/-}$ mice colonized with SIHUMI *-E. col* consortium developed severe inflammation in the distal colon (histolgical score: 5.7 ± 2.5), while the degree of colitis was significantly lower in the SIHUMI control group (histological score: 3.1 ± 2.3; see 4.4) (Figure 28A). Interestingly, in contrast to the colon, the severity of inflammation in the cecum tip of SIHUMI *-E. col* colonized IL-10$^{-/-}$ mice was significantly reduced compared to SIHUMI colonized IL-10$^{-/-}$ mice (Figure 28B). All colonized WT mice remained disease free (Figure 28A and B). In SIHUMI colonized IL-10$^{-/-}$ mice, on average higher inflammatory scores were observed in females, whereas in SIHUMI *-E.col* colonized IL-10$^{-/-}$ mice no influence of sex on the severity of disease could be observed (Figure 28A and B). Increased spleen weights and a high level of TNFα and IFNγ expression in colon tissue accompanied the histological inflammation in IL-10$^{-/-}$ mice (Figure 28C).
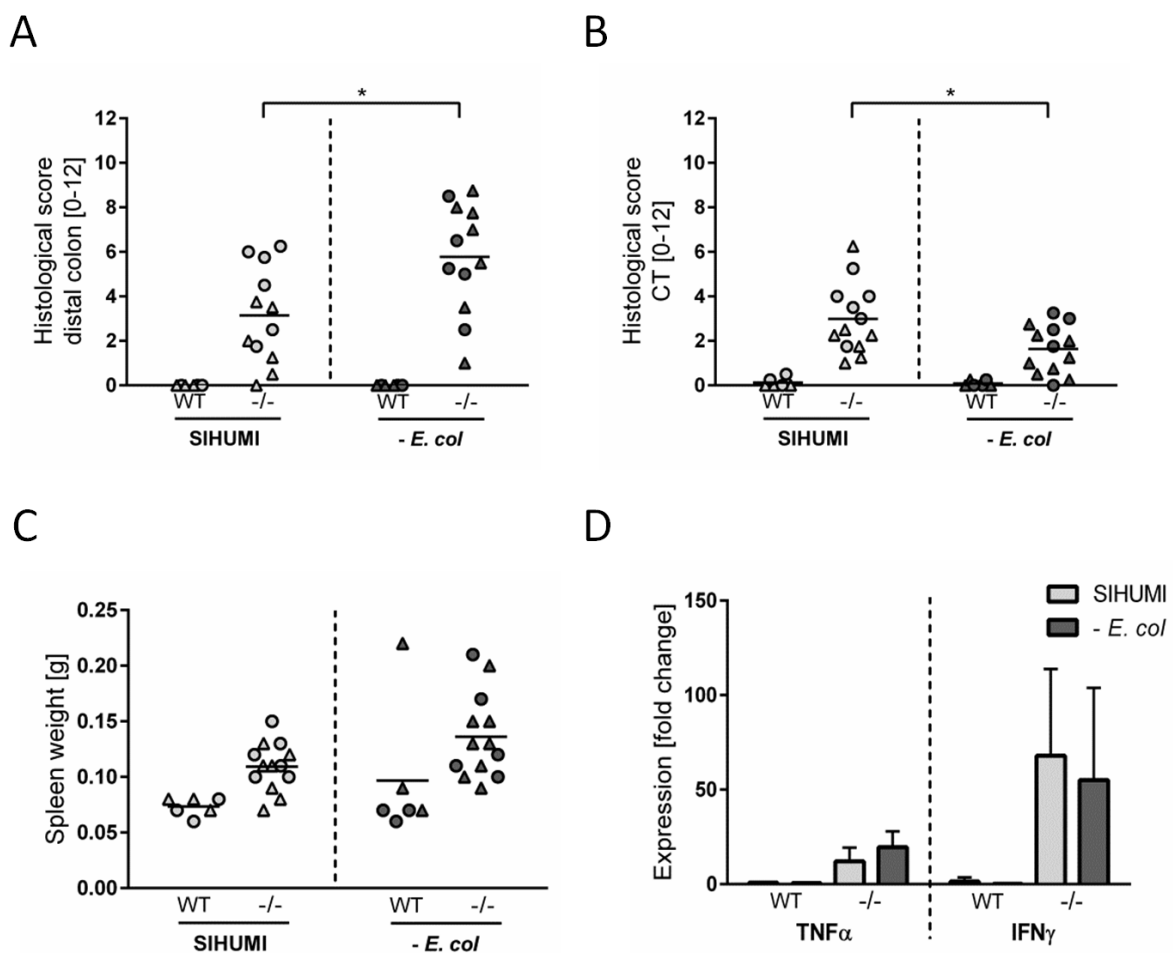
Figure 28: The presence of *E. coli* alleviates the inflammation in the distal colon, but exacerbates the inflammation in the cecum tip in IL-10$^{-/-}$ mice colonized with a complex bacterial consortium.

Germfree IL-10$^{-/-}$ and WT mice were colonized with SIHUMI consortium (see 4.4) or SIHUMI consortium without *E. coli* (SIHUMI -*E. col*) for a period of 16 weeks. **(A)** Histological inflammation in the distal colon or **(B)** cecum tip. Male mice are displayed as triangle, female mice as circles. **(C)** Spleen weight. Male mice are displayed as triangle, female mice as circles. **(D)** TNFα and IFNγ expression in colon tissue sections shown as fold change normalized to cytokine expression levels in WT mice colonized with SIHUMI consortium.

Since colonization of IL-10$^{-/-}$ mice with the omission of *E. coli* resulted in an exacerbation of the severity of inflammation in the distal colon, *E. coli* appears not to be the trigger of colitis in this environment. In the cecum tip, however, omission of *E. coli* resulted in a less severe inflammatory phenotype, indicating that *E. coli* is in part responsible for the development of cecal inflammation in SIHUMI colonized IL-10$^{-/-}$ mice.

To indentify the species that drive inflammation development in the absence of *E. coli*, we analyzed bacterial antigen-specific immune responses and serum IgG reactivity to bacterial lysates. As previously shown, MLN cells isolated from IL-10$^{-/-}$ mice colonized with SIHUMI produced maximal levels of IFNγ and IL-12p40 when stimulated with *E. coli* lysate (Figure 29A and B). In the absence of *E. coli*, however, MLN cells secreted the highest values of IFNγ when stimulated with *E. faecalis* lysate, while all other lysates failed to activate the MLN cell cultures (Figure 29A and B).

Sera from SIHUMI colonized IL-10$^{-/-}$ mice showed the highest IgG reactivity against *E. coli*, *B. vulgatus* and *R. gnavus* lysates. In the absence of *E. coli* (SIHUMI -*E.col*), however, no immunoreactive IgG bands against *E. coli* lysate could be observed. Here, we observed an increased number and intensity of immunoreactive bands against *E. faecalis* and *R. gnavus* lysates (Figure 29C). This indicates increased levels of IgG antibodies against these species in mice colonized with SIHUMI in the absence of *E. coli*.
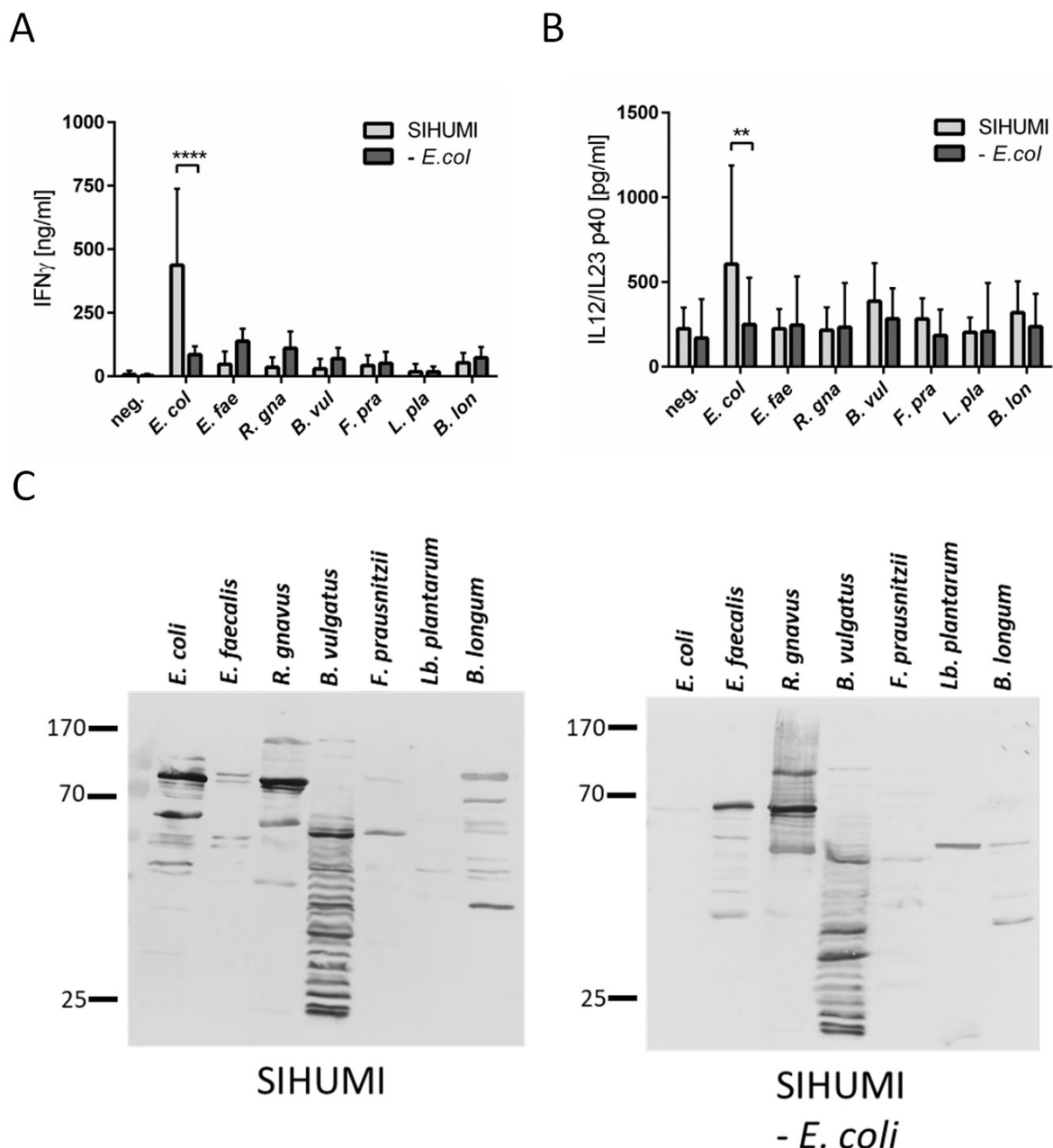
Figure 29: Increased MLN response and serum IgG reactivity to *E. faecalis* in the absence of *E. coli.*
Germfree IL-10$^{-/-}$ and WT mice were colonized with SIHUMI consortium (see 4.4) or SIHUMI consortium without *E. coli* (SIHUMI -*E. col*) for a period of 16 weeks. **(A)** IFNγ and **(B)** IL-12p40 secretion of MLN cells isolated from SIHUMI or SIHUMI -*E. col* colonized mice that were re-activated with the respective bacterial lysate after 16 weeks of colonization. *E. col*, *Escherichia coli*; *E. fae*, *Enterococcus faecalis*; *R. gna*, *Ruminococcus gnavus*; *B. vul*, *Bacteroides vulgatus*; *L. pla*, *Lactobacillus plantarum*; *B. lon*, *Bifidobacterium longum* **(C)** Serum IgG against SIHUMI species: Western blots of the indicated bacterial lysates using sera from SIHUMI or SIHUMI -*E. col* colonized IL10 $^{-/-}$ mice.

E. faecalis colonization density was significantly increased in WT, but not in IL-10$^{-/-}$ mice colonized with SIHUMI -*E. col* (Figure 30A). The only significant correlation between bacterial abundance and the level of colonic inflammation was detected for *R. gnavus* with a reduced abundance beeing

associated with higher inflammatory scores (Figure 30B). This is consistent with the results of chapter 4.4.
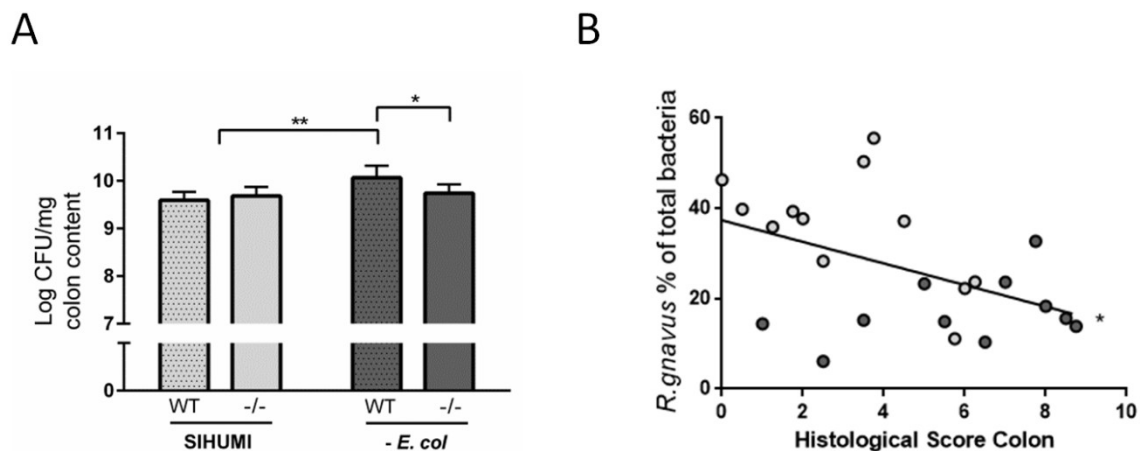
Figure 30: Bacterial concentrations do not positively correlate with tissue inflammation.
Germfree IL-10$^{-/-}$ and WT mice were colonized with SIHUMI consortium (see 4.4) or SIHUMI consortium without *E. coli* (SIHUMI *-E. col*) for a period of 16 weeks. **(A)** *E. faecalis* presence in luminal contents from colon according to the CFU counts/ml. **(B)** Correlation between *R. gnavus* relative abundance (luminal colon content) and histological scores of distal colon. Light grey indicates SIHUMI experimental group, dark grey indicates SIHUMI *-E. col* experimental group.

4. DISCUSSION

In this study, we demonstrate that *E. faecalis* functionally adapts to chronic inflammation, supporting the hypothesis tht host-related mechanisms contribute to the colitogenic activity of opportunistic pathogens. *E. faecalis* is a desease-relevant pathobiont and colonization of IBD-related mouse models, such as IL-10$^{-/-}$ mice, supports the concept that commensal bacteria harboring pathogenic traits drive chronic inflammation in genetically susceptible but not wild type hosts. In addition to previous identified genes modulating the colitogenic activity of *E. faecalis* (Ocvirk et al., 2015), we performed transcriptional profiling of *E. faecalis* under inflammatory conditions and identified 876 genes to be differentially regulated compared to normal conditions. Among the highest upregulated genes in monoassociated inflamed mice, a gene encoding for a major facilitator superfamily transporter (*mfs*) and genes of the ethanolamine utilization (*eut*) locus were identified. Despite their considerable up-regulation, the deletion of ethanolamine utilization (Δ*eutVW*) or *mfs* (Δ*mfs*) had no influence on bacterial colonization density and colitogenic activity in monoassociated mice. Interestingly, *E. coli* responds to inflammation in monoassociated IL-10$^{-/-}$ mice by the up-regulation of stress response genes, but targeted deletion these genes aggravated the inflammatory phenotype (Patwa et al., 2011; Tchaptchet et al., 2013). This supports our observation that bacterial adaptation processes correlating with intestinal inflammation are not necessarily harmful for the host. In line with this, we have shown in a previous study that genes that produce two colitis-relevant structures in *E. faecalis* are not transcriptionally regulated in inflamed IL-10$^{-/-}$ mice relative to WT controls (Ocvirk et al., 2015).

Although *eut* genes were up-regulated during *E. faecalis* growth in an inflammatory environment, this is not necessarily an indication of *in vivo* utilization of EA. The measurement of luminal intestinal EA allowed us to demonstrate that *E. faecalis* utilizes this substrate *in-vivo* in WT mice and not inflamed IL-10$^{-/-}$ mice. However, EA concentrations in inflamed IL-10$^{-/-}$ mice were similar for both *E. faecalis* OG1RF and Δ*eut* mutant colonization. This is surprising as *E. faecalis eut* genes were massively up-regulated in inflamed IL-10$^{-/-}$ mice relative to WT controls. This paradox could be explained by limitations of our model as we only analyzed gene expression and not *eut* protein levels. Additional studies to understand *E. faecalis eut* gene expression and *in-vivo* EA metabolism are needed.

We provide for the first time evidence for a protective effect of bacterial EA utilization in the context of chronic intestinal inflammation. Using a simplified microbial consortium based on human strains (SIHUMI), we demonstrate that *E. faecalis* EA utilization attenuated colitis in mice colonized with a complex bacterial community. The replacement of *E. faecalis* WT strain by a Δ*eut* mutant resulted in exacerbated colitis in SIHUMI colonized IL-10$^{-/-}$ mice, as indicated by increased

histological inflammation, increased tissue expression of TNF and IL-12p40 and increased spleen weights. The colonization density of Δ*eut* mutant was slightly increased compared to WT *E. faecalis*. However, the relative abundance of *E. faecalis* did not correlate with the histological inflammation, suggesting that increased *E. faecalis* Δ*eut* numbers do not explain the aggravated inflammatory phenotype. MLN cells secreted high amounts of IL-12p40 in response to *E. coli* lysate, but the highest IgA immunoreactivity was observed for *B. vulgatus* and *R. gnavus*, the two most abundant species. Though, a negative correlation between *R. gnavus* concentration and the severity of intestinal inflammation indicates that this bacterium is not involved in pathogenesis.

Our data indicate that *E. faecalis* is not the driver of inflammation in the SIHUMI community, but modulates disease by interaction with co-colonizing bacteria. The catabolism of EA by *E. faecalis* may prevent the utilization of this metabolite by the more colitogenic species *E. coli*. It has been shown that EA can promote *E. coli* growth and virulence (Bertin et al., 2011; Kendall et al., 2012) . Interestingly, a recent study demonstrated that *E. coli* LF82 *eut* operon is upregulated in the presence of bile salts. The authors showed that EA can be utilized as sole source of nitrogen by the LF82 *E. coli* and provides a growth advantage in the intestine of DSS treated mice (Delmas et al., 2019). Yet, the expression of selected *E. coli* LF82 virulence genes (*fliC*, *fimH*, *ompA*, *ompC*) and ethanolamine utilization genes (*eutR*, *eutC*, *eutQ*) was not affected in our model (data not shown) and also the relative abundance of *E. coli* was not increased in the presence of *E. faecalis* Δ*eut* mutant. Additional studies to identify the specific mechanism contributing to the protective effect of *E. faecalis eut* gene expression are required.

Our data provide new insights into the role of EA utilization in microbiota-host interactions. EA plays a well-recognized role in host adaption and virulence of enteric pathogens including EHEC, *Salmonella* and *Listeria monocytogenes* (Joseph et al., 2006; Bertin et al., 2011; Kendall et al., 2012; Luzader et al., 2013; Anderson et al., 2015). In contrast, we show that *E. faecalis* EA utilization has a protective function in IL-10$^{-/-}$ mice. These discrepancies might arise from differences in bacterial physiology and pathogenicity. The pathogen salmonella requires alternative electron acceptors released from inflamed host tissue for EA utilization (Price-Carter et al., 2001; Thiennimitr et al., 2011), whereas *E. faecalis* can grow anaerobically on EA in the absence of alternative electron acceptors (Garsin, 2010). In addition, others have demonstrated a protective effect of EA utilization by opportunistic pathogens as well. The metabolism of EA resulted in reduced virulence together with a delayed onset of disease in a hamster model of *Clostridium difficile* infection (Nawrocki et al., 2018). Furthermore, EA utilization by commensal *E. coli* isolates allowed them to outcompete the pathogen EHEC (Rowley et al., 2018).

Consistent with our data, the colonization efficiency of *E. faecalis* Δ*eutVW* in the murine gastrointestinal tract was increased relative to the WT strain (Kaval et al., 2018). This stands in contrast to enteric pathogens, where the loss of EA utilization resulted in a competitive disadvantage (Bertin et al., 2011; Thiennimitr et al., 2011; Anderson et al., 2015). In *Caenorhabditis elegans*, an *E. faecalis eut* mutant was attenuated in virulence, but in this host some *E. faecalis* strains are regared as a pathogenic organisms resulting in the death of infected nematodes (Maadani et al., 2007). The interesting correlation between bacterial lifestyle and the role of EA utilization for bacterial survival and virulence awaits further investigation.

To the best of our knowledge, this is the first published study that analyzed the influence of co-colonization with a bacterial consortium on gene expression and function of an opportunistic pathogen. Most importantly, we demonstrate that complex bacterial consortia interactions reprogram the gene expression profile and the colitogenic activity of *E. faecalis* towards a protective function. Transcriptional interactions between bacteria have already been illustrated for two members of the dominant gut bacterial phyla. *Eubacterium rectale* and *Bacteroides thetaiotaomicron* adapt their profile of utilized substrates in response to the co-colonizing species in gnotobiotic mice (Mahowald et al., 2009). In addition, Plichta et al. demonstrated transcriptional species-specific interactions in a complex bacterial community with central metabolisms being strongly affected by coexistence with other microbes (Plichta et al., 2016). Using immuno-magnetic separation, we were able to isolate *E. faecalis* cells from SIHUMI colonized mice. This allowed us to study for the first time the transcriptional response of an opportunistic pathogen to host inflammation depending on the microbial environment. Interestingly, the majority of regulated genes were not shared between *E. faecalis* colonizing in monoassociation or in the SIHUMI community. This shows that *E. faecalis* transcriptionally adapts to the co-colonizing microbes.

In monoassociated IL-10$^{-/-}$ mice, *E. faecalis* gene expression was characterized by an enrichment of functions important for bacterial stress adaption. General stress-response genes, amino acid biosynthesis genes and genes involved in the utilization of alternative carbon sources were up regulated. A similar regulation pattern has been observed by others analyzing *E. faecalis* transcriptome during mammalian infection. For instance, the intraperitoneal transcriptome of *E. faecalis* in gnotobiotic mice is characterized by the up-regulation of stress-response genes and a metabolic adaption to an inflamed environment (Muller et al., 2015). Frank et al. demonstrated that *E. faecalis* cells undergo transcriptional adaption and exist in a stringent response state in a rabbit subdermal abscess model (Frank et al., 2014). The stringent response, a bacterial stress adaption mechanism, is characterized by the repression of fundamental cellular pathways, whereas amino acid biosynthesis genes and stress-survival genes are strongly induced. In addition,

metabolic rearrangements including the utilization of alternative carbon sources are a hallmark of the stringent response (Traxler et al., 2008; Gaca et al., 2012).

In co-colonization with other microbes, however, *E. faecalis* gene expression in inflamed mice is not primarily characterized by the induction of stress-response pathways, but rather by an enrichment of pathways important for bacterial growth and replication. Although some genes important for bacterial adaption to environmental stress were up regulated (e.g. arginine deaminase pathway genes, *opuC*, *phrB*) (van de Guchte et al., 2002; Maadani et al., 2007), the transcriptional profile does not indicate a stringent response state as observed in monoassociated *E. faecalis*. Fundamental cellular pathways like replication and translation were induced and the expression of general stress-response genes like *clpE*, *clpP*, *dnaK*, *dnaJ*, *groEL*, *groES* was repressed (Giard et al., 2001; Gaca et al., 2012; Muller et al., 2015).

Previous studies analyzing *E. faecalis* function in chronic inflammation were conducted in monoassociated IL-10$^{-/-}$ mice and revealed a colitogenic behavior (Balish and Warner, 2002; Kim et al., 2005; Steck et al., 2011; Ocvirk et al., 2015). By characterizing *E. faecalis* as part of a microbial consortium, we are adding new knowledge to the complex interdependence of opportunistic pathogens, the genetically predisposed host and the microbial environment. Colonization of IL10$^{-/-}$ mice with SIHUMI under omission of *E. faecalis* resulted in a more severe phenotype as indicated by the histological inflammation, spleen weights and the pro-inflammatory cytokine expression in colon tissue. This supports the hypothesis that *E. faecalis* provides protective mechanisms in complex consortia by the utilization of EA. A massive pro-inflammatory response of re-activated MLN cells to *E. coli* lysate stimulation and a positive correlation between histopathology and *E. coli* abundance pointed to this bacterium as main driver of SIHUMI mediated colitis.

Surprisingly, colonization of IL-10$^{-/-}$ mice with SIHUMI under omission of supposedly colitogenic *E. coli* resulted again in a more severe inflammatory phenotype in colon. This suggests that the colitogenic activity of *E. coli* is compensated by other members of the consortium. The protective function of *E. coli* presence was only observed in colon, not in cecum, where the absence of *E. coli* led to less severe inflammation. Kim and colleagues showed that *E. coli*-driven inflammation is most prevalent in cecum in IL-10$^{-/-}$ mice (Kim et al., 2005) which supports our finding that *E. coli* is partly responsible for the development of cecal but not colonic inflammation in SIHUMI colonized IL-10$^{-/-}$ mice.

Bacterial antigen-specific immune responses by MLN cells and serum IgG reactivity suggest *E. faecalis* as the species that mainly triggers the inflammation in colon when *E. coli* is not present. This stands in marked contrast to our previous experiment, where we observed a protective effect of *E. faecalis* in SIHUMI colonized mice. This indicates a reciprocal interaction between the opportunistic

pathogens *E. faecalis* and *E. coli*. In the absence of one, the other becomes more colitogenic than in the presence of both. In conclusion, our experiments with the SIHUMI consortium emphasize the dualistic character of opportunistic pathogens and show that the colitogenic function of a bacterial strain is not only defined by its gene repertoire, but also by co-colonizing microbes.

Some examples can be found in literature that microbe-host interactions can be influenced by the microbial environment. Simultaneous colonization of IL-10$^{-/-}$ mice with *E. coli* and *E. faecalis* resulted in more aggressive colitis as compared to disease induced by each species individually (Kim et al., 2007). *Helicobacter hepaticus*, an opportunistic mouse pathogen, causes disease in mouse models of experimental colitis in combination with a complex SPF microbiota (Cahill et al., 1997). *H. hepaticus* and *Lactobacillus reuteri* do not induce disease in monoassociated IL-10$^{-/-}$ mice, but when both strains are used in a dual-association system, they induce severe colitis (Whary et al., 2011). This indicates that *H. hepaticus* requires the presence of other microbes to trigger or exacerbate disease in susceptible IL-10$^{-/-}$ mice.

The presence of *Klebsiella pneumoniae* and *Proteus mirabili*, both opportunistic pathogens associated with nosocomial infections, correlated with colitis in a mouse model of ulcerative colitis. The infection of Rag2-deficient and WT mice with *K. pneumoniae*, *P. mirabilis*, or a combination of both strains triggered inflammation in the presence of a complex specific-pathogen free (SPF) microbiota. However, *K. pneumoniae* and *P. mirabilis* dual-association of germfree mice did not result in the development of colitis (Garrett et al., 2010).

Similarly, in the SCID mouse model, segmented filamentous bacteria were only effective in triggering intestinal inflammation in combination with a complex SPF microbiota (Stepankova et al., 2007). Vice versa, *E. coli* induces colitis in gnotobiotic IL-2-deficient mice, but co-association with *B. vulgatus* prevents colitis development (Waidmann et al., 2003). In addition, Ganesh and colleagues were able to demonstrate that *Akkermansia municiphila*, a mucin-degrading commensal, exacerbates *S. typhimurium*-induced intestinal inflammation in gnotobiotic mice by disturbance of the host-mucus homeostasis (Ganesh et al., 2013).

5. CONCLUSION & PERSPECTIVE

In summary, we demonstrate that *E. faecalis* gene expression and colitogenic activity is influenced by co-colonizing microbes. This emphasizes the use of microbial consortia to investigate bacterial functions that may not be apparent in monoassociated studies. The protective effect of *E. faecalis* EA utilization was only apparent in SIHUMI colonized mice, not in monoassociation. Further work is needed to identify the mechanisms contributing to the protective effect of *E. faecalis eut* gene expression. A first step would be to measure EA concentrations in luminal content of mice colonized with SIHUMI, including either *E. faecalis* OG1RF or Δ*eut* mutant. This would clarify whether *E. faecalis* utilizes EA in co-colonization with the consortium and whether this prevents the utilization of EA by another member of the bacterial community.

We showed that in the absence of the opportunistic pathogens *E. faecalis* or *E. coli*, other SIHUMI species increase their colitogenic potential, leading to a worsening of the inflammatory phenotype. This indicates that biodiversity is important even on such a small scale and highlights bacterial interaction and competition for the maintenance of a homeostatic ecosystem. Our data suggest that it is important to study interactions between intestinal species in detail, as bacteria can change their colitogenic potential depending on co-colonizing bacteria. Future experiments with minimal bacterial consortia may help to dissect the complex disease-relevant microbe-microbe and microbe-host interactions in chronic intestinal inflammation. A reasonable approach to unravel those complex mechanisms would be to reduce the diversity and colonize susceptible mice with all possible combinations of a minimal consortium consisting of only *E. faecalis*, *E. coli* and an obligate anaerobic species like *B. vulgatus*.

The investigation of disease progression and the measurement of immune cell subsets and antigen-specific immune responses can contribute to a better understanding of the complex interplay between microbes and the host's immune system. In addition, the generation of fluorescence-labeled bacterial species would make it possible to easily determine absolute bacterial counts and their specific intestinal location within the consortium.

Transcriptional interactions between members of the minimal bacterial consortium could be investigated by the use of metatranscriptomics. Based on the transcriptomic data set, targeted deletion of bacterial genes and the targeted measurement of metabolites, like short-chain fatty acids, bile acids and EA would give functional insight into microbe-microbe interactions relevant for the development of chronic inflammation.

Starting with a simple system and gradually adding more complexity is a complementary approach to screening for disease-associated microbial signatures in complex ecosystems by sequencing

techniques. Only a combination of both approaches will finally contribute to a basic understanding of the pathogenesis of human IBD.

ADDENDUM

Supplementary figures

A

B
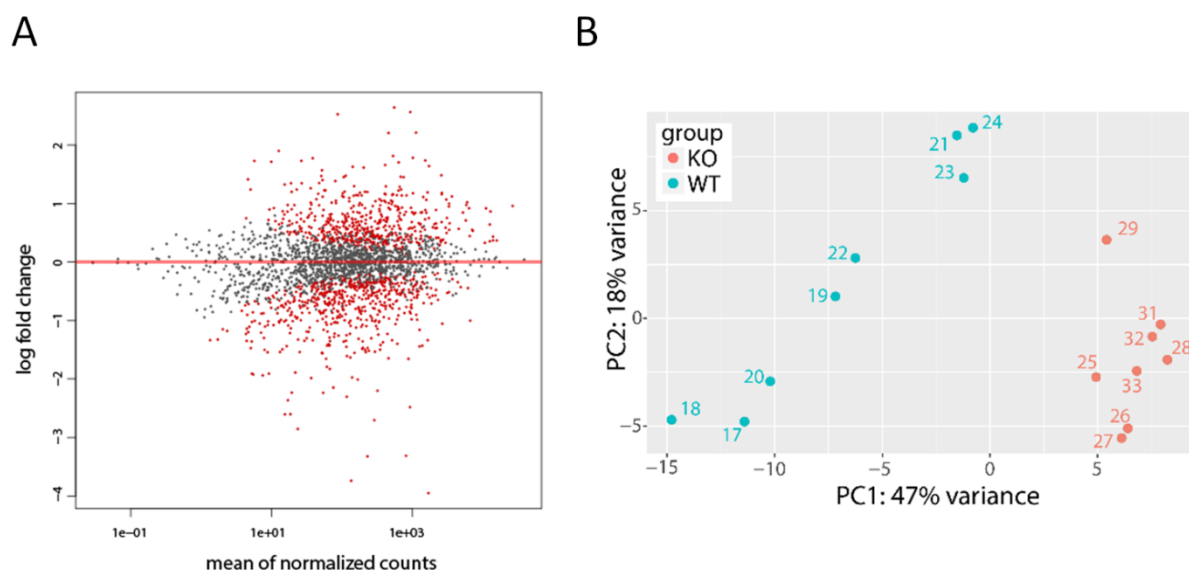
Figure S1
(A) Differentially expressed genes in *E. faecalis* isolated from monoassociated IL-10$^{-/-}$ (KO) vs. WT mice. MA plot shows the distribution of log2 fold changes in gene expression, the average of the counts normalized by size factor is shown on the x-axis. Each gene is represented with a dot. Genes with an adjusted p-value below 0.05 are indicated in red. **(B)** PCA plot showing sample-to-sample distances according to their gene expression profiles for *E. faecalis* isolated from monoassociated IL-10$^{-/-}$ vs. WT mice.

A

B
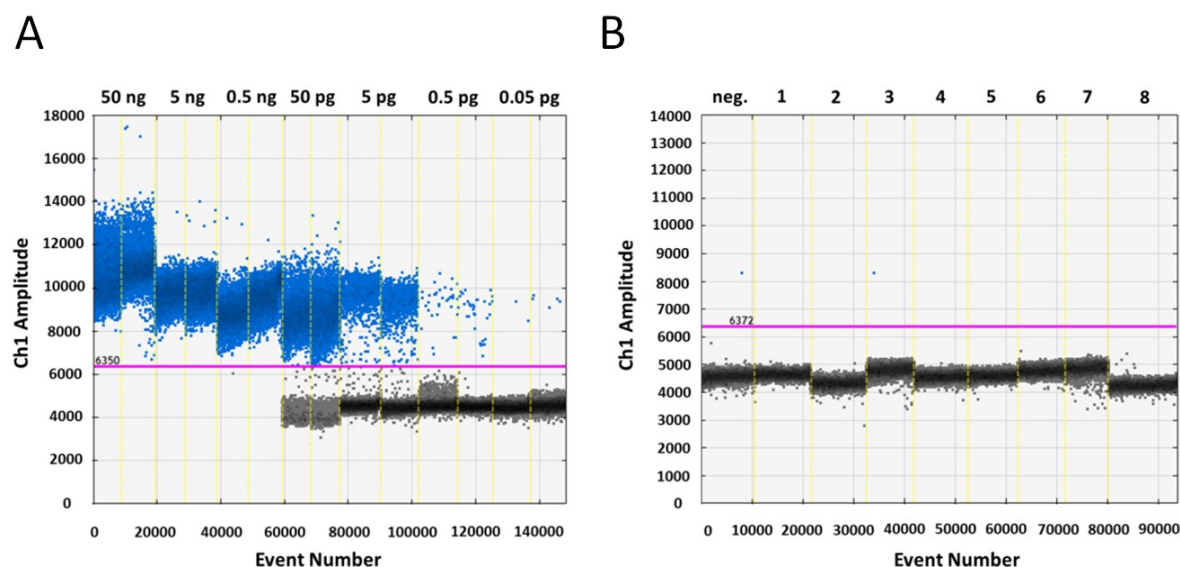
Figure S2
Droplet digital PCR: PCR positive droplets are color-coded in blue, primers are targeted against *F. prausnitzii* 16S rRNA. **(A)** Standard curve with *F. prausnitzii* DNA isolated from culture, DNA concentration per reaction (blue). **(B)** Droplet digital PCR reaction with 50 ng of total DNA isolated from luminal colon content of germfree (neg.) and SIHUMI colonized IL-10$^{-/-}$ (#1-4) and WT (#5-8) mice after a colonization period of 4 (#1,2,5,6) and 16 weeks (#3,4,7,8).
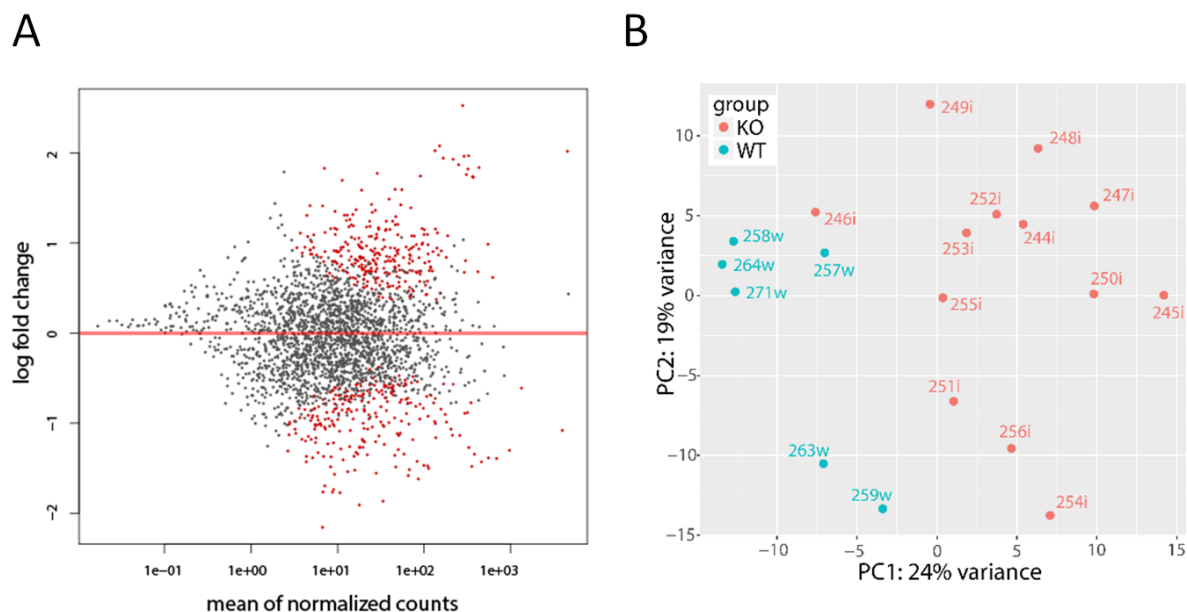
Figure S3
Differentially expressed genes in *E. faecalis* isolated from SIHUMI colonized IL-10$^{-/-}$ (KO) vs. WT mice. **(A)** MA plot shows the distribution of log2 fold changes in the gene expression, the average of the counts normalized by size factor is shown on the x-axis. Each gene is represented with a dot. Genes with an adjusted p-value below 0.5 are indicated in red. **(B)** PCA plot showing sample-to-sample distances according to their gene expression profiles**.**
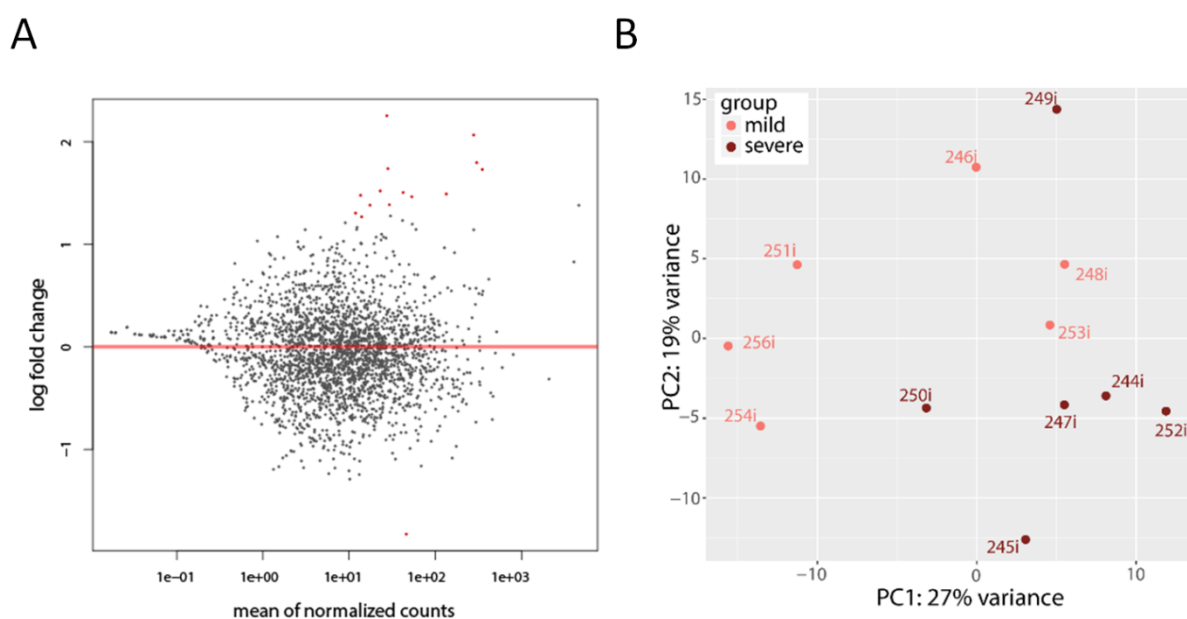
Figure S4
Differentially expressed genes in *E. faecalis* isolated from SIHUMI colonized severely inflamed IL-10$^{-/-}$ vs. mildly inflamed IL-10$^{-/-}$ mice. **(A)** MA plot shows the distribution of log2 fold changes in the gene expression, the average of the counts normalized by size factor is shown on the x-axis. Each gene is represented with a dot. Genes with an adjusted p-value below 0.5 are indicated in red. **(B)** PCA plot showing sample-to-sample distances according to their gene expression profiles.
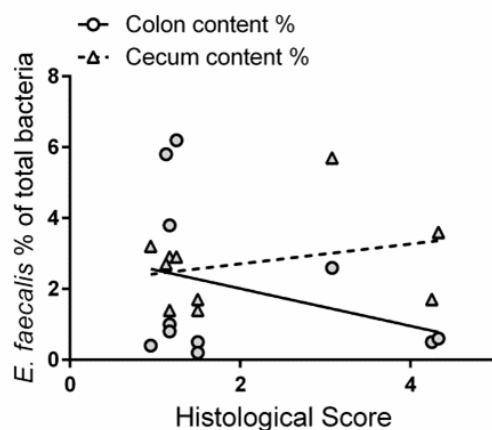
Figure S5
Germfree IL10$^{-/-}$ and WT mice were colonized with SIHUMI consortium or SIHUMI consortium without *E. faecalis* (*-E. fae*). Correlation between *E. faecalis* abundance (colon and cecum luminal content) and mean histological scores of cecum tip and distal colon after 16 weeks of colonization.
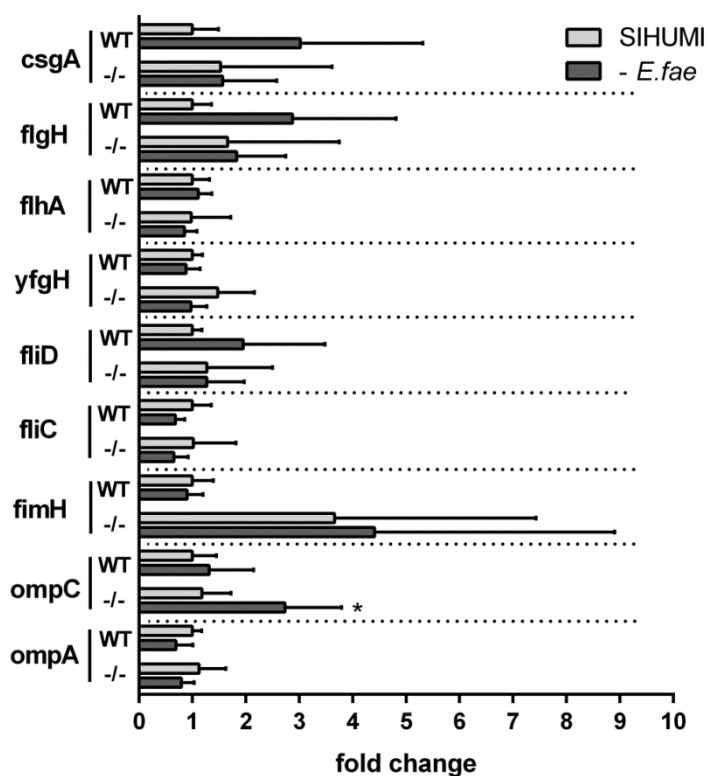
Figure S6
Germfree IL10$^{-/-}$ and WT mice were colonized with SIHUMI consortium or SIHUMI consortium without *E. faecalis* (*-E. fae*) for a period of 16 weeks. Expression of selected *E. coli* LF82 virulence genes shown as fold change normalized to expression levels in WT mice colonized with SIHUMI consortium.

Supplementary tables

Table S1: Significantly differentially regulated genes between *E. faecalis* isolated from monoassociated IL-10^{-/-} vs. WT mice

Gene_ID	Description	log2(FC)	P-adj
EBG00001209378	RatA	-1,00788781	0,01015785
EBG00001209390	tracrRNA	-1,01596151	0,00508251
EBG00001209416	rli28	-0,55492442	0,00349241
EBG00001209423	BsrC	-0,41891108	0,04007474
EBG00001209427	rli28	-0,87641007	0,01850041
EBG00001209441	rli28	-0,5749175	1,95E-05
EBG00001209458	rliD	-0,97202493	5,50E-05
OG1RF_10002	DNA-directed DNA polymerase III beta subunit	0,23124277	0,04448236
OG1RF_10010	DHH family protein	0,34302665	0,03304811
OG1RF_10011	50S ribosomal protein L9	0,40269309	0,02165049
OG1RF_10018	PTS family mannose/fructose/sorbose porter component IIB	0,35924567	0,03364785
OG1RF_10019	PTS family mannose porter, IIAB component	0,433301	0,00239349
OG1RF_10020	PTS family mannose/fructose/sorbose porter component IIC	0,32721885	0,04381245
OG1RF_10021	PTS family mannose/fructose/sorbose porter component IID	0,36856151	0,00407813
OG1RF_10024	hypothetical protein	-0,83929923	0,00200567
OG1RF_10030	ABC superfamily ATP binding cassette transporter permease subunit	1,23957087	0,00332783
OG1RF_10039	DNA repair protein RadA	0,24794883	0,00788907
OG1RF_10041	2-C-methyl-D-erythritol 2,4-cyclodiphosphate synthase	0,21010427	0,02445913
OG1RF_10042	glutamate--tRNA ligase	0,36944772	0,00011805
OG1RF_10043	serine O-acetyltransferase	0,85540798	5,83E-06
OG1RF_10044	cysteine--tRNA ligase	0,61260914	6,24E-05
OG1RF_10045	cysteine--tRNA ligase	0,7468755	0,00055138
OG1RF_10046	RNA methyltransferase	0,69542991	8,71E-05
OG1RF_10047	protein of hypothetical function DUF901	0,72379828	0,00020619
OG1RF_10049	Veg protein	-0,34644162	0,00200213

OG1RF_10050	4-diphosphocytidyl-2-C-methyl-D-erythritol kinase	-0,58211074	0,0030243
OG1RF_10052	ABC superfamily ATP binding cassette transporter, ABC protein	0,5309233	0,00335156
OG1RF_10056	5'-nucleotidase	-0,70294044	0,00032534
OG1RF_10057	oligopeptide ABC superfamily ATP binding cassette transporter, binding protein	-0,67126877	0,03020629
OG1RF_10060	crossover junction ATP-dependent DNA helicase RuvA	-0,46266755	0,00361598
OG1RF_10063	N-acylglucosamine-6-phosphate 2-epimerase	0,45957928	0,00755114
OG1RF_10064	glycoside hydrolase family protein	1,12019121	2,23E-12
OG1RF_10065	cro/CI family transcriptional regulator	-2,8524993	7,14E-18
OG1RF_10066	crp/Fnr family transcriptional regulator	-1,82837262	8,56E-13
OG1RF_10074	hypothetical protein	-0,9032558	0,03304811
OG1RF_10079	major facilitator family transporter	2,52566857	1,58E-06
OG1RF_10080	hypothetical protein	1,8988133	0,00042639
OG1RF_10083	M protein trans-acting positive regulator	-0,68680891	0,01978443
OG1RF_10084	cell wall surface anchor protein	0,92069332	0,00209309
OG1RF_10085	diacylglycerol kinase catalytic domain protein	0,75346236	0,02991567
OG1RF_10086	M protein trans-acting positive regulator	1,00677309	3,38E-10
OG1RF_10088	cell wall surface anchor family protein	0,42103158	0,00775566
OG1RF_10089	formate/nitrite transporter	1,03704092	2,22E-05
OG1RF_10104	ThiJ/PfpI family protein	-0,43978328	0,0475461
OG1RF_10106	oxidoreductase	-0,57376854	0,01683046
OG1RF_10107	family 20 glycosyl hydrolase	0,68292864	1,47E-05
OG1RF_10109	hypothetical protein	0,43149404	0,03994447
OG1RF_10110	GntR family transcriptional regulator	0,48816322	0,00919019
OG1RF_10121	pyrimidine-nucleoside phosphorylase	0,9291014	1,71E-09
OG1RF_10122	deoxyribose-phosphate aldolase	0,9010508	2,29E-08
OG1RF_10123	cytidine deaminase	1,19710536	3,73E-10
OG1RF_10124	ABC superfamily ATP binding cassette transporter, binding protein	1,13882769	3,73E-10
OG1RF_10125	ABC superfamily ATP binding cassette transporter, binding protein	0,99826101	1,72E-10

OG1RF_10126	ABC superfamily ATP binding cassette transporter, ABC protein	0,64730304	1,56E-07
OG1RF_10127	ABC superfamily, ATP binding cassette transporter, membrane protein	0,83746677	2,76E-07
OG1RF_10128	ABC superfamily, ATP binding cassette transporter, membrane protein	0,92690646	5,34E-10
OG1RF_10133	phosphopentomutase	0,58686618	6,31E-06
OG1RF_10134	purine-nucleoside phosphorylase	0,58093601	9,65E-08
OG1RF_10135	purine nucleoside phosphorylase	0,59166369	2,40E-11
OG1RF_10139	iron ABC superfamily ATP binding cassette transporter, membrane protein	0,62428609	0,00568331
OG1RF_10140	putative alcohol dehydrogenase (NADP(+))	0,8394048	0,00139012
OG1RF_10149	cyclopropane-fatty-acyl-phospholipid synthase	0,95847386	1,87E-07
OG1RF_10151	50S ribosomal protein L3	0,42219305	0,01710261
OG1RF_10153	50S ribosomal protein L23	0,46643243	0,01610637
OG1RF_10156	50S ribosomal protein L22	0,40232703	0,04802135
OG1RF_10182	ABC superfamily ATP binding cassette transporter, ABC protein	-0,38581425	0,01196534
OG1RF_10188	GNAT family acetyltransferase	1,71320821	0,00078465
OG1RF_10192	hypothetical protein	0,41560165	0,01231316
OG1RF_10195	maltose O-acetyltransferase	0,36503046	0,00028641
OG1RF_10197	N-acetylmuramoyl-L-alanine amidase	-0,4273096	0,02046738
OG1RF_10212	lysine--tRNA ligase	-0,28332842	0,03392153
OG1RF_10218	thioesterase	-0,35879058	0,04100758
OG1RF_10221	DNA-3-methyladenine glycosylase I	0,50176959	0,01304159
OG1RF_10223	CDF family cation diffusion facilitator	0,58091345	0,00144981
OG1RF_10224	hypothetical protein	0,77430795	1,07E-08
OG1RF_10226	3-oxoacyl-(acyl-carrier-protein) synthase II	0,45890681	0,01761967
OG1RF_10227	(3R)-hydroxymyristoyl-[acyl-carrier-protein] dehydratase	0,57607405	0,04277537
OG1RF_10229	fibronectin-binding protein	0,69306663	0,00607995
OG1RF_10231	hypothetical protein	0,50165076	0,02965952
OG1RF_10233	cystathionine gamma-synthase	0,86069144	0,00810067
OG1RF_10234	6-phospho-beta-glucosidase	1,73467198	3,38E-17

OG1RF_10235	PTS family lactose-N,N'-diacetylchitobiose-beta-glucoside (lac) porter component IIBC	0,84955026	1,36E-06
OG1RF_10236	RpiR family transcriptional regulator	-2,20145996	3,03E-33
OG1RF_10241	copper-exporting ATPase	0,50500946	4,43E-06
OG1RF_10242	MerTP family copper permease, binding protein CopZ	0,55892383	0,01010817
OG1RF_10243	hypothetical protein	1,22154914	6,81E-09
OG1RF_10244	GntR family transcriptional regulator	0,83409095	0,00134904
OG1RF_10245	aminopeptidase C	0,2180949	0,00106315
OG1RF_10246	flavin reductase domain protein, FMN-binding protein	1,12486745	0,00125592
OG1RF_10247	lactoylglutathione lyase	1,04918853	0,00144981
OG1RF_10250	chitinase C1	-0,77304375	0,04958873
OG1RF_10255	aspartate kinase	-0,50141449	0,00249852
OG1RF_10256	HAD-superfamily hydrolase	-0,45987501	0,01880379
OG1RF_10259	response regulator	-0,57477249	0,00192282
OG1RF_10260	sensor histidine kinase	-0,57392	0,00323307
OG1RF_10261	S-layer protein	-0,92739993	3,74E-05
OG1RF_10262	S-layer protein	-0,87252096	4,24E-06
OG1RF_10263	S-layer protein	-1,64663399	1,13E-11
OG1RF_10265	ankyrin repeat family protein	-1,45006785	7,53E-12
OG1RF_10266	amidohydrolase	-1,00449839	8,15E-09
OG1RF_10269	hypothetical protein	0,83877709	5,63E-05
OG1RF_10270	hypothetical protein	0,75193886	5,04E-05
OG1RF_10271	hypothetical protein	-0,44759375	0,01555932
OG1RF_10273	major facilitator family transporter	-0,54554505	0,0032949
OG1RF_10274	carbamate kinase	-0,73068837	0,00025633
OG1RF_10275	sodium/dicarboxylate symporter family protein	-0,79545289	7,16E-06
OG1RF_10276	ureidoglycolate dehydrogenase	-0,89982891	8,53E-05
OG1RF_10277	UIT9 family protein	-1,12159199	1,03E-05
OG1RF_10278	N-isopropylammelide isopropylaminohydrolase	-1,01265834	5,79E-05

OG1RF_10281	secreted antigen	-0,44611903	0,02557174
OG1RF_10286	membrane protein	0,49877863	0,02671868
OG1RF_10287	pyroglutamyl-peptidase I	0,44149713	0,0113822
OG1RF_10288	Na+/H+ antiporter NhaC	0,74053415	0,01560135
OG1RF_10295	hypothetical protein	-2,1471761	7,52E-26
OG1RF_10301	efflux transporter	-0,38505403	0,03193611
OG1RF_10314	RhiN protein	-0,94859099	0,00125408
OG1RF_10315	TRAP-T family tripartite ATP-independent periplasmic transporter, binding protein	-1,4293094	2,02E-17
OG1RF_10316	TRAP-T family tripartite ATP-independent periplasmic transporter, membrane protein	-1,32541771	5,84E-09
OG1RF_10317	TRAP-T family tripartite ATP-independent periplasmic transporter, membrane protein	-1,24971716	1,65E-12
OG1RF_10319	rhamnulokinase	-1,22333139	7,98E-08
OG1RF_10320	L-rhamnose isomerase	-1,29251863	3,01E-13
OG1RF_10321	rhamnulose-1-phosphate aldolase	-0,93278378	3,72E-05
OG1RF_10322	L-rhamnose 1-epimerase	-1,08460254	3,31E-05
OG1RF_10323	AraC family transcriptional regulator	-1,03818914	9,89E-06
OG1RF_10324	family 2 AP endonuclease	-1,18930598	2,87E-06
OG1RF_10328	peptidoglycan binding protein	1,20012135	9,78E-05
OG1RF_10336	putative glucosamine-6-phosphate deaminase	-0,7643091	0,01004625
OG1RF_10339	hypothetical protein	-0,57375111	0,03453243
OG1RF_10350	transcriptional regulator	-0,33499204	0,00359267
OG1RF_10358	glutaredoxin	0,5598743	0,01611004
OG1RF_10359	ferrous iron transport protein A	0,82215852	0,00028498
OG1RF_10360	FeoB family ferrous iron (Fe2+) uptake protein	0,96915061	3,79E-08
OG1RF_10361	hypothetical protein	0,76166538	0,00080955
OG1RF_10367	decarboxylase	1,63921853	4,92E-15
OG1RF_10368	amino acid permease	1,45007633	8,62E-11
OG1RF_10369	Na+/H+ antiporter NhaC	1,14010984	3,01E-06
OG1RF_10370	hypothetical protein	1,06733979	0,00034052

OG1RF_10374	hypothetical protein	-0,53026458	0,01793744
OG1RF_10380	nitroreductase	-0,58637902	0,00899964
OG1RF_10382	hypothetical protein	-1,50589089	1,09E-21
OG1RF_10388	DeoR family transcriptional regulator	1,26013256	1,28E-07
OG1RF_10389	Xaa-Pro aminopeptidase	0,61115616	0,00948055
OG1RF_10390	uracil-DNA glycosylase	0,96996172	2,73E-05
OG1RF_10394	glucose-1-phosphate adenylyl transferase	0,55706469	0,00061741
OG1RF_10395	C_GCAxxG_C_C family protein	0,40752529	0,00263567
OG1RF_10396	hypothetical protein	0,76097143	0,02470595
OG1RF_10397	lactoylglutathione lyase	1,13835228	5,91E-05
OG1RF_10402	dipeptidase PepV	0,5199899	4,92E-05
OG1RF_10404	csn1 family CRISPR-associated protein	-0,9032818	9,93E-07
OG1RF_10405	CRISPR-associated protein cas1	-1,14167172	8,34E-09
OG1RF_10406	CRISPR-associated protein cas2	-1,03052249	5,87E-07
OG1RF_10407	csn2 family CRISPR-associated protein	-0,99146478	7,87E-08
OG1RF_10408	hypothetical protein	-1,35224508	1,00E-17
OG1RF_10416	ribosomal large subunit pseudouridine synthase	0,55982733	0,00545008
OG1RF_10423	peptidyl-prolyl cis-trans isomerase	-0,39008088	0,01234478
OG1RF_10429	tRNA (guanine-N(7)-)-methyltransferase	-0,53624074	0,02364283
OG1RF_10431	1-phosphofructokinase	1,46953092	8,82E-10
OG1RF_10432	PTS family fructose porter component IIBC	0,61953166	0,01037304
OG1RF_10433	PTS family fructose/mannitol (fru) porter component IIA	0,68376287	0,0075383
OG1RF_10434	tagatose-bisphosphate aldolase	0,65643011	0,02681753
OG1RF_10444	ATP-dependent Clp protease	1,48323734	2,06E-10
OG1RF_10447	PTS family porter, phosphocarrier protein HPR	0,32250733	0,00520254
OG1RF_10449	hypothetical protein	-0,8196161	0,01016955
OG1RF_10452	trigger factor	-0,29664109	0,02436934
OG1RF_10453	hypothetical protein	-0,41662594	0,02480989

OG1RF_10459	NAD-dependent DNA ligase LigA	0,33830778	0,00954597
OG1RF_10479	sodium/dicarboxylate symporter family protein	-0,58030818	0,00219061
OG1RF_10497	excision endonuclease subunit UvrB	0,46226901	0,01418949
OG1RF_10498	excision endonuclease subunit UvrA	0,5421912	3,60E-08
OG1RF_10499	hypothetical protein	-1,97350693	2,44E-37
OG1RF_10502	protein of hypothetical function DUF199	0,302782	0,00086574
OG1RF_10503	PEP phosphonomutase family protein	-0,42826289	0,04259326
OG1RF_10504	thioredoxin superfamily protein	0,72855603	0,00154234
OG1RF_10505	ATP-dependent Clp protease proteolytic subunit	0,57747958	0,0008151
OG1RF_10511	glycerophosphoryl diester phosphodiesterase	0,36769896	0,00986308
OG1RF_10513	cold shock protein B	-0,51481561	0,02387764
OG1RF_10514	DNA-directed RNA polymerase sigma subunit RpoN	0,77405731	2,70E-07
OG1RF_10518	MFS family drug resistance transporter	1,07365135	1,02E-10
OG1RF_10519	esterase	0,70129746	7,18E-08
OG1RF_10526	ABC superfamily ATP binding cassette transporter, membrane protein	1,00617366	0,000752
OG1RF_10527	ABC superfamily ATP binding cassette transporter, ABC protein	1,11482688	9,46E-05
OG1RF_10531	hypothetical protein	-0,44290288	5,46E-05
OG1RF_10532	hypothetical protein	-0,66519641	0,00033837
OG1RF_10546	GntR family transcriptional regulator	-0,75863939	0,03392153
OG1RF_10548	PTS family mannose/fructose/sorbose porter component IIC	-0,77223328	0,00037234
OG1RF_10549	PTS family mannose/fructose/sorbose porter component IID	-0,67503398	0,00851158
OG1RF_10550	family 8 polysaccharide lyase	-1,09332709	5,27E-07
OG1RF_10552	50S ribosomal protein L25	0,84316298	0,00815942
OG1RF_10554	HAD-superfamily hydrolase	0,40070273	0,0475461
OG1RF_10581	hypothetical protein	-1,90843464	1,78E-08
OG1RF_10582	hypothetical protein	-1,88993418	3,05E-10
OG1RF_10583	hypothetical protein	-1,90927699	8,45E-06
OG1RF_10584	signal peptidase I	-1,50287676	5,46E-05

OG1RF_10585	M protein trans-acting positive regulator	-1,03314013	1,92E-09
OG1RF_10586	putative protein-tyrosine-phosphatase	-0,68278509	0,00153734
OG1RF_10590	APC family amino acid-polyamine-organocation transporter	0,49285469	0,03916049
OG1RF_10598	S-adenosylmethionine:tRNA ribosyltransferase-isomerase	0,36094353	0,0380268
OG1RF_10601	potassium uptake protein	0,53156989	0,02834342
OG1RF_10605	aldo/keto reductase 2 family oxidoreductase	0,50284088	4,18E-05
OG1RF_10608	dephospho-CoA kinase	-0,36501745	0,04870643
OG1RF_10621	amino acid ABC superfamily ATP binding cassette transporter, membrane protein	0,7803299	0,02643437
OG1RF_10626	hypothetical protein	-0,67836323	0,00840846
OG1RF_10640	transposase	-0,52835954	0,04277537
OG1RF_10651	hypothetical protein	0,64377861	0,04372348
OG1RF_10652	hypothetical protein	0,74117763	0,00239349
OG1RF_10653	response regulator	0,44169319	0,0126155
OG1RF_10659	hypothetical protein	-0,86731684	0,00938841
OG1RF_10661	TatD family hydrolase	-0,41477477	0,00077886
OG1RF_10662	primase-like protein	-0,27390645	0,04372348
OG1RF_10663	dimethyladenosine transferase	-0,26997388	0,00217517
OG1RF_10666	methylglyoxal synthase	0,76261703	0,00086576
OG1RF_10667	hypothetical protein	0,68930786	0,00214519
OG1RF_10668	ABC superfamily ATP binding cassette transporter, membrane protein	0,31177843	0,01924342
OG1RF_10672	GNAT family acetyltransferase	-1,00835738	1,98E-05
OG1RF_10674	exopolyphosphatase	-0,30253141	0,00212907
OG1RF_10676	phosphate acetyltransferase	-0,64511544	0,00251551
OG1RF_10679	hypothetical protein	0,51197445	0,03238592
OG1RF_10680	LacI family sugar-binding transcriptional regulator	-1,33742756	1,42E-10
OG1RF_10681	aldose 1-epimerase	-2,0101365	1,62E-11
OG1RF_10682	beta-phosphoglucomutase	-3,32274835	3,10E-17
OG1RF_10683	family 65 glycosyl hydrolase	-3,31311317	7,41E-19

OG1RF_10684	PTS family porter component IIABC	-3,95168245	2,42E-55
OG1RF_10685	endonuclease/exonuclease/phosphatase family protein RgfB	-3,73998909	2,71E-54
OG1RF_10699	hypothetical protein	-0,61051051	0,0006487
OG1RF_10708	xaa-Pro dipeptidase	0,42449253	0,00025379
OG1RF_10709	MagZ family protein	0,57114142	2,24E-05
OG1RF_10710	alkaline shock protein	-0,23724896	0,00075505
OG1RF_10711	transcription antitermination factor NusB	-0,25104865	0,0099453
OG1RF_10712	bifunctional methylenetetrahydrofolate dehydrogenase/methylenetetrahydrofolate cyclohydrolase	-0,4233088	0,00389471
OG1RF_10713	exodeoxyribonuclease VII large subunit	-0,35325913	0,02679187
OG1RF_10720	putative lipoprotein	-0,57133234	0,02958407
OG1RF_10721	cell division protein MraZ	-0,51859421	0,00024258
OG1RF_10722	S-adenosyl-methyltransferase MraW	-0,44352098	0,00282131
OG1RF_10723	cell division protein	-0,47837855	0,00539058
OG1RF_10740	sugar fermentation stimulation protein	-0,49109198	0,01173222
OG1RF_10745	PTS family porter, enzyme I	-1,43871163	2,39E-05
OG1RF_10746	PTS family lactose/cellobiose porter component IIC	-0,8239363	0,00101272
OG1RF_10748	hypothetical protein	-0,69818154	0,04367727
OG1RF_10753	6-phospho-beta-glucosidase	-0,89837795	6,47E-05
OG1RF_10755	hypothetical protein	0,8898	0,02282718
OG1RF_10758	CBS domain protein	-0,71504576	0,00926081
OG1RF_10766	amidase	-0,94508763	2,28E-05
OG1RF_10768	lipoprotein	-0,54378667	0,01544933
OG1RF_10769	nucleoside diphosphate kinase	-0,35586622	0,01555421
OG1RF_10770	aspartate aminotransferase	0,73047512	0,04367654
OG1RF_10771	putative lipoprotein	-0,83569022	0,00016782
OG1RF_10774	xanthine/uracil permease family protein	-1,06039029	0,02654089
OG1RF_10775	drug:H+ antiporter-1 family protein	0,48269008	0,02121762

OG1RF_10776	hypothetical protein	0,58776765	0,00381346
OG1RF_10777	DNA-directed DNA polymerase III alpha subunit	0,33266581	0,00462029
OG1RF_10778	6-phosphofructokinase	0,35855334	0,02480989
OG1RF_10779	pyruvate kinase	0,4951237	0,00070979
OG1RF_10780	nucleic acid-binding protein	-0,35975938	0,04493124
OG1RF_10783	response regulator	-0,30966744	0,01866494
OG1RF_10800	conjugative transposon ATP/GTP-binding protein	-0,65929833	0,02643437
OG1RF_10802	NLP/P60 family lipoprotein	-1,02620006	0,01266342
OG1RF_10806	hypothetical protein	1,41266533	0,0011451
OG1RF_10809	hypothetical protein	0,6986317	0,02260501
OG1RF_10810	hypothetical protein	0,97473177	0,00025797
OG1RF_10811	collagen adhesion protein	0,65751383	1,12E-11
OG1RF_10824	UvrD/REP helicase	-0,31140372	0,03752414
OG1RF_10827	hypothetical protein	-0,59982851	0,01133748
OG1RF_10828	membrane protein	-0,67944788	0,02244114
OG1RF_10830	membrane protein	-0,68426019	0,00628397
OG1RF_10837	tunicamycin resistance protein	-0,48303815	0,04576982
OG1RF_10849	galactokinase	0,284144	0,04801571
OG1RF_10852	galactose operon repressor GalR	0,2640962	0,03959316
OG1RF_10856	streptomycin 3''-adenylyltransferase	0,89009376	0,00097669
OG1RF_10857	GNAT family acetyltransferase	0,57633133	0,04719055
OG1RF_10858	MFS family major facilitator transporter	-0,51272428	0,03431125
OG1RF_10859	Y family DNA-directed DNA polymerase	0,80943472	0,00052682
OG1RF_10860	hypothetical protein	0,86771217	0,00986308
OG1RF_10867	integral membrane protein	1,00881432	6,28E-05
OG1RF_10872	sortase	-0,96687138	2,21E-06
OG1RF_10873	hypothetical protein	-0,96481791	6,88E-06
OG1RF_10875	hypothetical protein	1,62856571	0,0024271

OG1RF_10876	hypothetical protein	1,34673659	0,01544933
OG1RF_10878	collagen adhesin protein	-0,86928245	0,00503952
OG1RF_10881	hypothetical protein	-1,35988366	0,01511386
OG1RF_10895	glutamine ABC superfamily ATP binding cassette transporter, membrane protein	-1,01660731	0,00209897
OG1RF_10896	amino acid ABC superfamily ATP binding cassette transporter, membrane protein	-1,03413719	0,00190162
OG1RF_10897	glutamine ABC superfamily ATP binding cassette transporter, binding protein	-1,21478944	2,83E-05
OG1RF_10898	ABC superfamily ATP binding cassette transporter, ABC protein	-0,99532929	4,52E-05
OG1RF_10900	ribonuclease PH/Ham1 protein	0,39599886	0,00038657
OG1RF_10901	phosphoesterase	0,47645248	0,00116151
OG1RF_10909	L-ribulose-5-phosphate 4-epimerase	0,53077577	0,04663151
OG1RF_10913	mechanosensitive ion channel	-0,3818136	0,00822483
OG1RF_10915	2,5-diketo-D-gluconate reductase	0,57887922	0,03929468
OG1RF_10920	HD domain protein	0,34545227	0,02426292
OG1RF_10921	lipoate--protein ligase A	0,43884425	0,00025379
OG1RF_10933	GntR family transcriptional regulator	0,64151907	0,01922926
OG1RF_10935	N4-(beta-N-acetylglucosaminyl)-L-asparaginase	-1,22772613	0,00758342
OG1RF_10936	PTS family porter, enzyme I	-1,33830496	0,00640224
OG1RF_10937	PTS family oligomeric beta-glucoside porter component IIC	-1,49891259	0,0006487
OG1RF_10938	hypothetical protein	-1,34634455	0,00257607
OG1RF_10939	hypothetical protein	-1,42678337	0,00153734
OG1RF_10940	DNA-directed DNA polymerase III epsilon subunit	0,62600133	2,66E-07
OG1RF_10941	asparaginase	0,72347365	2,94E-11
OG1RF_10942	HD domain protein	0,6063318	8,33E-06
OG1RF_10954	S-ribosylhomocysteine lyase	0,38842938	0,0201271
OG1RF_10955	aspartate-semialdehyde dehydrogenase	-0,26059884	0,02145815
OG1RF_10956	dihydrodipicolinate synthase	-0,32272634	0,00243507
OG1RF_10964	MIP family major intrinsic protein water channel AqpZ	0,80491837	0,03205537
OG1RF_10973	protein of hypothetical function DUF1212	-0,41965786	0,04653728

OG1RF_10977	cro/CI family TPR domain transcriptional regulator	1,09446717	1,75E-07
OG1RF_10984	transcriptional regulator	-0,4382374	0,0027445
OG1RF_10997	putative thiamine biosynthesis lipoprotein	0,39138291	0,044015
OG1RF_10998	NADPH-dependent FMN reductase domain protein	0,80219815	5,63E-05
OG1RF_10999	NADPH-dependent FMN reductase domain protein	0,97651931	2,29E-06
OG1RF_11000	M protein trans-acting positive regulator	0,51793481	0,01610455
OG1RF_11003	ABC superfamily ATP binding cassette transporter, membrane protein	0,82591101	1,06E-09
OG1RF_11004	ABC superfamily ATP binding cassette transporter, membrane protein	1,01431884	9,26E-09
OG1RF_11005	ABC superfamily ATP binding cassette transporter, substrate-binding protein	0,90564131	1,13E-10
OG1RF_11008	endonuclease/exonuclease/phosphatase	0,56624449	0,01077035
OG1RF_11009	putative beta-glucosidase	0,53736402	0,00170067
OG1RF_11012	hypothetical protein	0,6854368	0,00690116
OG1RF_11013	GntR family transcriptional regulator	-0,40952261	0,00995914
OG1RF_11019	fibronectin binding protein A	-0,53264242	7,84E-05
OG1RF_11021	hypothetical protein	-0,76338634	0,00065267
OG1RF_11025	integral membrane protein	-0,56802435	0,00425274
OG1RF_11036	E1-E2 family cation-transporting ATPase	0,6423542	2,62E-05
OG1RF_11047	cro/CI family transcriptional regulator	-0,63545625	0,00168895
OG1RF_11051	hypothetical protein	0,62969159	0,02671868
OG1RF_11070	FtsW/RodA/SpovE family cell division protein	0,73643015	0,00550026
OG1RF_11071	FtsW/RodA/SpovE family cell division protein	0,70139126	0,00813519
OG1RF_11078	chaperone DnaK	0,55150583	0,00650643
OG1RF_11079	hypothetical protein	0,69368764	0,00121755
OG1RF_11080	chaperone DnaJ	0,54933939	0,0111364
OG1RF_11085	aspartate aminotransferase	-0,32566043	0,02897908
OG1RF_11087	cro/CI family transcriptional regulator	-0,66148147	0,00318418
OG1RF_11093	hypothetical protein	-0,39127287	0,01028725
OG1RF_11094	SPFH domain/band 7 family protein	-0,525128	0,00090136

OG1RF_11095	hypothetical protein	-0,54932632	0,0432645
OG1RF_11096	hypothetical protein	-0,42244596	0,00629843
OG1RF_11097	TetR family transcriptional regulator	-0,48540197	0,0053368
OG1RF_11100	virulence factor EsxA	-2,48053269	1,66E-30
OG1RF_11101	YhgE/Pip domain protein	-1,65513169	7,48E-09
OG1RF_11102	hypothetical protein	-1,49338115	0,00069816
OG1RF_11103	YukD superfamily protein	-1,53747713	6,68E-05
OG1RF_11104	hypothetical protein	-2,23641747	3,01E-13
OG1RF_11105	cell division protein FtsK/SpoIIIE	-2,70455012	1,84E-20
OG1RF_11106	hypothetical protein	-2,60492355	6,25E-11
OG1RF_11107	hypothetical protein	-2,60077133	2,09E-11
OG1RF_11108	hypothetical protein	-2,36361911	2,67E-08
OG1RF_11109	hypothetical protein	-2,30466726	3,01E-13
OG1RF_11110	hypothetical protein	-2,23430192	2,24E-08
OG1RF_11111	hypothetical protein	-1,9232629	5,11E-05
OG1RF_11112	hypothetical protein	-1,33707496	0,01746518
OG1RF_11113	hypothetical protein	-1,93909986	3,53E-06
OG1RF_11114	hypothetical protein	-1,14044526	0,02407197
OG1RF_11115	putative virulence protein EssC	-0,66246671	0,02353539
OG1RF_11121	exopolyphosphatase	-1,29820617	0,0007344
OG1RF_11123	hypothetical protein	-1,23007114	0,00626555
OG1RF_11133	sugar ABC superfamily ATP binding cassette transporter, membrane protein	-1,63222985	5,46E-07
OG1RF_11134	sugar ABC superfamily ATP binding cassette transporter, membrane protein	-1,48571389	1,49E-05
OG1RF_11135	sugar ABC superfamily ATP binding cassette transporter, sugar-binding protein	-1,33706333	0,00010449
OG1RF_11136	neopullulanase	-1,01813057	0,00030435
OG1RF_11137	glucan 1,6-alpha-glucosidase	-0,96644794	0,00181123
OG1RF_11138	oligo-1,6-glucosidase	-0,98455588	0,00145592
OG1RF_11146	glycerol dehydrogenase	0,86434375	0,00796686

OG1RF_11147	glycerone kinase PTS family porter component IIA	0,9500304	0,00227091
OG1RF_11148	dihydroxyacetone kinase	0,91738908	0,00284648
OG1RF_11149	dihydroxyacetone kinase	0,97504842	0,00084902
OG1RF_11151	hydroxymethylglutaryl-CoA synthase	-0,41756748	0,04533503
OG1RF_11153	membrane protein	-0,32461073	0,01396626
OG1RF_11154	integral membrane protein	-0,33121337	0,04177475
OG1RF_11155	cold shock protein CspA	-0,53027565	0,00454392
OG1RF_11156	hypothetical protein	0,83619342	0,01813609
OG1RF_11162	alkylphosphonate uptake protein	-0,35120282	0,01361848
OG1RF_11166	transcriptional regulator	-0,54248285	0,00489886
OG1RF_11168	SAM-dependent methyltransferase	0,55823279	3,03E-06
OG1RF_11169	protein of hypothetical function DUF34	0,67952079	8,93E-11
OG1RF_11170	M20 family tripeptide aminopeptidase	0,68381177	1,02E-07
OG1RF_11174	FNT family formate-nitrite transporter	-0,74662252	0,04098265
OG1RF_11177	NADH-quinone oxidoreductase subunit F	-0,86743806	0,00237271
OG1RF_11178	NAD-dependent formate dehydrogenase, alpha subunit	-0,75103206	0,00088589
OG1RF_11179	molybdenum cofactor biosynthesis family protein	-0,80127911	0,00038828
OG1RF_11188	ABC superfamily ATP binding cassette transporter, ABC protein	-0,62182872	0,00153734
OG1RF_11189	zinc-exporting ATPase	-0,39305665	0,02671868
OG1RF_11190	hypothetical protein	-0,43915424	8,80E-05
OG1RF_11191	colicin V production protein CvpA family protein	-0,31282668	0,01326871
OG1RF_11193	thioredoxin	0,46708645	0,03821705
OG1RF_11198	LacI family sugar-binding transcriptional regulator	-0,55674993	0,00153734
OG1RF_11199	6-phospho-beta-glucosidase	-0,78882078	0,00638627
OG1RF_11200	hypothetical protein	-0,88426418	0,00043123
OG1RF_11201	ABC superfamily ATP binding cassette transporter, ABC protein	-0,87759285	0,01688671
OG1RF_11203	glutamate dehydrogenase	0,27492382	0,00500293
OG1RF_11204	glucose-6-phosphate isomerase	0,38136338	0,00038349

OG1RF_11207	V-type ATPase, subunit F	-0,9585687	3,23E-08
OG1RF_11208	proton (H+) or sodium (Na+) translocating V-type ATPase (V-ATPase), subunit I	-0,7939642	4,61E-05
OG1RF_11209	proton (H+) or sodium (Na+) translocating V-type ATPase (V-ATPase), subunit K	-0,67639771	0,00044927
OG1RF_11210	proton (H+) or sodium (Na+) translocating V-type ATPase (V-ATPase), subunit E	-0,78796177	0,00018862
OG1RF_11211	proton (H+) or sodium (Na+) translocating V-type ATPase (V-ATPase), subunit C	-0,82676062	0,0003819
OG1RF_11212	V-type ATP synthase subunit F	-0,79946128	0,0002966
OG1RF_11213	ATP synthase F1 sector alpha subunit	-0,98679166	3,06E-07
OG1RF_11214	proton (H+) or sodium (Na+) translocating V-type ATPase (V-ATPase), subunit B	-0,97978396	1,01E-05
OG1RF_11215	V-type ATP synthase subunit D	-0,94226796	4,57E-05
OG1RF_11216	hypothetical protein	-1,25811641	6,51E-06
OG1RF_11218	hypothetical protein	-1,05239769	0,00971662
OG1RF_11221	diaminopimelate decarboxylase	-0,36753647	0,04435354
OG1RF_11226	N-6 adenine-specific DNA methylase YitW	-0,49700186	8,40E-06
OG1RF_11230	SacPA operon antiterminator	-0,7012548	0,00428874
OG1RF_11231	PTS family glucose porter, IICBA component	-0,73880345	0,00060286
OG1RF_11232	DNA-binding/PRD domain protein	0,50758923	0,00680924
OG1RF_11233	PTS family porter component IIA	0,92206844	0,00221184
OG1RF_11234	PTS family fructose porter, IIB component	0,7342324	0,00638627
OG1RF_11235	PTS family porter component IIA	0,49814498	0,04937707
OG1RF_11236	PTS family porter component IIC	0,44052154	0,01925744
OG1RF_11237	ribulose-phosphate 3-epimerase	0,53585784	0,01389688
OG1RF_11240	E1-E2 family cation-transporting ATPase	-0,54182448	0,00011805
OG1RF_11241	DNA primase	-0,291741	0,02078478
OG1RF_11243	hypothetical protein	-0,46938965	3,74E-05
OG1RF_11244	S1 RNA binding domain protein	-0,75121831	7,11E-07
OG1RF_11245	ferric uptake regulation protein	-1,0040389	5,12E-08
OG1RF_11246	glyceraldehyde-3-phosphate dehydrogenase	0,66151359	0,03692611
OG1RF_11250	TetR family transcriptional regulator	-1,3484645	0,00731378

OG1RF_11252	hypothetical protein	-1,30220842	0,0011451
OG1RF_11253	peptidylprolyl isomerase	-0,57025227	2,78E-06
OG1RF_11266	cytidylate kinase	-0,42014074	0,01406273
OG1RF_11267	30S ribosomal protein S1	-0,29402538	0,00899284
OG1RF_11268	ribosome-associated GTPase EngA	-0,40782637	0,00979557
OG1RF_11269	DNA-binding protein HU	0,55252383	0,00070979
OG1RF_11276	tRNA adenylyltransferase	-0,36219561	0,04533503
OG1RF_11282	3-dehydroquinate synthase	0,70009131	0,01585672
OG1RF_11283	chorismate synthase	0,69254571	0,00168763
OG1RF_11284	prephenate dehydrogenase	0,60016076	0,03063495
OG1RF_11285	3-phosphoshikimate 1-carboxyvinyltransferase	0,56161894	0,03396499
OG1RF_11287	prephenate dehydratase	0,51653196	0,04311635
OG1RF_11289	DegV family protein	-0,60102515	9,69E-07
OG1RF_11298	repressor lexA	-0,47511617	0,00014018
OG1RF_11303	cysteine synthase	0,99012163	0,00279646
OG1RF_11306	MutT/NUDIX family protein	-0,73756413	0,00221644
OG1RF_11309	AraC family transcriptional regulator	0,7198113	3,58E-05
OG1RF_11310	multidrug ABC superfamily ATP binding cassette transporter, ABC protein	-0,60746648	0,03794981
OG1RF_11313	putative lipoprotein	-0,83590033	2,76E-07
OG1RF_11317	PTS family beta-glucosides porter, IIABC component	-1,30389454	2,92E-05
OG1RF_11318	oligo-1,6-glucosidase	-1,31261218	6,28E-06
OG1RF_11319	sucrose-6-phosphate dehydrogenase	-1,79144671	4,94E-10
OG1RF_11320	sucrose operon repressor ScrR	-0,72159241	9,83E-05
OG1RF_11323	phosphotransferase system (PTS) beta-glucoside-specific enzyme IIBCA component	-0,54283914	0,01784692
OG1RF_11326	hypothetical protein	-0,67498029	0,00255249
OG1RF_11331	DNA topoisomerase (ATP-hydrolyzing) ParE	-0,37057297	0,00152141
OG1RF_11332	CoA-binding domain protein	0,94544364	2,73E-08
OG1RF_11333	ethanolamine utilization protein EutQ	1,5688118	6,37E-06

OG1RF_11334	ethanolamine utilization protein EutH	1,47407008	7,30E-06
OG1RF_11335	ethanolamine utilization protein EutN	1,77325779	2,30E-07
OG1RF_11336	ethanolamine utilization protein	1,39978045	6,24E-05
OG1RF_11337	ethanolamine utilization protein	1,45070652	3,15E-05
OG1RF_11338	hypothetical protein	1,38295436	0,00019046
OG1RF_11339	ribonuclease III	1,61482621	1,34E-07
OG1RF_11340	acetaldehyde dehydrogenase	1,2930717	0,0001854
OG1RF_11341	microcompartment protein	1,18492346	0,00055738
OG1RF_11342	ethanolamine utilization protein EutL	1,14279397	0,00039594
OG1RF_11343	ethanolamine ammonia-lyase small subunit	0,86619886	0,00431758
OG1RF_11344	ethanolamine ammonia-lyase large subunit	0,77822104	0,02362704
OG1RF_11350	ATP:cob(I)alamin adenosyltransferase	1,01656563	0,00180849
OG1RF_11351	ethanolamine utilization protein	0,60427519	0,02430808
OG1RF_11354	iron (Fe) ABC superfamily ATP binding cassette transporter, binding protein	0,40136886	0,03431125
OG1RF_11356	aldose epimerase	0,40302288	0,01924342
OG1RF_11357	GTP-sensing transcriptional pleiotropic repressor CodY	0,31715166	0,04709149
OG1RF_11358	ATP-dependent hsl protease ATP-binding subunit HslU	0,47072033	0,00389949
OG1RF_11359	ATP-dependent protease HslVU	0,66478043	0,00221644
OG1RF_11366	ribosome biogenesis GTP-binding protein YlqF	-0,49105486	0,00994991
OG1RF_11367	2-dehydropantoate 2-reductase	-0,8777055	1,36E-06
OG1RF_11368	LysR family transcriptional regulator	-0,76300696	5,04E-05
OG1RF_11369	regulatory protein	-0,65180502	0,00032179
OG1RF_11370	branched-chain alpha-keto acid	-0,60617996	0,00051944
OG1RF_11371	3-methyl-2-oxobutanoate dehydrogenase	-0,5945015	0,00209702
OG1RF_11372	3-methyl-2-oxobutanoate dehydrogenase	-0,55891705	0,00137124
OG1RF_11373	dihydrolipoyl dehydrogenase	-0,48259119	0,00890907
OG1RF_11374	butyrate kinase	-0,48665482	0,01659153
OG1RF_11375	branched-chain phosphotransacylase	-0,48885431	0,00708076

OG1RF_11376	hypothetical protein	-0,59865817	0,00034261
OG1RF_11377	hypothetical protein	-0,77452247	0,01203008
OG1RF_11383	putative NADPH:quinone reductase	1,1578289	0,00070979
OG1RF_11384	permease protein	-0,73585292	0,00019853
OG1RF_11392	S41A family carboxy-terminal peptidase	-0,35454411	0,00353566
OG1RF_11394	peptide-methionine-(S)-S-oxide reductase	-0,39692483	0,00312938
OG1RF_11398	hemolysin III	-0,31258147	0,00260562
OG1RF_11399	hypothetical protein	-0,34046359	0,01305706
OG1RF_11400	adenine phosphoribosyltransferase	0,37900028	0,01291655
OG1RF_11401	single-stranded-DNA-specific exonuclease RecJ	0,19612683	0,02322471
OG1RF_11402	hypothetical protein	0,29743464	0,01924342
OG1RF_11418	family 38 glycosyl hydrolase	0,57705742	0,00041509
OG1RF_11421	LysR family transcriptional regulator	-0,70853924	0,04895193
OG1RF_11422	carbonate dehydratase	-1,15986803	0,00085877
OG1RF_11423	orotate phosphoribosyltransferase	-1,46988285	0,00063895
OG1RF_11424	orotidine-5'-phosphate decarboxylase	-1,35706711	0,0017547
OG1RF_11425	dihydroorotate oxidase	-1,53243799	0,00038828
OG1RF_11426	dihydroorotate dehydrogenase electron transfer subunit	-1,54284903	0,00032431
OG1RF_11427	carbamoyl-phosphate synthase, large subunit	-1,431603	2,18E-05
OG1RF_11428	carbamoyl-phosphate synthase, small subunit	-1,24167014	0,0007344
OG1RF_11429	dihydroorotase	-1,03202419	0,00520254
OG1RF_11430	aspartate carbamoyltransferase, catalytic subunit	-0,9967212	2,88E-05
OG1RF_11434	signal peptidase II	0,46062986	0,03982138
OG1RF_11436	formate--tetrahydrofolate ligase	0,49735127	0,0433989
OG1RF_11440	YbaK/ebsC protein	0,33342336	0,01361848
OG1RF_11442	multidrug ABC superfamily ATP binding cassette transporter, ABC protein	-0,71940518	0,0075823
OG1RF_11443	multidrug ABC superfamily ATP binding cassette transporter, ABC protein	-0,60493308	0,00255249
OG1RF_11445	deoxyribonuclease IV (phage-T(4)-induced)	-0,5123501	0,00038617

OG1RF_11446	hypothetical protein	-0,6497502	0,00061061
OG1RF_11447	hypothetical protein	-0,54320507	0,00281515
OG1RF_11449	tyrosine--tRNA ligase	0,42795197	0,00084166
OG1RF_11455	general stress protein	0,45520611	0,00027595
OG1RF_11456	methyl-accepting chemotaxis family protein	0,49095598	0,00506755
OG1RF_11458	glycerol-3-phosphate dehydrogenase (NAD(P)(+))	-0,36332595	0,01859194
OG1RF_11462	membrane protein of hypothetical function	-0,67792688	1,48E-06
OG1RF_11463	PspC domain protein	-0,54061043	0,00023982
OG1RF_11464	hypothetical protein	-0,71032009	0,00045558
OG1RF_11474	peptide chain release factor RF2	-0,35363793	0,02680845
OG1RF_11476	preprotein translocase subunit SecA	-0,21676985	0,01010566
OG1RF_11477	ribosomal subunit interface protein	0,64029905	0,0001929
OG1RF_11481	PTS family cellobiose porter, IIA component	0,43464315	0,03138615
OG1RF_11483	protein of hypothetical function UPF0029	-0,6233514	0,00127069
OG1RF_11489	phosphoribosylamine-glycine ligase	-1,55445822	0,00038631
OG1RF_11490	bifunctional purine biosynthesis protein PurH	-1,46596986	0,00247413
OG1RF_11491	phosphoribosylglycinamide formyltransferase	-1,56344406	0,0005007
OG1RF_11492	phosphoribosylaminoimidazole synthetase	-1,55033392	0,00110586
OG1RF_11493	amidophosphoribosyltransferase	-1,42367896	0,00483666
OG1RF_11494	phosphoribosylformylglycinamidine synthase	-1,60798027	0,00120635
OG1RF_11495	phosphoribosylformylglycinamidine synthase	-1,53977289	0,00128037
OG1RF_11496	phosphoribosylformylglycinamidine synthase subunit PurS	-1,47201553	0,00567713
OG1RF_11500	SPFH domain/Band 7 family protein	0,97085695	2,32E-08
OG1RF_11502	oligopeptide ABC superfamily ATP binding cassette transporter, binding protein	-0,52010944	0,012646
OG1RF_11507	hypothetical protein	-0,56911692	0,00187626
OG1RF_11509	hypothetical protein	-1,16017369	0,00014966
OG1RF_11520	general stress protein A	-1,07751745	0,03193601
OG1RF_11521	phosphatidylglycerol--membrane-oligosaccharide	0,83693546	2,39E-05

	glycerophosphotransferase		
OG1RF_11523	LysR family transcriptional regulator	1,16637192	1,53E-07
OG1RF_11525	SprE protein	1,65774283	0,00210371
OG1RF_11526	gelatinase	1,70310502	0,00145592
OG1RF_11527	sensor histidine kinase FsrC	1,29597191	0,00314454
OG1RF_11528	FsrB protein	1,17119962	0,00498296
OG1RF_11530	N-acetylmuramoyl-L-alanine amidase	-0,85112072	4,71E-06
OG1RF_11531	glycosyl hydrolase	-0,79866896	1,30E-05
OG1RF_11533	alcohol dehydrogenase	0,72969526	0,00425274
OG1RF_11539	membrane protein	0,66811582	0,02211529
OG1RF_11540	PP-loop family protein	0,76843355	0,00020126
OG1RF_11549	PTS family mannose/fructose/sorbose porter component IID	1,22402068	0,02205638
OG1RF_11550	PTS system, IIC component	1,35040648	0,00430876
OG1RF_11551	phospotransferase system PTS, mannose-specific IIB component	1,73029833	0,00023219
OG1RF_11552	PTS family porter, mannose/fructose-specific component IIA	1,19894714	0,03074428
OG1RF_11553	hypothetical protein	1,72758915	0,00095189
OG1RF_11555	galactose-6-phosphate isomerase LacB subunit	-0,92285246	0,04474476
OG1RF_11558	PTS system, IIB component	-0,91424102	0,04372348
OG1RF_11559	PTS family galactitol (gat) porter component IIC	-1,0550325	0,01813609
OG1RF_11560	lactose PTS family porter repressor LacR	-0,62006079	0,00255249
OG1RF_11561	hypothetical protein	1,20094231	5,37E-10
OG1RF_11562	HD domain protein	0,64351005	0,03144301
OG1RF_11569	integral membrane protein	-0,57380897	0,00822483
OG1RF_11570	glycerophosphoryl diester phosphodiesterase	-0,89190314	6,99E-08
OG1RF_11575	hypothetical protein	0,58832926	0,02876204
OG1RF_11576	hypothetical protein	-0,57601191	0,02165049
OG1RF_11585	putative ribosylpyrimidine nucleosidase	-0,48662719	0,04805467
OG1RF_11587	M protein trans-acting positive regulator	-0,62871378	0,0008151

OG1RF_11591	glycerol-3-phosphate oxidase	0,84533192	0,00908175
OG1RF_11593	M protein trans-acting positive regulator	-0,85708377	3,87E-05
OG1RF_11594	pyridine nucleotide-disulfide family oxidoreductase	-0,87280522	1,36E-05
OG1RF_11595	hypothetical protein	-1,01309554	0,04879478
OG1RF_11596	hypothetical protein	-0,72428602	0,00986308
OG1RF_11598	PTS family porter component IIABC	-1,01129297	1,43E-05
OG1RF_11599	GntR family transcriptional regulator	-0,6852531	0,00015031
OG1RF_11614	PTS family mannose/fructose/sorbose porter component IIC	-0,65893304	0,01881512
OG1RF_11619	hypothetical protein	-0,96003796	5,21E-10
OG1RF_11620	hypothetical protein	-1,34713138	1,36E-06
OG1RF_11623	enolase	0,53376698	0,00122237
OG1RF_11624	triose-phosphate isomerase	0,39881593	0,03040559
OG1RF_11625	phosphoglycerate kinase	0,42259261	0,0162781
OG1RF_11627	central glycolytic genes regulator	-0,53239978	0,00913879
OG1RF_11628	YitT family protein	-0,28703063	0,02236675
OG1RF_11634	hypothetical protein	-0,70982439	0,00034639
OG1RF_11635	D-tyrosyl-tRNA(Tyr) deacylase	-0,38292063	0,01199748
OG1RF_11636	GTP diphosphokinase	-0,47348091	6,50E-05
OG1RF_11637	RsmE family RNA methyltransferase	0,38100074	0,00010659
OG1RF_11638	ribosomal protein L11 methyltransferase	0,2054387	0,02958407
OG1RF_11639	hypothetical protein	0,39574241	0,00677279
OG1RF_11641	replication-associated recombination protein A	0,34208333	0,0019345
OG1RF_11642	hypothetical protein	-0,93035444	0,00424443
OG1RF_11663	ABC superfamily ATP binding cassette transporter, ABC/membrane protein	-0,5281742	0,00674304
OG1RF_11664	ABC superfamily ATP binding cassette transporter, ABC/membrane protein	-0,43584332	0,03587504
OG1RF_11666	cytochrome D ubiquinol oxidase subunit I	0,32857349	0,04068931
OG1RF_11671	hypothetical protein	0,90171194	0,00360441
OG1RF_11672	major facilitator family transporter	0,76858942	0,00212625

OG1RF_11677	ABC superfamily ATP binding cassette transporter, ABC protein	-0,90961262	0,02834342
OG1RF_11678	ABC superfamily ATP binding cassette transporter, membrane protein	-1,07815694	0,01274879
OG1RF_11679	ABC superfamily ATP binding cassette transporter, binding protein	-0,89701949	0,00039328
OG1RF_11685	hypothetical protein	-1,19890356	0,02654089
OG1RF_11686	hypothetical protein	-0,85329678	2,86E-06
OG1RF_11689	hypothetical protein	-0,64821099	0,00593616
OG1RF_11694	ABC superfamily ATP binding cassette transporter, ABC protein	-0,67130832	0,00069343
OG1RF_11696	phosphoglucosamine mutase	0,22471142	0,03947826
OG1RF_11701	glutamate--ammonia ligase	-0,55600425	0,0004446
OG1RF_11702	regulatory protein GlnR	-0,62179022	1,73E-05
OG1RF_11705	glycerophosphodiester phosphodiesterase	-0,78600136	0,00192133
OG1RF_11706	group 2 glycosyl transferase	-0,49423606	9,94E-05
OG1RF_11720	group 2 glycosyl transferase	-0,65583871	0,00650643
OG1RF_11723	brp/Blh family beta-carotene 15,15'-monooxygenase	-0,54349011	0,02287238
OG1RF_11726	ABC superfamily ATP binding cassette transporter, ABC protein	-0,36048727	0,04477572
OG1RF_11727	ABC superfamily ATP binding cassette transporter, membrane protein	-0,4988201	0,00395399
OG1RF_11735	group 2 glycosyl transferase	-0,51908543	0,00564761
OG1RF_11736	group 2 glycosyl transferase	-0,75387277	3,38E-05
OG1RF_11737	group 2 glycosyl transferase	-0,60067473	0,01388868
OG1RF_11745	protein of hypothetical function DUF1696	-0,53923325	0,00107098
OG1RF_11746	cytidine/deoxycytidylate deaminase	-0,44028483	0,04653728
OG1RF_11748	phenazine biosynthesis protein PhzF family protein	-0,41069284	0,00181001
OG1RF_11760	hypothetical protein	0,81939134	1,03E-07
OG1RF_11761	ABC superfamily ATP binding cassette transporter, binding protein	0,95769429	8,39E-15
OG1RF_11762	carbohydrate ABC superfamily ATP binding cassette transporter, membrane protein	1,02133249	3,16E-12
OG1RF_11763	ABC superfamily ATP binding cassette transporter, membrane protein	0,84597861	2,34E-08
OG1RF_11765	MerR family transcriptional regulator	0,9063075	0,00029182
OG1RF_11768	tryptophan--tRNA ligase	-0,37593258	0,03056986

OG1RF_11769	hypothetical protein	-1,37366897	3,05E-09
OG1RF_11770	hypothetical protein	-1,19071476	1,30E-05
OG1RF_11771	brp/Blh family beta-carotene 15,15'-monooxygenase	-1,1941802	0,0001616
OG1RF_11772	sugar ABC superfamily ATP binding cassette transporter, membrane protein	-1,03472938	0,00060264
OG1RF_11773	ABC superfamily ATP binding cassette transporter, membrane protein	-1,0393931	0,00209309
OG1RF_11774	sugar ABC superfamily ATP binding cassette transporter, sugar-binding protein	-0,84956502	0,00019693
OG1RF_11775	glucuronyl hydrolase	-0,53002993	0,04448236
OG1RF_11779	hypothetical protein	0,39174789	0,00304853
OG1RF_11780	PTS family cellobiose porter component IIB	0,90430369	0,00182712
OG1RF_11781	sodium:solute symporter family protein	0,85855324	0,00648719
OG1RF_11782	myo-inositol catabolism protein IolE	1,17567926	4,76E-05
OG1RF_11783	inositol 2-dehydrogenase	1,45545383	4,31E-07
OG1RF_11784	inositol 2-dehydrogenase	1,81211647	8,56E-13
OG1RF_11785	methylmalonate-semialdehyde dehydrogenase (acylating)	2,21212401	1,02E-16
OG1RF_11786	myo-inositol catabolism protein IolB	2,6404714	2,36E-21
OG1RF_11787	3D-(3,5/4)-trihydroxycyclohexane-1,2-dione hydrolase	2,56392741	4,95E-24
OG1RF_11788	5-dehydro-2-deoxygluconokinase	2,20657141	8,93E-11
OG1RF_11789	DNA binding protein	1,13882461	5,48E-12
OG1RF_11791	GNAT family acetyltransferase	-0,28108634	0,01726008
OG1RF_11792	nucleoside 2-deoxyribosyltransferase superfamily protein	-0,29992074	0,04277537
OG1RF_11801	hypothetical protein	0,7136993	0,00071696
OG1RF_11802	hypothetical protein	0,44210942	0,0029324
OG1RF_11809	hypothetical protein	-0,93098372	0,00024297
OG1RF_11812	hypothetical protein	1,23853552	6,18E-07
OG1RF_11813	hypothetical protein	1,3239715	6,78E-05
OG1RF_11820	glucose 1-dehydrogenase	-0,74311304	0,01924342
OG1RF_11834	GNAT family acetyltransferase	0,35174971	0,0111407

OG1RF_11849	Fur family transcriptional regulator ZurR	0,60939333	0,01354092
OG1RF_11850	protein of hypothetical function DUF299	-0,52783166	1,74E-05
OG1RF_11853	homoserine dehydrogenase	0,37270178	7,17E-05
OG1RF_11854	metal transport repressor protein CzrA	0,35247042	0,02671868
OG1RF_11855	putative pyrroline-5-carboxylate reductase	-0,58375042	0,00952643
OG1RF_11860	GMP reductase	-0,83287103	0,04010031
OG1RF_11861	NCS2 family xanthine/uracil permease	-1,12099648	0,00758342
OG1RF_11862	guanine deaminase	-1,07280068	0,00192282
OG1RF_11866	PTS family porter, enzyme I	0,73513328	6,15E-07
OG1RF_11867	N-acetylmuramic acid 6-phosphate etherase	0,81085272	0,00723034
OG1RF_11868	outer surface protein	0,58518317	0,01098281
OG1RF_11869	PTS system, IIA component	0,4676085	0,01231979
OG1RF_11871	hypothetical protein	-0,98521698	1,15E-07
OG1RF_11872	hypothetical protein	-0,71823741	0,0061412
OG1RF_11873	phosphate transporter	-0,96090206	2,34E-09
OG1RF_11874	30S ribosomal protein S20	-0,40349825	0,04482883
OG1RF_11876	2-dehydropantoate 2-reductase	1,24066095	6,86E-13
OG1RF_11877	DNA-directed DNA polymerase III delta subunit	-0,29509534	0,03392153
OG1RF_11892	GTP-binding protein TypA/BipA	-0,57743771	0,04650937
OG1RF_11893	inositol-phosphate phosphatase	0,39071556	0,01553404
OG1RF_11895	voltage-gated chloride channel family protein	-0,78475213	0,02282718
OG1RF_11900	cro/CI family transcriptional regulator	0,68679765	0,00038349
OG1RF_11902	arginine--tRNA ligase	0,43443781	0,02915
OG1RF_11903	O-sialoglycoprotein endopeptidase	0,34206426	0,01169675
OG1RF_11908	hypothetical protein	-0,26804532	0,02680845
OG1RF_11909	hypothetical protein	-0,31720596	0,02578255
OG1RF_11912	hypothetical protein	0,80720599	0,00762745
OG1RF_11914	phosphatidate cytidylyltransferase	-0,30922741	0,02540599

OG1RF_11915	di-trans,poly-cis-decaprenylcistransferase	-0,29966876	0,04994598
OG1RF_11916	ABC superfamily ATP binding cassette transporter, binding protein	0,55120521	0,01681679
OG1RF_11931	uracil phosphoribosyltransferase	-0,35481365	0,00606022
OG1RF_11938	fumarate reductase	-0,55133959	0,00639009
OG1RF_11939	Trk family potassium (K+) transporter, membrane protein	-0,56644235	0,00537286
OG1RF_11940	pyruvate:ferredoxin oxidoreductase	-0,64799463	0,00221796
OG1RF_11941	glutamate synthase	-0,60820349	0,01455429
OG1RF_11942	ferredoxin--NADP(+) reductase subunit alpha	-0,55711612	0,02643437
OG1RF_11944	YqeB family selenium-dependent molybdenum hydroxylase system protein	-0,77888468	0,00045558
OG1RF_11945	hypothetical protein	-0,74628992	0,00046602
OG1RF_11946	hypothetical protein	-0,74226299	0,00038617
OG1RF_11947	selenium metabolism protein YedF	-0,66829125	0,00894056
OG1RF_11948	selenide, water dikinase	-0,64520929	0,00508251
OG1RF_11949	putative cysteine desulfurase	-0,47502369	0,01740094
OG1RF_11951	selenium-dependent molybdenum hydroxylase 1	-0,42934957	0,02407197
OG1RF_11954	xanthine/uracil permease	-0,76909254	0,00210789
OG1RF_11955	endoribonuclease inhibitor of translation	-0,70991147	0,00746156
OG1RF_11956	carbamate kinase	-0,67424329	0,00624533
OG1RF_11957	carbamoyltransferase YgeW	-0,49851616	0,04057161
OG1RF_11969	beta-lactamase	0,57156696	0,00111033
OG1RF_11970	glyoxalase	0,441623	0,00519327
OG1RF_11975	beta-glucosidase	0,85021605	0,00174185
OG1RF_11976	PTS family porter, enzyme I	0,79376109	0,00424162
OG1RF_11977	transcription antiterminator LicT	-0,79998886	0,000631
OG1RF_11979	FMN-dependent NADH-azoreductase	-0,88372074	1,49E-05
OG1RF_11985	ATP synthase F1 sector epsilon subunit	1,11045506	6,93E-08
OG1RF_11986	ATP synthase F1 sector beta subunit	1,15827149	2,87E-10

OG1RF_11987	ATP synthase F1 sector gamma subunit	1,19084832	8,51E-12
OG1RF_11988	ATP synthase F1 sector alpha subunit	1,1820642	1,15E-11
OG1RF_11989	ATP synthase F1 sector delta subunit	1,14213993	1,39E-11
OG1RF_11990	ATP synthase F0 sector subunit B	1,14748003	3,73E-10
OG1RF_11991	ATP synthase F0 sector subunit C	1,02318722	2,25E-08
OG1RF_11992	ATP synthase F0 sector subunit A	0,8500818	3,72E-05
OG1RF_11996	preprotein translocase subunit SecG	-0,72101047	1,99E-07
OG1RF_11997	GNAT family acetyltransferase	1,07394437	3,74E-05
OG1RF_11998	hypothetical protein	1,11214042	6,26E-06
OG1RF_11999	P-ATPase superfamily P-type ATPase cadmium transporter	0,95630111	0,0011296
OG1RF_12000	NAD(+) synthase	0,55149622	0,00053388
OG1RF_12001	nicotinate phosphoribosyltransferase	0,37161347	0,00284985
OG1RF_12003	N-acetylmuramoyl-L-alanine amidase	-1,98407606	6,62E-10
OG1RF_12004	hypothetical protein	-1,54399593	8,27E-05
OG1RF_12005	transcriptional regulator	-1,15009685	0,03304811
OG1RF_12006	chaperonin GroEL	0,91827944	3,84E-07
OG1RF_12007	chaperone GroES	1,28492549	2,06E-10
OG1RF_12011	ABC superfamily ATP binding cassette transporter, ABC protein	-0,34763593	0,01997588
OG1RF_12020	hypothetical protein	-1,06106318	7,99E-11
OG1RF_12026	alcohol dehydrogenase	0,33372372	0,00053388
OG1RF_12027	phosphopantothenate-cysteine ligase	0,3931321	0,00012193
OG1RF_12028	phosphopantothenoylcysteine decarboxylase	0,36475593	0,00239349
OG1RF_12029	hypothetical protein	0,32987317	0,01242966
OG1RF_12039	23S rRNA pseudouridylate synthase RluD	0,33249347	0,0238855
OG1RF_12045	competence protein	-0,80106453	0,00832878
OG1RF_12047	regulatory protein Spx	-0,47652172	0,00137681
OG1RF_12048	tryptophan--tRNA ligase	-0,43778276	0,00278012
OG1RF_12050	HAD-superfamily hydrolase	-1,39881411	1,06E-15

OG1RF_12068	MutT/NUDIX family protein	-0,2182593	0,04719055
OG1RF_12071	transcriptional regulator	0,43474717	0,01024869
OG1RF_12073	recombination regulator RecX	-0,40091589	0,01713368
OG1RF_12077	amino acid permease	0,75841933	0,00974864
OG1RF_12084	ABC superfamily ATP binding cassette transporter, ABC protein	0,31142743	0,0477191
OG1RF_12093	preprotein translocase	-0,66024452	0,00033837
OG1RF_12094	50S ribosomal protein L33	-0,62604551	0,00152141
OG1RF_12102	thioredoxin-disulfide reductase	-1,44421577	1,03E-06
OG1RF_12103	peroxiredoxin	-1,65644678	3,19E-11
OG1RF_12105	lipoate-protein ligase	-0,26212074	0,01361848
OG1RF_12106	metallo-beta-lactamase	-0,4075006	0,00013784
OG1RF_12115	anaerobic ribonucleoside-triphosphate reductase large subunit	0,34239664	0,01353379
OG1RF_12116	pyruvate formate-lyase activating enzyme	0,50049402	0,00094338
OG1RF_12117	DNA-directed DNA polymerase IV	0,47108952	0,01724589
OG1RF_12118	YbbM family protein	-0,83772669	1,73E-05
OG1RF_12119	ABC superfamily ATP binding cassette transporter, ABC protein	-0,74173829	0,00096219
OG1RF_12120	tetrapyrrole methylase	-0,81331047	4,62E-08
OG1RF_12124	protein of hypothetical function DUF970	0,42847705	0,01616239
OG1RF_12134	MarR family transcriptional regulator	0,69455096	0,00360441
OG1RF_12142	UDP-glucose 4-epimerase	-0,32261784	0,0153226
OG1RF_12144	hypothetical protein	0,7188147	0,000631
OG1RF_12145	protein of hypothetical function DUF488	0,92048888	0,00041505
OG1RF_12146	rhodanese family protein	0,51660332	0,00607995
OG1RF_12147	glucokinase	0,34711053	0,00994991
OG1RF_12148	hypothetical protein	0,52773076	0,03550237
OG1RF_12149	rhomboid family protein	0,34123196	0,02680845
OG1RF_12151	hydrolase	0,98209167	0,00067365
OG1RF_12159	threonine--tRNA ligase	0,65741949	0,00422036

OG1RF_12160	4-oxalocrotonate tautomerase	0,71433534	8,69E-05
OG1RF_12168	PFL4705 family integrating conjugative element protein	0,8630163	1,01E-05
OG1RF_12169	glucose-1-phosphate adenylyltransferase	0,88656976	1,39E-07
OG1RF_12170	nucleotidyltransferase	-0,33834749	0,01209234
OG1RF_12171	methyltransferase	-0,20462786	0,0214179
OG1RF_12174	nicotinate-nucleotide adenylyltransferase	-0,34273959	0,01389688
OG1RF_12187	acyl carrier protein	0,70778097	0,01064018
OG1RF_12190	hypothetical protein	-0,25829167	0,0080159
OG1RF_12192	group 1 glycosyl transferase	-0,34075135	0,04368979
OG1RF_12193	group 1 glycosyl transferase	-0,35808259	0,02528842
OG1RF_12198	hypothetical protein	-1,17966238	0,02052138
OG1RF_12199	peptidylprolyl isomerase	-0,34509566	0,04267376
OG1RF_12202	5'-nucleotidase	0,40616249	0,04367511
OG1RF_12210	Trk family potassium (K+) transporter, NAD+ binding protein	-0,43429584	0,00125194
OG1RF_12217	UDP-N-acetylglucosamine 2-epimerase	0,28179675	0,02364283
OG1RF_12225	cold shock protein CspA	0,41795703	0,02395128
OG1RF_12227	HAD superfamily hydrolase	0,3725301	0,01368845
OG1RF_12228	tetrahydrofolate synthase	0,38432184	0,01231316
OG1RF_12231	valine--tRNA ligase	0,73985114	0,00178723
OG1RF_12242	DMT superfamily drug/metabolite transporter	0,80254829	1,23E-07
OG1RF_12243	ribose ABC superfamily ATP binding cassette transporter, membrane protein	0,81761202	7,31E-07
OG1RF_12244	ribokinase	0,9564628	5,92E-11
OG1RF_12258	L-seryl-tRNA(Sec) selenium transferase	0,71695959	0,03396499
OG1RF_12260	PTS family mannose/fructose/sorbose porter component IIC	0,51570771	0,04663151
OG1RF_12266	transcriptional regulator	-0,85984656	0,02979196
OG1RF_12268	ABC superfamily ATP binding cassette transporter, ABC protein	-1,104343	0,03870802
OG1RF_12270	rhodanese family protein	0,89819331	0,00355075
OG1RF_12280	cytosine/purine permease	-0,79187966	0,01026035

OG1RF_12281	N-acetyltransferase	0,5220745	0,01064018
OG1RF_12291	hypothetical protein	-0,51333003	0,02713619
OG1RF_12294	P-ATPase superfamily P-type ATPase cation transporter	-0,70109038	0,00527328
OG1RF_12295	DAACS family dicarboxylate/amino acid:sodium (Na+) or proton (H+) symporter	-0,51312062	0,00565194
OG1RF_12298	hypothetical protein	-0,51085651	0,00730592
OG1RF_12299	hypothetical protein	1,22569161	1,08E-11
OG1RF_12300	sigma-70 family protein	1,34566012	2,69E-09
OG1RF_12302	DAACS family dicarboxylate/amino acid:cation symporter	-0,86892563	0,01615633
OG1RF_12303	family 8 polysaccharide lyase	-1,41739116	1,94E-10
OG1RF_12307	universal stress protein	0,75196918	0,00011224
OG1RF_12308	thioredoxin family protein	0,75256188	7,34E-05
OG1RF_12309	glutamyl aminopeptidase	0,70992404	0,00036155
OG1RF_12311	peptide ABC superfamily ATP binding cassette transporter, binding protein	-0,78846042	2,24E-05
OG1RF_12328	hypothetical protein	-1,09158317	2,34E-08
OG1RF_12329	protein-tyrosine-phosphatase	-0,67382066	2,96E-05
OG1RF_12336	peptide deformylase	0,62292256	0,00019693
OG1RF_12345	hypothetical protein	-0,42119156	0,04372348
OG1RF_12356	hypothetical protein	-0,74458591	0,00733177
OG1RF_12357	glutathione synthase	0,52915854	0,01389688
OG1RF_12359	YitT family protein	-0,84770461	0,00083784
OG1RF_12362	cell division protein FtsY	0,44911572	0,01248288
OG1RF_12370	ABC superfamily ATP binding cassette transporter, ABC protein	-0,47838441	0,00244412
OG1RF_12380	50S ribosomal protein L28	-0,61178075	0,00058184
OG1RF_12383	ribosome small subunit-dependent GTPase A	-0,35495416	0,00123544
OG1RF_12385	serine/threonine protein phosphatase 1	0,33661793	0,03119508
OG1RF_12387	methionyl-tRNA formyltransferase	0,40659267	0,02781543
OG1RF_12388	formylmethionine deformylase	0,40285269	0,02930869
OG1RF_12390	DNA-directed RNA polymerase subunit omega	-0,42621288	0,00212625

OG1RF_12391	guanylate kinase	-0,56031178	0,00084902
OG1RF_12393	hypothetical protein	0,43907783	0,00908175
OG1RF_12394	YicC like protein	0,59629541	1,52E-07
OG1RF_12395	hypothetical protein	0,59028743	2,18E-06
OG1RF_12397	2-dehydro-3-deoxyphosphogluconate aldolase/4-hydroxy-2-oxoglutarate aldolase	0,81385885	0,00076288
OG1RF_12398	mannonate dehydratase	0,88499432	0,00025797
OG1RF_12399	PTS family mannose/fructose/sorbose porter component IIA	1,03895153	1,15E-05
OG1RF_12400	PTS family mannose/fructose/sorbose porter, IIB component	1,04543832	4,14E-06
OG1RF_12401	PTS family mannose/fructose/sorbose porter component IID	0,92549506	3,82E-05
OG1RF_12402	PTS family mannose/fructose/sorbose porter component IIC	0,69780077	0,00255249
OG1RF_12403	putative glycerol dehydrogenase	0,78393177	0,00123544
OG1RF_12404	D-isomer specific 2-hydroxyacid dehydrogenase	0,93055767	1,18E-05
OG1RF_12405	6-phosphogluconate dehydrogenase	1,15522891	3,09E-07
OG1RF_12411	hypothetical protein	-0,60340939	0,0437277
OG1RF_12414	hypothetical protein	-0,60859915	0,00137681
OG1RF_12415	hypothetical protein	-0,99599049	9,13E-05
OG1RF_12416	hypothetical protein	-1,20823095	0,00119031
OG1RF_12420	large conductance mechanosensitive channel protein	0,67212795	0,00813519
OG1RF_12428	hypothetical protein	-0,88225255	0,02319932
OG1RF_12429	hypothetical protein	-0,70744447	0,0014726
OG1RF_12436	hypothetical protein	0,42357067	0,03928862
OG1RF_12442	FMN reductase	0,67481624	7,34E-05
OG1RF_12447	hypothetical protein	0,78045178	0,00239448
OG1RF_12449	M protein trans-acting positive regulator	0,59428276	0,00050785
OG1RF_12451	cell wall surface anchor family protein	0,43364826	0,04061175
OG1RF_12452	UbiD family decarboxylase	1,03145153	8,15E-09
OG1RF_12453	WxL domain surface protein	1,04739686	3,56E-08
OG1RF_12454	UbiD family decarboxylase	1,05117729	1,12E-07

OG1RF_12455	hypothetical protein	1,13277929	9,69E-07
OG1RF_12456	WxL domain surface protein	1,06297153	3,85E-07
OG1RF_12464	ABC superfamily ATP binding cassette transporter, binding protein	-0,67977031	0,00239448
OG1RF_12465	metal ion ABC superfamily ATP binding cassette transporter, membrane protein	-0,82159665	0,00507157
OG1RF_12468	30S ribosomal protein S14	0,56650181	0,01573354
OG1RF_12474	ABC superfamily ATP binding cassette transporter, membrane protein	0,67797629	0,00290551
OG1RF_12476	PTS family fructose/mannitol (fru) porter component IIA	-1,36085662	8,45E-05
OG1RF_12477	PTS family ascorbate porter, IIB component	-1,09504287	0,00101238
OG1RF_12478	PTS family fructose/mannitol (fru) porter component IIC	-1,10772076	0,00075187
OG1RF_12479	PTS family porter component II	-1,07158267	6,50E-05
OG1RF_12480	DEAH-box family ATP-dependent helicase	-1,51571142	3,73E-10
OG1RF_12481	choline binding protein	-1,22934996	7,31E-07
OG1RF_12482	hypothetical protein	-1,32614927	0,01800402
OG1RF_12494	ChpA/MazF transcriptional modulator	0,43873125	0,01996084
OG1RF_12495	antitoxin MazE	0,44738255	0,04163469
OG1RF_12497	hypothetical protein	-1,10696161	0,0147281
OG1RF_12498	biotin--[acetyl-CoA-carboxylase] ligase	-0,63791569	3,18E-06
OG1RF_12499	chitin binding protein	-1,0036981	0,00171834
OG1RF_12501	hypothetical protein	-1,13406948	0,00167638
OG1RF_12506	cell wall surface anchor family protein	-0,6181596	0,01342765
OG1RF_12508	thiamine biosynthesis lipoprotein	0,62781706	0,0094777
OG1RF_12509	pheromone cAD1 lipoprotein	0,56712105	0,0118015
OG1RF_12510	NADH dehydrogenase	0,57928266	0,00038617
OG1RF_12519	glutathione-disulfide reductase	0,56894891	0,00049167
OG1RF_12520	hypothetical protein	0,8390384	0,00016599
OG1RF_12521	cro/CI family zinc-binding transcriptional regulator	0,79091577	6,26E-06
OG1RF_12522	hypothetical protein	0,51661216	0,04574571
OG1RF_12526	hypothetical protein	0,49645385	1,79E-06

OG1RF_12529	brp/Blh family beta-carotene 15,15'-monooxygenase	-0,61221813	9,64E-05
OG1RF_12532	putative methionine gamma-lyase	-1,28029916	2,40E-11
OG1RF_12533	PTS family oligomeric beta-glucoside porter component IIC	-1,40635475	8,51E-12
OG1RF_12537	serine--tRNA ligase	0,65191509	1,17E-05
OG1RF_12540	hypothetical protein	0,46388642	0,01368845
OG1RF_12541	GTP-binding protein YchF	0,69084126	1,29E-05
OG1RF_12542	protein of hypothetical function DUF951	0,69125667	0,00612892
OG1RF_12546	hypothetical protein	1,1677523	2,69E-06
OG1RF_12547	myosin-cross-reactive antigen	1,78059469	3,85E-07
OG1RF_12556	tRNA uridine 5-carboxymethylaminomethyl modification enzyme GidA	0,59738755	0,01305706
OG1RF_12557	tRNA modification GTPase TrmE	0,61157232	0,00107916
OG1RF_12572	citrate transporter	-0,48718409	0,00214932
OG1RF_12573	GntR family transcriptional regulator	-0,36278944	0,02344089
OG1RF_12574	response regulator	-0,33431431	0,04958873
OG1RF_12578	50S ribosomal protein L34	-0,55566432	0,00982451

Table S2: Significantly differentially regulated genes between *E. faecalis* isolated from SIHUMI colonized IL-10^{-/-} vs. WT mice

Gene_ID	Description	log2(FC)	P-adj
EBG00001209428	RatA	-1,06415269	0,02566304
OG1RF_10007	30S ribosomal protein S6	0,68021555	0,00433353
OG1RF_10013	adenylosuccinate synthase	1,59145182	7,48E-08
OG1RF_10050	4-diphosphocytidyl-2-C-methyl-D-erythritol kinase	-1,03010155	0,0020006
OG1RF_10051	metal ABC superfamily ATP binding cassette transporter, binding protein	-0,74339477	0,04241773
OG1RF_10053	metal cation ABC superfamily ATP binding cassette transporter, membrane protein	-1,07992124	0,02522899
OG1RF_10054	purine operon repressor	0,95790125	0,00993607
OG1RF_10056	5'-nucleotidase	-0,62243605	0,00133125
OG1RF_10081	DNA-binding protein	1,78895813	0,00722505
OG1RF_10099	arginine deiminase	1,8338633	2,00E-08
OG1RF_10100	ornithine carbamoyltransferase	1,72725966	4,82E-06
OG1RF_10101	carbamate kinase	1,73273113	7,48E-08
OG1RF_10102	global nitrogen regulator NtcA	1,96682644	3,98E-09
OG1RF_10103	UIT3 family protein	1,75724787	7,48E-08
OG1RF_10116	pantothenate kinase	1,01298877	0,00141095
OG1RF_10129	membrane protein	1,51635352	0,00925498
OG1RF_10141	phosphoglycerate mutase	0,68857666	0,00722505
OG1RF_10145	30S ribosomal protein S7	0,77698899	0,00118306
OG1RF_10146	elongation factor G	0,6767967	0,00987272
OG1RF_10147	elongation factor EF1A	0,61567916	0,00161501
OG1RF_10150	30S ribosomal protein S10	1,08884813	5,32E-05
OG1RF_10151	50S ribosomal protein L3	1,1533398	8,35E-06
OG1RF_10152	ribosomal protein L4/L1 family protein	1,16358049	1,03E-07
OG1RF_10153	50S ribosomal protein L23	1,15453024	2,93E-05
OG1RF_10154	50S ribosomal protein L2	0,86207076	0,0080218

OG1RF_10155	30S ribosomal protein S19	0,92506496	0,00101497
OG1RF_10156	50S ribosomal protein L22	0,96334537	0,01139406
OG1RF_10157	30S ribosomal protein S3	0,97810086	0,00052531
OG1RF_10158	50S ribosomal protein L16	0,81948083	0,01151901
OG1RF_10159	50S ribosomal protein L29	0,772312	0,0199474
OG1RF_10160	30S ribosomal protein S17	0,95561909	0,00258719
OG1RF_10161	50S ribosomal protein L14	0,9315438	7,15E-06
OG1RF_10164	ribosomal protein S14p/S29e	1,04404575	0,01061708
OG1RF_10165	30S ribosomal protein S8	0,9982049	2,55E-06
OG1RF_10166	50S ribosomal protein L6	0,79520244	0,00221769
OG1RF_10167	50S ribosomal protein L18	0,86744153	0,00465641
OG1RF_10168	30S ribosomal protein S5	0,93975374	0,00084754
OG1RF_10169	50S ribosomal protein L30	0,88525235	0,00066353
OG1RF_10170	50S ribosomal protein L15	0,8267992	0,00225557
OG1RF_10171	preprotein translocase subunit SecY	0,90428163	4,93E-05
OG1RF_10172	adenylate kinase	0,87960515	0,0010056
OG1RF_10173	translation initiation factor IF-1	0,74728259	0,00282497
OG1RF_10175	30S ribosomal protein S13	0,88388367	3,68E-06
OG1RF_10176	30S ribosomal protein S11	0,68588998	0,0082183
OG1RF_10177	DNA-directed RNA polymerase subunit alpha	0,8326903	2,60E-06
OG1RF_10178	50S ribosomal protein L17	0,7262649	0,00479037
OG1RF_10180	hypothetical protein	0,85616839	0,0448757
OG1RF_10184	ABC superfamily ATP binding cassette transporter, membrane protein	1,32413401	0,00117834
OG1RF_10197	N-acetylmuramoyl-L-alanine amidase	0,63130698	0,02538908
OG1RF_10203	heat shock protein	-0,97491766	0,00190351
OG1RF_10212	lysine--tRNA ligase	0,43304217	0,03102904
OG1RF_10213	transcription antiterminator LicT	-1,5102183	1,25E-07
OG1RF_10214	phosphotransferase system (PTS) beta-glucoside-specific enzyme IIBCA component	-1,41192287	0,00051768

OG1RF_10215	6-phospho-beta-glucosidase	-1,46998843	0,00162909
OG1RF_10225	enoyl-[acyl-carrier-protein] reductase (NADH)	0,73209637	0,00570011
OG1RF_10257	septation ring formation regulator EzrA	0,73539503	0,00084754
OG1RF_10259	response regulator	-1,52356518	0,0002921
OG1RF_10262	S-layer protein	-1,19727532	0,02177902
OG1RF_10281	secreted antigen	0,72735293	0,04951938
OG1RF_10288	Na+/H+ antiporter NhaC	-1,86326856	2,98E-06
OG1RF_10314	RhiN protein	-1,35833752	0,006304
OG1RF_10315	TRAP-T family tripartite ATP-independent periplasmic transporter, binding protein	-1,01781385	0,01381663
OG1RF_10317	TRAP-T family tripartite ATP-independent periplasmic transporter, membrane protein	-1,54210891	0,00037766
OG1RF_10324	family 2 AP endonuclease	-1,02201075	0,01413689
OG1RF_10326	POT family proton (H+)-dependent oligopeptide transporter	0,93680118	0,00898682
OG1RF_10356	ribonucleotide-diphosphate reductase subunit alpha	-0,97353787	0,03769629
OG1RF_10357	ribonucleotide-diphosphate reductase subunit gamma	-1,08002852	0,00037237
OG1RF_10366	tyrosine--tRNA ligase	-0,77222262	0,0386425
OG1RF_10367	decarboxylase	1,78049255	3,06E-06
OG1RF_10368	amino acid permease	1,7247697	2,93E-05
OG1RF_10375	hypothetical protein	-0,93304862	0,0133405
OG1RF_10379	phage integrase family site-specific recombinase	-1,03045223	0,01510647
OG1RF_10387	glyoxalase	-1,09726993	0,0242677
OG1RF_10388	DeoR family transcriptional regulator	-2,15291391	0,00022192
OG1RF_10389	Xaa-Pro aminopeptidase	-1,90439383	7,85E-05
OG1RF_10390	uracil-DNA glycosylase	-1,67181661	0,00254911
OG1RF_10397	lactoylglutathione lyase	-0,98019178	0,04241773
OG1RF_10408	hypothetical protein	-1,11199834	0,02117876
OG1RF_10411	ABC superfamily ATP binding cassette transporter, ABC protein	-0,85125369	0,00381556
OG1RF_10412	ABC superfamily ATP binding cassette transporter, membrane protein	2,01565416	0,00031034
OG1RF_10423	peptidyl-prolyl cis-trans isomerase	1,1435225	0,00550504

OG1RF_10428	phosphotransferase enzyme family protein	0,66845066	0,04472849
OG1RF_10439	peptide chain release factor RF3	0,96335469	0,00215275
OG1RF_10443	hypothetical protein	-1,48109995	0,00027579
OG1RF_10444	ATP-dependent Clp protease	-1,14896951	0,00384235
OG1RF_10445	hypothetical protein	-1,32249423	0,02126127
OG1RF_10458	ATP-dependent DNA helicase PcrA	0,85498374	0,00104315
OG1RF_10468	LuxR family transcriptional regulator	-1,12028651	0,00670059
OG1RF_10505	ATP-dependent Clp protease proteolytic subunit	-1,00439026	0,01974905
OG1RF_10534	leucine--tRNA ligase	0,79684679	0,00285395
OG1RF_10552	50S ribosomal protein L25	-1,06319952	0,00986953
OG1RF_10555	GNAT family acetyltransferase	1,10864925	0,04792745
OG1RF_10562	hypothetical protein	-0,89135141	0,02452105
OG1RF_10577	hypothetical protein	-1,30620962	0,01317065
OG1RF_10587	hypothetical protein	1,41270547	1,90E-07
OG1RF_10611	primosomal protein DnaI	-0,57804888	0,01012511
OG1RF_10627	aldehyde-alcohol dehydrogenase	-0,61306831	0,04508538
OG1RF_10649	integral membrane protein	0,73008098	0,04619307
OG1RF_10657	methionine--tRNA ligase	1,1147673	1,51E-05
OG1RF_10671	extracellular protein	1,33746868	7,66E-06
OG1RF_10676	phosphate acetyltransferase	1,03460895	0,00632622
OG1RF_10703	50S ribosomal protein L21	1,2918358	2,84E-06
OG1RF_10704	putative ribosomal protein	1,08749702	7,48E-08
OG1RF_10705	50S ribosomal protein L27	0,68019464	0,00190351
OG1RF_10716	hemolysin A	0,68286614	0,03921868
OG1RF_10717	arginine repressor	2,01934401	0,00073047
OG1RF_10724	penicillin-binding protein C	0,68517171	0,00351201
OG1RF_10725	phospho-N-acetylmuramoyl-pentapeptide- transferase	0,86639433	0,00354104
OG1RF_10726	UDP-N-acetylmuramoylalanine--D-glutamate ligase	1,29890268	0,00010793

OG1RF_10728	cell division protein FtsQ	0,72260322	0,01641578
OG1RF_10758	CBS domain protein	-0,94738303	0,01139406
OG1RF_10761	alpha/beta hydrolase fold family hydrolase	-1,69158852	4,55E-05
OG1RF_10779	pyruvate kinase	0,90833858	0,00225557
OG1RF_10800	conjugative transposon ATP/GTP-binding protein	1,48953502	0,02867859
OG1RF_10834	hypothetical protein	-1,34391867	0,00012395
OG1RF_10837	tunicamycin resistance protein	-1,0317097	0,04508538
OG1RF_10872	sortase	-1,20065768	0,0071564
OG1RF_10884	hypothetical protein	-1,35529482	0,00337431
OG1RF_10903	L-ascorbate 6-phosphate lactonase	-1,15905133	0,03037651
OG1RF_10918	MutT/NUDIX family protein	-0,85331959	0,00640791
OG1RF_10932	endonuclease III	-0,8448167	0,03787285
OG1RF_10933	GntR family transcriptional regulator	0,83268025	0,01699052
OG1RF_10945	fructose-bisphosphate aldolase	0,67231292	0,0142681
OG1RF_10948	50S ribosomal protein L31	0,79341774	0,00025112
OG1RF_10949	hypothetical protein	1,76841108	0,00218887
OG1RF_10954	S-ribosylhomocysteine lyase	-0,58706362	0,01852267
OG1RF_10955	aspartate-semialdehyde dehydrogenase	0,74412358	0,00821461
OG1RF_10966	sensor histidine kinase	-0,60671668	0,04373982
OG1RF_10967	hypothetical protein	-0,69589152	0,0123965
OG1RF_10974	protein of hypothetical function DUF965	-0,72178262	0,02849259
OG1RF_10976	protein of hypothetical function DUF1292	-0,89122728	0,00361631
OG1RF_10990	spermidine/putrescine ABC superfamily ATP binding cassette transporter, membrane protein	1,38632497	0,01413689
OG1RF_10992	ABC superfamily ATP binding cassette transporter, ABC protein	1,33419206	0,00012714
OG1RF_10993	spermidine/putrescine ABC superfamily ATP binding cassette transporter	1,19339981	0,00034951
OG1RF_11010	cellobiose-phosphorylase	1,10778391	0,02149165
OG1RF_11021	hypothetical protein	-0,79578278	0,03503447
OG1RF_11025	integral membrane protein	-0,98677196	0,04470339

OG1RF_11038	protein of hypothetical function DUF150	-0,74105876	0,02927703
OG1RF_11043	translation initiation factor IF2	-0,77121253	0,03888065
OG1RF_11076	heat-inducible transcription repressor HrcA	-1,50038662	8,23E-05
OG1RF_11077	co-chaperone GrpE	-1,33593379	5,96E-05
OG1RF_11078	chaperone DnaK	-1,13612375	1,82E-05
OG1RF_11079	hypothetical protein	-0,6172706	0,04506268
OG1RF_11080	chaperone DnaJ	-0,90289363	0,00780723
OG1RF_11081	hypothetical protein	-1,16319398	0,00161025
OG1RF_11082	serine/threonine protein phosphatase	-0,94821197	0,02149165
OG1RF_11099	GntR family transcriptional regulator	-1,48057879	0,00053724
OG1RF_11131	ABC superfamily ATP binding cassette transporter, ABC protein	-1,36840153	0,00026609
OG1RF_11133	sugar ABC superfamily ATP binding cassette transporter, membrane protein	-1,261595	0,00195379
OG1RF_11135	sugar ABC superfamily ATP binding cassette transporter, sugar-binding protein	-1,29283928	0,00173899
OG1RF_11146	glycerol dehydrogenase	2,07304541	3,41E-06
OG1RF_11147	glycerone kinase PTS family porter component IIA	1,95812706	1,82E-05
OG1RF_11148	dihydroxyacetone kinase	1,86307548	8,35E-06
OG1RF_11149	dihydroxyacetone kinase	1,93427899	1,97E-06
OG1RF_11167	alanine--tRNA ligase	1,22589422	2,49E-05
OG1RF_11179	molybdenum cofactor biosynthesis family protein	-0,97594675	0,04080297
OG1RF_11188	ABC superfamily ATP binding cassette transporter, ABC protein	-0,70946535	0,02240282
OG1RF_11232	DNA-binding/PRD domain protein	1,34626227	0,01120398
OG1RF_11240	E1-E2 family cation-transporting ATPase	0,94003802	0,02279085
OG1RF_11242	RNA polymerase sigma factor rpoD	-0,69417968	0,03556452
OG1RF_11249	PTS family porter component IIC	-0,60710051	0,0386425
OG1RF_11268	ribosome-associated GTPase EngA	0,69314665	0,01619735
OG1RF_11282	3-dehydroquinate synthase	-1,05428023	0,00799641
OG1RF_11284	prephenate dehydrogenase	-1,34258681	0,00063101
OG1RF_11285	3-phosphoshikimate 1-carboxyvinyltransferase	-1,78092286	7,48E-08

OG1RF_11286	shikimate kinase	-1,26344764	0,01557083
OG1RF_11287	prephenate dehydratase	-1,34720394	0,00022748
OG1RF_11300	transketolase	0,44244812	0,04457356
OG1RF_11309	AraC family transcriptional regulator	-0,86754694	0,01510647
OG1RF_11315	deoxyribodipyrimidine photolyase	2,52403223	3,92E-06
OG1RF_11317	PTS family beta-glucosides porter, IIABC component	-0,96947475	0,03102904
OG1RF_11324	cardiolipin synthetase	-0,75822484	0,02538908
OG1RF_11329	formate acetyltransferase	0,9855267	0,02613442
OG1RF_11331	DNA topoisomerase (ATP-hydrolyzing) ParE	0,82515732	0,0022846
OG1RF_11361	tRNA:M(5)U-54 methyltransferase	1,16763268	0,0011669
OG1RF_11365	ribonuclease H	1,34879244	0,0007735
OG1RF_11400	adenine phosphoribosyltransferase	0,80317264	0,04173793
OG1RF_11404	ribonuclease Z	1,15015744	0,00394246
OG1RF_11406	KH domain protein	1,24140735	0,00697829
OG1RF_11407	30S ribosomal protein S16	1,0591031	0,00112116
OG1RF_11436	formate--tetrahydrofolate ligase	-0,64526434	0,03037651
OG1RF_11448	hypothetical protein	-1,75085232	0,00188363
OG1RF_11453	catabolite control protein A	0,83049813	0,01510647
OG1RF_11457	UTP--glucose-1-phosphate uridylyltransferase	0,69016973	0,00222562
OG1RF_11460	HPr(Ser) kinase/phosphatase	0,82234534	0,00742605
OG1RF_11472	cell division protein FtsX	0,74771948	0,01753905
OG1RF_11473	ABC superfamily ATP binding cassette transporter, ABC protein	0,82199091	0,01852267
OG1RF_11476	preprotein translocase subunit SecA	0,42079353	0,00292381
OG1RF_11497	phosphoribosylaminoimidazole-succinocarboxamide synthetase	0,95255194	0,04076856
OG1RF_11498	phosphoribosylaminoimidazole carboxylase ATPase subunit PurK	0,95395793	0,02522899
OG1RF_11500	SPFH domain/Band 7 family protein	-0,95223468	0,00023231
OG1RF_11511	PTS family mannose/fructose/sorbose porter component IID	-0,96300286	0,03071001
OG1RF_11513	PTS family mannose/fructose/sorbose porter, IIB component	-0,84280196	0,03769629

OG1RF_11521	phosphatidylglycerol--membrane-oligosaccharide glycerophosphotransferase	1,87503284	0,00084754
OG1RF_11545	hypothetical protein	1,60632384	0,0166276
OG1RF_11567	NRAMP family Mn2+/Fe2+ transporter	-0,89588798	0,00556527
OG1RF_11602	putative calcium-transporting ATPase	0,57511269	0,02032364
OG1RF_11616	PTS family mannose/fructose/sorbose porter component IIA	1,4267293	0,00821461
OG1RF_11618	hypothetical protein	-1,07974739	1,82E-05
OG1RF_11645	adenine-specific methyltransferase	0,95430898	0,00600199
OG1RF_11648	hypothetical protein	1,82576232	0,00221769
OG1RF_11655	cfr family radical SAM enzyme	1,06098833	0,00595507
OG1RF_11674	hypothetical protein	-1,1352451	2,02E-05
OG1RF_11685	hypothetical protein	1,24263244	0,01579726
OG1RF_11694	ABC superfamily ATP binding cassette transporter, ABC protein	0,92344449	0,01160653
OG1RF_11713	CDP-glycerol:poly(glycerophosphate) glycerophosphotransferase	0,67687306	0,0334839
OG1RF_11714	group 2 glycosyl transferase	1,17180308	0,0005397
OG1RF_11720	group 2 glycosyl transferase	0,93209399	0,04792745
OG1RF_11726	ABC superfamily ATP binding cassette transporter, ABC protein	1,05325661	0,00017356
OG1RF_11729	hypothetical protein	-1,08697305	0,04173793
OG1RF_11734	glucose-1-phosphate thymidylyltransferase	0,76174012	0,00731038
OG1RF_11751	hypothetical protein	-1,34107217	0,00804589
OG1RF_11753	PTS family trehalose porter, IIBC component	-1,55269522	1,24E-05
OG1RF_11760	hypothetical protein	1,15848538	0,01753905
OG1RF_11763	ABC superfamily ATP binding cassette transporter, membrane protein	1,19466118	0,0404947
OG1RF_11773	ABC superfamily ATP binding cassette transporter, membrane protein	-1,14948156	0,02033643
OG1RF_11774	sugar ABC superfamily ATP binding cassette transporter, sugar-binding protein	-1,19330023	3,35E-05
OG1RF_11775	glucuronyl hydrolase	-0,94488143	0,00802722
OG1RF_11776	hypothetical protein	-1,21834767	0,00089551
OG1RF_11780	PTS family cellobiose porter component IIB	-1,46712025	5,32E-05
OG1RF_11781	sodium:solute symporter family protein	-1,48203241	5,33E-05

OG1RF_11782	myo-inositol catabolism protein IolE	-1,30257862	0,00190037
OG1RF_11783	inositol 2-dehydrogenase	-1,34414049	0,00066353
OG1RF_11784	inositol 2-dehydrogenase	-1,26868173	0,00084754
OG1RF_11785	methylmalonate-semialdehyde dehydrogenase (acylating)	-1,42835886	4,03E-06
OG1RF_11786	myo-inositol catabolism protein IolB	-1,3870189	1,82E-05
OG1RF_11787	3D-(3,5/4)-trihydroxycyclohexane-1,2-dione hydrolase	-1,39334164	2,93E-05
OG1RF_11788	5-dehydro-2-deoxygluconokinase	-1,13473941	0,00093221
OG1RF_11789	DNA binding protein	-1,19151571	0,00089844
OG1RF_11793	chaperone protein ClpB	-0,72849926	0,03816311
OG1RF_11798	xanthine phosphoribosyltransferase	0,95802981	0,00381556
OG1RF_11807	peptidase propeptide and YPEB domain protein	0,86598885	0,01585065
OG1RF_11810	amino acid permease	0,82911572	0,03206269
OG1RF_11811	DNA polymerase III PolC	-0,52406626	0,01165143
OG1RF_11831	UMP kinase	0,61571561	0,0117112
OG1RF_11839	glycyl-tRNA synthetase beta subunit	0,74261853	0,01662916
OG1RF_11856	bifunctional phosphoglucomutase/phosphomannomutase	0,44771486	0,04390326
OG1RF_11862	guanine deaminase	0,8279018	0,006304
OG1RF_11865	RpiR family phosphosugar-binding transcriptional regulator	-1,04208209	0,00655823
OG1RF_11874	30S ribosomal protein S20	0,90951851	0,00642612
OG1RF_11892	GTP-binding protein TypA/BipA	0,79440119	0,02844986
OG1RF_11929	hypothetical protein	-1,22548075	0,00898317
OG1RF_11931	uracil phosphoribosyltransferase	0,80700253	0,00361631
OG1RF_11938	fumarate reductase	0,65467036	0,0162156
OG1RF_11940	pyruvate:ferredoxin oxidoreductase	-0,76562312	0,00735101
OG1RF_11950	YgfJ family molybdenum hydroxylase accessory protein	-0,99515797	0,00188363
OG1RF_11951	selenium-dependent molybdenum hydroxylase 1	-0,80649712	0,01720308
OG1RF_11975	beta-glucosidase	-1,61864208	0,00180546

OG1RF_11976	PTS family porter, enzyme I	-1,57627522	0,00141095
OG1RF_11977	transcription antiterminator LicT	-1,14432295	0,00012207
OG1RF_11992	ATP synthase F0 sector subunit A	0,77256563	0,03647397
OG1RF_12006	chaperonin GroEL	-0,98534838	1,07E-06
OG1RF_12007	chaperone GroES	-1,2547631	2,93E-05
OG1RF_12029	hypothetical protein	-0,92762076	0,02431947
OG1RF_12039	23S rRNA pseudouridylate synthase RluD	1,18183561	0,01874254
OG1RF_12042	adenylate cyclase	-0,84807278	0,03647397
OG1RF_12045	competence protein	-1,40054178	0,00409181
OG1RF_12048	tryptophan--tRNA ligase	0,88429291	0,03982111
OG1RF_12050	HAD-superfamily hydrolase	-0,87719953	0,00534412
OG1RF_12080	ribosomal protein L7/L12	0,87697327	0,00012158
OG1RF_12081	50S ribosomal protein L10	0,98071358	0,00381556
OG1RF_12082	50S ribosomal protein L1	1,09360315	0,00011032
OG1RF_12083	50S ribosomal protein L11	0,86728684	0,00595061
OG1RF_12087	D-aminopeptidase superfamily protein	-1,30606239	0,01354248
OG1RF_12109	D-alanyl-lipoteichoic acid biosynthesis protein DltD	-0,73040782	0,03647397
OG1RF_12112	D-alanine--D-alanyl carrier protein ligase subunit 1	-1,04537037	0,02380807
OG1RF_12115	anaerobic ribonucleoside-triphosphate reductase large subunit	0,64417442	0,03503447
OG1RF_12121	initiation-control protein YabA	-0,75565082	0,00361631
OG1RF_12141	galactose-1-phosphate uridylyltransferase	0,74280362	0,01510647
OG1RF_12160	4-oxalocrotonate tautomerase	1,19733592	0,00595061
OG1RF_12161	serine-type D-Ala-D-Ala carboxypeptidase	1,6925512	0,00325667
OG1RF_12169	glucose-1-phosphate adenylyltransferase	-0,56133842	0,00821461
OG1RF_12179	acetyl-coA carboxylase carboxyl transferase subunit beta	0,83674414	0,01870118
OG1RF_12180	acetyl-CoA carboxylase subunit A	0,91252768	0,00369838
OG1RF_12181	(3R)-hydroxymyristoyl-[acyl-carrier-protein] dehydratase	1,31542188	0,00047884
OG1RF_12182	acetyl-CoA carboxylase biotin carboxyl carrier subunit	0,9078623	0,0369945

OG1RF_12183	beta-ketoacyl-acyl-carrier-protein synthase II	0,94040138	0,0011669
OG1RF_12184	3-oxoacyl-[acyl-carrier-protein] reductase	0,92802654	0,00959096
OG1RF_12186	enoyl-(acyl-carrier-protein) reductase II	1,06071608	0,00225557
OG1RF_12187	acyl carrier protein	1,20614418	2,93E-05
OG1RF_12188	beta-ketoacyl-acyl-carrier-protein synthase III	0,83708562	0,00084754
OG1RF_12189	MarR family transcriptional regulator	1,07219404	0,00087288
OG1RF_12203	ABC superfamily ATP binding cassette transporter, substrate-binding protein	0,8224453	0,00077029
OG1RF_12204	hypothetical protein	0,72015991	0,00928343
OG1RF_12205	sugar ABC superfamily ATP binding cassette transporter, membrane protein	0,90116341	0,0379922
OG1RF_12207	ABC superfamily ATP binding cassette transporter, ABC protein	0,70240455	0,02566304
OG1RF_12214	transcription elongation factor GreA	1,31207517	0,00088438
OG1RF_12225	cold shock protein CspA	0,81270732	0,01204568
OG1RF_12228	tetrahydrofolate synthase	-0,63478082	0,00322151
OG1RF_12231	valine--tRNA ligase	0,49803345	0,03283276
OG1RF_12267	permease protein	-1,25757823	0,01767841
OG1RF_12269	PFL4705 family integrating conjugative element protein	-1,51597761	0,01100962
OG1RF_12290	FdrA protein	1,81103376	0,00557112
OG1RF_12299	hypothetical protein	-1,23660771	0,02779489
OG1RF_12300	sigma-70 family protein	-1,76965417	0,00072314
OG1RF_12322	hypothetical protein	-1,20545613	0,00692884
OG1RF_12325	putative lipoprotein	-0,82523677	0,0384615
OG1RF_12328	hypothetical protein	-1,23605077	0,00722505
OG1RF_12329	protein-tyrosine-phosphatase	1,23025039	0,03816311
OG1RF_12334	polyribonucleotide nucleotidyltransferase	0,69896599	0,00846524
OG1RF_12339	formate/nitrite transporter	1,11454466	0,01510647
OG1RF_12340	30S ribosomal protein S4	1,0924548	2,93E-05
OG1RF_12356	hypothetical protein	-1,43379595	0,00722505
OG1RF_12360	lactoylglutathione lyase	-0,86512068	0,0489884

OG1RF_12366	peptide ABC superfamily ATP binding cassette transporter, binding protein	-0,92395472	0,01857256
OG1RF_12367	ABC superfamily ATP binding cassette transporter, ABC protein	-0,85937961	0,00850911
OG1RF_12370	ABC superfamily ATP binding cassette transporter, ABC protein	-1,05753421	0,00267587
OG1RF_12374	DAK2 domain protein	-0,83991602	0,00014976
OG1RF_12380	50S ribosomal protein L28	0,82198087	0,0142681
OG1RF_12381	thiamine diphosphokinase	-1,26591874	0,00351201
OG1RF_12388	formylmethionine deformylase	0,78516539	0,02566304
OG1RF_12390	DNA-directed RNA polymerase subunit omega	1,0629273	0,00298291
OG1RF_12391	guanylate kinase	1,15676471	0,00325123
OG1RF_12405	6-phosphogluconate dehydrogenase	1,07709194	0,03503447
OG1RF_12487	50S ribosomal protein L13	0,77390904	0,00084754
OG1RF_12499	chitin binding protein	-1,19352294	3,64E-05
OG1RF_12507	1,4-dihydroxy-2-naphthoate octaprenyltransferase	-0,87886692	0,00645975
OG1RF_12510	NADH dehydrogenase	0,9728324	7,98E-07
OG1RF_12519	glutathione-disulfide reductase	-0,72986279	0,00722505
OG1RF_12530	ATPase/chaperone ClpC, probable specificity factor for ClpP protease	-0,9562743	0,02498897
OG1RF_12531	transcriptional regulator CtsR	-0,86976136	0,04095633
OG1RF_12540	hypothetical protein	-0,64222507	0,00188363
OG1RF_12541	GTP-binding protein YchF	0,70570404	0,03292881
OG1RF_12545	16S rRNA methyltransferase GidB	1,36206551	0,00184812
OG1RF_12546	hypothetical protein	-0,69056808	0,03519354
OG1RF_12571	hypothetical protein	1,2367689	0,01514468
OG1RF_12575	RNA-binding protein	-0,88907924	0,02060367
OG1RF_12578	50S ribosomal protein L34	1,03436243	0,00090219

List of figures

List of tables

List of abbreviations

Δ*eut*	*E. faecalis* OG1RF *eutV* and *eutW* double deletion mutant
Δ*mfs*	*E. faecalis* OG1RF *mfs* deletion mutant
AdoCbl	adenosylcobalamin
AIEC	adherent and invasive *E. coli*
AMP	antimicrobial peptide
ATG16L1	autophagy-related protein 16-1
B. longum	*Bifidobacterium longum*
B. vulgatus	*Bacteroides vulgatus*
BHI	brain heart infusion
CD	cluster of differntiation
CD	Crohn's disease
cDNA	complementary DNA
CEACAM6	carcinoembryonic antigen-related cell adhesion molecule 6
CFU	colony forming units
Cm	chloramphenicol
Ct	threshold cycle
DC	dendritic cell
ddPCR	digital droplet PCR
DSS	dextran sulfate sodium
DTT	dithiothretiol
E. coli; *E. col*	*Escherichia coli*
E. faecalis; *E. fae*	*Enterococcus faecalis*
EA	ethanolamine
EDTA	ethylenediaminetetraacetic acid
EHEC	enterohemorrhagic *E. coli*
ELISA	enzyme linked immunosorbent assay
epa	enterococcal polysaccharide antigen
ER	endoplasmatic reticulum
Eut	ethanolamine utilization
eut	ethanolamine utilization genes
F. prausnitzii	*Faecalibacterium prausnitzii*
FMT	fecal microbiota transplantation
gDNA	genomic DNA
GelE	gelatinase E
GF	germfree
GI	gastrointestinal
GSEA	*Gene Set Enrichment Analysis*
HLA	human leukocyte antigen
IBD	inflammatory bowel diseases
IEC	intestinal epithelial cells
IFN	interferon
IgA	immunoglobulin A
IgG	immunoglobulin G
IL	interleukin

IL-10$^{-/-}$	IL-10-deficient mouse
IMS	immunomagnetic separation
IPTG	Isopropyl-β-D-thiogalactopyranosid
IRGM	immunity-related GTPase family M protein
KEGG	Kyoto Encyclopedia of Genes and Genomes
Lb. plantarum	*Lactobacillus plantarum*
LB	lysogeny broth
MAPK	mitogen-activated protein kinase
mfs	major facilitator superfamily transporter gene
MFS	major facilitator superfamily transporter protein
MLN	mesenteric lymph node
NCF4	neutrophil cytosol factor 4
NF-κB	nuclear factor-κB
NOD2	nucleotide-binding oligomerization domain 2
OD	optical density
ON	over night
ORF	open reading frame
PBS	phosphate-buffered saline
PCA	principal component analysis
PCR	polymerase chain reaction
PRR	pattern recognition receptor
PVDF	polyvinylidene difluoride
qPCR	real-time quantitative PCR
R. gnavus	*Ruminococcus gnavus*
RNAseq	RNA sequencing
rRNA	ribosomal RNA
S. Typhimurium	*Salmonella* Typhimurium
SCFA	short-chain fatty acids
SCID	severe combined immunodeficiency
SDS-PAGE	discontinuous denaturing polyacrylamid gel electrophoresis
SIHUMI	simplified human microbiota consortium
SNP	single nucleotide polymorphism
SPF	specific pathogen free
TBST	Tris-buffered saline with Tween20
TLR	toll-like receptor
TM-IEC C1galt1(-/-)	mice deficient in core 1-derived O-glycans
TNBS	2,4,6-trinitrobenzene sulfonic acid
TNF	tumor necrosis factor
Treg cells	T-regulatory cells
UC	Ulcerative colitis
UPL	universal probe library
WCA	Wilkins-Chalgren-Agar
WT	wild type
X-Gal	5-Brom-4-chlor-3-indoxyl-β-D-galactopyranosid

References figure 2

[1] E. Balish, T. Warner, Enterococcus faecalis induces inflammatory bowel disease in interleukin-10 knockout mice, Am J Pathol, 160 (2002) 2253-2257.

[2] S.C. Kim, S.L. Tonkonogy, C.A. Albright, J. Tsang, E.J. Balish, J. Braun, M.M. Huycke, R.B. Sartor, Variable phenotypes of enterocolitis in interleukin 10-deficient mice monoassociated with two different commensal bacteria, Gastroenterology, 128 (2005) 891-906.

[3] S.C. Kim, S.L. Tonkonogy, T. Karrasch, C. Jobin, R.B. Sartor, Dual-association of gnotobiotic IL-10-/- mice with 2 nonpathogenic commensal bacteria induces aggressive pancolitis, Inflamm Bowel Dis, 13 (2007) 1457-1466.

[4] L.G. Patwa, T.J. Fan, S. Tchaptchet, Y. Liu, Y.A. Lussier, R.B. Sartor, J.J. Hansen, Chronic intestinal inflammation induces stress-response genes in commensal Escherichia coli, Gastroenterology, 141 (2011) 1842-1851 e1841-1810.

[5] U.P. Singh, S. Singh, R. Singh, R.K. Karls, F.D. Quinn, M.E. Potter, J.W. Lillard, Jr., Influence of Mycobacterium avium subsp. paratuberculosis on colitis development and specific immune responses during disease, Infect Immun, 75 (2007) 3722-3728.

[6] J.P. Moran, J. Walter, G.W. Tannock, S.L. Tonkonogy, R.B. Sartor, Bifidobacterium animalis causes extensive duodenitis and mild colonic inflammation in monoassociated interleukin-10-deficient mice, Inflamm Bowel Dis, 15 (2009) 1022-1031.

[7] M.T. Whary, N.S. Taylor, Y. Feng, Z. Ge, S. Muthupalani, J. Versalovic, J.G. Fox, Lactobacillus reuteri promotes Helicobacter hepaticus-associated typhlocolitis in gnotobiotic B6.129P2-IL-10(tm1Cgn) (IL-10(-/-)) mice, Immunology, 133 (2011) 165-178.

[8] C.S. Eun, Y. Mishima, S. Wohlgemuth, B. Liu, M. Bower, I.M. Carroll, R.B. Sartor, Induction of bacterial antigen-specific colitis by a simplified human microbiota consortium in gnotobiotic interleukin-10-/- mice, Infect Immun, 82 (2014) 2239-2246.

[9] M. Schultz, C. Veltkamp, L.A. Dieleman, W.B. Grenther, P.B. Wyrick, S.L. Tonkonogy, R.B. Sartor, Lactobacillus plantarum 299V in the treatment and prevention of spontaneous colitis in interleukin-10-deficient mice, Inflamm Bowel Dis, 8 (2002) 71-80.

[10] B.C. Sydora, M.M. Tavernini, J.S. Doyle, R.N. Fedorak, Association with selected bacteria does not cause enterocolitis in IL-10 gene-deficient mice despite a systemic immune response, Dig Dis Sci, 50 (2005) 905-913.

[11] M. Stehr, M.C. Greweling, S. Tischer, M. Singh, H. Blocker, D.A. Monner, W. Muller, Charles River altered Schaedler flora (CRASF) remained stable for four years in a mouse colony housed in individually ventilated cages, Lab Anim, 43 (2009) 362-370.

List of references

Afgan, E., Baker, D., Batut, B., van den Beek, M., Bouvier, D., Cech, M., et al. (2018). The Galaxy platform for accessible, reproducible and collaborative biomedical analyses: 2018 update. *Nucleic Acids Res* 46(W1)**,** W537-W544. doi: 10.1093/nar/gky379.

Agus, A., Massier, S., Darfeuille-Michaud, A., Billard, E., and Barnich, N. (2014). Understanding host-adherent-invasive Escherichia coli interaction in Crohn's disease: opening up new therapeutic strategies. *Biomed Res Int* 2014**,** 567929. doi: 10.1155/2014/567929.

Albenberg, L., Esipova, T.V., Judge, C.P., Bittinger, K., Chen, J., Laughlin, A., et al. (2014). Correlation between intraluminal oxygen gradient and radial partitioning of intestinal microbiota. *Gastroenterology* 147(5)**,** 1055-1063 e1058. doi: 10.1053/j.gastro.2014.07.020.

Anderson, C.J., Clark, D.E., Adli, M., and Kendall, M.M. (2015). Ethanolamine Signaling Promotes Salmonella Niche Recognition and Adaptation during Infection. *PLoS Pathog* 11(11)**,** e1005278. doi: 10.1371/journal.ppat.1005278.

Atarashi, K., Tanoue, T., Oshima, K., Suda, W., Nagano, Y., Nishikawa, H., et al. (2013). Treg induction by a rationally selected mixture of Clostridia strains from the human microbiota. *Nature* 500(7461)**,** 232-236. doi: 10.1038/nature12331.

Balish, E., and Warner, T. (2002). Enterococcus faecalis induces inflammatory bowel disease in interleukin-10 knockout mice. *Am J Pathol* 160(6)**,** 2253-2257. doi: 10.1016/S0002-9440(10)61172-8.

Barnett, M.P., McNabb, W.C., Cookson, A.L., Zhu, S., Davy, M., Knoch, B., et al. (2010). Changes in colon gene expression associated with increased colon inflammation in interleukin-10 gene-deficient mice inoculated with Enterococcus species. *BMC Immunol* 11**,** 39. doi: 10.1186/1471-2172-11-39.

Barnich, N., Carvalho, F.A., Glasser, A.L., Darcha, C., Jantscheff, P., Allez, M., et al. (2007). CEACAM6 acts as a receptor for adherent-invasive E. coli, supporting ileal mucosa colonization in Crohn disease. *J Clin Invest* 117(6)**,** 1566-1574. doi: 10.1172/JCI30504.

Bauer, H., Horowitz, R.E., Levenson, S.M., and Popper, H. (1963). The response of the lymphatic tissue to the microbial flora. Studies on germfree mice. *Am J Pathol* 42**,** 471-483.

Baumgart, D.C., and Sandborn, W.J. (2012). Crohn's disease. *Lancet* 380(9853)**,** 1590-1605. doi: 10.1016/S0140-6736(12)60026-9.

Baumgart, M., Dogan, B., Rishniw, M., Weitzman, G., Bosworth, B., Yantiss, R., et al. (2007). Culture independent analysis of ileal mucosa reveals a selective increase in invasive Escherichia coli of novel phylogeny relative to depletion of Clostridiales in Crohn's disease involving the ileum. *ISME J* 1(5)**,** 403-418. doi: 10.1038/ismej.2007.52.

Baumler, A.J., and Sperandio, V. (2016). Interactions between the microbiota and pathogenic bacteria in the gut. *Nature* 535(7610)**,** 85-93. doi: 10.1038/nature18849.

Becker, N., Kunath, J., Loh, G., and Blaut, M. (2011). Human intestinal microbiota: characterization of a simplified and stable gnotobiotic rat model. *Gut Microbes* 2(1)**,** 25-33. doi: 10.4161/gmic.2.1.14651.

Benveniste, J., Lespinats, G., Adam, C., and Salomon, J.C. (1971). Immunoglobulins in intact, immunized, and contaminated axenic mice: study of serum IgA. *J Immunol* 107(6)**,** 1647-1655.

Berg, D.J., Davidson, N., Kuhn, R., Muller, W., Menon, S., Holland, G., et al. (1996). Enterocolitis and colon cancer in interleukin-10-deficient mice are associated with aberrant cytokine production and CD4(+) TH1-like responses. *J Clin Invest* 98(4)**,** 1010-1020. doi: 10.1172/JCI118861.

Berry, D., Kuzyk, O., Rauch, I., Heider, S., Schwab, C., Hainzl, E., et al. (2015). Intestinal Microbiota Signatures Associated with Inflammation History in Mice Experiencing Recurring Colitis. *Front Microbiol* 6**,** 1408. doi: 10.3389/fmicb.2015.01408.

Bertin, Y., Girardeau, J.P., Chaucheyras-Durand, F., Lyan, B., Pujos-Guillot, E., Harel, J., et al. (2011). Enterohaemorrhagic Escherichia coli gains a competitive advantage by using ethanolamine as

a nitrogen source in the bovine intestinal content. *Environ Microbiol* 13(2)**,** 365-377. doi: 10.1111/j.1462-2920.2010.02334.x.

Beutler, B. (2000). Tlr4: central component of the sole mammalian LPS sensor. *Curr Opin Immunol* 12(1)**,** 20-26.

Bevins, C.L., and Salzman, N.H. (2011). Paneth cells, antimicrobial peptides and maintenance of intestinal homeostasis. *Nat Rev Microbiol* 9(5)**,** 356-368. doi: 10.1038/nrmicro2546.

Bloom, S.M., Bijanki, V.N., Nava, G.M., Sun, L., Malvin, N.P., Donermeyer, D.L., et al. (2011). Commensal Bacteroides species induce colitis in host-genotype-specific fashion in a mouse model of inflammatory bowel disease. *Cell Host Microbe* 9(5)**,** 390-403. doi: 10.1016/j.chom.2011.04.009.

Bonen, D.K., Ogura, Y., Nicolae, D.L., Inohara, N., Saab, L., Tanabe, T., et al. (2003). Crohn's disease-associated NOD2 variants share a signaling defect in response to lipopolysaccharide and peptidoglycan. *Gastroenterology* 124(1)**,** 140-146. doi: 10.1053/gast.2003.50019.

Brant, S.R. (2011). Update on the heritability of inflammatory bowel disease: the importance of twin studies. *Inflamm Bowel Dis* 17(1)**,** 1-5. doi: 10.1002/ibd.21385.

Brugiroux, S., Beutler, M., Pfann, C., Garzetti, D., Ruscheweyh, H.J., Ring, D., et al. (2016). Genome-guided design of a defined mouse microbiota that confers colonization resistance against Salmonella enterica serovar Typhimurium. *Nat Microbiol* 2**,** 16215. doi: 10.1038/nmicrobiol.2016.215.

Cadwell, K., Liu, J.Y., Brown, S.L., Miyoshi, H., Loh, J., Lennerz, J.K., et al. (2008). A key role for autophagy and the autophagy gene Atg16l1 in mouse and human intestinal Paneth cells. *Nature* 456(7219)**,** 259-263. doi: 10.1038/nature07416.

Cahill, R.J., Foltz, C.J., Fox, J.G., Dangler, C.A., Powrie, F., and Schauer, D.B. (1997). Inflammatory bowel disease: an immunity-mediated condition triggered by bacterial infection with Helicobacter hepaticus. *Infect Immun* 65(8)**,** 3126-3131.

Carvalho, F.A., Barnich, N., Sivignon, A., Darcha, C., Chan, C.H., Stanners, C.P., et al. (2009). Crohn's disease adherent-invasive Escherichia coli colonize and induce strong gut inflammation in transgenic mice expressing human CEACAM. *J Exp Med* 206(10)**,** 2179-2189. doi: 10.1084/jem.20090741.

Chassaing, B., Ley, R.E., and Gewirtz, A.T. (2014). Intestinal epithelial cell toll-like receptor 5 regulates the intestinal microbiota to prevent low-grade inflammation and metabolic syndrome in mice. *Gastroenterology* 147(6)**,** 1363-1377 e1317. doi: 10.1053/j.gastro.2014.08.033.

Costello, S.P., Soo, W., Bryant, R.V., Jairath, V., Hart, A.L., and Andrews, J.M. (2017). Systematic review with meta-analysis: faecal microbiota transplantation for the induction of remission for active ulcerative colitis. *Aliment Pharmacol Ther* 46(3)**,** 213-224. doi: 10.1111/apt.14173.

Crost, E.H., Tailford, L.E., Le Gall, G., Fons, M., Henrissat, B., and Juge, N. (2013). Utilisation of mucin glycans by the human gut symbiont Ruminococcus gnavus is strain-dependent. *PLoS One* 8(10)**,** e76341. doi: 10.1371/journal.pone.0076341.

Dale, J.L., Beckman, K.B., Willett, J.L.E., Nilson, J.L., Palani, N.P., Baller, J.A., et al. (2018). Comprehensive Functional Analysis of the Enterococcus faecalis Core Genome Using an Ordered, Sequence-Defined Collection of Insertional Mutations in Strain OG1RF. *mSystems* 3(5). doi: 10.1128/mSystems.00062-18.

Darfeuille-Michaud, A., Boudeau, J., Bulois, P., Neut, C., Glasser, A.L., Barnich, N., et al. (2004). High prevalence of adherent-invasive Escherichia coli associated with ileal mucosa in Crohn's disease. *Gastroenterology* 127(2)**,** 412-421.

Davidson, N.J., Leach, M.W., Fort, M.M., Thompson-Snipes, L., Kuhn, R., Muller, W., et al. (1996). T helper cell 1-type CD4+ T cells, but not B cells, mediate colitis in interleukin 10-deficient mice. *J Exp Med* 184(1)**,** 241-251.

DebRoy, S., Gao, P., Garsin, D.A., Harvey, B.R., Kos, V., Nes, I.F., et al. (2014a). "Transcriptional and Post Transcriptional Control of Enterococcal Gene Regulation," in *Enterococci: From Commensals to Leading Causes of Drug Resistant Infection,* eds. M.S. Gilmore, D.B. Clewell, Y. Ike & N. Shankar. (Boston).

DebRoy, S., Gebbie, M., Ramesh, A., Goodson, J.R., Cruz, M.R., van Hoof, A., et al. (2014b). Riboswitches. A riboswitch-containing sRNA controls gene expression by sequestration of a response regulator. *Science* 345(6199)**,** 937-940. doi: 10.1126/science.1255091.

Debroy, S., van der Hoeven, R., Singh, K.V., Gao, P., Harvey, B.R., Murray, B.E., et al. (2012). Development of a genomic site for gene integration and expression in Enterococcus faecalis. *J Microbiol Methods* 90(1)**,** 1-8. doi: 10.1016/j.mimet.2012.04.011.

Del Papa, M.F., and Perego, M. (2008). Ethanolamine activates a sensor histidine kinase regulating its utilization in Enterococcus faecalis. *J Bacteriol* 190(21)**,** 7147-7156. doi: 10.1128/JB.00952-08.

Delmas, J., Gibold, L., Fais, T., Batista, S., Leremboure, M., Sinel, C., et al. (2019). Metabolic adaptation of adherent-invasive Escherichia coli to exposure to bile salts. *Sci Rep* 9(1)**,** 2175. doi: 10.1038/s41598-019-38628-1.

Donaldson, G.P., Lee, S.M., and Mazmanian, S.K. (2016). Gut biogeography of the bacterial microbiota. *Nat Rev Microbiol* 14(1)**,** 20-32. doi: 10.1038/nrmicro3552.

Durfee, T., Hansen, A.M., Zhi, H., Blattner, F.R., and Jin, D.J. (2008). Transcription profiling of the stringent response in Escherichia coli. *J Bacteriol* 190(3)**,** 1084-1096. doi: 10.1128/JB.01092-07.

Duvallet, C., Gibbons, S.M., Gurry, T., Irizarry, R.A., and Alm, E.J. (2017). Meta-analysis of gut microbiome studies identifies disease-specific and shared responses. *Nat Commun* 8(1)**,** 1784. doi: 10.1038/s41467-017-01973-8.

Elinav, E., Strowig, T., Kau, A.L., Henao-Mejia, J., Thaiss, C.A., Booth, C.J., et al. (2011). NLRP6 inflammasome regulates colonic microbial ecology and risk for colitis. *Cell* 145(5)**,** 745-757. doi: 10.1016/j.cell.2011.04.022.

Eun, C.S., Mishima, Y., Wohlgemuth, S., Liu, B., Bower, M., Carroll, I.M., et al. (2014). Induction of bacterial antigen-specific colitis by a simplified human microbiota consortium in gnotobiotic interleukin-10-/- mice. *Infect Immun* 82(6)**,** 2239-2246. doi: 10.1128/IAI.01513-13.

Fite, A., Macfarlane, S., Furrie, E., Bahrami, B., Cummings, J.H., Steinke, D.T., et al. (2013). Longitudinal analyses of gut mucosal microbiotas in ulcerative colitis in relation to patient age and disease severity and duration. *J Clin Microbiol* 51(3)**,** 849-856. doi: 10.1128/JCM.02574-12.

Fox, K.A., Ramesh, A., Stearns, J.E., Bourgogne, A., Reyes-Jara, A., Winkler, W.C., et al. (2009). Multiple posttranscriptional regulatory mechanisms partner to control ethanolamine utilization in Enterococcus faecalis. *Proc Natl Acad Sci U S A* 106(11)**,** 4435-4440. doi: 10.1073/pnas.0812194106.

Frank, D.N., Robertson, C.E., Hamm, C.M., Kpadeh, Z., Zhang, T., Chen, H., et al. (2011). Disease phenotype and genotype are associated with shifts in intestinal-associated microbiota in inflammatory bowel diseases. *Inflamm Bowel Dis* 17(1)**,** 179-184. doi: 10.1002/ibd.21339.

Frank, K.L., Colomer-Winter, C., Grindle, S.M., Lemos, J.A., Schlievert, P.M., and Dunny, G.M. (2014). Transcriptome analysis of Enterococcus faecalis during mammalian infection shows cells undergo adaptation and exist in a stringent response state. *PLoS One* 9(12)**,** e115839. doi: 10.1371/journal.pone.0115839.

Frick, J.S., Zahir, N., Muller, M., Kahl, F., Bechtold, O., Lutz, M.B., et al. (2006). Colitogenic and non-colitogenic commensal bacteria differentially trigger DC maturation and Th cell polarization: an important role for IL-6. *Eur J Immunol* 36(6)**,** 1537-1547. doi: 10.1002/eji.200635840.

Furrie, E., Macfarlane, S., Cummings, J.H., and Macfarlane, G.T. (2004). Systemic antibodies towards mucosal bacteria in ulcerative colitis and Crohn's disease differentially activate the innate immune response. *Gut* 53(1)**,** 91-98.

Gaca, A.O., Abranches, J., Kajfasz, J.K., and Lemos, J.A. (2012). Global transcriptional analysis of the stringent response in Enterococcus faecalis. *Microbiology* 158(Pt 8)**,** 1994-2004. doi: 10.1099/mic.0.060236-0.

Ganesh, B.P., Klopfleisch, R., Loh, G., and Blaut, M. (2013). Commensal Akkermansia muciniphila exacerbates gut inflammation in Salmonella Typhimurium-infected gnotobiotic mice. *PLoS One* 8(9)**,** e74963. doi: 10.1371/journal.pone.0074963.

Garrett, W.S., Gallini, C.A., Yatsunenko, T., Michaud, M., DuBois, A., Delaney, M.L., et al. (2010). Enterobacteriaceae act in concert with the gut microbiota to induce spontaneous and maternally transmitted colitis. *Cell Host Microbe* 8(3)**,** 292-300. doi: 10.1016/j.chom.2010.08.004.

Garsin, D.A. (2010). Ethanolamine utilization in bacterial pathogens: roles and regulation. *Nat Rev Microbiol* 8(4)**,** 290-295. doi: 10.1038/nrmicro2334.

Geva-Zatorsky, N., Sefik, E., Kua, L., Pasman, L., Tan, T.G., Ortiz-Lopez, A., et al. (2017). Mining the Human Gut Microbiota for Immunomodulatory Organisms. *Cell* 168(5)**,** 928-943 e911. doi: 10.1016/j.cell.2017.01.022.

Gevers, D., Kugathasan, S., Denson, L.A., Vazquez-Baeza, Y., Van Treuren, W., Ren, B., et al. (2014). The treatment-naive microbiome in new-onset Crohn's disease. *Cell Host Microbe* 15(3)**,** 382-392. doi: 10.1016/j.chom.2014.02.005.

Giard, J.C., Laplace, J.M., Rince, A., Pichereau, V., Benachour, A., Leboeuf, C., et al. (2001). The stress proteome of Enterococcus faecalis. *Electrophoresis* 22(14)**,** 2947-2954. doi: 10.1002/1522-2683(200108)22:14<2947::AID-ELPS2947>3.0.CO;2-K.

Giard, J.C., Riboulet, E., Verneuil, N., Sanguinetti, M., Auffray, Y., and Hartke, A. (2006). Characterization of Ers, a PrfA-like regulator of Enterococcus faecalis. *FEMS Immunol Med Microbiol* 46(3)**,** 410-418. doi: 10.1111/j.1574-695X.2005.00049.x.

Girardin, S.E., Boneca, I.G., Viala, J., Chamaillard, M., Labigne, A., Thomas, G., et al. (2003). Nod2 is a general sensor of peptidoglycan through muramyl dipeptide (MDP) detection. *J Biol Chem* 278(11)**,** 8869-8872. doi: 10.1074/jbc.C200651200.

Golinska, E., Tomusiak, A., Gosiewski, T., Wiecek, G., Machul, A., Mikolajczyk, D., et al. (2013). Virulence factors of Enterococcus strains isolated from patients with inflammatory bowel disease. *World J Gastroenterol* 19(23)**,** 3562-3572. doi: 10.3748/wjg.v19.i23.3562.

Haberman, Y., Tickle, T.L., Dexheimer, P.J., Kim, M.O., Tang, D., Karns, R., et al. (2014). Pediatric Crohn disease patients exhibit specific ileal transcriptome and microbiome signature. *J Clin Invest* 124(8)**,** 3617-3633. doi: 10.1172/JCI75436.

Hansen, J.J., and Sartor, R.B. (2015). Therapeutic Manipulation of the Microbiome in IBD: Current Results and Future Approaches. *Curr Treat Options Gastroenterol* 13(1)**,** 105-120. doi: 10.1007/s11938-014-0042-7.

Harmsen, H.J., Pouwels, S.D., Funke, A., Bos, N.A., and Dijkstra, G. (2012). Crohn's disease patients have more IgG-binding fecal bacteria than controls. *Clin Vaccine Immunol* 19(4)**,** 515-521. doi: 10.1128/CVI.05517-11.

Harper, R.W., Xu, C., Eiserich, J.P., Chen, Y., Kao, C.Y., Thai, P., et al. (2005). Differential regulation of dual NADPH oxidases/peroxidases, Duox1 and Duox2, by Th1 and Th2 cytokines in respiratory tract epithelium. *FEBS Lett* 579(21)**,** 4911-4917. doi: 10.1016/j.febslet.2005.08.002.

Hisamatsu, T., Suzuki, M., and Podolsky, D.K. (2003). Interferon-gamma augments CARD4/NOD1 gene and protein expression through interferon regulatory factor-1 in intestinal epithelial cells. *J Biol Chem* 278(35)**,** 32962-32968. doi: 10.1074/jbc.M304355200.

Hooper, L.V., and Macpherson, A.J. (2010). Immune adaptations that maintain homeostasis with the intestinal microbiota. *Nat Rev Immunol* 10(3)**,** 159-169. doi: 10.1038/nri2710.

Hormannsperger, G., Schaubeck, M., and Haller, D. (2015). Intestinal Microbiota in Animal Models of Inflammatory Diseases. *ILAR J* 56(2)**,** 179-191. doi: 10.1093/ilar/ilv019.

Hugot, J.P., Chamaillard, M., Zouali, H., Lesage, S., Cezard, J.P., Belaiche, J., et al. (2001). Association of NOD2 leucine-rich repeat variants with susceptibility to Crohn's disease. *Nature* 411(6837)**,** 599-603. doi: 10.1038/35079107.

Human Microbiome Project, C. (2012). Structure, function and diversity of the healthy human microbiome. *Nature* 486(7402)**,** 207-214. doi: 10.1038/nature11234.

Johansen, F.E., and Kaetzel, C.S. (2011). Regulation of the polymeric immunoglobulin receptor and IgA transport: new advances in environmental factors that stimulate pIgR expression and its role in mucosal immunity. *Mucosal Immunol* 4(6)**,** 598-602. doi: 10.1038/mi.2011.37.

Johansson, M.E., Larsson, J.M., and Hansson, G.C. (2011). The two mucus layers of colon are organized by the MUC2 mucin, whereas the outer layer is a legislator of host-microbial interactions. *Proc Natl Acad Sci U S A* 108 Suppl 1**,** 4659-4665. doi: 10.1073/pnas.1006451107.

Johansson, M.E., Phillipson, M., Petersson, J., Velcich, A., Holm, L., and Hansson, G.C. (2008). The inner of the two Muc2 mucin-dependent mucus layers in colon is devoid of bacteria. *Proc Natl Acad Sci U S A* 105(39)**,** 15064-15069. doi: 10.1073/pnas.0803124105.

Joossens, M., Huys, G., Cnockaert, M., De Preter, V., Verbeke, K., Rutgeerts, P., et al. (2011). Dysbiosis of the faecal microbiota in patients with Crohn's disease and their unaffected relatives. *Gut* 60(5)**,** 631-637. doi: 10.1136/gut.2010.223263.

Joseph, B., Przybilla, K., Stuhler, C., Schauer, K., Slaghuis, J., Fuchs, T.M., et al. (2006). Identification of Listeria monocytogenes genes contributing to intracellular replication by expression profiling and mutant screening. *J Bacteriol* 188(2)**,** 556-568. doi: 10.1128/JB.188.2.556-568.2006.

Jostins, L., Ripke, S., Weersma, R.K., Duerr, R.H., McGovern, D.P., Hui, K.Y., et al. (2012). Host-microbe interactions have shaped the genetic architecture of inflammatory bowel disease. *Nature* 491(7422)**,** 119-124. doi: 10.1038/nature11582.

Kang, S., Denman, S.E., Morrison, M., Yu, Z., Dore, J., Leclerc, M., et al. (2010). Dysbiosis of fecal microbiota in Crohn's disease patients as revealed by a custom phylogenetic microarray. *Inflamm Bowel Dis* 16(12)**,** 2034-2042. doi: 10.1002/ibd.21319.

Katakura, K., Lee, J., Rachmilewitz, D., Li, G., Eckmann, L., and Raz, E. (2005). Toll-like receptor 9-induced type I IFN protects mice from experimental colitis. *J Clin Invest* 115(3)**,** 695-702. doi: 10.1172/JCI22996.

Kau, A.L., Ahern, P.P., Griffin, N.W., Goodman, A.L., and Gordon, J.I. (2011). Human nutrition, the gut microbiome and the immune system. *Nature* 474(7351)**,** 327-336. doi: 10.1038/nature10213.

Kaval, K.G., and Garsin, D.A. (2018). Ethanolamine Utilization in Bacteria. *MBio* 9(1). doi: 10.1128/mBio.00066-18.

Kaval, K.G., Singh, K.V., Cruz, M.R., DebRoy, S., Winkler, W.C., Murray, B.E., et al. (2018). Loss of Ethanolamine Utilization in Enterococcus faecalis Increases Gastrointestinal Tract Colonization. *MBio* 9(3). doi: 10.1128/mBio.00790-18.

Kawamoto, S., Maruya, M., Kato, L.M., Suda, W., Atarashi, K., Doi, Y., et al. (2014). Foxp3(+) T cells regulate immunoglobulin a selection and facilitate diversification of bacterial species responsible for immune homeostasis. *Immunity* 41(1)**,** 152-165. doi: 10.1016/j.immuni.2014.05.016.

Kendall, M.M., Gruber, C.C., Parker, C.T., and Sperandio, V. (2012). Ethanolamine controls expression of genes encoding components involved in interkingdom signaling and virulence in enterohemorrhagic Escherichia coli O157:H7. *MBio* 3(3). doi: 10.1128/mBio.00050-12.

Kim, S.C., Tonkonogy, S.L., Albright, C.A., Tsang, J., Balish, E.J., Braun, J., et al. (2005). Variable phenotypes of enterocolitis in interleukin 10-deficient mice monoassociated with two different commensal bacteria. *Gastroenterology* 128(4)**,** 891-906.

Kim, S.C., Tonkonogy, S.L., Karrasch, T., Jobin, C., and Sartor, R.B. (2007). Dual-association of gnotobiotic IL-10-/- mice with 2 nonpathogenic commensal bacteria induces aggressive pancolitis. *Inflamm Bowel Dis* 13(12)**,** 1457-1466. doi: 10.1002/ibd.20246.

Klaring, K., Hanske, L., Bui, N., Charrier, C., Blaut, M., Haller, D., et al. (2013). Intestinimonas butyriciproducens gen. nov., sp. nov., a butyrate-producing bacterium from the mouse intestine. *Int J Syst Evol Microbiol* 63(Pt 12)**,** 4606-4612. doi: 10.1099/ijs.0.051441-0.

Kobayashi, K.S., Chamaillard, M., Ogura, Y., Henegariu, O., Inohara, N., Nunez, G., et al. (2005). Nod2-dependent regulation of innate and adaptive immunity in the intestinal tract. *Science* 307(5710)**,** 731-734. doi: 10.1126/science.1104911.

Kruis, W. (2013). Probiotics. *Dig Dis* 31(3-4)**,** 385-387. doi: 10.1159/000354706.

Kruis, W., Fric, P., Pokrotnieks, J., Lukas, M., Fixa, B., Kascak, M., et al. (2004). Maintaining remission of ulcerative colitis with the probiotic Escherichia coli Nissle 1917 is as effective as with standard mesalazine. *Gut* 53(11)**,** 1617-1623. doi: 10.1136/gut.2003.037747.

Lane, D.J. (1991). 16S/23S rRNA sequencing. *In: Stackebrandt E, Goodfellow M, editors. Nucleic acid techniques in bacterial systematics. Chichester, United Kingdom: John Wiley and Sons*, 115–175.

Laubitz, D., Harrison, C.A., Midura-Kiela, M.T., Ramalingam, R., Larmonier, C.B., Chase, J.H., et al. (2016). Reduced Epithelial Na+/H+ Exchange Drives Gut Microbial Dysbiosis and Promotes Inflammatory Response in T Cell-Mediated Murine Colitis. *PLoS One* 11(4), e0152044. doi: 10.1371/journal.pone.0152044.

Law, C.J., Maloney, P.C., and Wang, D.N. (2008). Ins and outs of major facilitator superfamily antiporters. *Annu Rev Microbiol* 62, 289-305. doi: 10.1146/annurev.micro.61.080706.093329.

Lebreton, F., Willems, R.J.L., and Gilmore, M.S. (2014). "Enterococcus Diversity, Origins in Nature, and Gut Colonization," in *Enterococci: From Commensals to Leading Causes of Drug Resistant Infection,* eds. M.S. Gilmore, D.B. Clewell, Y. Ike & N. Shankar. (Boston).

Lewis, J.D., Chen, E.Z., Baldassano, R.N., Otley, A.R., Griffiths, A.M., Lee, D., et al. (2015). Inflammation, Antibiotics, and Diet as Environmental Stressors of the Gut Microbiome in Pediatric Crohn's Disease. *Cell Host Microbe* 18(4), 489-500. doi: 10.1016/j.chom.2015.09.008.

Lindenstrauss, A.G., Ehrmann, M.A., Behr, J., Landstorfer, R., Haller, D., Sartor, R.B., et al. (2014). Transcriptome analysis of Enterococcus faecalis toward its adaption to surviving in the mouse intestinal tract. *Arch Microbiol* 196(6), 423-433. doi: 10.1007/s00203-014-0982-2.

Liu, B., Gulati, A.S., Cantillana, V., Henry, S.C., Schmidt, E.A., Daniell, X., et al. (2013). Irgm1-deficient mice exhibit Paneth cell abnormalities and increased susceptibility to acute intestinal inflammation. *Am J Physiol Gastrointest Liver Physiol* 305(8), G573-584. doi: 10.1152/ajpgi.00071.2013.

Liu, Y.F., Yan, J.J., Lei, H.Y., Teng, C.H., Wang, M.C., Tseng, C.C., et al. (2012). Loss of outer membrane protein C in Escherichia coli contributes to both antibiotic resistance and escaping antibody-dependent bactericidal activity. *Infect Immun* 80(5), 1815-1822. doi: 10.1128/IAI.06395-11.

Loftus, E.V., Jr. (2004). Clinical epidemiology of inflammatory bowel disease: Incidence, prevalence, and environmental influences. *Gastroenterology* 126(6), 1504-1517.

Low, D., Tran, H.T., Lee, I.A., Dreux, N., Kamba, A., Reinecker, H.C., et al. (2013). Chitin-binding domains of Escherichia coli ChiA mediate interactions with intestinal epithelial cells in mice with colitis. *Gastroenterology* 145(3), 602-612 e609. doi: 10.1053/j.gastro.2013.05.017.

Lundberg, J.O., Hellstrom, P.M., Lundberg, J.M., and Alving, K. (1994). Greatly increased luminal nitric oxide in ulcerative colitis. *Lancet* 344(8938), 1673-1674.

Luzader, D.H., Clark, D.E., Gonyar, L.A., and Kendall, M.M. (2013). EutR is a direct regulator of genes that contribute to metabolism and virulence in enterohemorrhagic Escherichia coli O157:H7. *J Bacteriol* 195(21), 4947-4953. doi: 10.1128/JB.00937-13.

Maadani, A., Fox, K.A., Mylonakis, E., and Garsin, D.A. (2007). Enterococcus faecalis mutations affecting virulence in the Caenorhabditis elegans model host. *Infect Immun* 75(5), 2634-2637. doi: 10.1128/IAI.01372-06.

Macpherson, A.J., Hunziker, L., McCoy, K., and Lamarre, A. (2001). IgA responses in the intestinal mucosa against pathogenic and non-pathogenic microorganisms. *Microbes Infect* 3(12), 1021-1035.

Macpherson, A.J., Martinic, M.M., and Harris, N. (2002). The functions of mucosal T cells in containing the indigenous commensal flora of the intestine. *Cell Mol Life Sci* 59(12), 2088-2096.

Macpherson, A.J., and Uhr, T. (2004). Induction of protective IgA by intestinal dendritic cells carrying commensal bacteria. *Science* 303(5664), 1662-1665. doi: 10.1126/science.1091334.

Mähler M, L.E. (2002). Genetic and environmental context determines the course of colitis developing in IL-10-deficient mice. *Inflamm Bowel Dis* Sep(8(5)), 347-355.

Mahowald, M.A., Rey, F.E., Seedorf, H., Turnbaugh, P.J., Fulton, R.S., Wollam, A., et al. (2009). Characterizing a model human gut microbiota composed of members of its two dominant bacterial phyla. *Proc Natl Acad Sci U S A* 106(14), 5859-5864. doi: 10.1073/pnas.0901529106.

Marchix, J., Goddard, G., and Helmrath, M.A. (2018). Host-Gut Microbiota Crosstalk in Intestinal Adaptation. *Cell Mol Gastroenterol Hepatol* 6(2)**,** 149-162. doi: 10.1016/j.jcmgh.2018.01.024.

McGuckin, M.A., Linden, S.K., Sutton, P., and Florin, T.H. (2011). Mucin dynamics and enteric pathogens. *Nat Rev Microbiol* 9(4)**,** 265-278. doi: 10.1038/nrmicro2538.

Meena, N.K., Verma, R., Verma, N., Ahuja, V., and Paul, J. (2013). TLR4 D299G polymorphism modulates cytokine expression in ulcerative colitis. *J Clin Gastroenterol* 47(9)**,** 773-780. doi: 10.1097/MCG.0b013e31828a6e93.

Moayyedi, P., Surette, M.G., Kim, P.T., Libertucci, J., Wolfe, M., Onischi, C., et al. (2015). Fecal Microbiota Transplantation Induces Remission in Patients With Active Ulcerative Colitis in a Randomized Controlled Trial. *Gastroenterology* 149(1)**,** 102-109 e106. doi: 10.1053/j.gastro.2015.04.001.

Moller, F.T., Andersen, V., Wohlfahrt, J., and Jess, T. (2015). Familial risk of inflammatory bowel disease: a population-based cohort study 1977-2011. *Am J Gastroenterol* 110(4)**,** 564-571. doi: 10.1038/ajg.2015.50.

Molodecky, N.A., Soon, I.S., Rabi, D.M., Ghali, W.A., Ferris, M., Chernoff, G., et al. (2012). Increasing incidence and prevalence of the inflammatory bowel diseases with time, based on systematic review. *Gastroenterology* 142(1)**,** 46-54 e42; quiz e30. doi: 10.1053/j.gastro.2011.10.001.

Moolenbeek, C., and Ruitenberg, E.J. (1981). The "Swiss roll": a simple technique for histological studies of the rodent intestine. *Lab Anim* 15(1)**,** 57-59.

Mow, W.S., Vasiliauskas, E.A., Lin, Y.C., Fleshner, P.R., Papadakis, K.A., Taylor, K.D., et al. (2004). Association of antibody responses to microbial antigens and complications of small bowel Crohn's disease. *Gastroenterology* 126(2)**,** 414-424.

Muller, C., Cacaci, M., Sauvageot, N., Sanguinetti, M., Rattei, T., Eder, T., et al. (2015). The Intraperitoneal Transcriptome of the Opportunistic Pathogen Enterococcus faecalis in Mice. *PLoS One* 10(5)**,** e0126143. doi: 10.1371/journal.pone.0126143.

Murray, B.E., Singh, K.V., Ross, R.P., Heath, J.D., Dunny, G.M., and Weinstock, G.M. (1993). Generation of restriction map of Enterococcus faecalis OG1 and investigation of growth requirements and regions encoding biosynthetic function. *J Bacteriol* 175(16)**,** 5216-5223.

Nallapareddy, S.R., Singh, K.V., Sillanpaa, J., Garsin, D.A., Hook, M., Erlandsen, S.L., et al. (2006). Endocarditis and biofilm-associated pili of Enterococcus faecalis. *J Clin Invest* 116(10)**,** 2799-2807. doi: 10.1172/JCI29021.

Nawrocki, K.L., Wetzel, D., Jones, J.B., Woods, E.C., and McBride, S.M. (2018). Ethanolamine is a valuable nutrient source that impacts Clostridium difficile pathogenesis. *Environ Microbiol* 20(4)**,** 1419-1435. doi: 10.1111/1462-2920.14048.

Neuhaus, K., Lamparter, M.C., Zolch, B., Landstorfer, R., Simon, S., Spanier, B., et al. (2017). Probiotic Enterococcus faecalis Symbioflor(R) down regulates virulence genes of EHEC in vitro and decrease pathogenicity in a Caenorhabditis elegans model. *Arch Microbiol* 199(2)**,** 203-213. doi: 10.1007/s00203-016-1291-8.

Nolle, N. (2017). *Salmonella Typhimurium-Infektion: Ernährungsabhängiges Transkriptom und Charakterisierung eines Galaktitol-spezifischen Aufnahmesystems* Dissertation, Technische Universität München.

Ocvirk, S., Sava, I.G., Lengfelder, I., Lagkouvardos, I., Steck, N., Roh, J.H., et al. (2015). Surface-Associated Lipoproteins Link Enterococcus faecalis Virulence to Colitogenic Activity in IL-10-Deficient Mice Independent of Their Expression Levels. *PLoS Pathog* 11(6)**,** e1004911. doi: 10.1371/journal.ppat.1004911.

Ogura, Y., Bonen, D.K., Inohara, N., Nicolae, D.L., Chen, F.F., Ramos, R., et al. (2001). A frameshift mutation in NOD2 associated with susceptibility to Crohn's disease. *Nature* 411(6837)**,** 603-606. doi: 10.1038/35079114.

Ordas, I., Eckmann, L., Talamini, M., Baumgart, D.C., and Sandborn, W.J. (2012). Ulcerative colitis. *Lancet* 380(9853)**,** 1606-1619. doi: 10.1016/S0140-6736(12)60150-0.

Osaka, T., Moriyama, E., Arai, S., Date, Y., Yagi, J., Kikuchi, J., et al. (2017). Meta-Analysis of Fecal Microbiota and Metabolites in Experimental Colitic Mice during the Inflammatory and Healing Phases. *Nutrients* 9(12). doi: 10.3390/nu9121329.

Pabst, O. (2012). New concepts in the generation and functions of IgA. *Nat Rev Immunol* 12(12)**,** 821-832. doi: 10.1038/nri3322.

Palm, N.W., de Zoete, M.R., Cullen, T.W., Barry, N.A., Stefanowski, J., Hao, L., et al. (2014). Immunoglobulin A coating identifies colitogenic bacteria in inflammatory bowel disease. *Cell* 158(5)**,** 1000-1010. doi: 10.1016/j.cell.2014.08.006.

Pao, S.S., Paulsen, I.T., and Saier, M.H., Jr. (1998). Major facilitator superfamily. *Microbiol Mol Biol Rev* 62(1)**,** 1-34.

Paramsothy, S., Kamm, M.A., Kaakoush, N.O., Walsh, A.J., van den Bogaerde, J., Samuel, D., et al. (2017). Multidonor intensive faecal microbiota transplantation for active ulcerative colitis: a randomised placebo-controlled trial. *Lancet* 389(10075)**,** 1218-1228. doi: 10.1016/S0140-6736(17)30182-4.

Pascal, V., Pozuelo, M., Borruel, N., Casellas, F., Campos, D., Santiago, A., et al. (2017). A microbial signature for Crohn's disease. *Gut* 66(5)**,** 813-822. doi: 10.1136/gutjnl-2016-313235.

Patwa, L.G., Fan, T.J., Tchaptchet, S., Liu, Y., Lussier, Y.A., Sartor, R.B., et al. (2011). Chronic intestinal inflammation induces stress-response genes in commensal Escherichia coli. *Gastroenterology* 141(5)**,** 1842-1851 e1841-1810. doi: 10.1053/j.gastro.2011.06.064.

Perez-Munoz, M.E., Bergstrom, K., Peng, V., Schmaltz, R., Jimenez-Cardona, R., Marsteller, N., et al. (2014). Discordance between changes in the gut microbiota and pathogenicity in a mouse model of spontaneous colitis. *Gut Microbes* 5(3)**,** 286-295. doi: 10.4161/gmic.28622.

Petnicki-Ocwieja, T., Hrncir, T., Liu, Y.J., Biswas, A., Hudcovic, T., Tlaskalova-Hogenova, H., et al. (2009). Nod2 is required for the regulation of commensal microbiota in the intestine. *Proc Natl Acad Sci U S A* 106(37)**,** 15813-15818. doi: 10.1073/pnas.0907722106.

Piddock, L.J. (2006). Multidrug-resistance efflux pumps - not just for resistance. *Nat Rev Microbiol* 4(8)**,** 629-636. doi: 10.1038/nrmicro1464.

Pierik, M., Joossens, S., Van Steen, K., Van Schuerbeek, N., Vlietinck, R., Rutgeerts, P., et al. (2006). Toll-like receptor-1, -2, and -6 polymorphisms influence disease extension in inflammatory bowel diseases. *Inflamm Bowel Dis* 12(1)**,** 1-8.

Plichta, D.R., Juncker, A.S., Bertalan, M., Rettedal, E., Gautier, L., Varela, E., et al. (2016). Transcriptional interactions suggest niche segregation among microorganisms in the human gut. *Nat Microbiol* 1(11)**,** 16152. doi: 10.1038/nmicrobiol.2016.152.

Png, C.W., Linden, S.K., Gilshenan, K.S., Zoetendal, E.G., McSweeney, C.S., Sly, L.I., et al. (2010). Mucolytic bacteria with increased prevalence in IBD mucosa augment in vitro utilization of mucin by other bacteria. *Am J Gastroenterol* 105(11)**,** 2420-2428. doi: 10.1038/ajg.2010.281.

Price-Carter, M., Tingey, J., Bobik, T.A., and Roth, J.R. (2001). The alternative electron acceptor tetrathionate supports B12-dependent anaerobic growth of Salmonella enterica serovar typhimurium on ethanolamine or 1,2-propanediol. *J Bacteriol* 183(8)**,** 2463-2475. doi: 10.1128/JB.183.8.2463-2475.2001.

Prindiville, T., Cantrell, M., and Wilson, K.H. (2004). Ribosomal DNA sequence analysis of mucosa-associated bacteria in Crohn's disease. *Inflamm Bowel Dis* 10(6)**,** 824-833.

Qin, J., Li, R., Raes, J., Arumugam, M., Burgdorf, K.S., Manichanh, C., et al. (2010). A human gut microbial gene catalogue established by metagenomic sequencing. *Nature* 464(7285)**,** 59-65. doi: 10.1038/nature08821.

Ramanan, D., and Cadwell, K. (2016). Intrinsic Defense Mechanisms of the Intestinal Epithelium. *Cell Host Microbe* 19(4)**,** 434-441. doi: 10.1016/j.chom.2016.03.003.

Ramesh, A., DebRoy, S., Goodson, J.R., Fox, K.A., Faz, H., Garsin, D.A., et al. (2012). The mechanism for RNA recognition by ANTAR regulators of gene expression. *PLoS Genet* 8(6)**,** e1002666. doi: 10.1371/journal.pgen.1002666.

Ran, S., Liu, B., Jiang, W., Sun, Z., and Liang, J. (2015). Transcriptome analysis of Enterococcus faecalis in response to alkaline stress. *Front Microbiol* 6**,** 795. doi: 10.3389/fmicb.2015.00795.

Rath, H.C., Wilson, K.H., and Sartor, R.B. (1999). Differential induction of colitis and gastritis in HLA-B27 transgenic rats selectively colonized with Bacteroides vulgatus or Escherichia coli. *Infect Immun* 67(6)**,** 2969-2974.

Rembacken, B.J., Snelling, A.M., Hawkey, P.M., Chalmers, D.M., and Axon, A.T. (1999). Non-pathogenic Escherichia coli versus mesalazine for the treatment of ulcerative colitis: a randomised trial. *Lancet* 354(9179)**,** 635-639.

Riboulet-Bisson, E., Hartke, A., Auffray, Y., and Giard, J.C. (2009). Ers controls glycerol metabolism in Enterococcus faecalis. *Curr Microbiol* 58(3)**,** 201-204. doi: 10.1007/s00284-008-9308-4.

Riboulet-Bisson, E., Sanguinetti, M., Budin-Verneuil, A., Auffray, Y., Hartke, A., and Giard, J.C. (2008). Characterization of the Ers regulon of Enterococcus faecalis. *Infect Immun* 76(7)**,** 3064-3074. doi: 10.1128/IAI.00161-08.

Ridaura, V.K., Faith, J.J., Rey, F.E., Cheng, J., Duncan, A.E., Kau, A.L., et al. (2013). Gut microbiota from twins discordant for obesity modulate metabolism in mice. *Science* 341(6150)**,** 1241214. doi: 10.1126/science.1241214.

Rigottier-Gois, L. (2013). Dysbiosis in inflammatory bowel diseases: the oxygen hypothesis. *ISME J* 7(7)**,** 1256-1261. doi: 10.1038/ismej.2013.80.

Rioux, J.D., Xavier, R.J., Taylor, K.D., Silverberg, M.S., Goyette, P., Huett, A., et al. (2007). Genome-wide association study identifies new susceptibility loci for Crohn disease and implicates autophagy in disease pathogenesis. *Nat Genet* 39(5)**,** 596-604. doi: 10.1038/ng2032.

Roberts, R.L., Hollis-Moffatt, J.E., Gearry, R.B., Kennedy, M.A., Barclay, M.L., and Merriman, T.R. (2008). Confirmation of association of IRGM and NCF4 with ileal Crohn's disease in a population-based cohort. *Genes Immun* 9(6)**,** 561-565. doi: 10.1038/gene.2008.49.

Roche-Lima, A., Carrasquillo-Carrion, K., Gomez-Moreno, R., Cruz, J.M., Velazquez-Morales, D.M., Rogozin, I.B., et al. (2018). The Presence of Genotoxic and/or Pro-inflammatory Bacterial Genes in Gut Metagenomic Databases and Their Possible Link With Inflammatory Bowel Diseases. *Front Genet* 9**,** 116. doi: 10.3389/fgene.2018.00116.

Rossen, N.G., Fuentes, S., van der Spek, M.J., Tijssen, J.G., Hartman, J.H., Duflou, A., et al. (2015). Findings From a Randomized Controlled Trial of Fecal Transplantation for Patients With Ulcerative Colitis. *Gastroenterology* 149(1)**,** 110-118 e114. doi: 10.1053/j.gastro.2015.03.045.

Rowley, C.A., Anderson, C.J., and Kendall, M.M. (2018). Ethanolamine Influences Human Commensal Escherichia coli Growth, Gene Expression, and Competition with Enterohemorrhagic E. coli O157:H7. *MBio* 9(5). doi: 10.1128/mBio.01429-18.

Ruiz, P.A., Shkoda, A., Kim, S.C., Sartor, R.B., and Haller, D. (2005). IL-10 gene-deficient mice lack TGF-beta/Smad signaling and fail to inhibit proinflammatory gene expression in intestinal epithelial cells after the colonization with colitogenic Enterococcus faecalis. *J Immunol* 174(5)**,** 2990-2999.

Salzman, A., Denenberg, A.G., Ueta, I., O'Connor, M., Linn, S.C., and Szabo, C. (1996). Induction and activity of nitric oxide synthase in cultured human intestinal epithelial monolayers. *Am J Physiol* 270(4 Pt 1)**,** G565-573. doi: 10.1152/ajpgi.1996.270.4.G565.

Sartor, R.B. (2006). Mechanisms of disease: pathogenesis of Crohn's disease and ulcerative colitis. *Nat Clin Pract Gastroenterol Hepatol* 3(7)**,** 390-407. doi: 10.1038/ncpgasthep0528.

Sartor, R.B. (2008). Microbial influences in inflammatory bowel diseases. *Gastroenterology* 134(2)**,** 577-594. doi: 10.1053/j.gastro.2007.11.059.

Sartor, R.B., and Mazmanian, S.K. (2012). Intestinal Microbe in Inflammatory Bowel Disease. *Am J Gastroenterol Suppl* 1(1)**,** 15-21. doi: 10.1038/ajgsup.2012.4.

Sartor, R.B., and Wu, G.D. (2017). Roles for Intestinal Bacteria, Viruses, and Fungi in Pathogenesis of Inflammatory Bowel Diseases and Therapeutic Approaches. *Gastroenterology* 152(2)**,** 327-339 e324. doi: 10.1053/j.gastro.2016.10.012.

Sava, I.G., Heikens, E., and Huebner, J. (2010). Pathogenesis and immunity in enterococcal infections. *Clin Microbiol Infect* 16(6)**,** 533-540. doi: 10.1111/j.1469-0691.2010.03213.x.

Schaffler, H., Herlemann, D.P., Alberts, C., Kaschitzki, A., Bodammer, P., Bannert, K., et al. (2016). Mucosa-attached bacterial community in Crohn's Disease coheres with the Clinical Disease Activity Index. *Environ Microbiol Rep*. doi: 10.1111/1758-2229.12411.

Schirmer, M., Denson, L., Vlamakis, H., Franzosa, E.A., Thomas, S., Gotman, N.M., et al. (2018). Compositional and Temporal Changes in the Gut Microbiome of Pediatric Ulcerative Colitis Patients Are Linked to Disease Course. *Cell Host Microbe* 24(4)**,** 600-610 e604. doi: 10.1016/j.chom.2018.09.009.

Scortti, M., Lacharme-Lora, L., Wagner, M., Chico-Calero, I., Losito, P., and Vazquez-Boland, J.A. (2006). Coexpression of virulence and fosfomycin susceptibility in Listeria: molecular basis of an antimicrobial in vitro-in vivo paradox. *Nat Med* 12(5)**,** 515-517. doi: 10.1038/nm1396.

Sellon, R.K., Tonkonogy, S., Schultz, M., Dieleman, L.A., Grenther, W., Balish, E., et al. (1998). Resident enteric bacteria are necessary for development of spontaneous colitis and immune system activation in interleukin-10-deficient mice. *Infect Immun* 66(11)**,** 5224-5231.

Shiga, H., Kajiura, T., Shinozaki, J., Takagi, S., Kinouchi, Y., Takahashi, S., et al. (2012). Changes of faecal microbiota in patients with Crohn's disease treated with an elemental diet and total parenteral nutrition. *Dig Liver Dis* 44(9)**,** 736-742. doi: 10.1016/j.dld.2012.04.014.

Singh, S.B., Davis, A.S., Taylor, G.A., and Deretic, V. (2006). Human IRGM induces autophagy to eliminate intracellular mycobacteria. *Science* 313(5792)**,** 1438-1441. doi: 10.1126/science.1129577.

Slack, E., Balmer, M.L., Fritz, J.H., and Hapfelmeier, S. (2012). Functional flexibility of intestinal IgA - broadening the fine line. *Front Immunol* 3**,** 100. doi: 10.3389/fimmu.2012.00100.

Sokol, H., Pigneur, B., Watterlot, L., Lakhdari, O., Bermudez-Humaran, L.G., Gratadoux, J.J., et al. (2008). Faecalibacterium prausnitzii is an anti-inflammatory commensal bacterium identified by gut microbiota analysis of Crohn disease patients. *Proc Natl Acad Sci U S A* 105(43)**,** 16731-16736. doi: 10.1073/pnas.0804812105.

Sood, A., Midha, V., Makharia, G.K., Ahuja, V., Singal, D., Goswami, P., et al. (2009). The probiotic preparation, VSL#3 induces remission in patients with mild-to-moderately active ulcerative colitis. *Clin Gastroenterol Hepatol* 7(11)**,** 1202-1209, 1209 e1201. doi: 10.1016/j.cgh.2009.07.016.

Sorbara, M.T., and Pamer, E.G. (2018). Interbacterial mechanisms of colonization resistance and the strategies pathogens use to overcome them. *Mucosal Immunol*. doi: 10.1038/s41385-018-0053-0.

Spehlmann, M.E., Begun, A.Z., Burghardt, J., Lepage, P., Raedler, A., and Schreiber, S. (2008). Epidemiology of inflammatory bowel disease in a German twin cohort: results of a nationwide study. *Inflamm Bowel Dis* 14(7)**,** 968-976. doi: 10.1002/ibd.20380.

Steck, N., Hoffmann, M., Sava, I.G., Kim, S.C., Hahne, H., Tonkonogy, S.L., et al. (2011). Enterococcus faecalis metalloprotease compromises epithelial barrier and contributes to intestinal inflammation. *Gastroenterology* 141(3)**,** 959-971. doi: 10.1053/j.gastro.2011.05.035.

Stepankova, R., Powrie, F., Kofronova, O., Kozakova, H., Hudcovic, T., Hrncir, T., et al. (2007). Segmented filamentous bacteria in a defined bacterial cocktail induce intestinal inflammation in SCID mice reconstituted with CD45RBhigh CD4+ T cells. *Inflamm Bowel Dis* 13(10)**,** 1202-1211. doi: 10.1002/ibd.20221.

Sun, J., Deng, Z., and Yan, A. (2014). Bacterial multidrug efflux pumps: mechanisms, physiology and pharmacological exploitations. *Biochem Biophys Res Commun* 453(2)**,** 254-267. doi: 10.1016/j.bbrc.2014.05.090.

Sutherland, D.B., Suzuki, K., and Fagarasan, S. (2016). Fostering of advanced mutualism with gut microbiota by Immunoglobulin A. *Immunol Rev* 270(1)**,** 20-31. doi: 10.1111/imr.12384.

Sydora, B.C., Tavernini, M.M., Doyle, J.S., and Fedorak, R.N. (2005). Association with selected bacteria does not cause enterocolitis in IL-10 gene-deficient mice despite a systemic immune response. *Dig Dis Sci* 50(5)**,** 905-913.

Tchaptchet, S., Fan, T.J., Goeser, L., Schoenborn, A., Gulati, A.S., Sartor, R.B., et al. (2013). Inflammation-induced acid tolerance genes gadAB in luminal commensal Escherichia coli attenuate experimental colitis. *Infect Immun* 81(10)**,** 3662-3671. doi: 10.1128/IAI.00355-13.

Thiennimitr, P., Winter, S.E., Winter, M.G., Xavier, M.N., Tolstikov, V., Huseby, D.L., et al. (2011). Intestinal inflammation allows Salmonella to use ethanolamine to compete with the microbiota. *Proc Natl Acad Sci U S A* 108(42)**,** 17480-17485. doi: 10.1073/pnas.1107857108.

Thurlow, L.R., Thomas, V.C., and Hancock, L.E. (2009). Capsular polysaccharide production in Enterococcus faecalis and contribution of CpsF to capsule serospecificity. *J Bacteriol* 191(20)**,** 6203-6210. doi: 10.1128/JB.00592-09.

Traxler, M.F., Summers, S.M., Nguyen, H.T., Zacharia, V.M., Hightower, G.A., Smith, J.T., et al. (2008). The global, ppGpp-mediated stringent response to amino acid starvation in Escherichia coli. *Mol Microbiol* 68(5)**,** 1128-1148. doi: 10.1111/j.1365-2958.2008.06229.x.

Tsoy, O., Ravcheev, D., and Mushegian, A. (2009). Comparative genomics of ethanolamine utilization. *J Bacteriol* 191(23)**,** 7157-7164. doi: 10.1128/JB.00838-09.

Turnbaugh, P.J., Hamady, M., Yatsunenko, T., Cantarel, B.L., Duncan, A., Ley, R.E., et al. (2009). A core gut microbiome in obese and lean twins. *Nature* 457(7228)**,** 480-484. doi: 10.1038/nature07540.

Turnbaugh, P.J., Ley, R.E., Mahowald, M.A., Magrini, V., Mardis, E.R., and Gordon, J.I. (2006). An obesity-associated gut microbiome with increased capacity for energy harvest. *Nature* 444(7122)**,** 1027-1031. doi: 10.1038/nature05414.

Turpin, W., Goethel, A., Bedrani, L., and Croitoru Mdcm, K. (2018). Determinants of IBD Heritability: Genes, Bugs, and More. *Inflamm Bowel Dis* 24(6)**,** 1133-1148. doi: 10.1093/ibd/izy085.

Tursi, A., Brandimarte, G., Papa, A., Giglio, A., Elisei, W., Giorgetti, G.M., et al. (2010). Treatment of relapsing mild-to-moderate ulcerative colitis with the probiotic VSL#3 as adjunctive to a standard pharmaceutical treatment: a double-blind, randomized, placebo-controlled study. *Am J Gastroenterol* 105(10)**,** 2218-2227. doi: 10.1038/ajg.2010.218.

van de Guchte, M., Serror, P., Chervaux, C., Smokvina, T., Ehrlich, S.D., and Maguin, E. (2002). Stress responses in lactic acid bacteria. *Antonie Van Leeuwenhoek* 82(1-4)**,** 187-216.

Waidmann, M., Bechtold, O., Frick, J.S., Lehr, H.A., Schubert, S., Dobrindt, U., et al. (2003). Bacteroides vulgatus protects against Escherichia coli-induced colitis in gnotobiotic interleukin-2-deficient mice. *Gastroenterology* 125(1)**,** 162-177.

Wehkamp, J., Harder, J., Weichenthal, M., Schwab, M., Schaffeler, E., Schlee, M., et al. (2004). NOD2 (CARD15) mutations in Crohn's disease are associated with diminished mucosal alpha-defensin expression. *Gut* 53(11)**,** 1658-1664. doi: 10.1136/gut.2003.032805.

Whary, M.T., Taylor, N.S., Feng, Y., Ge, Z., Muthupalani, S., Versalovic, J., et al. (2011). Lactobacillus reuteri promotes Helicobacter hepaticus-associated typhlocolitis in gnotobiotic B6.129P2-IL-10(tm1Cgn) (IL-10(-/-)) mice. *Immunology* 133(2)**,** 165-178. doi: 10.1111/j.1365-2567.2011.03423.x.

Willing, B.P., Dicksved, J., Halfvarson, J., Andersson, A.F., Lucio, M., Zheng, Z., et al. (2010). A pyrosequencing study in twins shows that gastrointestinal microbial profiles vary with inflammatory bowel disease phenotypes. *Gastroenterology* 139(6)**,** 1844-1854 e1841. doi: 10.1053/j.gastro.2010.08.049.

Wilmore, J.R., Gaudette, B.T., Gomez Atria, D., Hashemi, T., Jones, D.D., Gardner, C.A., et al. (2018). Commensal Microbes Induce Serum IgA Responses that Protect against Polymicrobial Sepsis. *Cell Host Microbe* 23(3)**,** 302-311 e303. doi: 10.1016/j.chom.2018.01.005.

Winter, S.E., and Baumler, A.J. (2014). Why related bacterial species bloom simultaneously in the gut: principles underlying the 'Like will to like' concept. *Cell Microbiol* 16(2)**,** 179-184. doi: 10.1111/cmi.12245.

Winter, S.E., Thiennimitr, P., Winter, M.G., Butler, B.P., Huseby, D.L., Crawford, R.W., et al. (2010). Gut inflammation provides a respiratory electron acceptor for Salmonella. *Nature* 467(7314)**,** 426-429. doi: 10.1038/nature09415.

Winter, S.E., Winter, M.G., Xavier, M.N., Thiennimitr, P., Poon, V., Keestra, A.M., et al. (2013). Host-derived nitrate boosts growth of E. coli in the inflamed gut. *Science* 339(6120)**,** 708-711. doi: 10.1126/science.1232467.

Xavier, R.J., and Podolsky, D.K. (2007). Unravelling the pathogenesis of inflammatory bowel disease. *Nature* 448(7152)**,** 427-434. doi: 10.1038/nature06005.

Yamada, H., Kurose-Hamada, S., Fukuda, Y., Mitsuyama, J., Takahata, M., Minami, S., et al. (1997). Quinolone susceptibility of norA-disrupted Staphylococcus aureus. *Antimicrob Agents Chemother* 41(10)**,** 2308-2309.

Yen, D., Cheung, J., Scheerens, H., Poulet, F., McClanahan, T., McKenzie, B., et al. (2006). IL-23 is essential for T cell-mediated colitis and promotes inflammation via IL-17 and IL-6. *J Clin Invest* 116(5)**,** 1310-1316. doi: 10.1172/JCI21404.

Yu, G., Wang, L.G., Han, Y., and He, Q.Y. (2012). clusterProfiler: an R package for comparing biological themes among gene clusters. *OMICS* 16(5)**,** 284-287. doi: 10.1089/omi.2011.0118.

Zhou, Y., Chen, H., He, H., Du, Y., Hu, J., Li, Y., et al. (2016). Increased Enterococcus faecalis infection is associated with clinically active Crohn disease. *Medicine (Baltimore)* 95(39)**,** e5019. doi: 10.1097/MD.0000000000005019.

Zhu, L., Shen, D.X., Zhou, Q., Liu, C.J., Li, Z., Fang, X., et al. (2014). Universal Probe Library based real-time PCR for rapid detection of bacterial pathogens from positive blood culture bottles. *World J Microbiol Biotechnol* 30(3)**,** 967-975. doi: 10.1007/s11274-013-1515-x.

Acknowledgements

Publications and presentations

Peer-reviewed original research articles

Ocvirk, S., Sava, I.G., **Lengfelder, I.**, Lagkouvardos, I., Steck, N., Roh, J.H., Tchaptchet, S., Bao, Y., Hansen, J.J., Huebner, J., Carrol, I.M., Murray B.E., Sartor R.B., Haller, D. (2015). Surface-Associated Lipoproteins Link Enterococcus faecalis Virulence to Colitogenic Activity in IL-10-Deficient Mice Independent of Their Expression Levels. *PLoS Pathog* 11(6)**,** e1004911. doi: 10.1371/journal.ppat.1004911.

Original research articles in preparation

Lengfelder, I., Sava, I.G., Hansen, J.J., Kleigrewe, K., Herzog, J., Neuhaus, K., Hofmann, T., Sartor, R.B., Haller, D. Complex bacterial consortia reprogram the colitogenic activity of *Enterococcus faecalis* in a gnotobiotic mouse model of chronic, immune-mediated colitis. Accepted at Frontiers in Immunology.

Oral presentations

- Beyond the intestinal microbiome-- From signatures to therapy, Hannover (2014)
- 7th Seeon conference: Microbiota, Probiota and Host, Seeon (2014)
- External workshop of German Research Foundation (DFG) research training group GRK 1482, Spitzingsee (2015)
- Science Camp of German Research Foundation (DFG) research training group GRK 1482, Seeon (2017)
- 5th Joint Conference of the DGHM & VAAM, Würzburg (2017)

Poster presentations

- Beyond the intestinal microbiome-- From signatures to therapy, Hannover (2014)
- 52. Wissenschaftlicher Kongress der DGE: Ernährung und Umwelt – Determinanten unseres Stoffwechsels, Halle (2015)
- 71. Jahrestagung der Deutschen Gesellschaft für Hygiene und Mikrobiologie, Göttingen (2019)
- 8th Seeon conference: From Sequencing to Function, Seeon (2015)
- 11th Seeon conference: From Sequencing to Function, Seeon (2018)

Curriculum vitae

Personal information:

Surname/ First names	Lengfelder Isabella Brigitta
Date of birth	06.03.1989
Nationality	German
Email	isabella.lengfelder@hotmail.de
linkedin	https://www.linkedin.com/in/isabella-lengfelder-755065173/

Work experience:

04/2014 – 12/2018   Research associate, Technische Universität München
Chair of Nutrition and Immunology

Title of PhD thesis:
Complex bacterial consortia reprogram the colitogenic activity of *Enterococcus faecalis* in a gnotobiotic mouse model of chronic, immune-mediated colits

11/2011 – 02/2012   Research assistant, University Hospital Würzburg
Institute for Clinical Neurobiology

Education:

04/2014 – 05/2017   Scholarship, Graduiertenkolleg 1482

10/2008 – 11/2013   Studies in Biology, Universität Würzburg

Degree: Master of Science, with distinction
Master thesis (Chair of Microbiology): The role of the ER-mitochondrial interface (MAM) on infection with *Simkania*

Degree: Bachelor of Science, with distinction
Bachelor thesis (Institute for Clinical Neurobiology): Parkin and its role in the Ca^{2+}-homeostatis of neuronal cells

09/1999 – 07/2008   High school Gabrieli-Gymnasium-Eichstätt